METABOLIC AND MOLECULAR INSIGHTS ON LIMONIN BIOTRANSFORMATION BY *PSEUDOMONAS PUTIDA*

A thesis
submitted in fulfillment of the requirement
for the award of the degree of

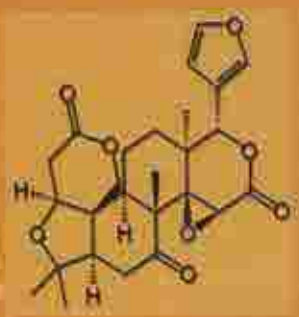

DOCTOR OF PHILOSOPHY
IN
BIOTECHNOLOGY

Meenakshi Malik
(Reg No 9051006)

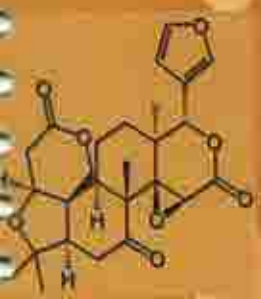

Department of Biotechnology and Environmental Sciences,
Thapar University, Patiala –147004
Punjab (India)

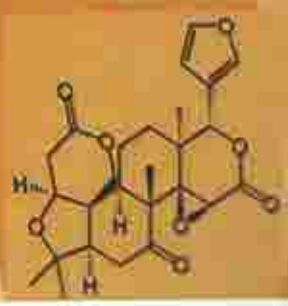

THAPAR
UNIVERSITY

CERTIFICATE

Certified that the thesis **"Metabolic and Molecular insights on Limonin Biotransformation by *Pseudomonas putida*"** which is submitted by **Meenakshi Malik**, in fulfillment of the requirement for the award of the degree of **Doctor of Philosophy** in the Department of Biotechnology and Environmental Sciences, Thapar University, Patiala, is a record of the candidate's own independent and original research work carried out by her under my supervision and guidance. The matter embodied in this thesis has not been submitted in part or full to any other University or Institute for the award of any degree.

(Dr. Moushumi Ghosh)
Associate Professor,
DBTES, Thapar University,
Patiala-147004

(Dr. M. Sudhakara Reddy)
Professor & Head,
DBTES, Thapar University,
Patiala-147004

THAPAR UNIVERSITY

CANDIDATE DECLARATION

I hereby declare that the work which is being presented in this thesis **"Metabolic and Molecular insights on Limonin Biotransformation by *Pseudomonas putida*"** submitted by me for the award of the degree of **Doctor of Philosophy** in the **Department of Biotechnology and Environmental Sciences, Thapar University, Patiala,** is true and original record of my own independent and original research work carried out under the supervision of **Dr. Moushumi Ghosh,** Associate Professor, **Department of Biotechnology and Environmental Sciences, Thapar University, Patiala, India**. The matter embodied in this thesis has not been submitted in part or full to any other university or institute for the award of any degree in India or abroad.

(Mrs. Meenakshi Malik)

ACKNOWLEDGEMENT

Firstly, I would like to recompense my veneration and gratitude to the Almighty for his eternal love and blessing that He has bestowed upon me.

Since my first day at Thapar University as a PhD student, till date I had come across many individuals who are to be acknowledged for their immense support towards the completion of this research work. I appreciate that I now have the opportunity to express my gratitude to all of them.

The first person I would like to thank is my revered supervisor ***Dr. Moushumi Ghosh,*** *Associate Professor, Thapar University, Patiala. It is difficult to overstate my gratitude to her. Throughout my PhD, her inspiring and encouraging ways have guided me to a deeper understanding of knowledge work. Her persistence and very optimistic attitude kept me moving forward and learning despite the highs and lows. It is through her patient advice that I have grown up with knowledge during these years and has developed a dedicated understanding into science.*

I am extremely thankful to ***Dr. Abhijit Mukherjee, Director****, Thapar University;* ***Dr. P. K. Bajpai,*** *Dean (Research and Sponsored Projects) for all the amenities, encouragement and support throughout this tenure; which have been immeasurably helpful for the completion of this research work.*

I hereby take an opportunity to express my deep sense of gratitude to ***M Sudhakara Reddy,*** *Professor and Head, Department of Biotechnology and Environmental Science and* ***Dr. Susheel Mittal****, Professor, Department of Chemistry and Biochemistry (my venerated doctoral committee members) for their invaluable suggestion, constant support and encouragement during the course of my study.*

I wish to express my thanks to ***Dr. Abhijit Ganguli,*** *Associate Professor, Department of Biotechnology and Environmental Sciences and* ***Dr. Manmohan Chibber,*** *Assistant Professor, School of Chemistry and Biochemistry for providing their invaluable suggestions, their decisive insights, meticulous and straightforward approach toward science.*

I am especially thankful to ***CSIR (Council of Scientific and Industrial Research)****, Human Resource Development Group, New Delhi, for the financial support during my research tenure as senior research fellow.*

I am highly gratified to all my colleagues and friends ***Santosh pathak, Richu Singla, Mukesh Kumar, Seema Bhanwar, Gurpreet Kaur Khaira, Taranpreet Kaur,***

Gatha Sharma, Shashi Bhanwar, Mr. Rajesh Dhankar, and Zinki Jindal *for their marvelous help and moral support during the crucial times.*

I feel lacunae of words to owe my personal gratitude and benevolence to my parents and brothers Ashish and Manish for their love, care, patience, inspiration, encouragement, motivation and constant driving force which has enabled me to complete this task.

Final and incalculable heartfelt gratitude goes to my husband, Mr. Sanjay Verma, for his constant encouragement and for being a backbone during all the thick and thin times. His support has been invaluable and I couldn't have done this without him.

*Date:*3-11-2011 *Meenakshi Malik*

Place: Patiala

LIST OF PUBLICATIONS

Publications in peer reviewed journals

1. **Meenakshi Malik, Abhijit Ganguli, Moushumi Ghosh (2012)** Modeling of permeabilization process in *Pseudomonas putida* G7 for enhanced Limonin bioconversion, Applied Microbiology and Biotechnology, 95(1): 223-231

2. **Meenakshi Malik, Abhijit Ganguli, Moushumi Ghosh (2012)** Enhancement of Bioconversion efficiency of Limonin by *Pseudomonas putida* G7, Journal of Food Science and Nutrition, 63(1): 59-65

3. **Raina Puri, Meenakshi Malik, Moushumi Ghosh, (2012),** An amperometric biosensor developed for detection of limonin levels in kinnow-mandarin juices, Annals of Microbiology, 62:1301–1309

4. **Moushumi Ghosh, Abhijit Ganguli, Meenakshi Malik (2006)** Evidence of Indigenous NAH Plasmid of Naphthalene Degrading *Pseudomonas putida* PpG7 Strain Implicated in Limonin Degradation, The Journal of Microbiology, 473-479

5. **Meenakshi Malik, Moushumi Ghosh (2012)** Immobilization parameters statistically optimized for whole cells of *P. putida* G7 to enhance limonin biotransformation, Journal of Advanced Laboratory Research in Biology **(Accepted)**

6. **Meenakshi Malik, Moushumi Ghosh (2012)** Statistical optimization of process parameters influencing the biotransformation of limonin by *Pseudomonas putida* G7, Research Journal of Biotechnology **(Accepted)**

Conference Proceedings

1. **Malik M, Ghosh M,** Molecular detection of limonin biotransforming enzyme and evaluation of antioxidant properties of the biotransformed products" (oral presentation) in National Conference on Emerging trends in Biopharmacheuticals: Relevance to human health & 4th Annual convention of Association of Biotechnology and Pharmacy, Thapar University (Nov 11-13, 2010)
2. **Malik M, Ghosh M,** Characterization of NAH plasmid coded, periplasmic limonoate dehydrogenase in *Pseudomonas putida* PpG7" (poster presentation) at 49th Association of Microbiologists of India (AMI) Conference, South campus, New Delhi (Nov 18-20Dec, 2008)

3. **Malik M, Ghosh M,** Evidence of Indigenous NAH Plasmid of Naphthalene Degrading *Pseudomonas putida* PpG7 Strain Implicated in Limonin Biotransformation" (poster presentation) at 47th AMI National Annual Conference, Barkatullah University, Bhopal (Dec 6-8, 2006)

ABSTRACT

Microbial whole cells and their enzymes are implicated as potential biocatalysts in several biotechnological processes. However suitable biocatalysts for removal of bitter triterpenoids in citrus juices are currently lacking and requires due consideration. Limonin, a triterpenoid is generated in freshly squeezed citrus juices and imparts bitterness making it unacceptable to consumers thereby impeding industrial processing of citrus juices. In this study, the unique metabolic feature of *Pseudomonas putida* G7 to biotransform polycyclic aromatic compounds was exploited based on its ability to utilize limonin as a sole carbon and energy source.

First, an attempt was made to elucidate the limonin catabolic abilities, enzyme(s) and gene(s) in *P. putida* G7. Then, these results were used to formulate a process for limonin biotransformation, viable under real time conditions in citrus juice. Physiological studies revealed that *P. puitda* G7 could biotransform limonin in synthetic minimal medium by 64% at an alkaline pH 8, 37°C, in 36h. The molecular characterization of limonin biotransformation revealed the association of glutamate symporter in limonin utilization and established the role of an indigenous 83 kb NAH plasmid for limonin bioconversion in *P. putida* G7. The biochemical insights suggested the potential involvement of a periplasmic isofunctional dehydrogenase in biotransformation of limonin. A 26 fold purification of the periplasmic dehydrogenase was achieved, the purified enzyme was a monomer of 26 kDa and converted limonin by 76% to non bitter defuran limonin upon incubation at pH 8 for 150 min at 30°C. The Michaelis constant (K_M) measured for limonin was 4.5µM and V_{max} was 8µmoles/min. However both whole cells as well as application of pure enzyme for limonin

biotransformation in citrus juices were not practicable, therefore improvements in whole cells was sought.

Substantial enhancement in limonin biotransformation was achieved by using alginate immobilized whole cells and conferred reusability of *P. putida* cells. Lower bioconversion rates observed during subsequent batch cycles was possibly due to diffusional restriction of substrate or products across the cellular membrane. Permeabilization of *P. putida* with EDTA (1 µg/ml) for 15 min alleviated diffusional restriction and enhanced limonin bioconversion to 73% within 180 min. Entrapment of permeabilized *P. putida* cells in dialysis membrane prior to application further enhanced the biotransformation rate to 76.7% presumably by affording mechanical stability to permeabilized cells. The residual limonin level in the treated citrus juice obtained using permeabilized cells, remained far below the threshold limit of human detection and retained its inherent antioxidative properties assuring consumer acceptance. The viability of dialysis membrane based bioreactor developed by employing the permeabilized *P. putida* G7 promises an important industrial strategy in reducing limonin levels in mandarin juices.

CONTENTS

LIST OF ABBREVIATIONS

ANOVA	Analysis of variance
BLAST	Basic Local Alignment Search Tool
$CaCl_2$	Calcium chloride
CCRD	Central Composite Rotatable Design
CTAB	N,N,N,N-Cetyl trimethyl ammonium bromide
CV	Coefficient of variation
DNA	Deoxyribonucleic acid
dNTP	2'-deoxynucleoside-5'-triphosphate
DVB	Divinyl benzene styrene
EDTA	Ethylenediamminetetraacetic acid
EtBr	Ethidium bromide
HPLC	High Performance Liquid Chromatography
IPTG	Isopropyl- -D- thioglactopyranoside
LA	Luria Agar
LB	Luria Broth
Na_2EDTA	Disodium Ethylenediaminetetraacetic acid
NaCl	Sodium chloride
OD	Optical Density
ORF	Open Reading Frame
PCR	Polymerase Chain Reaction
rDNA	Ribosomal deoxyribonucleic acid
rRNA	Ribosomal ribonucleic acid
RSM	Response surface methodology
SDS	Sodium dodecyl sulphate
SE	Standard error
SEM	Scanning Eelectron Microscopy
TBE	Tris Borate EDTA
TE	Tris EDTA
TEM	Transmission Eelectron Microscopy
TLC	Thin layer chromatography
Tris	Tris-(hydroxymethyl)- aminomethane
TTC	2,3,5- Triphenyl Tetrazolium Chloride
UV	Ultraviolet
X-gal	5- Bromo-4- Chloro-3- indolyl-D- galactoside

LIST OF SYMBOLS

%	Percentage
µ	Micron
bp	Base pair
cm	Centimeter
Da	Dalton
g	Gram
H	Hydrogen
H_2O_2	Hydrogen peroxide
hr	Hours
kb	Kilo base
KDa	Kilo Dalton
kV	Kilo volt
L	Litre
M	Molar
mA	Milli ampere
mg	Milligram
Min	Minutes
ml	Milliliter
mm	Millimeter
mM	Millimolar
ppm	Parts per million
rpm	Revolution per minute
Sec	Seconds
U	Unit
V	Volt
v/v	Volume by volume
w/v	Weight by volume
α	Alpha
β	Beta
µg	Microgram
µl	Microlitre

LIST OF TABLES

LIST OF FIGURES

Chapter 1

Introduction

Limonin, a Phytochemical which is a highly oxygenated triterpene derivative (composed of a furan ring and an epoxide group) belongs to a class of limonoids, responsible for causing delayed bitterness in certain citrus fruit juices. Citrus tissues possess limonoate A-ring lactone (LARL), a nonbitter limonoid and a natural precursor of limonin, present endogenously in the membranous sacs of citrus fruits. Juice extraction causes physical disruption of the juice sacs in the citrus fruits, initiating a biochemical transformation of the tasteless limonoid aglycone precursor i.e. limonate A-ring lactone, (LARL) to get converted to limonin (a bitter limonoid aglycone) - a process, known as delayed bitterness. The biochemical transformation is catalyzed by an enzyme limonin D-ring lactone hydrolase at lower pH of 6.5. This phenomenon of delayed bitterness continues to be an important economic impediment for the citrus industry worldwide in terms of achieving consumer acceptability (Manners 2007). The presence of limonin in excess of 6 ppm has been established as an objectionable level of bitterness in citrus and processed citrus products (Roy et al. 2006). The negative impact created by bitter taste in citrus juices made debittering a generally incorporated step in industrial juice processing technology. Therefore, over decades, it has been a major goal of researchers to develop methods for the eradication of bitterness from the citrus juices.

Bitterness due to limonin can be eliminated by: a) preventing its biosynthesis (preharvest treatment with 1-naphthalene acetic acid); b) removing the rag and pulp from freshly expressed juice as soon as possible to prevent the precursor, limonic acid A-ring (mono) lactone, from being converted to limonin or, c) enzymatic hydrolysis of limonin to non-bitter products by use of immobilized microbial cells containing an NADP-dependent limonin dehydrogenase (Puri et al. 2002). Based on these approaches, a number of physicochemical and enzymatic treatments have been devised, in order to reduce bitterness below a threshold level for consumer acceptability. The adsorptive debittering method involves the use of

polyamides, cellulose acetate, nylon-based matrices, porous polymers, ion exchangers, ultrafiltration and activated magnesium silicate (Florisil). These methods reduce bitterness and acidity in juices without adversely affecting its nutritional quality (vitamin C, sugars). The chemical methods for debittering orange juices involves treatment with ethylene (20pg/ml) for 3 h to accelerate ripening in navel oranges, carbon dioxide at pressures of 21 to 41 MPA and pH adjustment of the juice after extraction and immediately prior to (Kimball 1987). In batch operations, bitterness of citrus juices was reduced by passing the juice through cross-linked divinyl benzene-styrene resins and soluble β-cyclodextrin reduced limonin (Puri et al. 1996). Efforts were also made for limonin removal by ultrafiltration and adsorption to polystyrene divinylbenzene resins, XAD-7HP adsorbent resin (Ribeiro et al. 2002; Ribero et al. 2003; Kranz et al. 2011). However, all these methods faces numerous disadvantages like alteration in the chemical composition of the juice, non specificity, introduction of batch-to-batch variations due to undesirable changes along with the desirable ones, lacked reproducibility and low yields i.e. debittering was achieved at the cost of nutritional quality, flavour, color and stability of the citrus juices (Puri et al. 1996).

In order to overcome these limitations, research efforts have been directed to exploitation of the metabolic versatility of microbes and their enzymes for limonin metabolism. Whole bacterial cells or their enzyme(s) were used directly or immobilized in some solid matrices to debitter citrus juices. The application of prospective bacterial isolates like *Pseudomonas* 321 – 18; *Arthrobacter globifomis*; *Bacterium* 342-152-1, *Acinetobacter* sp. have been attempted. The limonin degrading enzymes of some of these isolates were entrapped in various immobilizing agents and were used for debittering citrus juices. For instance, *Corynebacterium fasciuns* and *Rhodococcus fuscians* (Martinez-Madrid et al. 1989) having constitutive enzymes were employed in immobilized forms for the degradation of limonin to non bitter metabolites (Canovas et al. 1996; Canovas et al. 1998).

Amongst such microbial sources, the potential pseudomonads include a diverse set of bacteria whose metabolic versatility and genetic plasticity have enabled their survival in a broad range of environments. *Pseudomonas putida* is ubiquitous and possesses diverse metabolic capability for utilizing different complex aliphatic and aromatic compounds. In fact a substantial volume of studies indicate *Pseudomonas putida* to be a nutritional opportunist par excellence and paradigm of metabolically versatile microorganism. An arsenal degradative function presumably reflects its extensive spectrum of housekeeping catabolic pathways and enzymes. One of the putative strains of Pseudomonads – *Pseudomonas putida* G7 could potentially metabolize limonin. Many of such alien phenotypes of *Pseudomonas putida* are based on plasmid and chromosomally encoded pathways which channelize substrates to metabolites. In order to exploit such potential of *P. putida* G7, for an industrial application to develop a debittering strategy, it was important to explore physiology, biochemistry and genetic robustness of the microbial strain.

The industrial application of immobilized enzymes has been limited due to several factors like low stability, low recovery, low yield and expensive steps involved in isolation and purification of enzymes. Therefore, whole cell immobilization had been employed and had offered many advantages over immobilized or free enzymes and free microbial cells. Immobilized whole microbial cells (viable or non viable) or their enzymes have distinct advantages over employing free cells in bioprocesses (Busto et al., 2006; Birgisson et al. 2007). Whole cell immobilisation provides a physical incarceration or localization of microbial cells or enzymes to a certain defined space for the preservation of certain desired catalytic activity and subsequent continuous operation stability (Karel et al. 1985). This method is cost effective, offers continuous operational stability and carry out multi-step cofactor requiring bioconversion (Haiau et al. 1997; Babu & Panda 1991) with minimum downstream processing, decreased product inhibition, simplified biocatalyst recovery, high

reusability of cells, relative ease of product separation, high volumetric productivity and reduced susceptibility of cells to contamination (Bernal, Sevilla, Cánovas, & Iborra, 2007).

For real time applications whole cell biocatalysts provide several advantages over purified enzymes as the low pH of the citrus juices result in inactivation of the microbial enzyme(s) that are implicated in limonin bioconversion. Thus far microorganisms that have been explored for a commercial viable debitterring strategy in batch, continuous mode and by immobilization (Canovas et al., 1998) in several matrices have met with limited success. The possible reason being the diffusional restriction or the permeability barrier of cell envelope for substrates and or products that often results in low reaction rates when whole cells are used (Babu et al., 1991).

Therefore it is pertinent to develop effective method(s) to reduce the permeability barrier of whole cell biocatalysts to enhance limonin bioconversion (Kondo et al., 2000). Perforation of cellular membrane (permeabilization) might ease and alleviate the permeability barrier to allow the free movement of substances across the cell envelope and produce high and stable enzymatic activities of the whole cell. The permeabilized microbial cells retain their inner organization, as well as cofactors necessary for functioning of several enzymes (Cheng et al., 2006). It may be envisaged that for application of whole cells require prior information on physiology, biochemical mechanist and genetic mechanisms for limonin bioconversion by the selected microorganism. Besides, adequately optimized cultural parameters for limonin bioconversion as well as knowledge of the products formed during bioconversion of limonin are important for achieving practicability for a bioprocess to reduce limonin and thus debitter citrus juices. In the present study a systematic approach was adopted in elucidating the physiological response, biochemical and genetic mechanisms involved in limonin bioconversion. The insights developed during these studies were important in developing a feasible whole cell biocatalytic process for limonin bioconversion.

Objectives

- Physiological and biochemical characterization of *Pseudomonas putida G7* in biotransformation of limonin
- Molecular studies and real time application of *P. putida* G7 for limonin biotransformation

Chapter2

Review of Literature

Citrus juices are recognized as an important component of human diet due to its established health promoting properties (Lam et al. 1989; 2000; Miller et al. 2000; Tian et al. 2001; Guthrie, et al. 2000). Recent reports have indicated that Vitamin C, folic acid, dietry fibre and bioactive compounds (limonoids, flavonoids, coumarins, carotenoids) (Appendix II) present in the citrus juices are associated with anticancerous activities and reduced risks of chronic diseases (Murthy et al. 2011) following regular consumption of citrus juices. But, along with these promising properties, fresh pressed juices of several varieties of citrus are susceptible to the development of delayed bitterness attributable to changes in limonin content (Manners 2007).

2.1 Delayed Bitterness in Citrus juices

Scientific basis of bitterness in literature dates back to 1857, however till date 'bitterness' has been a long-standing consumer acceptance problem in the industry (Premi et al. 1994; Puri et al. 1996). The susceptibility of citrus to delayed bitterness development restricts certain commercial citrus varieties (e.g., navel orange) to marketing primarily as table fruit rather than as a source of orange juice (Manners 2007) and has contributed to freeze losses up to $90 million in California in 1992 and 2006. Over decades research efforts had identified limonin, a bitter limonoid, as the principle source for the developed delayed bitterness in citrus juices after extraction.

Limonin ($C_{26}H_{30}O_8$) was first isolated by Highby in 1938 from Washington navel orange and established as the primary source of bitterness in orange juice (even low concentrations of this compound i.e. 6 parts per million may cause significant bitterness in citrus juices) (Emerson et al. 1949; Guadagni et al. 1973). Arnott et al. (1960) had elucidated the chemical structure of limonin by the combination of chemical and physical (X-ray crystallography) methods (Maier and Beverly, 1968). Limonin includes an epoxide, two lactone rings, a five-

membered ether ring, and a furan ring while all other citrus limonoids have been reported to have the furan ring and at least one of the lactone rings (Maier et al. 1977) (Fig. 2.1). Limonin is only slightly soluble in water and alcohol (although its water solubility is increased in the presence of sugar and pectin) and is soluble in glacial acetic acid, acetonitrile, and chloroform (Dreyer, 1965). Limonin is an esterification product of a non

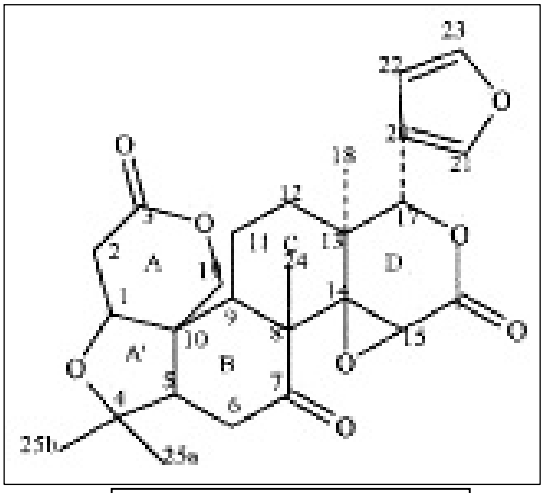

Fig. 2.1 Structure of Limonin

bitter precursor limonoic acid A-ring lactone (LARL) (Maier and Beverly, 1968; Hasegawa et al. 1972). During citrus juice processing LARL undergoes an enzyme-induced (Limonoid D-ring lactone hydrolase acid-catalyzed), esterification to form the bitter compound limonin (Maier et al. 1968; 69), the processes referred as "delayed bitterness" (Fig. 2.2) (Kefford

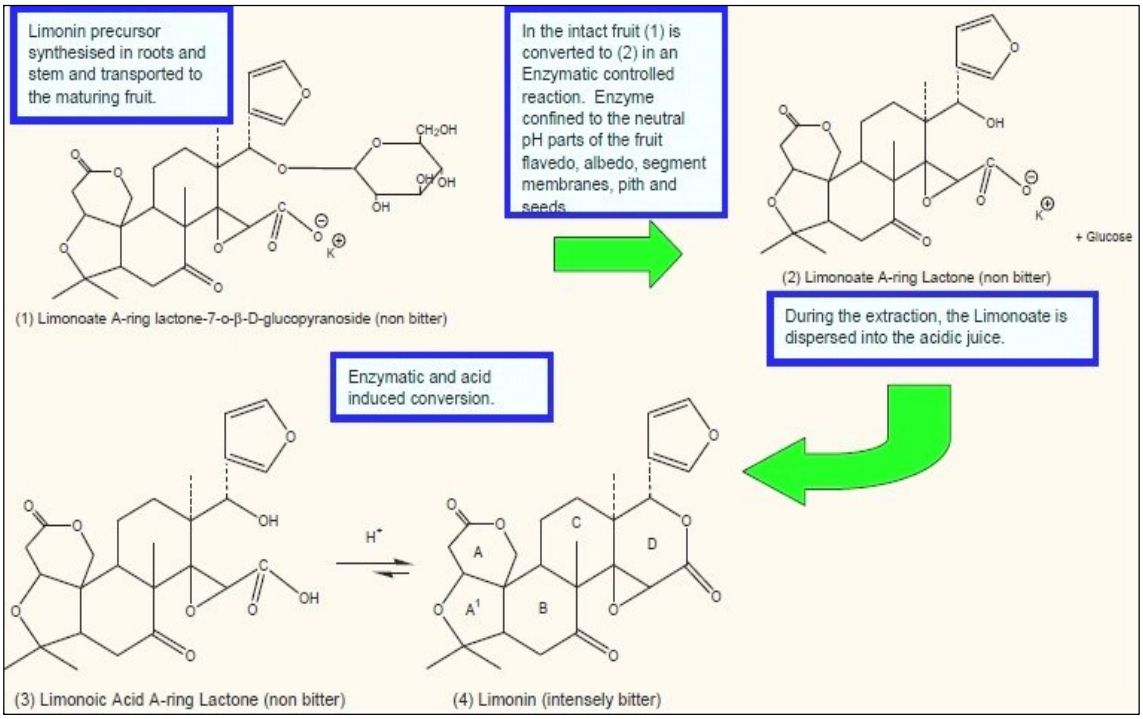

Fig. 2.2 Mechanism of delayed bitterness

1959; Hasegawa et al. 1996; Ghosh et al. 2006). The development of delayed bitterness i.e. conversion of limonoate-A-ring lactone to limonin gets completed by 48h of juice extraction at 12°C and in 4h when kept at 25°C (Premi et.al.1995; Verma et al. 2010). In addition to limonin, another triterpenoid, nomilin has also been associated with delayed bitterness, present lower concentrations (e.g., <2 ppm) in citrus juice and is of less commercial significance than limonin (Rouseff, 1980; 1990; Kimball et al. 1990).

Chemistry of limonoids

Thirty-six limonoids aglycones and seventeen glucosides have been isolated till date, from citrus and its hybrids (Maier et al. 1968). It has also been found that four limonoids namely limonin, nomilin, ichangin, nomilinate are bitter (Hasegawa and Maier, 1990).

Limonoid Aglycones

Bitter limonoid aglycones are only present in citrus juice if the enzymatic biochemical transformation of a tasteless open A-ring limonoid aglycone precursor has been initiated. Limonin is consistently the most abundant limonoid aglycone found in citrus seeds and is one of only six (limonin, nomilin, obacunoic acid, ichangin, deoxylimonoic acid and nomilinic acid) limonoid aglycones that have been identified to be inherently bitter (Hasegawa et al. 1996). The correlation of citrus limonoid structural character and perceived bitterness has established the presence of a closed D-ring, a C14–C15 epoxide, a C-7 keto group, and an acetyl ester group at C-1 in a seven membered A-ring as requirements for bitterness (Hasegawa et al. 1996). The need to monitor delayed bitterness in citrus juices has spawned a wide variety of analytical methods to quantify limonoid aglycones. The citrus limonoids can be semiquantitatively monitored by thin-layer chromatography (Albach et al. 1981; Hasegawa et al. 2000) utilizing Ehrlich's reagent (Dryer et al. 1965) as a specific detection method. Quantitative methods for analysis of limonoid aglycones primarily involve high-performance liquid chromatography (HPLC) coupled with ultraviolet (UV) detection

(Manners et al. 2000). Radioimmunoassy (Mansell et al. 1980) and enzyme-linked immunoassay (Jorudan et al. 1984) methods have also been developed to detect limonoids at very low concentrations (Rouseff et al. 1990; Widmer et al. 1991).

Limonoid Glycosides

The difference in susceptibility of different varieties of citrus to the development of bitterness and the intra seasonal change in susceptibility of particular bitterness susceptible varieties suggested that citrus possesses a natural mechanism to alleviate bitterness (Manners et al. 2005). The discovery of tasteless limonoid glycosides in the juice of citrus in the late 1980s (Manners 2007), coupled with the earlier observation that the concentration of the bitter limonin precursor LARL decreased as citrus matured (Maier et al. 1980), which led to the elucidation of the mechanism of natural debittering in citrus. UDP-D-glucose:limonoid glucosyltransferase, purified from the albedo of Frost navel orange, was established as the enzyme catalyzing the glucosylation of LARL (Hasegawa et al. 1996). Intraseason analysis of the levels of LARL and the glucoside of limonin (limonin glucoside) in navel and Valencia fruit established that limonin glucoside concentration increased with fruit maturity while LARL concentration decreased (Hasegawa et al. 1991; Fong et al. 1992) (Fig. 2.3).

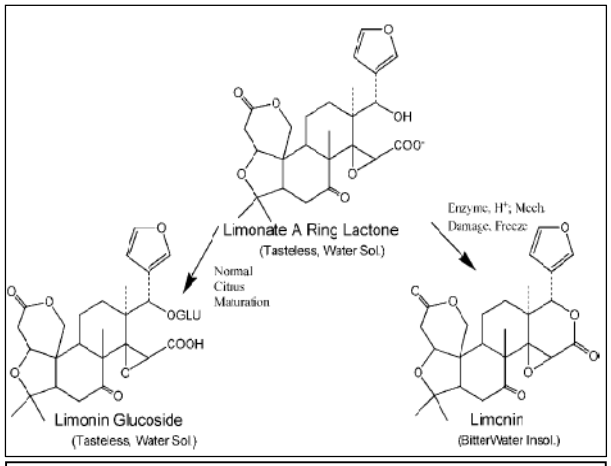

Fig. 2.3 Limonin and glucoside formation in citrus

More than 20 limonoid glycosides (all as glucosides) have been isolated and characterized from the tissues of citrus fruits and related genera in the plant family Rutaceae (Hasegawa et al. 1992). These tasteless, water-soluble limonoid glucosides occur in citrus fruit tissues, juice, and seeds in high concentrations. Limonin glucoside (Hasegawa et al. 1991), nomilin glucoside (Manners et al. 2005), and other limonoid glucosides have been obtained

chromatographically from polar extracts of defatted citrus seeds (Patil et al. 2006) and structurally characterized (Hasegawa et al. 1989; Sawabe et al. 1999). The characterized limonoid glucosides are mono-glucosylated mono- or dicarboxylic acid derivatives of A- and D-ring limonoid aglycones.

Limonoids in citrus juices are recognized as one of the significant component of functional foods, due to their antioxidant and chemopreventive potential against a variety of diseases, particularly cardiovascular diseases (Parez et al. 2009; Manners et al. 2005; 2007) and their imperative role in cancer prevention, (differential proliferation inhibition of leukemia, ovary, stomach and liver) (Jayaprakasha et al. 2007; Guthri et al. 2002; Tian et al. 2001; Poulose et al. 2005). Single oxygen and nitrogen radicals (e.g., superoxide and peroxynitrite respectively) are considered to be responsible to cause chronic degenerative diseases including heart disease and cancer, by altering the cellular structure and function (Kinsella et al. 1993). Presence of antioxidant bioactive compounds (limonoids, flavonoids, carotenoids, polyphenols, furocoumarins, sterols, folate), a well described property of citrus fruits, has been shown to reduce the frequency of these diseases (Guthrie 2000; Jayaprakasha et al. 2007; Manners et al. 2007). Limonin, a bitter component of citrus juices plays an important role in the inhibition of malarial parasite, radical scavenging activity, chemically induced carcinogenesis in mice, hamsters and cultured human breast cancer cells, and induction of phase II enzymes (Ghosh et al. 2006; Sun et al. 2005; Lam et al. 1989). Due to the numerous health benefits of citrus limonoids, intense research has been directed to them.

Generally, the effortless way of limonoid intake is by drinking citrus juice and eating its fruit itself but bitterness caused by this limonoid hinders consumer's acceptability. Therefore, it has been desired to develop strategies to eliminate the delayed bitterness and to produce the acceptable quality of juice by retaining its chemopreventive and antioxidant properties (Puri et al. 1996).

2.2 Strategies for Debittering citrus juices

Ever since limonin was discovered for its contribution to delayed bitterness in citrus juices, a great deal of research effort has been directed toward understanding its anabolism, role during the transition from raw to ripened fruit and its catabolism for improving juice palatability. To reduce bitterness in citrus juices below a threshold level for consumer acceptability, a number of physicochemical and enzymatic treatments have been devised. The approaches to bitterness reduction in citrus products fall into three category: 1) preharvest treatments that inhibit the formation of limonoids in citrus fruits, 2) conversion of bitter limonoids into non-bitter metabolites, and 3) limonoid removal by adsorption on polymer resins. However, a majority of them are restricted to debittering grapefruit juice. In many instances, the methods are patented and their details are sketchy, being guarded commercial secrets of a particular fruit processing company.

2.2.1 Physicochemical Methods

Adsorptive Debittering

The employment of polyamides and a variety of adsorbents such as cellulose acetate, nylon-based matrices, porous polymers, and ion exchangers have proved to exhibit intense affinity for limonin and reduce bitterness in citrus juices (Chandler and Kefford, 1968; Griffith, 1969; Johnson and Chandler, 1988). Treatment of citrus juice with activated magnesium silicate (Florisil) in a batch mode significantly reduced limonin, naringin, narirutin, and total acids without adversely affecting its nutritional quality (vitamin C, sugars) (Barmore et al., 1986), and the flavor of the Florisil-treated juice was improved significantly. Application of ultrafiltration in tandem with adsorption efficiently removed limonin from grapefruit juice at a pilot-plant scale (Fernandez et al., 1992), where the efficiency of limonin removal was independent of temperatures between 13 and 48°C.

Chemical Methods

Earlier methods of debittering orange juice used lengthy extraction techniques and involved pH adjustment of the juice after extraction and immediately before consumption (Pritchet, 1957; Swisher, 1958). Treatments with ethylene (20 pg/ml) for 3 h to accelerate ripening (limonin catabolism) in navel oranges, lemons, and grapefruits with a concomitant reduction in bitterness have been reported (Maier et al., 1973). Application of carbon dioxide at pressures of 21 to 41 MPA at 30 to 60°C for 1 h resulted in an average removal of 25% of the limonin from navel orange juice an extension of the treatment to 4 h led to the removal of 60% of the limonin (Kimball, 1987).

Debittering by Passage Through Polystyrene-DVB Resins

In batch operations, cross-linked divinyl benzene- styrene resin reduced naringin and limonin content in grapefruit juice by 80 and 90%, respectively (Puri, 1984 Wethern, 1991); the resultant juice was less bitter. Laboratory studies on the effect of mean pore diameter, percent cross-linkage, and specific area of polystyrene DVB resins for the adsorption of limonin and naringin from grapefruit juice have been reported (Manlan et al., 1990).Two other resins, Amberlite XAD-16HP and Dowex Optipore L285 was shown to remove limonin bitterness from Washington naval orange juice up to a desired level and resulted; the treatment had no effect on the minerals, acid, and amino acids content of the juice (Kimball et al. 1990; Kola et al. 2009).

Debittering by β-Cyclodexfrin

Polymers such as soluble 0.5% β -cyclodextrin has been used to reduce 58% of the initial bitter taste of juice from grapefruit, Iyo orange, and *C. natsudaidai* (Konno et al., 1982). The reduced bitterness was due to formation of an inclusion complex between k-cyclodextrin and naringin or limonin. The ability of cylcodextrin was subsequently exploited led to utilization of a β-cyclodextrin polymer in a batch/continuous column mode to remove limonin and

naringin from their aqueous solutions, orange and grapefruit juices (Shaw and Wilson, 1983). The regeneration of the *β*-cyclodextrin polymer by extraction with an organic solvent enhanced its use for scale-up trials. Using a continuous flow fluid column, significant quantities of limonin, nomilin, and naringin from grapefruit juice as well as limonin and nomilin from navel orange juice were removed (Shaw et al., 1984). Sensorial analysis indicated consumer preference for such debittered juice (incidentally, with an improved flavor) compared with the control which led to a scaled-up application of *β*-cyclodextrin polymer on a pilot-scale fluidized bed column, enhancing the possibilities of using such a system for commercial operations (Wagner et al., 1988).

Limitations

The various inherent limitations of the physicochemical approaches used for debittering approaches described thus far are listed as: Compromised nutritional quality, texture, flavor, taste, color, or stability following debitterring. Methods are nonspecific and therefore inherently inefficient, introducing batch-to-batch variations due to undesirable or non monitorable changes along with the desirable ones. Debitterring methods were cumbersome, lacked reproducibility, and exhibited lower yields with partial loss of desired nutrients in the process of removing bitter components.

2.2.2 Microbial Studies

The limitations with the physiochemical methods warranted investigations for innovative technique(s) using microbial approaches to debitter the fruit juices. With the successful commercial applications of microbial biomass in various biotechnological processes, it appeared feasible and cost effective to develop comparable process(s) for fruit juice processing.

Potential microbial strains and their applications for debittering

Micro-organism and their enzymes have proven to be versatile biocatalysts and are extensively used for utilizations of various terpenoids. (Chatterjee & Bhattacharya 2001).

A large variety of enzymes occur in several micro-organisms which are effective in utilizations of various terpenoids and can be used in vivo. The microbial transformation processes have therefore been explored for terpenoids with a view to achieving desired conversions, optical resolutions of products, as well as understanding of the metabolic pathway for biodegradation of terpenoids. Although few, attempts have been made to employ candidate microbes or their enzymes in immobilized forms to metabolize limonin. Six species of bacteria, each capable of metabolizing limonoids, have been isolated from soil by enrichment using limonoate (A-and D-rings of limonin), 1 or 3-furoic acid as a single carbon source (Table 2.1). *C. fascians* is known for its constitutive enzymes for limonoid metabolism as compared to others.

Table 2.1 Microorganims and their pathways involved in limonin biotransformation

Microorganisms	Pathways/Enzymes	References
Arthrobacter globiformis	17-dehydrolimonoids	Hasegawa et.al. 1972
***Pseudomonas* 321-18**	Deoxylimonoids, 17-Dehydrolimonoids	Hasegawa et.al. 1972, 1974
***Bacterium* 342-152-1**	Deoxylimonoids, 17-Dehydrolimonoids	Hasegawa and Kim 1975
Acinetobactor sp	Deoxylimonoids,	Vaks and Liftsitz, 1981
Arthrobactor globiformis11	Deoxylimonoids, 7-Hydrolimonoids	Hasegawa et.al. 1983
Corynebacterium fascians	17-Dehydrolimonoids, trans-19-HBA	Hasegawa et al. 1983; 1985
Rhodococcus facians		Manjon et al. 1991; Martinez-madrid et al. 1989
Aspergillus niger	*Naringinase*	Goldstein et al. 1971; Gray and Olson, 1981
Penicillium	*Naringinase*	Tsen et al. 1991; Manjon et al. 1985; Jimeno et al. 1987

Microbial whole cells and their enzyme(s) provide several advantages over various physico-chemical methods involved in bioconversion of the bitter principle limonin, in the citrus juices (Puri et al., 2002; Canovas et al., 1998). Based on the metabolites and enzymes

produced by these species of bacteria, five metabolic pathways of limonoids have been established, these pathways whose de brief description follows below.

Metabolic potential of microorganisms

17-Dehydrolimonoid pathway

Limonoate dehydrogenases catalyzing limonoids to 17-dehydrolimonoids, have been isolated from *A. globiformis* (Hasegawa et al. 1972), *P.* 321-18 (Hasegawa et al. 1974), Bacterium 342-152-1 (Hasegawa et al. 1975) and C. *fascians* (Hasegawa et al. 1983). Although dehydrogenases of different organisms had identical functions, but they differed based on their characteristic features like pH optima, cofactor requirements, stability against heat, hydrogen ion concentrations, and molecular weights. The dehydrogenases attack most citrus limonoids with the exception of however deoxylimonin, deoxylimonate and deoxylimonol. Dehydrogenases play an important role in the development of a biological process that uses immobilized bacterial cells for limonoid debittering of citrus juices. Comparative studies in microorganisms and citrus have led to the identification of this metabolic pathways in citrus (Fig. 2.4).

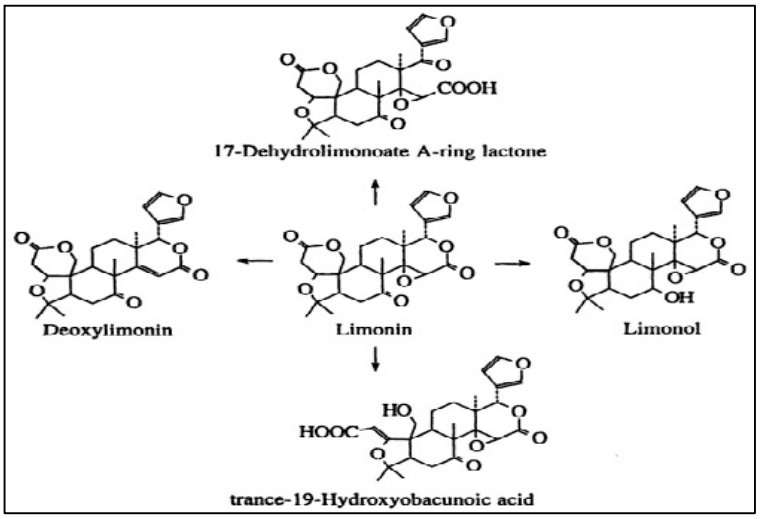

*Bacterial transformation of limonin

Fig. 2.4 Transformed products of limonin in citrus plants

Deoxylimonoid pathway

The isolation of deoxylimonin and deoxylimonate from limonoate growth media of Pseudomonas 321-18 led to the establishment of the deoxylimonoid pathway (Hasegawa et al. 1974; Hasegawa et al. 1995). Limonin epoxidase, which converts limonoids to deoxylimonoids along with deoxylimonin hydrolase, catalyzes the conversion of deoxylimonin to deoxylimonate by cell-free extracts of P. 321-18 and *Acinetobacter* (Vaks et al. 1981;Hasegawa et al. 1974). This enzyme catalyzes the addition of one molecule of water, but this hydrolysis is not simple since a C-C bond of the B-ring is cleaved and a double bond is shifted from the D-ring to the C-ring and requires sulfhydryl groups for its catalytic action. The presence of the deoxylimonoid pathway also has been demonstrated in citrus. The plant possesses limonin epoxidase activity (Hasegawa et al. 1982) as well as metabolites involved in the pathway such as deoxylimonin (Dreyer et al. 1965), deoxylimonate (Bennet et al. 1971) and deoxylimnol (Bennet et al. 1982).

7a-Hydroxylimonoid pathway

When citrus juice serum is passed through a column packed with *A. globiformis* II or C. *fascians* cells immobilized in acrylamide gel, the limonin present in the serum is exclusively converted to limonol (Hasegawa et al. 1983; Hasegawa et al. 1985). This conversion appears to be catalyzed by limonol dehydrogenase, observed in cell-free extracts of these organisms, but has not been isolated. The pathway is as important as the 17-dehydrolimonoid pathway for reduction of limonoid bitterness of citrus juices. However, the enzyme system involved in this pathway is less active and less effective than that of the 17-dehydrolimonoid pathway in converting bitter limonoids to nonbitter limonoids. The presence of deoxylimnol, 17-Dehydrolimonate A-ring lactone, limonoyl acetate and *7a.*obacunol (Bennett et al. 1982) in citrus suggests that this metabolic pathway is also operative in citrus.

Obacunone pathway

This pathway was first demonstrated in immobilized cells of *C. fascians* (Hasegawa et al. 1984) when grapefruit juice enriched with nomilin was passed through a column packed with *C. fascians* cells immobilized in acrylamide gel and nomilin was converted to obacunone. Later, nomilin acetyl-lyase isolated from cell-free extracts of this organism was characterized (Herman et al. 1985). Herman et al (1985) demonstrated that obacunone was further metabolized to obacunoate in C. *fascians* by obacunone A-ring lactone hydrolase.

Trans-19-Hydroxyobacunoate pathway

Trans-19-Hydroxyobacunoate was isolated from limonoate growth media of *C. fascians* (Hasegawa et al. 1983), apparently produced from limonoate by the action of a transeliminase (lyase). The activity of this enzyme was detected in cell-free extracts of the organism, but the enzyme has not been isolated. Thus far, there is no data available to suggest that this pathway operates in citrus. In the 17-dehydrolimonoid and deoxylimonoid pathways, the initial attack is on the D-ring of the limonoids, whereas in the trans-19-hydroxyobacunoate, nomilinate and obacunoate pathways the initial attack is on the A-ring. On the other hand, in the 7a-hydroxylimonoid pathway, the initial attack is on the B-ring.

Whole cell/enzyme immobilization

Performance of enzymes and whole cells in commercial applications can often be dramatically improved by immobilization of the biocatalysts, for instance by their covalent attachment to or adsorption on solid supports, entrapment, encapsulation and cross-linking (Gisby et al. 1987; Taghvaei et al. 2000). Immobilization of cells or enzymes helps in their economic reuse and development of continuous bioprocesses have been used in a variety of applications such as biotransformations, biosensors, production of ethanol, degradation of phenol etc (Phadtare et al. 2004; Cetinus et al. 2003). Immobilized biocatalysts - whole microbial cells (viable or non viable) or their enzymes have distinct benefits over employing

free cells in bioprocesses (Krasaekoopt et al., 2003; Plessas et al., 2005; Busto et al., 2006; Birgisson et al. 2007). Cell immobilization provides a physical incarceration or localization of microbial cells or enzymes to a certain defined space for the preservation of certain desired catalytic activity and subsequent continuous operation stability (Karel et al. 1985). Industrial application of immobilized enzymes has been limited due to several factors like low stability, low recovery, low yield and expensive steps involved in isolation and purification of enzymes. Therefore, whole cell immobilization has been employed and offers many advantages over immobilized or free enzymes and free microbial cells. This method is economical, offers continuous operational stability and carry out multi-step cofactor requiring bioconversion (Haiau et al. 1997; Babu & Panda 1991) with minimum downstream processing, decreased product inhibition, simplified biocatalyst recovery, high reusability of cells, relative ease of product separation, high volumetric productivity and reduced susceptibility of cells to contamination (Bernal, 2007).

Microbial cells and their enzymes (both in free form and immobilized forms) have been employed for the development of strategies for the eradication of bitterness from the citrus juices (Hasegawa et al. 1983; 1990; Manjon et al. 1991; Canovas et al. 1996). Inorder to overcome the difficulty related to inactivation of the microbial enzyme(s) due to the low pH of the citrus juices, entrapment of whole cells has been used for the bioconversion (Hasegawa et al., 1972; 1983; 85; Canovas et al., 1998). Previous studies reported the usage of various immobilizing matrixes (for immobilizing various limonin degrading microbes like *Rhodococcus fascians, Acinetobacter globiformis*, for debittering citrus juices) like dialysis, polyacryl amide gel, k-carrageenan and polyurethane foam. These methods have faced a number of constraints like limitations for human consumption, low stability matrix at low pH of juice and delayed reduction of bitterness in citrus juices (Vaks et al. 1981; Canovas et al. 1997). Whole bacterial cells are employed for citrus-juice debittering, as the enzymes are

protected from the external pH, and thus the problem related to the enzyme degradation, isolation, purification and low activity of immobilized enzymes are minimized (Hasegawa et al. 1983).

Immobilized cells of Arthrobacter globiformis

Microbial whole cells immobilized in acrylamide gel were used to debitter citrus juices. Cells of *A. globiformis* packed in acrylamide gel reduced 95% of the limonin (Hasegawa et al. 1982), with a reusability of the gel to 16 times before losing its effectiveness. Analyses of the treated serum showed that immobilized *A. globiformis* cells metabolized limonoids via 17-dehydrolimonoid pathway. Limonin was converted to nonbitter 17-dehydrolimonate A-ring lactone (Hasegawa et al. 1982; Hasegawa et al. 1983) catalysed by two enzymes, limonin D-ring lactone hydrolase and limonoate dehydrogenase in the presence of the cofactor NAD. The removal of bitter principle of Kinnow mandarin juice, were reported by raising pH, addition of sweetening agents, β-cyclodextrin - monomer for forming inclusion complexes of limonin, passing juice through adsorbent XAD-16 and by the action of immobilized bacteria (*Arthrobacter globiformis*) (Premi et al. 1995).

Immobilized cells of Arthrobacter globiformis II

Immobilized cells of *A. globiformis* II metabolize limonoids differently from those of *A. globiformis* when they are used in the bioreactor (Hasegawa et al. 1983) and converts limonin and nomilin to nonbitter limonol and nomilol, respectively, and reduced limonoid content to below the levels of the respective bitterness thresholds. However, a reactor operated using whole cells of *A. globiformis* II was less effective in reducing limonoid content of citrus juices, this is based on the fact that the 7a-hydroxylimonoid pathway is one of minor metabolic pathways present in the bacteria. The organism possesses much less limonol dehydrogenase activity, the enzyme responsible for this conversion, than limonoate dehydrogenase activity.

Immobilized cells of Corynebacterium fascians

C. fascians, isolated from soil by enrichment with 3-furoic acid as a single carbon source, produced constitutive enzymes for limonoid metabolism (Hasegawa et al. 1983; 1984). This differs from the other organisms mentioned, which require a limonoid inducer in their growth media to produce enzymes. Immobilized cells of *C. fascians* in acrylamide gel converted limonin to limnol in citrus juices, a process catalysed by limonol dehydrogenase, (Hasegawa et al. 1985). It is not clear why immobilized cells of C. *fascians* metabolize limonin via the minor metabolic pathway instead of the major pathway, limonin to 17-dehydrolimonate A-ring lactone. This appears to be the main explanation as to why the process with immobilized cells of C. *fascians* was less effective than that of *A. glohiformis* cells when applied in citrus juices for debitterring.

Immobilized cells of Acinetobacter and Pseudomonas 321-18

Debittering of citrus juice by *Acinetobacter* cells entrapped in a dialysis sac was demonstrated by placing the sac in the juice (Vaks et al. 1981) at an optimum pH of 6-7. Two non-bitter metabolites were isolated from the reaction mixture and identified as deoxylimonin and deoxylimonoic acid. A total of 120 mg of bacteria was found to convert 1L of bitter early season orange juice to drinkable juice (Vaks and Lifshitz, 1981). A pathway was proposed for debittering limonin by the bacteria: Limonin > Deoxylimonin > Deoxylimonic acid.

Immobilized cells of *Pseudomonas* 321-18 metabolize limonoate mainly through deoxylimonin by deoxylimonin hydrolase, isolated from cell-free extracts of the bacteria, which catalyses hydrolysis of deoxylimonin to form deoxylimonic acid and apparently attacks only the closed D ring of deoxylimonin (Hasegawa et.al. 1974b). The cell-free extracts also contained considerable amount of limonoate dehydrogenase activity, indicating the presence of another pathway involving 17-dehydrolimonoate. This enzyme was characterized as limonoate-NAD oxidoreductase (Hasegawa et.al. 1974).

Immobilized cells of Rhodococcus fascians

In Rhodococcus fascians, the limonin degrading enzymes are constitutive (Martinez-Madrid et.al. 1989) and the microorganism was entrapped in different matrices and evaluated. The gels were coated either with polyethylamine or cross linked with glutaraldehyde in lieu of coating. The coated system showed lower efficacy, doubtful stability, and unexpected diffusional limitations vis-a-vis the cross-linked system. *Rhodococcus fascians* cells entrapped in k-carrageenan and polyurethane have also been used for limonin degradation (Manjon et.al. 1991, Canovas et al. 1998). Their ability for continuous degradation of limonin as a function of pH showed optimal limonin degradation when pH was changed from 4.5 to 5. Recently, process parameters for the debittering of Kinnow mandarin juice by *R. facians* have been optimized by Marwaha et.al. (1994) and Puri et al. (2002).

Immobilized Aspergillus Naringinase

Naringinase from *Aspergillus niger* immobilized on copolymers of styrene, tannin aminohexylcellulose, on chitin with glutaraldehyde and sodium borohydride and maleic anhydride has been used to hydrolyze naringin (Goldstein et al. 1971; Ono et al. 1978; Tsen, 1984). But naringinase showed no visible adverse effect in a hollow-fiber reactor during the hydrolysis of naringin in unclarified grapefruit juice (Olson et al. 1979), and could be used for 4 h at 66% efficiency (Gray and Olson, 1981). The parameters (flow rates, hollow fiber membrane surface area, temperature, and enzyme loading) affecting naringin hydrolysis to prunin and naringenin were investigated in order to improve the debittering rate and quality of the processed juice.

Immobilized Penicillium Naringinase

Naringinase from *Penicillium* sp. entrapped in cellulose triacetate fiber (Tsen et al. 1989) showed higher K, values than its soluble form which hydrolyzed naringin and limonin when grapefruit juice was debittered without altering sugar components, total organic acids, and

turbidity levels remained unaltered (Tsen and Yu, 1991). In another case, a covalently linked naringinase from *Penicillium* sp. to glycophase-coated CPG was used for debittering naringin in fruit juices (Manjon et al. 1985), where its operational stability in a packed-bed reactor was tested with naringin as the substrate (Jimeno et al. 1987; Manjon et al. 1985). They found that the theoretically predicted results fitted well with the experimentally measured values.

Limitations

Although several different immobilized cells/enzyme systems have been operated, certain limitations of immobilization have come to the forefront. Techniques of immobilization perhaps occupy the same loci that are useful in the expression of enzyme activity; hence, the kinetics of debittering appeared disappointingly slow, a disqualification for scale-up purposes. This is one of the reasons that prompted us to opt for the use of free cells packed in a column in lieu of using immobilized cells (Puri, 1993). Due to the use of unclarified juice, the permeability of limonin and naringin or their limited solubility under operational conditions seemed to be affected. Pretreatment of juice with pectinase may alleviate this drawback partially. Inactivation of enzymes by particulate matter or their leaching appeared distinct in view of the milder entrapment conditions designed for an efficient enzyme system. These drawbacks limited the operational half-life, clogged columns, drops in pressure, etc. necessitating engineering inputs for rapid equilibrium and significant flow rates.

Cell permeability modification

Microbial whole cells play a significant role in the enzymatic biotransformation with recent advances in biotechnology. The efficiency of the microbial enzymes for the biotransformation is based on the location of the enzymes. A number of cell disruption processes has been employed for the availability of the intracellular enzymes for the desired enzymatic reactions. But such processes face a number of drawbacks as the leakage of all the intracellular constituents in the surroundings and purification of enzyme (Chisti et al., 1986).

In order to overcome such disadvantages the whole cells were employed for the enzymatic biotransformations. But the catalytic activity of the intracellular enzymes of the whole cells may be low as the cellular membrane is impermeable or partially permeable to the substrate or products to diffuse across the cell membrane (Siso et al., 1992). Permeabilization of whole cells therefore have emerged as a favourite option since it offers several advantages over cells disruption (Hewtter et al., 1986). Perforating the cellular membrane with efficient permeabilizing agents enhances the whole cell biocatalysis with high and stable enzyme activity. Permeabilization alters the permeability of the cellular membrane for the small molecules to cross freely and thereby preventing the cell lysis using various chemical and physical treatments (Naglak et al., 1990).

Molecular base of permeability limitations

The molecular frame of cellular wall of Gram negative bacteria is illustrated in Fig. 2.5 (Prescott et al. 2002). Gram-negative bacteria have two cell membranes, the outer membrane and inner membrane which consist of phospholipid bilayer decorated with over 200 different kinds of proteins. The structure of the outer membrane is

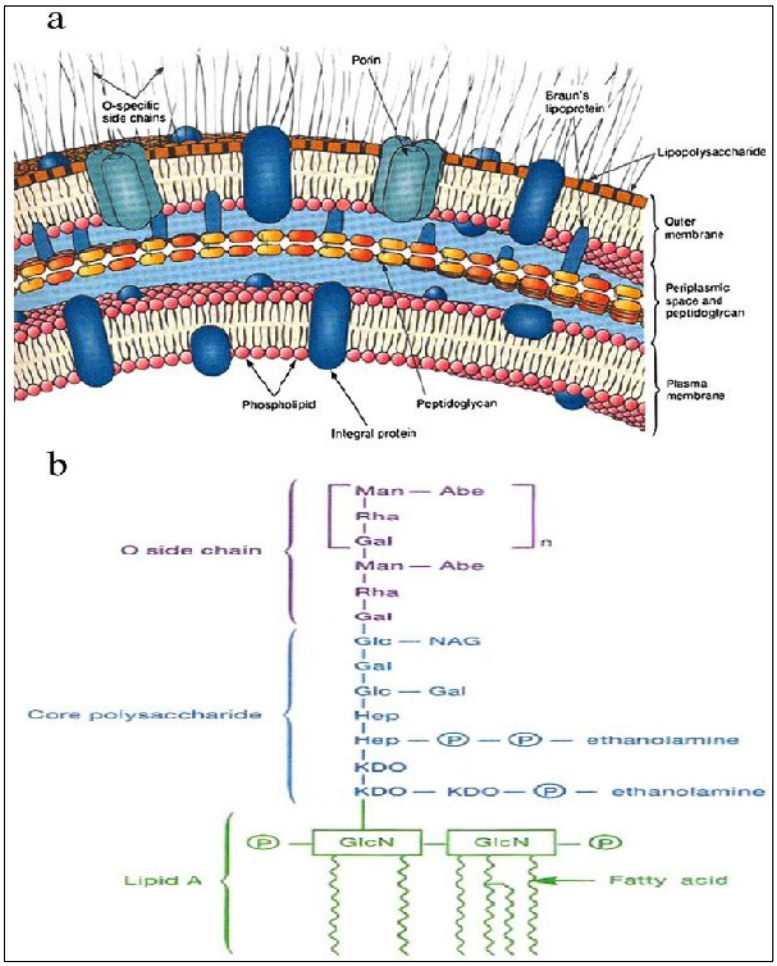

Fig. 2.5 (a) Gram-negative cell envelope. (b) Lipopolysaccharide structure (Prescott et al. 2002)

differs from the inner membrane with lipopolysaccharides (LPS) (Fig. 2.5a). Densely packed LPS limits the passage of hydrophobic and hydrophilic molecules due to its amphiphilicity and comprises of three components (Fig. 2.5b): lipophilic lipid A, an oligosaccharide core, and a long polysaccharides chain of a repeating unit commonly called O antigen. The hydrophilic nature of the polysaccharide component limits the penetration

of hydrophobic molecules as compared to the inner membrane, where it is relatively fast because of the lipophilic bilayer(Nikaido 1994). The transport of hydrophilic molecules relies on specific transport proteins that reside in the inner membrane (Neidhardt et al. 1990). The hydrophobic lipid A of LPS restricts hydrophilic compounds essential

to cell growth (such as sugars, amino acids, and ions), which rely on passive diffusion through special channels or porins (Fig. 1a) to cross the outer membrane barrier. LPS are non-covalently cross-linked and are held in position at the outer membrane surface by divalent cations such as Mg2+ and Ca2+, which exhibit a quasicrystalline structure and does not permit fast diffusion (Vaara 1993; Nikaido 1994). It was also reported that the peptidoglycan may play a role in the permeability of Gram-negative bacteria, either directly by forming a permeability barrier or indirectly by holding together the outer membrane (Burman et al. 1972). Hydrophilic molecules (smaller than 600Da) rely on nonspecific porins for entry and the bigger molecules are enter the cell through specific protein-based uptake systems, which is passive diffusion through the LPS layer. However, the rate of diffusion may vary due to its highly ordered quasicrystalline structure (Vaara and Nurminen 1999). For hydrophobic molecules, neither porins nor passive diffusion through LPS is a mechanism for their rapid uptake. In most biotechnological applications, the permeability issues are particularly important, as there is an intracellular consumption of substrate, which in most cases is the target to be maximized. For example, by overexpression of enzymes, the rate of reaction can be augmented by hundreds of times. The enhanced catalytic capability,

compounded by the factor that biocatalysis and bioremediation deal with many hydrophobic molecules, makes the permeability one of the most important limitation in these applications.

Permeabilization methods

The permeabilization reports specifies variable conditions for a given organism, substrate, or product varied widely. Several commonly used methods are illustrated as:

Solvent treatment

Permeabilization with variable solvents have proved to be quite promising as for *Saccharomyces cerevisiae* expressing glyoxalase and *Kluyveromyces lactis*, permeabilization with 40% ethanol and isopropyl alcohol remarkably increased the initial rate of whole-cell reaction by 380- and 580 fold, respectively, with an increase in its reusability (Liu et al. 1999; Lee et al. 2004). Solvent The use of 50% v/v and 10% (v/v) toluene for permeabilization of *S. cerevisiae* and *Zymomonas mobilis* respectively increased the whole-cell catalyzed reaction involving catalase by six fold (Silveira and Jonas 2002). Permeabilization of bacteria used much lower solvent concentrations as for example, only 5% v/v solvent (toluene, diethyl ether, chloroform) was used for permeabilizing *Pseudomonas rhodesiae* Fontanille and Larroche (2003). These variations in solvent concentrations reflect the differences in cell envelop between yeast and bacteria which are based on the nature of the solvent, concentration of the solvent, and time duration of the treatment are important parameters to optimize.

Detergent treatment

Detergent concentration, time duration of the treatment and cell density are three important parameters for optimizing an effective permeabilization. Among various permeabilization methods, detergent Triton X-100 was most effective method for *Pseudomonas pseusoalcaligene,* for the conversion of maleate to D-malic acid and for *Pichia anomala* to ameliorate the cellbound phytase activity to utilize the permeabilized cells in dephytinization

of soymilk (van der Werf et al. 1995; Upadhya et al. 2000; Kaur et al. 2009). Other detergent, such as cetyltrimethylammonium bromide (CTAB, 0.1% w/v) was found useful for permeabilizing *Z. mobilis* in sorbitol and gluconic acid production (Silveira and Jonas 2002), which was aimed for the release of the essential soluble cofactors necessary for the conversion of gluconic acid to ethanol so that ethanol production is minimized.

Salt concentration

Salt stress was used in a biocatalysis process to enhance the production of L (−) carnitine of *E. coli* cells in the presence of NaCl by two folds when increased the concentration of NaCl (from 40 to 80%) as compared with that of the control (Cavonas et al. 2003). Similar salt concentration induced permeabilization of the outer membrane of *Rhizobium leguminosarum* was observed for cyclic β-1,2-glucans in the presence of 0.2 M NaCl (Breedveld et al. 1992).

Electropermeabilization

Electopermeabilization had been used as a method for the release of secondary metabolite from living plant cells (Yang et al. 2003), when release of indole alkaloids and yohimbine from *Catharanthus roseus* in tubular membrane reactors was induced by applying low-level electric current (1–5 mA). And the permeabilization maintained high cell viability. A related method, pulsed electric field or electroporation was more commonly employed for macromolecule uptake or killing of microbes, may also be applicable for small molecule uptake by modification of conditions based to optimize electric field strength, energy input, pulse width, medium conductivity, pH, and cell growth phase (Muraji et al. 1999; Wouters et al. 2001).

Other physical and chemical methods

Using EDTA as a permeabilizer is also common which works by complexing divalent cations that are crucial in strengthening lateral LPS molecules, resulting in the weakening of its near-crystal structure. For biodiesel fuel production, recombinant *S. cerevisiae* expressing lipase

was permeabilized by air-drying at 42°C for 3 h for substrates (methanol and triglyceride) to cross cell membrane barriers (Matsumoto et al. 2001). Variation of susceptibility among different yeast strains was noted, highlighting the empirical nature of the process in deriving optimal protocol (Isoai et al. 2002). Reverse micelles of AOT/hexane/water were developed for selective release of periplasmically located recombinant penicillin acylase through outer membrane permeabilization (Bansal-Mutalik and Gaikar 2003). Maximum activity of glycolate oxidase was obtained from a recombinant *Pichia pastoris* by permeabilization with 0.1% benzalkonium chloride for 60 min at room temperature, which increased the intracellular glycolate oxidase activity by 10-fold with respect to untreated cells (Gough et al. 2001).

2.3 Response Surface Methodology (RSM) for optimization and modeling process parameters

Often biotechnology processes wish to find the conditions under which a certain process attains the optimal results. That is, they want to determine the levels of the design parameters at which the response reaches its optimum level. However, statistical methods provide an alternative methodology to optimize a particular process by considering the mutual interactions among the variables and to give an estimation of the combined effects of these variables on the final result (Lim et al. 2005). Of such methodologies, Response Surface Methodology (RSM) is a powerful statistical method based on the multivariate non-linear model and is useful for the evaluation and understanding the interactions of the various parameters affecting the process. This multivariate approach has advantages over the conventional methods in terms of maximum response in a bioprocess (Dwevedi & Kayastha, 2009; Lee et al., 2006; Potumarthi et al., 2008; Zhang et al., 2012).

Conventional methods are based on ‘one variable at time’ (OVAT) approach, which provides information regarding that variable alone. Furthermore, such methods suffer from disadvantages, such as being more time consuming, requiring large number of experiments,

being uneconomical, and most importantly, lacking the mutual interactions among the variables (Rathi et al. 2002; Kunamneni 2005). Response surface methodology (RSM) is a powerful tool and an efficient mathematical approach (Murthy et al. 2000; Xin et al. 2005) based on the fundamental principles of statistics, such as randomization, replication and duplication, which then simplifies the optimization by studying the mutual interactions among the variables over a range of values in a statistically valid manner widely applied in the optimization of fermentation and other bioprocesses (Chowdary et al. 2002; Xin et al. 2005; Chauhan et al. 2006).

Response surface methodology quantifies the relationship between the controllable input parameters and the obtained response surfaces (Raissi et al. 2009). At first some ideas are generated concerning which factors or variables are likely to be important in response surface study. It is usually called a screening experiment. The objective of factor screening is to reduce the list of candidate variables to a relatively few so that subsequent experiments will be more efficient and require fewer runs or tests. The purpose of this phase is the identification of the important independent variables.

Further, the main aim is to determine if the current settings of the independent variables result in a value of the response that is near the optimum. If the current settings or levels of the independent variables are not consistent with optimum performance, then the experimenter must determine a set of adjustments to the process variables that will move the process toward the optimum. This phase of RSM makes considerable use of the first-order model and an optimization technique called the method of steepest ascent.

This step begins when the process is near the optimum. At this point such a model is expected that will accurately approximate the true response function within a relatively small region around the optimum. Because the true response surface usually exhibits curvature near the optimum, a second-order model (or perhaps some higher-order polynomial) should be used.

Once an appropriate approximating model has been obtained, this model may be analyzed to determine the optimum conditions for the process. All variables are assumed to be measurable, the response surface can be expressed in the form of the second degree polynomial equation as:

$$Yi=\beta 0+\Sigma\beta iXi+\Sigma\beta iiX_i^2+\Sigma\beta ijXiXj,$$

Where Yi is the response variable, XiXj are input variables which influence the response variable Y; βo is the interception coefficient; βi is the ith linear coefficient; βii is the ith quadratic coefficient and βij is the ijth interaction coefficient.

The mathematical models were evaluated for each response by means of multiple linear regression analysis (Murthy et al. 2000; Gohel et al. 2005; Ratnam et al. 2005). Modeling was started with a quadratic model including linear, squared and interaction terms. The significant terms in the model were found by analysis of variance (ANOVA) for each response. Significance was judged by determining the probability level that the F-statistic calculated from the data is less than 5%. After model fitting was performed, residual analysis was conducted to validate the assumptions used in the ANOVA. This analysis included calculating case statistics to identify outliers and examining diagnostic plots such as normal probability plots and residual plots. Maximization and minimization of the polynomials thus fitted was usually performed by desirability function method, and mapping of the fitted responses was achieved using computer software such as Design Expert. Most applications of RSM are sequential in nature and can be carried out based on the following phases:

This sequential experimental process is usually performed within some region of the independent variable space called the operability region or experimentation region or region of interest.

Response Surface Methodology (RSM) was used for modeling limonin bioconversion in raw and sterilized orange juices by *Acinetobacter calcoaceticus* by optimizing reaction

conditions, as a function of temperature (23–37°C) and limonin content (8–16 ppm). In raw orange juice, after 7 h reaction time, the amount of converted limonin, increased upto 33% with temperature and low intial limonin level (11 mg l^{-1}) (Ribeiro et al. 2003). Investigations were carried out to investigate the optimum conditions for the efficient conversion of kinnow juice into wine using response surface methodology. The maximum levels of wine (11%) were established when the optimum parameters were 26° Brix total soluble solid concentrations, 5.4 pH, 29°C temperature and innoculum size of 7.5% and incubation period of 5 days (Panesar 2009). In an attempt to debitter the citrus juices, the maximum enzymatic hydrolysis of naringin with immobilized naringinase was studied by optimizing the significant parameters – pressure and temperature, by response surface methodology. A maximum 81% of naringin conversion was observed experimentally under the optimum levels (Riberio et al. 2010). The cells of *P. anomala* were subjected to permeabilization using the surfactant Triton X-100 to overcome the permeability barrier and prepare whole cell biocatalysts with high phytase activity. The statistical approach, response surface methodology (RSM) was used to optimize the conditions for permeabilization inorder to optimize the levels of significant parameters for an enhanced phytase activity. The treatment of cells with 5% Triton X-100 for 30 min resulted in 15% enhancement in cell-bound phytase activity (Kaur et al. 2009). The industrial applications of enzymatic hydrolysis processes are being hampered, due to intracellular location of the yeast enzyme, which makes its extraction difficult and expensive. However, the problem of enzyme extraction and poor permeability of cell membrane to lactose can be overcome using permeabilization technique which was further optimized by employing Response surface methodology to investigate the effect of different parameters (concentration, temperature and treatment time) on the permeabilization of *Kluyveromyces marxianus* cells.

However, observing the imperative role of response surface methodology in various biotechnological processes, the technique was employed for the optimization of various parameters during the present work.

2.4 *Pseudomonas putida* G7 and Plasmid mediated metabolism of aromatic compounds

Pseudomonas putida is one of the best studied species of the metabolically versatile and ubiquitous genus of the Pseudomonads, whose versatility and genetic plasticity have enabled their survival in a broad range of environments (Timmis et al. 2001; dos Santos et al. 2004; Moore et al. 2006). The fact that *P. putida* possesses such an arsenal of degradative functions presumably reflects it's extensive spectrum of housekeeping catabolic pathways and enzymes, it's tendency to freely acquire, plasmids from other bacteria and it's relaxed-specificity gene expression system, allowing the expression of genes derived from wide variety of different bacteria.

Whole genome analysis of *P. putida* revealed a wealth of genetic determinants that play a role in biocatalysis, such as those for the hyper-production of polymers (such as polyhydroxyalkanoates (Steinbuchel et al. 2001; Huijberts et al. 1996) and industrially relevant enzymes, the production of epoxides, substituted catechols, enantiopure alcohols, and heterocyclic compounds (Wackett et al. 2003; Schmid et al. 2001). These features, along with their renowned stress resistance, amenability for genetic manipulation and suitability as a host for heterologous expression, make *Pseudomonas putida* particularly attractive for biocatalysis. As a species, it exhibits a wide biotechnological potential, with numerous strains (some of which solvent-tolerant) (Mosqueda et al. 1999; de Bont et al. 1998) able to efficiently degrade toxic compounds or to efficiently produce high value compounds and are therefore of interest for both bioremediation and bulk chemical production.

Plasmids play a very pivotal role in characterizing Pseudomonads, as a nutritional opportunist par excellence and a paradigm of metabolically versatile microorganism and is responsible

for its degradative abilities for aromatic compounds (Foght & Westlake, 1996; Kiyohara et al. 1994; Johnsen et al. 1996; Obayori et. al. 2010) (Fig. 2.6). The genes that code for the enzymes of the degradative pathways for these compounds are sometimes located in the chromosomal DNA, although they are very often found on large (>50 kb) plasmids. Many examples of self-transmissible plasmids that carry genes for degradation of aromatic compounds are known (Table 2.2) and their role in spreading these genes to other microorganisms conferring new degradative potential has been clearly demonstrated (van der Meer et al. 1992; Johnsen et al., 2005).

A plasmid may encode a complete degradative pathway or partial degradative step. Some other plasmids code for enzymes that have specificity for several substrates. One of the features of the *Pseudomonas* peripheral metabolism is the broad substrate specificity of the enzymes involved in the primary attack on xenobiotics, i.e., the enzymes are not only capable of converting their substrate, but also its structural analogs and sometimes even compounds with a different structure. For example, the genes encoding the upper and lower pathways of naphthalene in the NAH plasmids of several Pseudomonads have broad specificities, allowing the host to grow on several two and three - ring PAHs, as sole carbon and energy sources (Foght and Westlake, 1996). This broad substrate specificity of enzymes is a characteristic of several other enzymes and wide bread

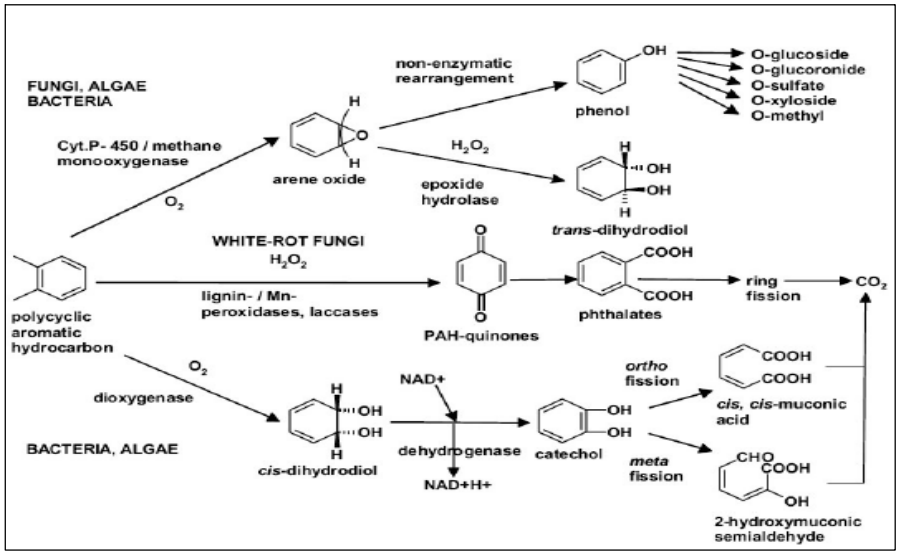

Fig. 2.6 Pathways of microbial degradation of polycyclic aromatic hydrocarbon
(Source: Obayori and Salam, 2010)

among several different degradative pathways. This fact allows these microorganisms to channel a wide range of foreign compounds into their metabolism (Golovleva et al. 1992).

Table 2.2 Degradative plasmids identified in *Pseudomonas* strains

Plasmid	Size(kb)	Conjugative	Substrates	References
TOL	117	+	Xylenes, toluene, toulate	Bayley et al. 1979; Lehrbach et al. 1982
NAH7	83	+	Naphthalene via salicilate	Bayley et al. 1979; Lehrbach et al. 1983
pWW60-1	87	+	Naphthalene via salicilate	Cane & Williams, 1982
SAL1	85	+	Salicilate	Bayley et al. 1979; Lehrbach et al. 1983
pKF1	82	-	Biphenyls via benzoate	Furukawa & Chakrabarty, 1982
pWW100	200	ND	Methylbiphenyls via toluates	Llyod-Jones et al., 1994
pCITI	100	ND	Aniline	Anson & Mackinnon, 1984
pRE4	105	ND	Isoproplybenzene	Eaton & Timmis, 1986
pWW174	200	+	Benzene	Winstanley et al. 1987
pEST100	544	ND	Phenol	Kivisaar et al., 1990
pVI150	Mega	+	Phenol, cresols, 3,4-dimethylphenol	Shingler et al., 1989
pAC25	117	+	3-Chlorobenzoate	Chatterjee et al., 1981
pJP4	77	+	3-Chlorobenzoate, 2,4-D	Don & Pemberton, 1981
pRC10	45	ND	1,2,4-Trichlorobenzene	Chaudhary & Huang, 1988
pMAB1	90	ND	2,4-D	Bhat et al. 1994

*ND, not determined

Degradative NAH plasmid encoding naphthalene degradation

The association of plasmids with the degradation of naphthalene by bacteria has been well reported (Dunn and Gunsalus 1973; Yen and Serdar 1988). *Pseudomonas putida* PpG7 was characterized for the presence of a naphthalene degrading NAH plasmid (Austen et al. 1980). All the genes for the initial step in the oxidation of the naphthalene were localized on the NAH plasmid in *Pseudomonas* PpG7 (Table 2.3). The plasmid was transmissible coded for naphthalene degradation via salicyclate and catechol, then, by the catechol meta cleavage pathway (Fig. 1). Enzymes for the meta-cleavage of catechol were found to be constitutive and the enzymes involved in the conversion of naphthalene to catechol were found to be inducible during growth on salicyclate. Thus, it was concluded that genes encoding the enzymes of the first 11 steps of the naphthalene oxidation pathway were located on the NAH7 plasmid but belonged to two separate operons i.e. nah and sal (Austen et al. 1980; Yen & Gunsalus 1982). The first operon includes genes nahABCDEF, coding for the conversion

of naphthalene to salicylate, and the second operon includes genes nahGHIJK, coding for the oxidation of salicylate via the catechol meta-cleavage pathway. Yen and Gunsalus (1985) further confirmed that the two catabolic operons in NAH7 are controlled by a positive regulator gene, nahR, that is located immediately upstream of the nahG gene.

Table 2.3 Genes harbored by NAH7 plasmid with respective enzymes in *P. putida*

Substrate	Gene	Encoded protein or function
Naphthalene (upper pathway)	nahAa	Reductase
	nahAb	Ferredoxin
	nahAc	Iron sulfur protein large subunit
	nahAd	Iron sulfur protein small submit
	nahB	cis-Napthalene dihydrodiol dehydrogenase
	nahF	salicyaldehyde dehydrogenase
	nahC	1,2-Dihydroxynaphthalene oxygenase
	nahE	2-Hydroxybenzalpyruvate aldolase
	nahD	2-Hydroxychromene-2-carboxylate isomerase
Salicylate (lower pathway)	nahG	Salicylate hydroxylase
	nahT	Chloroplast-type ferredoxin
	nahH	Catechol oxygenase
	nahI	2-Hydroxymuconic semialdehyde dehydrogenase
	nahN	2-Hydroxymuconic semialdehyde dehydrogenase
	nahL	2-Oxo-4-pentenoate hydratase
	nahO	4-Hydroxy-2-oxovalerate aldolase
	nahM	Acetaldehyde dehydrogenase
	nahK	4-Oxalocrotonate decarboxylase
	nahJ	2-Hydroxymuconate tautomerase
Regulator for both operons	nahR	Induced by salicyylate

NAH genes are highly versatile

The naphthalene degrading enzymes encoded by the NAH7 genes is known today to be a highly versatile enzyme system, encoding a wide range of reactions (Ensley et al., 1983; Parales et al., 2002) and belongs to the IncP-9 incompatibility group. It is one of the three completely sequenced IncP-9 plasmids alongside pWWO (Williams and Murray, 1974) and pDTG1 (Kurkela et al., 1988). The plasmids in this group are mainly large self-transmissible plasmids, associated with degradation, and antibiotic and toxic metal resistance markers. The first evidence of the versatility of the NAH plasmid encoded genes was provided independently by two research groups (Sanseverino et al., 1993). This led Sanseverino et al.

(1993) to conclude that maintaining and monitoring one catabolic bacterial population may be sufficient for degradation of a significant fraction of PAHs in contaminated soil. Kiyohara and Nagao (1978) had proposed that enzymes other than NahA catalysed dioxygenation in phenanthrene metabolism but findings by Sanseverino et al. (1993) confirmed that the enzymes were indeed NahA and were borne on NAH7- like plasmid. Menn et al. (1993) produced the first report which provides direct biochemical evidence that the naphthalene plasmid degradative enzyme system is involved in the degradation of higher-molecular-weight polycyclic aromatic hydrocarbons other than naphthalene. Plasmids that encode the degradation of naphthalene have also been found to be involved in the pathways of dibenzothiophene transformation, and it has been suggested that all the dibenzothiophene plasmids were actually naphthalene plasmids which are closely related to NAH7 (Eaton, 1994). Denome et al. (1993) completely sequenced the Dox genes in *Pseudomonas* strain C18 and showed that the same genes are responsible for the upper pathway of naphthalene degradation. The genes were found to be on a 75-kb plasmid doxABDFGHIJ. The authors concluded, therefore, that a single genetic pathway controls the metabolism of dibenzothiophene, naphthalene and phenanthrene in strain C18. At about the same time, Simon et al. (1993) reported that the DNA sequence for genes of nah (nahAb, nahAc and nahAd) were namely identical with the doxABD genes. The genes encoded the entire upper pathway of naphthalene and phenanthrene degradation. The gene nahY which code for the membrane protein that is a chemoreceptor for naphthalene or naphthalene metabolite is encoded by the NAH7 plasmid of *P. putida* G7 (Grimm and Harwood, 1997, 1999). Thus, the versatility of NAH plasmid (present in *P. putida* G7) for the degradation of structurally similar polycyclic aromatic compounds provoked the exploitation of triterpenoids by the organism.

2.5 Approaches for genetic characterization

Since the advent of bacterial genome sequencing, a great many molecular genetic manipulation tools have been developed and improved, via the application of genetic events that occur naturally in prokaryotes, in order to characterize the genes and their functions in a variety of environments (Azzolina et al. 2001; Reznikoff 2008; Bourhy et al. 2005; Albano et al. 1992). The study of any microorganism's functional properties can be greatly enhanced by the generation of mutations in genes of interest. Creation of mutations and subsequent genetic mapping can elucidate the identity, location, relative size, number, organization of genes and transcriptional units involved in a physiological process. In more sophisticated approaches, site-specific mutation of a gene can help to reveal the relationship of the structure of a protein to its function (Lorenzo et al. 1989; Jackman et al. 2001). Mutagenizing microorganisms is important, interesting, and potentially profitable in the most general term, mutation of a gene or genes under study can be achieved by first altering the DNA of the microorganism in some fashion and then screening or selecting for the desired phenotype.

General methods for microbial mutagenesis

The different sources to mutagens used for bacteria mutagenesis are:

Electromagnetic radiation

Mutation by electromagnetic radiation involves exposing the microbe to high energy electromagnetic waves (X-rays or more commonly UV light). This procedure damages the target DNA and sometimes, during repair, an improper base pair (or pairs) is incorporated in the DNA, causing a mutation.

Chemical mutagens

Chemical mutagens are also employed when added to a growing culture of an organism for a given time period and interfere with the replication of the DNA. Some mutagens achieve this by serving as base analogs eg. 5-bromo-deoxyuridine (5BU), others chemically modify the

DNA eg. alkylators include ethyl methane sulfonate (EMS), methyl methane sulfonate (MMS), diethylsulfate (DES), and nitrosoguanidine (NTG, NG, MNNG), and yet another class can insert or intercalate in between the base pairs of DNA causing DNA polymerase to make mistakes. In all cases, the mutagen causes incorrect copying of the DNA resulting in base substitutions (exchange of one base pair for another), insertions (addition of one or more base pairs), or deletions (removal of one or more base pairs).

Transposon Mutagenesis

Transposons are mobile genetic elements that can relocate from one genomic location to another. As well as modulating gene expression and contributing to genome plasticity and evolution, transposons are remarkably diverse molecular tools for both whole-genome and single-gene studies in bacteria, yeast, and other microorganisms. Transposon-based signature tagged mutagenesis and genetic foot printing strategies have pinpointed essential genes and has reaffirmed the usefulness of these elements as simple yet highly effective mutagens for both functional genomics and proteomic studies of microorganisms (Hayer 2003). The movement of transposable elements is highly regulated and can profoundly influence gene expression, as Barbara McClintock observed in the 1940s and 1950s during her discovery of transposition in maize (Comfort 2001). In the 1960s and 1970s, transposable elements were isolated in bacteria whose amenability to genetic manipulation facilitated both detailed molecular studies of the transposition process as well as the development of transposons as molecular tools. In bacteria, transposons were widely employed as random insertion mutagens both at a genomic level and in the analysis of the organization of individual genes.

Transposon mutagenesis has several advantages over the use of other methods of mutation. Firstly, chemicals and ionizing radiations techniques are very risky to handle and extreme caution as compared to transposons. Secondly, transposons used to mutate bacteria have selectable phenotypes, (usually drug resistances), which can be easily isolated followed by

screening this subset of microorganisms for the desired characteristic or deficiency. Also, since transposition happens at a frequency of 10^{-4} to 10^{-7}, thus eliminates the vast majority of un mutated organisms and cause very clean mutations.

Bacteria-derived transposons include various transposons [Tn(s)] such as Tn3, Tn5, modified Tn7, Tn10, Tn552, and so on. Among them, Tn5-based random mutagenesis was utilized in a vast variety of bacterial organisms for the identification of functional genes (Colegio et al. 2001; Das et al. 1998; Hamer et al. 2001; Hayes 2000; Maekawa et al. 1996; Manoil 2000; Mei et al. 1997; Perkins et al. 1986; Polard et al. 1996). Very recently, it was proposed that a minimal genome of *E. coli* required only for survival could be created by using the Tn5 system (Reznikoff et al. 2003).

Transposon organization and mobility

Transposable elements in bacteria range from simple insertion sequence (IS) elements that consist of a gene(s) for transposition bounded by inverted repeat sequences, to composite transposons composed of a pair of IS elements that bracket additional genetic information for antibiotic resistance or other properties, to more complex conjugative transposons that exhibit hybrid properties of transposons, plasmids, and bacteriophages (Hayes 2003). The transposons most favored as genetic tools are those that insert randomly or near-randomly, or can be manipulated to behave in this way, as is the case with the transposons discussed briefly here. Tn*5* was one of the first transposons to be identified (Berg et al. 1989; Bhasin et al. 2000) and is a composite transposon that consists of two inversely oriented copies of the IS*50* element that are separated by genes specifying resistance to kanamycin, bleomycin, and streptomycin (Fig 2.7).

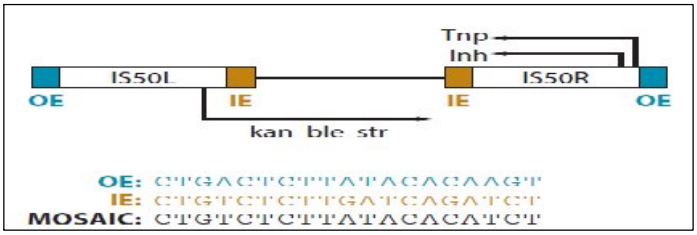

Fig. 2.7 Model structure of Tn5 Transposon

Overlapping genes on IS*50*R produce a transposase (Tnp) that is responsible, along with regulatory host factors, for the movement of Tn*5* between genomic locations, and a truncated version of Tnp that post translationally down regulates Tnp activity. Each IS*50* element harbors 19-bp repeat sequences at its termini with which Tnp interacts. Tn*5* transposition occurs through a "cut and paste" mechanism in which the transposon is precisely excised from its original location in the donor DNA and then is inserted into a target sequence (Berg 1989; Reznikoff 2003). The molecular mechanism of Tn*5* transposition is explained in Fig. 2.8.

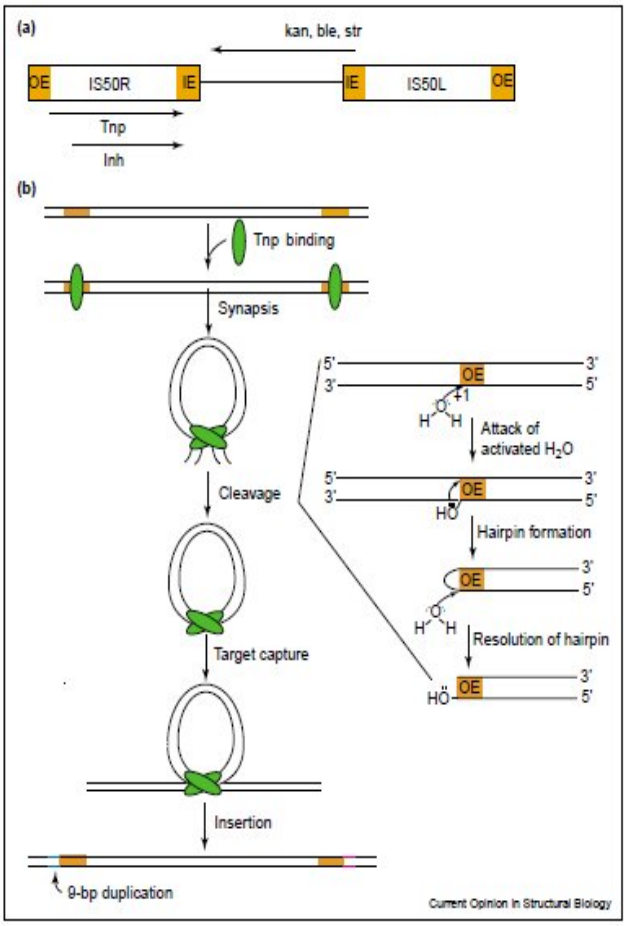

Fig. 2.8 Mechanism of Tn*5* transposition (Reznikoff , 2008)

Gene sequencing with transposons

The inherent ability of transposons to insert into novel DNA sites makes them ideal sources of portable priming sites for nucleotide sequence determination of uncharacterized regions. Using sequencing primers that anneal near the end(s) of the transposon, a collection of random transposon insertions into a cloned DNA fragment of interest can be used to generate a set of overlapping sequence contigs that can be assembled into the entire sequence of the fragment (Liu 1987; Butterfield et al. 2002; Griffin 1999). This method has been extended to sequence analysis of cDNA libraries (Shevchenko et al. 2002) and potentially is of special use in the analysis of regions whose sequences might otherwise be technically difficult to decipher (Devine et al. 1994).

A number of transposable elements, including Tn*3*, Tn*5*, and Mu, have been successfully developed as sequencing tools. Recently, sequencing reactions with transposon-specific primers have been used to localize transposon insertion sites directly in genomic DNA of yeast and bacteria without a requirement for prior cloning or amplification of the transposon-target junction region (Hoffman et al. 2000; Horecka et al. 2000). This strategy, although not yet in widespread application, has the potential to accelerate considerably the characterization of transposon disruptions in genes of interest that have been identified by signature-tagged mutagenesis or genetic footprinting. Thus, although high-throughput sequencing strategies that allow the rapid and precise sequencing of whole genomes have been developed in recent years (Green, 2001), transposon-mediated approaches to nucleotide sequencing remain highly relevant.

Chapter 3

Materials & Methods

4.1 Physiological insights for limonin utilization by *Pseudomonas putida* G7

4.1.1 Metabolic fingerprint for carbon source(s)

Members of Pseudomonas species have been ascribed to possess the capability of utilizing a wide gamut of carbon sources. Thus, a profile of carbon utilization is helpful in elucidating the metabolic versatility of the members. Fig. 4.1 shows a differential utilization profile of variable carbon sources in microtitre plate with TTC. The differential intensity of the color signified the bacterial growth with respect to the carbon source utilized. The *P. putida* G7 tested on 95 different carbon sources utilized 82 of the carbon sources, suggesting its metabolic robustness. The high specific growth rate of 0.62 h^{-1} was observed for glucose as carbon source (Fig. 4.2). The ability of *P. putida* G7 cells to utilize limonin as sole carbon source was demonstrated by an increase in cell density and a proportionate reduction of limonin from the medium; approximately 54% of limonin was metabolized by *P. putida* G7 in 48 h, appreciable limonin was utilized during the log phase of growth. The cells exhibited a lag time of approximately 1 h and exhibited a growth rate (μ) of 0.43 h^{-1} suggesting a slow utilization of the triterpenoid.

Both acetonitrile and chloroform, which have been commonly used in earlier studies, were examined for their effect on the growth of *P. putida* G7. Amongst acetonitrile (2%) and chloroform (1.5%), acetontrile supported cell viability to a tune of 98%. Attempts to make the cells more adaptable to organic solvent and thus increased limonin utilization were successful. In cells precultivated in acetonitrile the lag phase was shortened notably as compared to freshly inoculated cells and exhibited a higher growth rate of 0.43 h^{-1} in comparison to the untreated cells (growth rate of 0.25 h^{-1}).

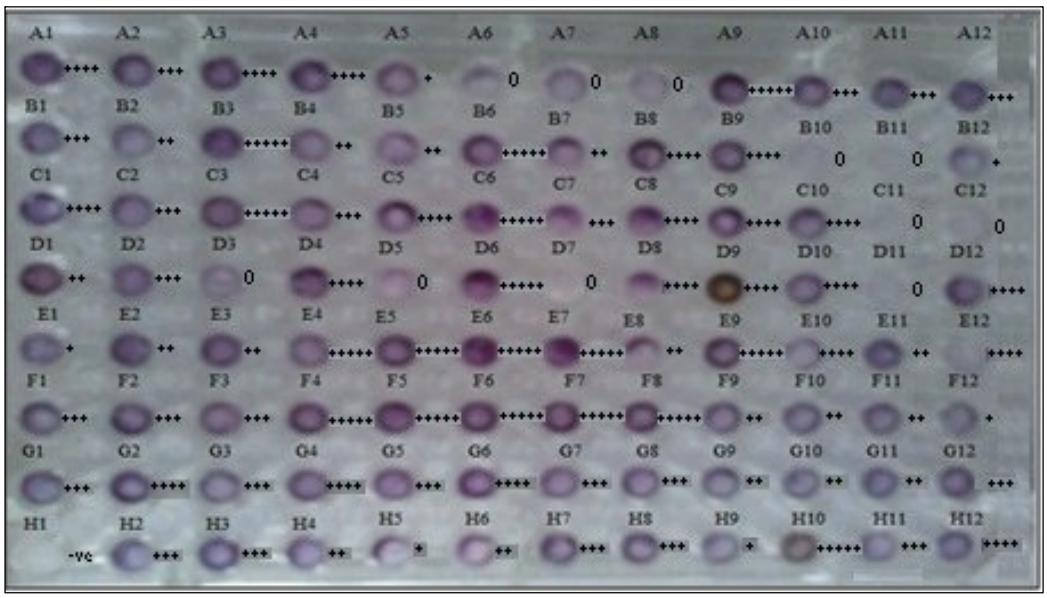

Fig. 4.1 Different carbon source(s) utilization profile of *P. putida* G7

(A1-Water, A2-α-Cyclodextrin, A3-Dextrin, A4-Glycogen, A5-Tween 40, **A6-Tween 80, A7-N-Acetyl-D-Galactosamine, A8-N-Acetyl-D-Glucosamine,** A9-Adonitol, A10-L-Arabinose, A11-D-Arabitol, A12-D-Cellobiose, B1-i-Erythritol, B2-D-Fucose, B3-L-Fructose, B4-D-Galactose, B5-Gentiobiose, B6-α-D-Glucose, B7-m-Inositol, B8-α-D-Lactose, B9-Lactulose, **B10-Maltose, B11- D-Mannitol,** B12- D-Mannose, C1- D-Melibiose, C2-β-Methyl-D-Glucoside, C3- D-Psicose, C4-D-Raffinose, C5-L-Rhamnose, C6-D-Sorbitol, C7-Sucrose, fdC8-D-Trehalose, C9-Turanose, C10-Xylitol**, C11-Pyruvic Acid Methyl Ester, C12-Succinic Acid Mono-Methyl-Ester**, D1-Acetic Acid, D2-Cis-Aconitic Acid, **D3-Citric Acid,** D4-Formic Acid, **D5-D-Galactonic Acid Lactone,** D6-D-Galacturonic Acid**, D7-D-Gluconic Acid,** D8-D-Glucosaminic Acid, D9-D-Glucuronic Acid, D10-α-Hydroxybutyric Acid, **D11-β-Hydroxybutyric Acid,** D12-γ-Hydroxybutyric Acid, E1-p-Hydroxy Phenylacetic Acid, E2-Itaconic Acid, E3-α-Keto Butyric Acid, E4- α-Keto Glutaric Acid, E5-α-Keto Valeric Acid, E6-D,L-Lactic Acid, E7-Malonic Acid, E8- Propionic Acid, E9-Quinic Acid, E10-D-Saccharic Acid, E11-Sebacic Acid, E12-Succinic Acid, F1-Bromosuccinic Acid, F2-Succinamic Acid, F3-Glucuronamide, F4-L-Alaninamide, F5-D-Alanine, F6-L-Alanine, F7-L-Alanylglycine, F8-L-Asparagine, F9-L-Aspartic Acid, F10-L-Glutamic Acid, F11-Glycyl-LAspartic Acid, F12-Glycyl-LGlutamic Acid, G1-L-Histidine, G2-Hydroxy-LProline, G3-L-Leucine, G4- L-Ornithine, G5- L Phenylalanine, G6-L-Proline, G7-L-Pyroglutamic Acid, G8-D-Serine, G9-L-Serine, G10-L-Threonine, G11-D,L-Carnitine, G12-γ-Amino Butyric Acid, **H1-Urocanic Acid,** H2-Inosine, H3-Uridine, H4-Thymidine, H5-Phenyethylamine, H6- Putrescine, H7-2-Aminoethanol, H8-2,3-Butanediol, H9-Glycerol, H10-D,L-α-Glycerol Phosphate, H11-α-D-Glucose-1-Phosphate, H12-D-Glucose-6-Phosphate)

*Differential growth score for variable carbon sources ([a] -vc = negative control ; +vc = positive control ; +++++ = excellent growth in glucose (standard),++++ = very good growth; +++ = average growth; ++ = less growth; + = poor growth; 0 = no growth

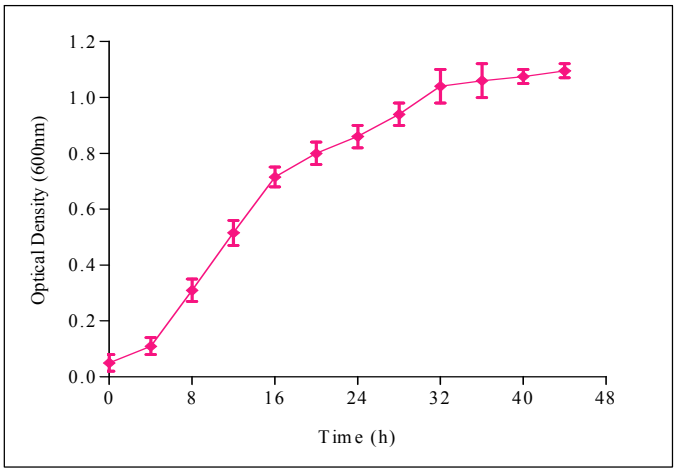

Fig. 4.2 Growth kinetics of *P. putida* G7 for utilizing glucose

4.1.2 Effect of Limonin concentration

Few if any earlier studies have examined the effect of limonin concentrations on growth of microorganisms; this is important for understanding both the tolerance and utilization at different concentrations. It was deemed necessary to examine a range of limonin concentrations on cell growth and subsequent utilization. A concentration of 50 µg/ml of limonin indicated adequacy in terms of growth rate of 0.43 h^{-1} and reduction in limonin level within 36 h; higher limonin concentrations were not favorable for cell growth as well as limonin utilization (Fig. 4.3). The residual limonin levels were estimated by HPLC. The chromatograms revealed the substrate retention time to be 9.3 minutes; a reduction in peak following utilization by the *P. putida* G7 cells was observed. The limonin was utilized and converted to metabolites which appeared as two new peaks at retention times of 15.9 and 25.2 minutes (Fig. 4.4) respectively. The limonin levels were reduced to a peak area of 46.4% this corresponded to reduction of initial levels of limonin by 55.2%.

4.1.3 Effect of pH

The effect of pH range 5.0 - 9.0 on the growth and limonin utilization of *P. putida* was determined. Optimal pH was considered the one which afforded maximum bacterial growth and limonin utilization in 48h (Fig. 4.5). Low pH impeded growth and limonin utilization. Significant reduction in limonin levels was however observed in the pH range of 7 to 9; the cells exhibited a maximum growth rate of 0.40 h^{-1} when the initial pH was adjusted to 8. The *P. putida* strain lacked both growth and limonin utilization at pH values above 8.

4.1.4 Effect of Temperature

Temperature is a prerequisite for growth and thus important for conferring optimal metabolism to bacterial cells. To determine the influence of temperature on the growth and limonin metabolism, growth and limonin levels were monitored over a temperature

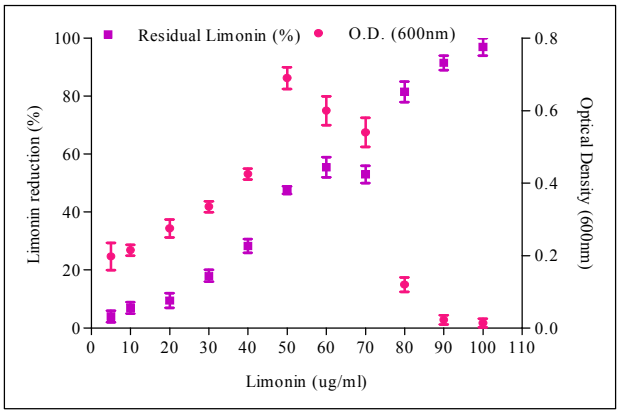

Fig. 4.3 Effect of limonin concentration

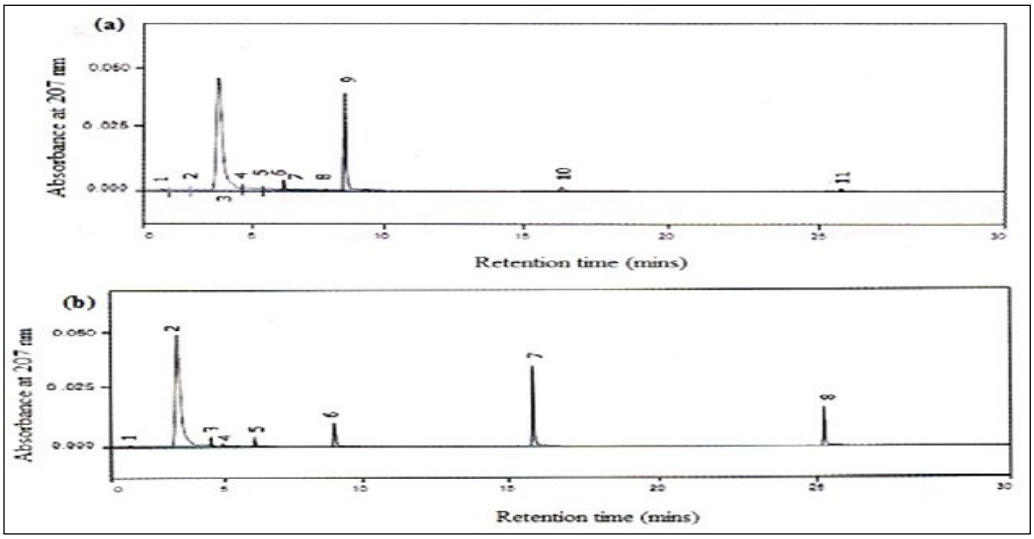

Fig. 4.4 (a) HPLC chromatograms of standard limonin (50µg/ml) and (b) chromatograms of standard limonin (90µg/ml) utilized by *P. putida* G7, using an acetonitrile/deionised water (32:68) with a flow rate 0.9 ml/min and an injection volume of 20 µl

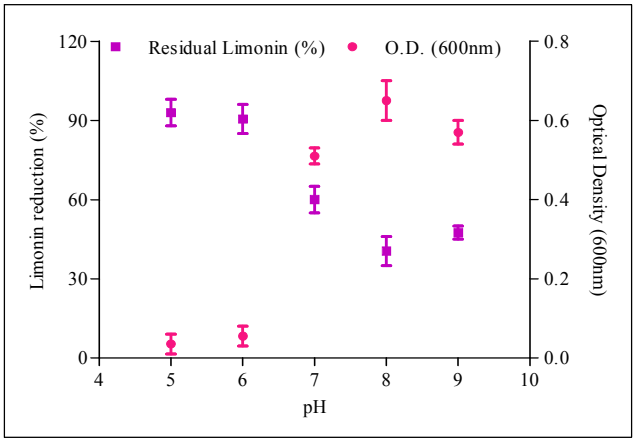

Fig. 4.5 Effect of pH on growth and limonin utilization ability of *P.putida G7*

range 20^{O}C- 35^{O}C (Fig. 4.6). Maximal growth was observed at 30^{O}C, at lower and high temperatures, the *P.putida* G7 cells lacked appreciable growth. Limonin utilized could be correlated to these observations.

4.1.5 Effect of Agitation

Agitation regulates the oxygen concentration and helps uniform exposure of bacterial cells to medium nutrients. However higher agitation speeds may mechanically damage cellular integrity, therefore it was desirable to optimize the most suited agitation speed for *P. putida* G7. Both maximal growth and limonin utilization ooccurred (53.5%) when the cells were incubated at an rpm of 120. At higher agitation speed (200 rpm and more) increase in growth (growth rate $0.41h^{-1}$) with an early induction of stationary phase was observed but limonin utilization was lower. Microscopic observation of cells agitated at higher speeds exhibited gross disruption. A comparison of the temperature, pH optima and corresponding growth rate and limonin utilization with reported limonin degrading strains revealed a higher utlization of limonin within a shorter time period. This corroborated with a higher specific growth rate of the strain as well. A comparison of various microorganisms utilizing limonin at various cultural parameters is shown in Table 4.1.

4.1.6 Statistical optimization of cultural parameters for maximal limonin utilization

The combined effect or the inter-relationship of the selected cultural parameters for limonin utilization response was observed with response surface methodology with central composite design in a face centred cube design of 2^3=8 + 6 centre points and 6 (2x3) star points which lead to a total of 20 experiments. The coded values of the significant variables are presented in Table 4.2. Based on the optimization of process parameters and the experimental results (obtained from CCD and regression analysis) (Table 4.3), the relationship between the limonin utilization and the significant parameters (A- limonin concentration, B- temperature, C- pH) was established in the form of a quadratic polynomial equation. The analysis of

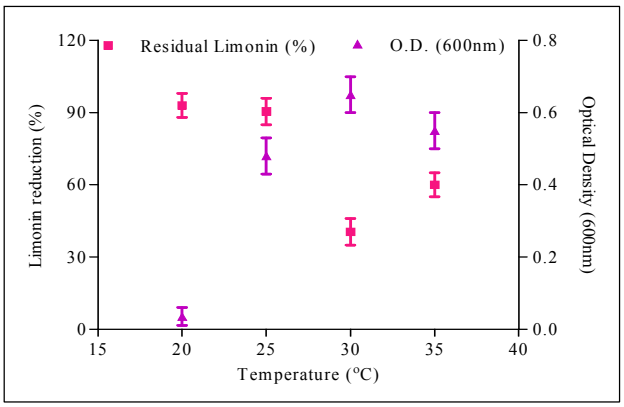

Fig. 4.6 Effect of temperature on growth and limonin utilization ability of *P.putida G7*

Table 4.1 Comparision of limonin utilization potential of different bacterial strains with their growth rate and physiological conditions

Microorganisms	Temperature (ºC)	pH	Limonin utilization (%)	Time	Growth rate (h^{-1})
Arthrobacter globiformis	30	3.5	28	56	0.22
Pseudomonas 321-18	30	7	45	54	0.33
Bacterium 342-152-1	37	7.5	36	60	0.25
Acinetobactor sp	35	4	42	72	0.31
Corynebacterium fascians	37	8	41	70	0.29
Rhodococcus facians	37	4.5	48	62	0.37
P. putida G7	30	8	54	48	0.43

*Data collected from literature references (Hasegawa et al. 1972; 1974; 1975; 1981; 1985; Manjon et al. 1989)

Table 4.2 Coded values of all the significant variables

Variables	Coded Values				
	-α	-1	0	+1	+ α
A-Limonin (µg/ml)	9.77	20	35	50	60.23
B- Temperature (°C)	16.59	20	25	30	33.41
C- pH	2.63	4	6	8	9.36

variance for this model is present in Table 4.4. The F value (43.08) of the model signifies the significance of the model and there was only 0.01 % chance that the model F value must have occurred due to noise. Regression analysis results has revealed R^2 (coefficient of determination, and the value more closer to 1 indicates the model fit of the experimental data) value of 0.9748, which signified the strength of the model and predicted a better response along with the enability of the model to explain only 2.52% of the total variations. The predicted R^2 of 0.78978 was in reasonable agreement with the adjusted R^2 (adjusted determination coefficient) value of 0.9522, which indicates the high reliability of the model and the quadratic polynomial equation. The statistical analysis also allowed us to determine the contribution of experimental factors (signals) in comparison to noise, where the signal should be fairly large in comparison to noise. The "adequate precision" which measures the signal to noise ratio (a ratio greater than 4 is desirable) and the ratio of 25.041 indicates an adequate signal. The values of "Prob>F" of the model far less than 0.05, indicates the significant and desirability of the model terms. The Fisher's "*F*" test of the model for limonin utilization response shows that fitted second order response surface model is significant i.e. 43.08425 (p= <0.0001). The parameters A, B, C (*p*= <0.0001) were significant and a significant interaction was observed among the parametrs AC & BC followed by AB, for the maximal response of limonin utilization (R1).The "Lack of Fit F-value" of 102.74 implies that the Lack of Fit is significant. There is only a 0.01% chance that this large "Lack of Fit F-value" could occur due to noise. A low value of CV (coefficient of variation) of 11.61% signifies a high degree of precision and a good deal of reliability of the experimental values. Values greater than 0.1 indicates the model terms are not significant. The equation for the model in terms of coded factors was determined as explained in Table 4.5.

The response model was developed further represented in the form of contour plots for a better understanding of the interaction among the three significant parameters and for the

Table 4.3 Response surface central composite design (CCD) and experimental limonin utilization

Run	A-Limonin (ug/ml)	B-Temperature (°C)	C-pH	Limonin Utilization (%)	
				Actual	Predicted
1	35	25	2.63	7	5.17
2	35	25	6	30	29.97
3	50	20	8	37	37.29
4	35	33.40	6	33	30.22
5	35	25	6	30	29.97
6	60.22	25	6	40	39.67
7	35	25	9.36	50	52.54
8	35	25	6	30	29.97
9	20	20	8	31	25.72
10	35	25	6	30	29.97
11	9.77	25	6	20	21.04
12	35	16.59	6	8	11.49
13	50	20	4	12	9.13
14	35	25	6	30	29.97
15	20	20	4	10	11.55
16	35	25	6	30	29.97
17	20	30	8	35	37.35
18	50	30	4	15	19.76
19	50	30	8	64	61.93
20	20	30	4	10	9.192

Table 4.4 Analysis of variance (ANOVA) for Response Surface Quadratic Model

Source	Sum of squares	df	Mean square	F -value	p-value Prob>F
Model	3984.054	9	442.6727	43.08425	< 0.0001 significant
A-Limonin	418.8946	*1*	418.8946	40.76999	< 0.0001
B- Temperature (°C)	423.4368	*1*	423.4368	41.21207	< 0.0001
C- pH	2708.227	*1*	2708.227	263.5851	< 0.0001
AB	84.5	*1*	84.5	8.224179	0.0167
AC	98	*1*	98	9.538101	0.0115
BC	98	*1*	98	9.538101	0.0115
A^2	0.262112	*1*	0.262112	0.025511	0.8763
B^2	149.7837	*1*	149.7837	14.57808	0.0034
C^2	2.253845	*1*	2.253845	0.219361	0.6496
Residual	102.7458	10	10.27458		
Lack of Fit	102.7458	*5*	20.54916		
Pure Error	0	5	0		
Cor Total	4086.8	19			

Table 4.5 Equation for the response surface model for limonin utilization

Final Equation in Terms of Actual Factors:
Limonin utilization (%) = -21.53654 -1.45607 * Limonin +3.94477* Temperature -4.60588 * pH +0.043333 * Limonin * Temperature +0.11667 * Limonin * pH +0.35000 * Temperature * pH +5.99390 E-004 * $Limonin^2$ -0.12896 * $Temperature^2$ -0.098867 * pH^2
Final Equation in Terms of coded factors:
Limonin utilization (%) = +29.98 +5.54 * A + 5.57 * B +14.08 * C +3.25 * A * B +3.50 * A * C +3.50 * B * C +0.13 * A^2 -3.22 * B^2 -0.40 * C^2

detection of the optimum level of each parameter for a maximum response. The contours plot showed the interaction of two independent parameters when the third parameter is fixed at zero (Fig 4.7 a-c), which represents the limonin utilization response. It is observed that if the contour is elliptical, the mutual interaction between the two factors is significant; or else if it is circular, the mutual interaction effect is non-significant. As shown in Fig. 4.7a the highest value of limonin utilization was obtained when the cells were grown at pH 8 with a limonin concentration of 50µg/ml over a time period of 36 h. The optimum operating conditions of pH (8) and temperature (30°C) was observed for effective response of limonin utilization (Fig. 4.7b). The response surface plotted in Fig. 4.7c, between temperature (30°C) and pH (8), depicted a higher activity of limonin utilization. Among the three significant variables A (limonin concentration), B (temperature) and C (pH); BC and AC exhibited the highest interaction which was most significant, followed by an interaction between BC. The experimental response for limonin utilization by *P. puitda* G7 was 64% when a limonin concentration of 50µg/ml was chosen as substrate and incubation carried out at 27.6°C and pH 8.

Thus, the response shown was based on the interaction of the significant variables. The close associations of the predicted and actual response were approximately 61.93% and 64% and signified the validity of the model.

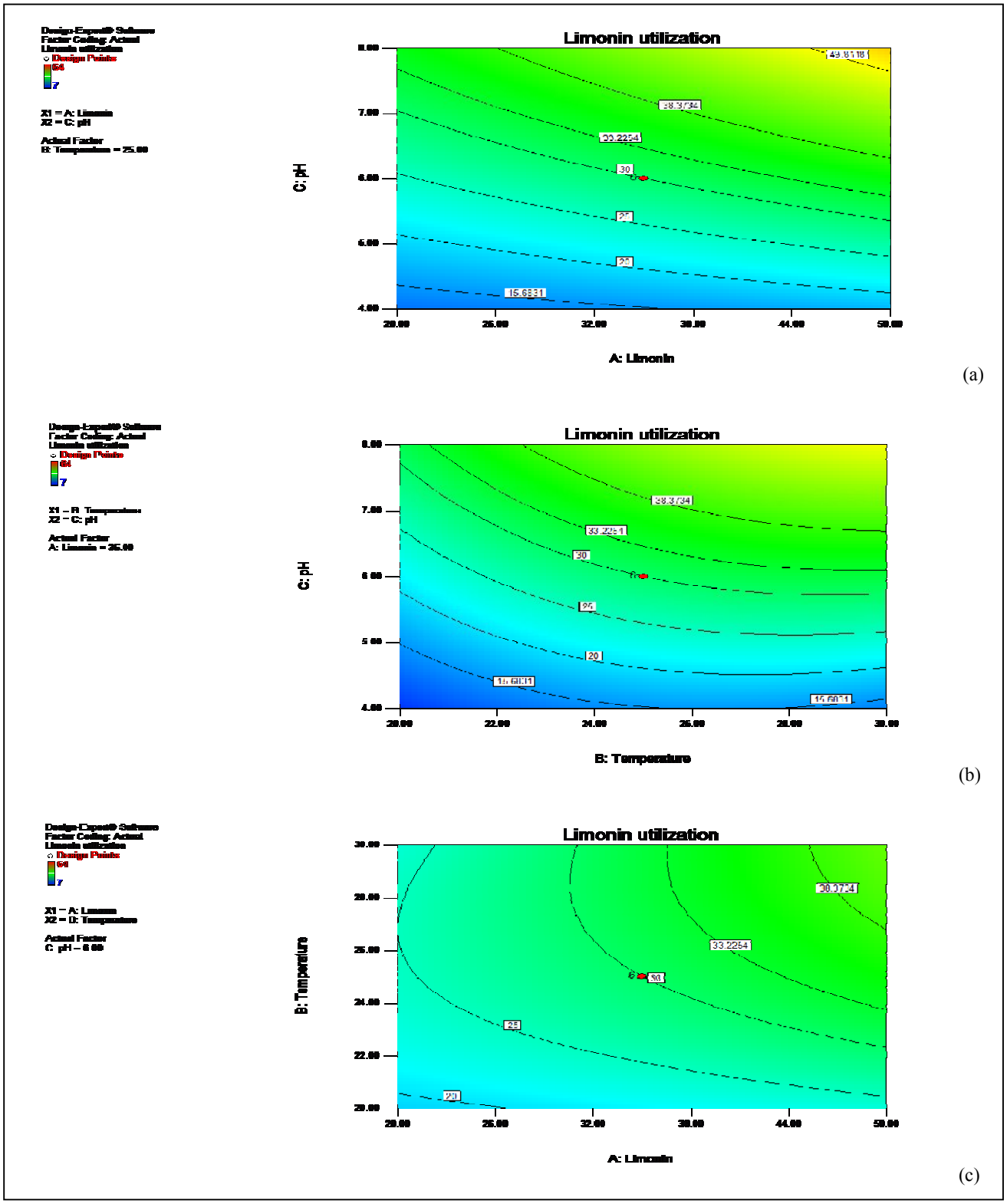

Fig. 4.7 Contour plots for limonin utilization by *P. putida* G7 in minimal medium depicting the interaction of significant factors (a) Interaction effect between limonin concentration and pH (b) Interaction effect between temperature and pH ; (c) interaction effect between limonin concentration and temperature

4.2 Genetic studies of *Pseudomonas putida G7* associated with limonin utilization

The most direct way to establish the function of a gene is by mutation. Insertional mutagenesis provides a short cut to isolating the gene in question without recourse to linkage mapping and the assembly of large clone contigs. Here the phenotype generated by transposon Tn5 insertion is absence of limonin utilizing ability (lim^-) in *P. putida* G7 because the insertion element had disrupted the corresponding gene, which means that the gene's sequence will flank the insertion site. Further a PCR based technique referred as inverse PCR was used for isolation of flanking sequence using different pair of primers that anneals to the transposon ends and detects the gene at the flanking sites to detect the disrupted gene. Where the genomic DNA from a lim^- mutant was cleaved with a restriction enzyme and self-circularized. PCR amplification was then carried out using primers that specifically anneal to the insertion transposon element but point outward rather than inward. In a circular DNA molecule, this will result in the amplification of sequences flanking the insert.

4.2.1 Transposon Tn5 insertional mutagenesis

Random Tn*5* transposon mutagenesis was accomplished for generation of a mutant library by mobilizing the suicide vector pGS9 (which harbored Tn5 transposon) from *E. coli* JB110 to generate mutants in *P. Putida G7*. A Tn5 transposition of 10^{-2} to 10^{-3} per cell generation occurred in *P. putida* G7. The total library consisted of >1,850 randomly picked mutants without discriminating by colony morphology or size. The mutants were arrayed in 96-well plates for phenotypic screening based on limonin utilization (Fig. 4.8). The color developed with TTC differentially depicted the growth in limonin. Those putative mutants were selected for further screening which did not turn up the formazan precipitates. This indicated absence of growth or inability to utilize limonin as the carbon source due to disruption by insertion of Tn5. Finally a stable mutant was selected and it was designated as *P. putida* strain lim A^- mutant.

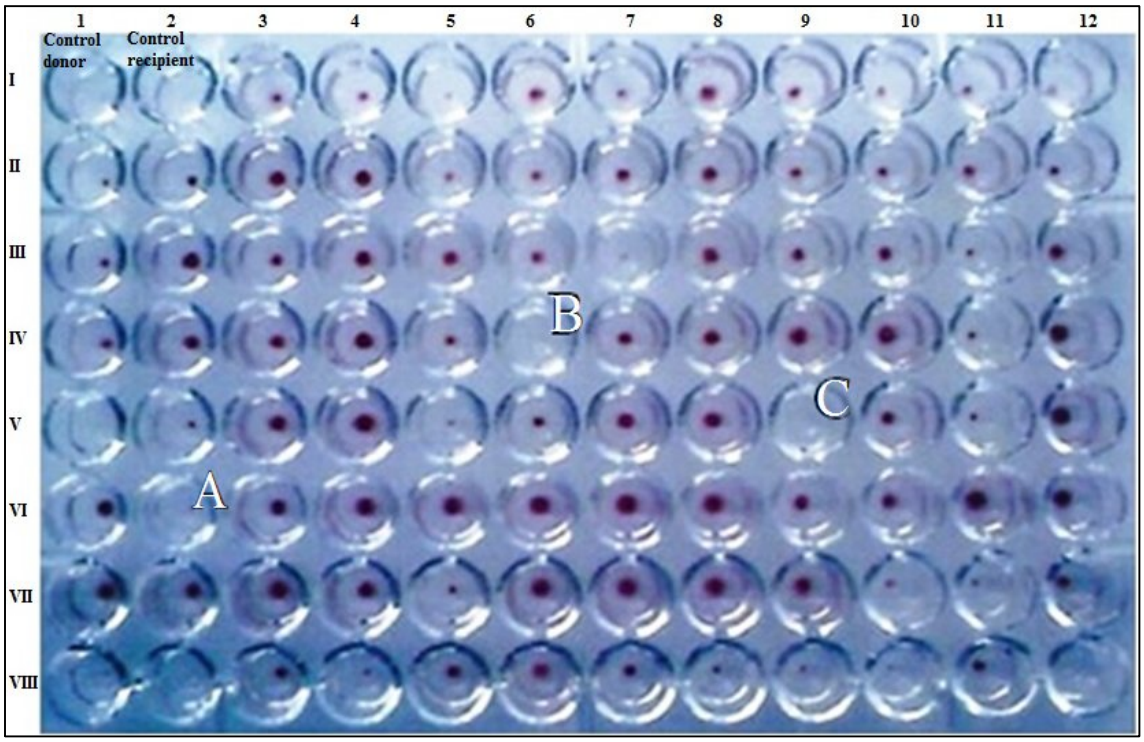

Fig. 4.8 Screening of mutant library generated by transposon mutagenesis for putative lim⁻ phenotypes; The three wells marked as A,B,C were the phenotypic mutants (unable to utilize limonin as carbon source), selected on the basis of absence of development of red precipitates of formazan as an indicator of growth

4.2.2 Detection of Tn5 in lim⁻A mutant

The transposition of Tn5 in the chromosome of *P. putida* G7 was confirmed by amplification of Tn5. The 625bp fragment based on IS50 element of Tn5 was amplified by PCR and amplification was positive in lim⁻ A mutant (Fig 4.9). No amplification was observed in the wild type *P. putida*.

4.2.3 Size approximation of Tn5 by Southern Hybridization

A highly sensitive Tn5 probe labelled with DIG-dUTP (as a visible marker) was generated and confirmed by resolution on a 0.8% agarose gel, where it showed less mobility as compared to the control (unlabelled Tn5) (Fig. 4.10). The genomic DNA of *P. putida* G7 (wild), lim⁻ A mutant and pGS9 plasmid DNA of *E.coli* (JB110) were isolated and digested with restriction enzymes Eco R1 and Hpa 1 (Fig. 4.11). The gel adhered with the digested profile of the target samples was denatured and unsterilized with various respective buffers followed by blotting the DNA profiles on the nitrocellulose membrane. The probe was employed for the detection of the copy number of Tn5 target sequence by hybridization. A visible signal for the target DNA sequence was immunodetected and documented. Fig. 4.12 showed no signal for *P. putida* G7 (wild), A signal was visible at 5.8kb in genomic DNA profile of *P. putida* G7 lim⁻ A. Also plasmid pGS9 of *E.coli* - JB110 was used as one of the controls for detecting the Tn5 signal.

4.2.4 Cloning and detection of the Tn5 flanking region

A high throughput inverse PCR approach was employed to detect the gene loci in lim⁻ A mutant. The gene sequence at the Tn5 flanking site was mapped by locating Tn5 insertion in the various restricted endonuclease digests of the lim⁻A mutant. The restriction fragments of variable restriction enzymes (Sal1, Bam H1, Bgl11, Not 1, Hpa1) were when circularized by ligation, gave various amplicons of varied sizes, with the respective primers (Fig. 4.13). Approximately, 18 amplicons corresponded to the variable circularized DNA were resulted

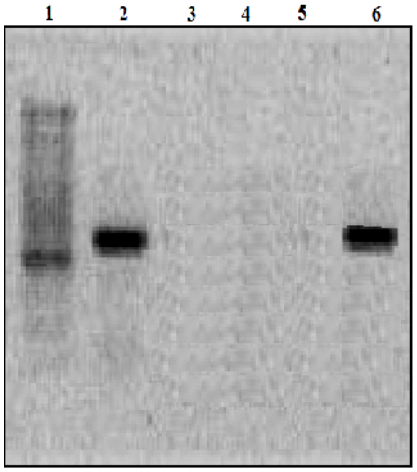

Fig. 4.9 Confirmation of Tn5 insertion in *P. putida* G7 by PCR amplification; Lane1: Molecular weight marker (100bp ladder); Lane2: Presence of Tn5 amplicon in Tn5 transconjugant "A" (Lim$^-$ mutant); Lane3,4: Absence of Tn5 amplification in Tn5 transconjugant B & C; Lane5: Absence of Tn5 amplification in *P. putida* G7 (wild type) (-ve control); Lane 6: Presence of Tn5 amplification in pGS9 plasmid (+ve control)

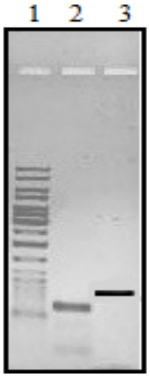

Fig. 4.10 DIG labeled Tn5 probe generated by PCR amplification; Lane 1: 100 bp Molecular weight marker; Lane2: Unlabelled control Tn5 probe; Lane3: DIG labeled Tn5 probe

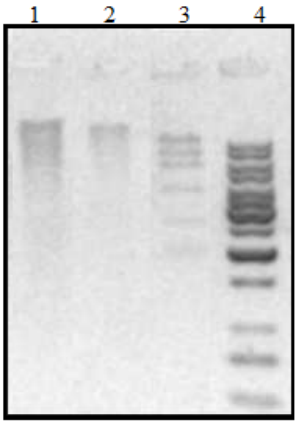

Fig. 4.11 Restriction digestion profile of *P. putida* G7 lim$^-$ A mutant; Lane 1: Eco R1 digested DNA sample of wild type of *P. putida* G7; Lane 2: Eco R1 digested DNA of lim$^-$ A mutant of *P. putida* G7; Lane 3: Hpa1 digested products of pGS9 plasmid; Lane4: 1 Kb DNA molecular weight marker

Fig. 4.12 Immunodetection of Tn5 insertion in lim⁻ A mutant of *P. putida* G7; Lane 1- Negative control (wild type of *P.putida* G7); Lane 2- lim⁻ A mutant confirms the presence of signal for Tn5; Lane 3- Positive control (suicidal vector pGS9 containing Tn5 of strain JB110)

Fig. 4.13 Gene amplification at the insertion sites of Tn5 by Inverse PCR in lim⁻ A mutant of *P. putida* G7; Lane1- three amplicons of Bam HI restriction digested product; Lane 2- three amplicons of Not 1 restriction digested product; Lane 3- four amplicons of Sal I restriction digested product; Lane 4- four amplicons of Bgl III restriction digested product; Lane 5- four amplicons of Hpa I restriction digested product; Lane 6- 1kb ladder

as a result of inverse PCR (Table 4.6). The amplicons were extracted and purified, cloned in the pGEM-T Easy vector system and transformed into *E.coli* (DH5α). A clone library was formed and nearly 215 clones were selected from the transformed colonies (corresponding to the various restriction enzymes) on IPTG/X-gal plates and were sequenced.

4.2.5 Sequence Analysis and gene identification

The clones sequences obtained were multaligned and restriction mapped. The deduced gene sequence had shown similarity with various chromosomal streches of variable identical restriction pattern, when identified using blast-n, blast-p and NCBI ORF finder bioinformatic tools. Of the various clones sequences, 9 clones had shown ORF'S which had similarities with partial genes sequences or with hypothetical genes (Table 4.7). One of the larger fragments of clones Sal 1 of 1.176 kb (Accession: BankIt1523539) had shown an ORF1 (tnA) with a putative function for a gltS glutamate transporter from its 78-846 position. ORF2 (tnB) has also shown an ORF with a similar putative function of gltS Sodium/glutamate symport carrier protein, from 677-967 position in the Sal 1 fragment. The physical map of the gene sequence and its translated protein sequence has been predicted by a Dnadynamo software as presented in Fig. 4.14. This revealed that the Tn5 insertion must have deactivated the glutamate transporter gene due to which the bacterial cell were unable to utilize limonin. Thus the gene sequence derived from the flanking region of Th5 only 2 ORF's are proposed to be the participants of the gene corresponding to limonin utilization/uptake on the basis of the sequence homologies and the effect of mutation. ORF1 (tnA) and ORF2 (tnB) showed a similarity with the ORF's of glutamate symporter/transporters located on the membranes of *E. coli* K12, MG1655 an *E. coli* CFT073 respectively. Disruption of this membranous protein was response for the inability of lim^- mutant of *P. putida* G7 to uptake and utilize limonin as the carbon source.

Table 4.6 Amplicons generated by Inverse PCR

E.coli strain /pGEMT Vector	Genotype	
	Restriction digested	Insert
Δ1/S1	Sal 1	560bp
Δ2/S2		730bp
Δ3/S3		1.3kb
Δ4/S4		450bp
Δ5/Bm1	Bam H1	493bp
Δ6/Bm2		684bp
Δ7/Bm3		1.12kb
Δ8/Bg1	Bgl 11	480bp
Δ9/Bg2		651bp
Δ10/Bg3		1.2kb
Δ11/Bg4	Not 1	550bp
Δ12/No1		538bp
Δ13/No2		854bp
Δ14/No3		630bp
Δ15/Hp1	Hpa 1	850 bp
Δ16/Hp2		750bp
Δ17/Hp3		954bp
Δ18/Hp4		325bp

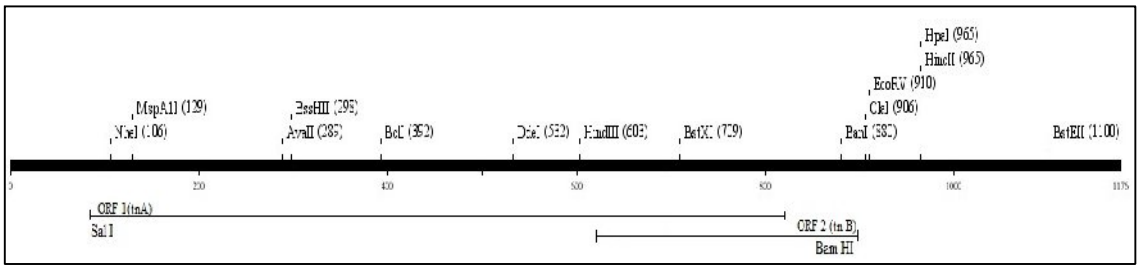

Fig. 4.14 Position of essential ORF's and the restriction map of the gene associated with limonin utilization

Table 4.7 Features of the ORF'S encoded in the 1.1 76kb DNA region from Lim⁻ A mutant of *P. putida* G7

ORF	Position	Identity %	Putative function	Organism	Accession no
ORF 1 (tnA)	79-846	98	gltS glutamate transporter	*Escherichia coli str. K-12 substr. MG1655*	NP_418110.1
ORF2 **(tnB)**	677-967	99	gltS Sodium/glutamate symport carrier protein	*Escherichia coli CFT073*	YP_002384972.1
ORF4 **(tnD)**	547-7 44	44	ECU08_0210 SEC31-like protein involved in vesicular transport from ER to golgi	*Encephalitozoon cuniculi GB-M1*	NP_597151.1
ORF5 **(tnE)**	930-1175	41	hypothetical protein B2_07867	Bacteroides sp. 2_1_7	ZP_05285934.1
ORF6 **(tnF)**	434-1051	39	CIMG_04173 hypothetical protein	*Coccidioides immitis RS*	XP_001244732.1
ORF7 (tnG)	74-316	100	ytfM hypothetical protein	*Shigella dysenteriae Sd197*	YP_405829.1
ORF8 (tnH)	22-261	26	BVU_0689 serine acetyltransferase	*Bacteroides vulgatus ATCC 8482*	YP_001298017.1
ORF10 (tnJ)	406-546	43	lysA diaminopimelate decarboxylase	*Shigella dysenteriae Sd197*	YP_404563.1
ORF12 (tnL)	500-616	52	CTU_34270 hypothetical protein	*Cronobacter turicensis z3032*	YP_003211790.1

4.2.6 Detection of Gltase activity in lim⁻ A mutant

The deactivation of the glutamate symporter gene due to Tn5 insertion was further confirmed by detecting the variation in the glutamate uptake of (50 µg/ml, as carbon source) potential of the lim⁻A mutant and wild type of *P. putida* G7. The spectrophotometric analysis when done for the detection of glutamate levels at O.D. 450 nm, showed a reduction in the absorbance (which corresponds to the reduction in the glutamate concentration of 15% in 30 min) after the incubation of the wild type cells of *P. putida* G7. This shows that the undisrupted glutamate symorter in wild type corresponded to the uptake of glutamate (as the carbon source). Whereas the lim⁻ A mutant of *P. putida* G7 showed an insignificant 1-2% ($p<0.05$) reduction in absorbance. This revealed that the lim⁻ A mutant which was unable to utilize limonin was also unable to uptake glutamate as the carbon source.

4.2.7 Chemotaxis for limonin by P. putida G7

Though motility is essential for gram negative bacteria, however it is important to understand whether the bacterial cells actually chemotax towards the compound of interest i.e. limonin. The *P. putida* G7 cells (Fig. 4.15), placed on one end of the filter paper and observed at regular intervals, exhibited positive motility on the filter paper by utilizing limonin present and reducing the TTC present into red color formazan. The observations indicated that *P.putida* G7 cells could utilize limonin, when present as sole carbon source.

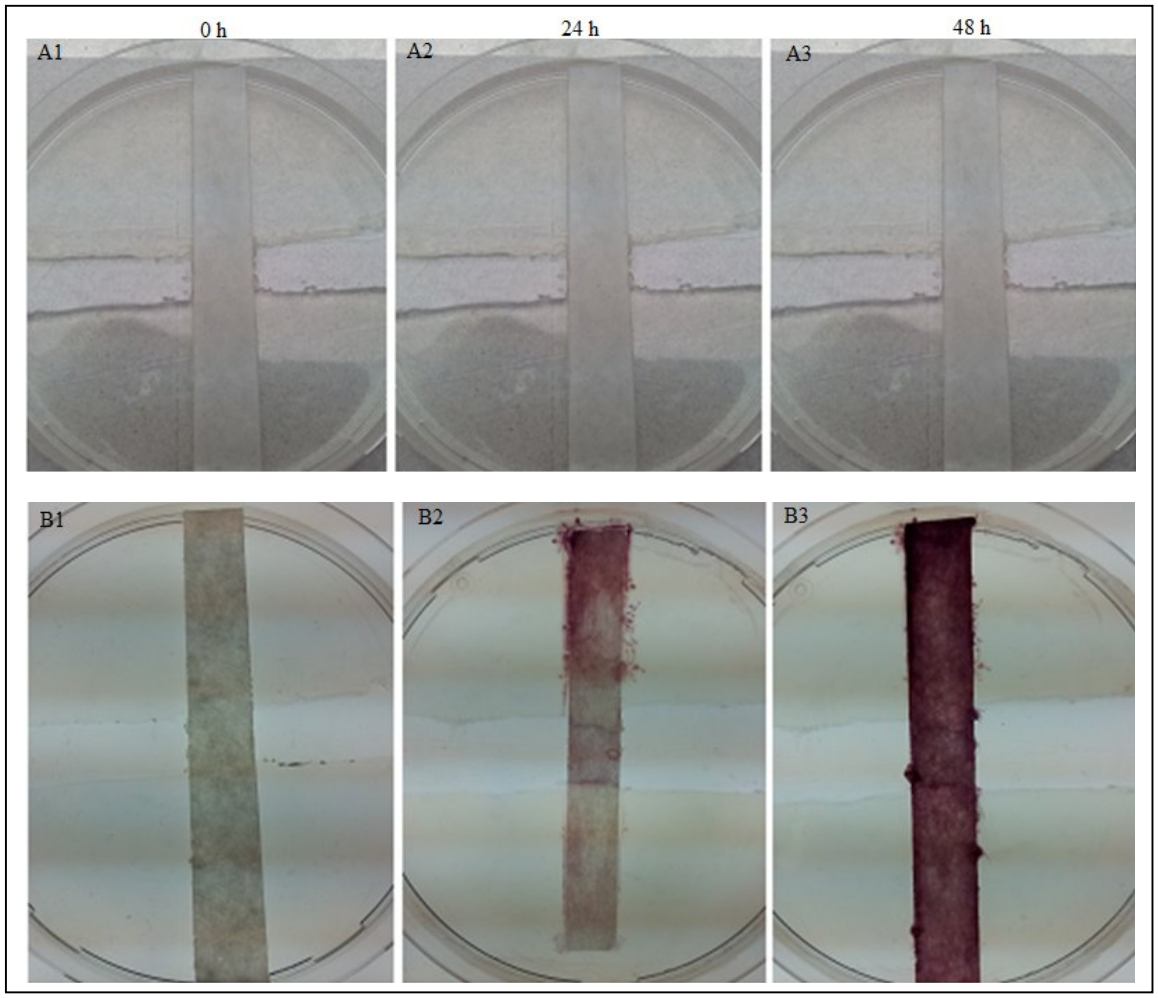

Fig. 4.15 Chemotaxis of *P. putida* G7 cells for chemo-attractant limonin; Growth was observed for *P. putida* G7 in B2 and B3, by red color due to TTC, which confirmed the mobility of cells to utilize limonin across the well. Absence of motility was observed in A2 and A3 which explained the inability of *E. coli* Dh5α to utilize limonin as cabon source

4.2.8 Role of NAH plasmid of *P. putida* G7 in Limonin biotransformation

As evident form the foregoing studies, that identity of the genes responsible for limonin bioconversion remained elusive. Therefore it was anticipated that the NAH plasmid responsible for naphthalene degradation in *P. putida* G7 might offer clues for characterizing limonin degrading genes. Plasmid curing was therefore attempted to examine whether cured strains retained the ability to utilize limonin. Prior to curing studies the plasmid characteristics were examined in a preliminary study.

Detection and molecular weight determination of plasmid in P. putida G7

The slow mobility of the purified plasmid DNA indicated its large size; comparison to the lambda marker suggested its size to be more than 23kb lambda marker (Fig. 4.16). The ability of *P. putida* to metabolize naphthalene signified its identity as low copy number NAH plasmids with size varying between 60-100kb. For obtaining a genetic fingerprint, the plasmid was subjected to restriction digestion and resolved on agarose gel. The profile of digested fragments was used to determine the molecular weight using the Mol Match program. The plasmid had a molecular weight of approximately 83 kb.

Plasmid curing

The role of plasmid borne structural gene(s) implicated in limonin utilization was determined by curing the wild type strain of its indigenous NAH plasmid. Among the various curing agents mitomycin C proved to be most efficient (Table 4.8). The number of viable cells was plotted as a function of mitomycin C (Fig. 4.17). A killing rate of 94.7% (±1.2, n=6) was observed in the presence of 20 µg/ml mitomycin C. Such a rate was considered sufficiently high for screening the remaining viable cells (5.3%) for plasmid loss. These cells were further grown and approximately 1600 colonies were screened in terms of their ability to utilize naphthalene and limonin as sole carbon and energy sources.

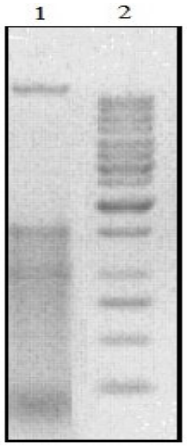

Fig. 4.16 Profile of plasmid of *P. putida G7*, Lane 1: Plasmid DNA, Lane 2: 1 Kb marker

Table 4.8 Effect of different curing agents on their ability of curing plasmid from *P. putida* G7

Curing agent	Sub inhibitory concentration	Total number of colonies examined	Colonies with lost plasmid	Frequency of curing (%)
Ethidium Bromide	80 µg/ml	952	0	0
SDS	0.1 g/ml	683	0	0
Elevated temperature	45°C	875	0	0
Mitomycin C	20 µg/ml	1600	4	2.47%

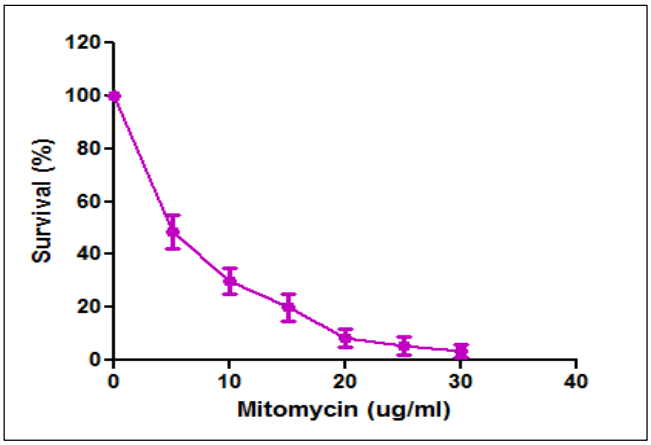

Fig. 4.17 Survival curve of *P. putida* G7 as function of mitomycin C

Amongst these four colonies, *viz*. PpC1–PpC4 were observed which did not reduce it to formazan (red color indicator) i.e. did showing their inability to utilize limonin as a carbon source as compared to the wild type. Similarly, no growth was observed in the presence of naphthalene vapors even after 24 h (Table 4.9). However in two (PpC2, PpC4) colonies, very faint growth was observed after 48 h. All the four suspected cured derivatives were analyzed for plasmid loss; however only one of the four strains (PpC1) showed the presence of plasmid (Fig. 4.18). Among the four suspected cured derivatives (PpC1-PpC4); only PpC3 was confirmed as a true cured strain (PpC3) as evidenced by loss of plasmid, and failure to grow on naphthalene and limonin as a sole carbon source. The other two cured strains viz. PpC2 and PpC4 appeared to have had the plasmid integrated into the genome, as evidenced by the absence of plasmid. PpC1 was essentially a mutant, as the strain harbored the plasmid, but lost the ability to grow on naphthalene for one reason or another. A curing frequency with a mean of 4×10^{-4} i.e 1 per cell 1.6×10^{2}, (n=6), was calculated.

Confirmation of plasmid encoded ndo gene by amplification

The plasmid encoded *ndo* gene (one of the gene responsible for naphthalene degradation) was ensured in the four suspected cured derivatives. The *ndo* gene specific primers resulted an amplification of 640 bp, which confirmed the presence of *ndo* gene in wild type and in two cured strains, viz. PpC2, PpC4. Absence of *ndo* specific amplification confirmed the absence of plasmid in PpC1 or PpC3 (Fig. 4.19).

Verification of cured strain and confirmation of plasmid encoded limonin utilization

The plasmid-encoded function for limonin utilization was verified in the PpC3 cured strain of *P. putida* G7. The strategy employed was to check the recuperation of the limonin utilization function after transmitting the indigenous plasmid from the donor wild type to the cured strain. The transconjugants obtained regained their potential to utilize naphthalene and limonin as a sole carbon and energy with a physical presence of plasmid (Fig. 4.20).

Table 4.9 Characteristic profile of four cured mutants

Putative cured derivatives	Growth on naphthalene (After 24 hrs)	Presence of ndo gene	Growth in limonin	Plasmid
PpC1	-	-	-	visible
PpC2	-	+	-	not visible
PpC3	-	-	-	not visible
PpC4	-	+	-	not visible

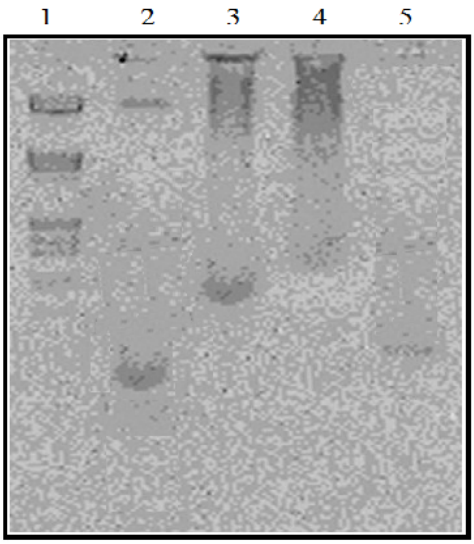

Fig.4.18 Plasmid detection in the cured derivatives of *P. putida* G7; Lane 1: 23kb ladder as marker Lane 2: Presence of plasmid in PpC1 cured strain Lane 3-5: Absence of plasmid in PpC2, PpC3, PpC4 cured derivatives

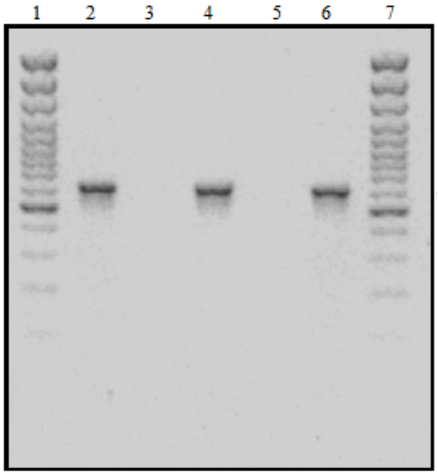

Fig. 4.19 Confirmation of plasmid encoded ndo gene located on NAH7 plasmid by amplification; Lane 1, 100 bp ladder, Lane 2,4,6, presence of ndo gene (640 bp fragment) in wild-type *P. putida* G7, PpC2 & PpC4 respectively; Lane 3& 5, absence of ndo gene in PpC1& PpC3 derivatives respectively, Lane 7, 100 bp molecular weight marker

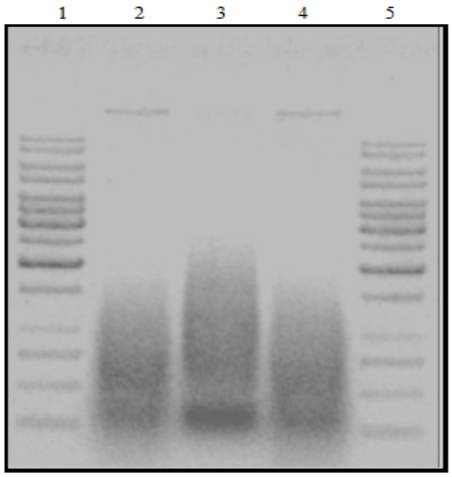

Fig. 4.20 Detection of plasmid DNA in the transconjugants screened; Lane 1: 1Kb molecular size marker, Lane 2: plasmid DNA of *P. putida* G7 (wild-type), Lane 3: Absence of plasmid in the cured strain, Lane 4: presence of plasmid DNA after conjugal transfer into cured derivative (transconjugant); Lane 5: 1 Kb molecular size marker

4.3 Biochemical attributes of limonin biotransformation

A complete understanding of the biochemical mechanism for limonin utilization by *P.putida* G7 can provide valuable insights and enable effective approaches for reducing limonin mediated bitterness in kinnow mandarin juices. Thus, the biochemical mechanism(s) of *P. putida* regarding its limonin utilization was studied. Comparison was drawn to its Tn5 mutant, which has lost its ability to utilize limonin as sole carbon source.

4.3.1 Limonin utilization kinetics by P. putida in minimal medium

Standard limonin was used as sole carbon source in minimal medium for studying limonin utilization by the wild type and mutant *P. putida*. The residual limonin level at each phase of growth was estimated for up to 50 hours. An overall reduction in initial limonin levels by 64% within 48 hours of growth was observed; the mutant survived but failed to grow (Fig. 4.21).

4.3.2 *Cellular locus of enzyme of P. putida G7*

The cell extracts of wild type and its mutant (PpC3) obtained by ultrasonic disruption were assayed for limonin degradation. A decrease in absorbance observed over time could be correlated with a proportionate decline in limonin levels; the final limonin content decreased by 03.4% (Table 4.10). A similar trend was not observed in case of cell extracts obtained from PpC3 mutant. In parallel experiments cell fractions were heat inactivated and treated with proteinase K and assayed for limonin degradation, however, initial levels of limonin did not decline in these cases. The observations indicated the involvement of enzyme for limonin degradation. Further, the cell proteins of both wild type and mutant *P. putida* cells resolved on SDS-PAGE revealed the absence of two polypeptides of molecular weight 43 KDa and 14 KDa (Fig. 4.22) suggesting a possible role of these polypeptides in limonin degradation. The cellular locus of the limonin degrading enzyme was ascertained by isolating the periplasmic, spheroplast fractions of *P. putida*. Limonin degradation assays conducted with

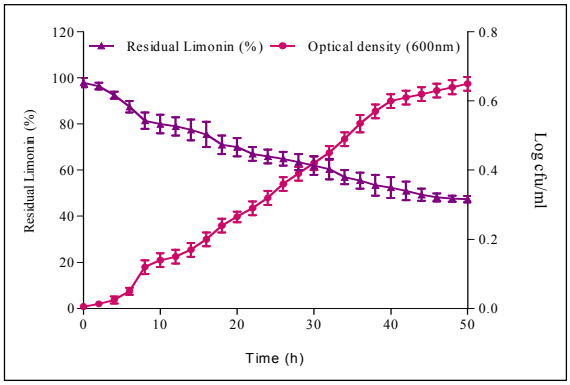

Fig. 4.21 Growth and limonin utilization profile of *P. putida* G7 in minimal medium

Table 4.10 Limonin utilization by various cellular fractions

Various cell fractions	*P. putida* (wild)	Cured *P. putida* (PpC3)
Cell free extracts	03.4%	ND
Periplasmic fraction	76.3%	ND
Spheroplast fraction	02.8%	ND

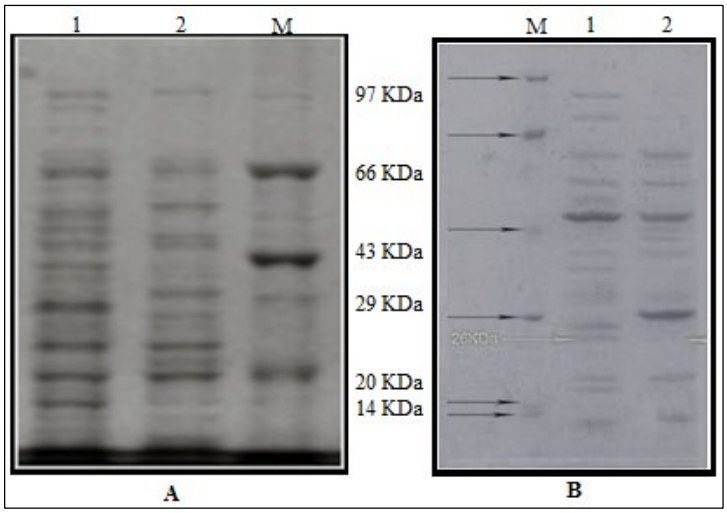

Fig. 4.22 SDS-PAGE profile for (a) cell free extract proteins of wild type of *P. putida* G7 and its PpC3 mutant; [Lane 1: Cell free extracts of wild type of *P. putida* G7; Lane 2: Cell free extracts of *P. putida* G7 (PpC3 mutant); Lane 3: Molecular weight marker]; **and (b) periplasmic fraction proteins of wild type of *P. putida* G7 and its PpC3 mutant [**Lane 1: Molecular weight marker; Lane 2: Periplasmic fraction of wild type of *P. putida* G7; Lane 3: Periplasmic fraction of *P. putida* G7 (PpC3 mutant)]

the periplasmic fraction exhibited a decline in limonin content by up to 76.3% (Table 4.10). In comparison, the periplasmic extracts of PpC3 mutant showed no change in the limonin concentration. The periplasmic fractions of both wild type and mutant *P. putida* cells were resolved on SDS- PAGE. The PpC3 mutant lacked at least five polypeptides - 22 KDa, 26 KDa, 38 KDa, 72 KDa and 89 KDa in comparison to its wild type counterpart (Fig. 4.22).

To examine whether spheroplast fractions retained limonin degrading activity, both wild type and PpC3 spheroplast fractions were assayed. Results indicated a reduction in limonin levels by 02.8% (Table 4.10). No decline in initial limonin level was detectable in case of PpC3 mutant. The requirement of cofactors was examined by extensively dialyzing the periplasmic fraction and re-assaying for limonin degradation in separate combinations comparing-dialyzate and retentate, retentate alone and retentate with NAD. The conversion of NAD to NADH was concomitant in retentate added with NAD; a five fold higher reduction in the limonin content was observed. These results suggested the requirement of the cofactor NAD for the limonin biotransforming enzyme.

4.3.3 Purification of limonin degrading enzyme

Since the limonin degrading activity was primarily obtained in the periplasmic fraction, purification was attempted in order to further characterize the enzyme. To achieve purification, the periplasmic fraction was subjected to a number of steps including gel filtration, hydroxyapatite, anion exchange and finally Mono Q (Table 4.11) to obtain 26-fold purification of the enzyme with an overall yield of 26%. SDS–PAGE of the purified enzyme revealed a single distinct band of a molecular mass of 26 kDa (Fig. 4.23), implying the integrity and purity of the purified enzyme. The molecular mass of the native enzyme was 26 kDa, indicating the enzyme to be a monomer.

4.434 Immunoblotting and Zymography

To determine whether the limonin degrading enzyme is homologous to other previously reported enzymes having similar function, the 26 kDa polypeptide was cross-reacted with monospecific anti-LDase antibodies raised against *A. globiformis* Limonin dehydrogenase. Cross reaction of the *P. putida* enzyme to that of *A. globiformis* could be clearly demonstrated (Fig. 4.24). To elucidate the nature of the enzyme, activity staining assay was carried out. The 26kDa band showed a strong fluorescence under UV light upon incubation with limonin (Fig. 4.25) suggesting a "dehydrogenase" nature of the enzyme.

4.3.5 Peptide mass fingerprinting

To further characterize the limonin degrading enzyme, purified enzyme was subjected to peptide mass fingerprinting. The MASCOT and Pro Found searches indicated this protein to be homologous to Salicylaldehyde dehydrogenase (DoxF, SaliADH, EC=1.2.1.65) involved in the upper naphthalene catabolic pathway of Pseudomonas strain C18. The salicylaldehyde dehydrogenase possessed 48% of amino acid identity (53% similarity) to DoxF from Pseudomonas C18, with alignment coverage of 82%. Similar results were obtained when the predicted peptide sequence was analyzed by BLAST (p), followed by an analysis of similar peptide sequences clustal alignment of the various sequences (Fig. 4.26). The conserved domains on the sequence from amino acid residues 65-190 were similar with aldehyde dehydrogenase super family (ALDH-SF) of NAD (P) dependent enzymes. The amino acid residues from 220-308 shows a similarity with the NADB Rossmann super family that shares Rossmann-fold NAD(P)H/NAD(P)(+) binding (NADB) domain. The NADB domain is found in numerous dehydrogenases of metabolic pathways such as glycolysis and many other redox enzymes. The proteins in this family comprise a second domain in addition to the NADB domain, which is responsible for specifically binding a substrate and catalyzing a particular

enzymatic reaction. The sequence of the limonin dehydrogenase has been submitted in Uniprot KB, the accession number of the protein is P86808.

Table 4.11 Purification profile of periplasmic limonin dehydrogenase of *P. putida* G7

Purification Step	Total protein (mg)	Specific activity ($IUmg^{-1}$)	Purification (fold)	Yield (%)
A- Periplasmic extract	300 (±0.06)	5.6(±0.02)	1(±0.03)	100(±0.03)
B- Gel filtration	130(±0.07)	9.9(±0.05)	1.8(±0.02)	78(±0.02)
C-Hydroxyapatite	32 (±0.02)	25(±0.03)	4.5(±0.03)	48(±0.01)
D-Anion exchange	6.5(±0.02)	110(±0.01)	20(±0.02)	43(±0.02)
E-Mono Q	3.0(±0.01)	145(±0.04)	26(±0.01)	26(±0.03)

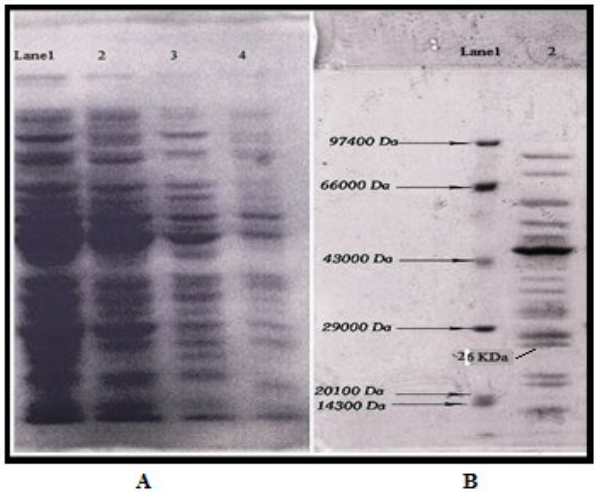

Fig. 4.23 SDS PAGE of periplasmic extract of *P. putida* G7; (A) Lanes 1-4, shows the protein profile of the periplasmic enzyme during various purification steps (B) shows the SDS-PAGE of the purified periplasmic enzyme, Lane1: Molecular markers; Lane2:Purified limonin dehydrogenase of *P.putida* G7

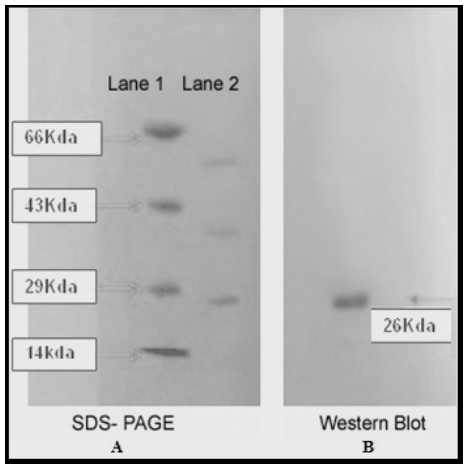

Fig. 4.24 Western blot analysis of the limonin degrading enzyme of *P. putida* G7 (A) SDS PAGE [Lane1: Molecular weight marker, Lane 2: Purified periplasmic fraction of *P. putida* G7] and (B) Western blot analysis of purified periplasmic fraction

Fig. 4.25 Zymogram of LDase activity; a single band of protein corresponds to *in situ* assay for LDase activity

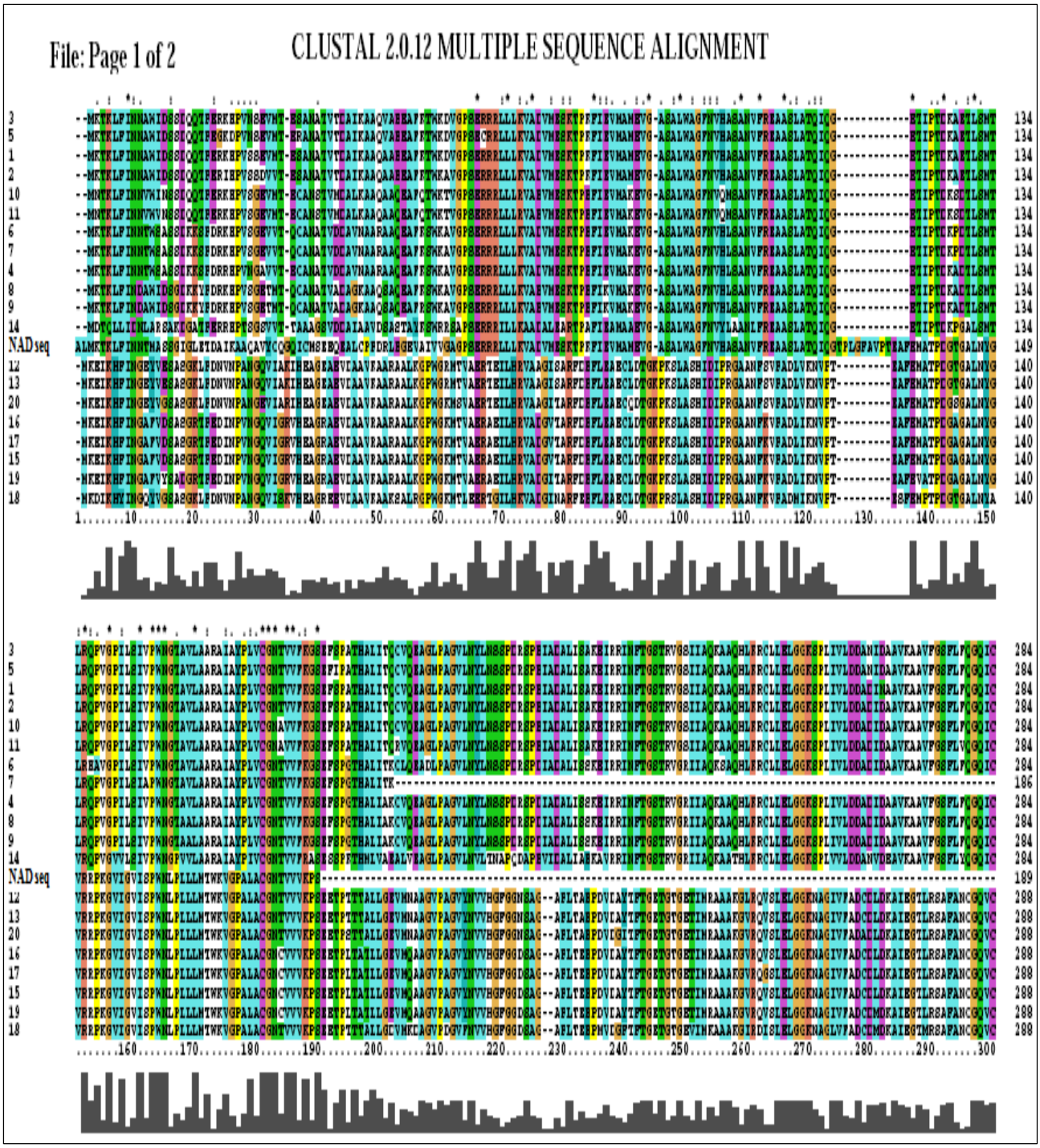
File: Page 1 of 2
CLUSTAL 2.0.12 MULTIPLE SEQUENCE ALIGNMENT
NADseq
NADseq

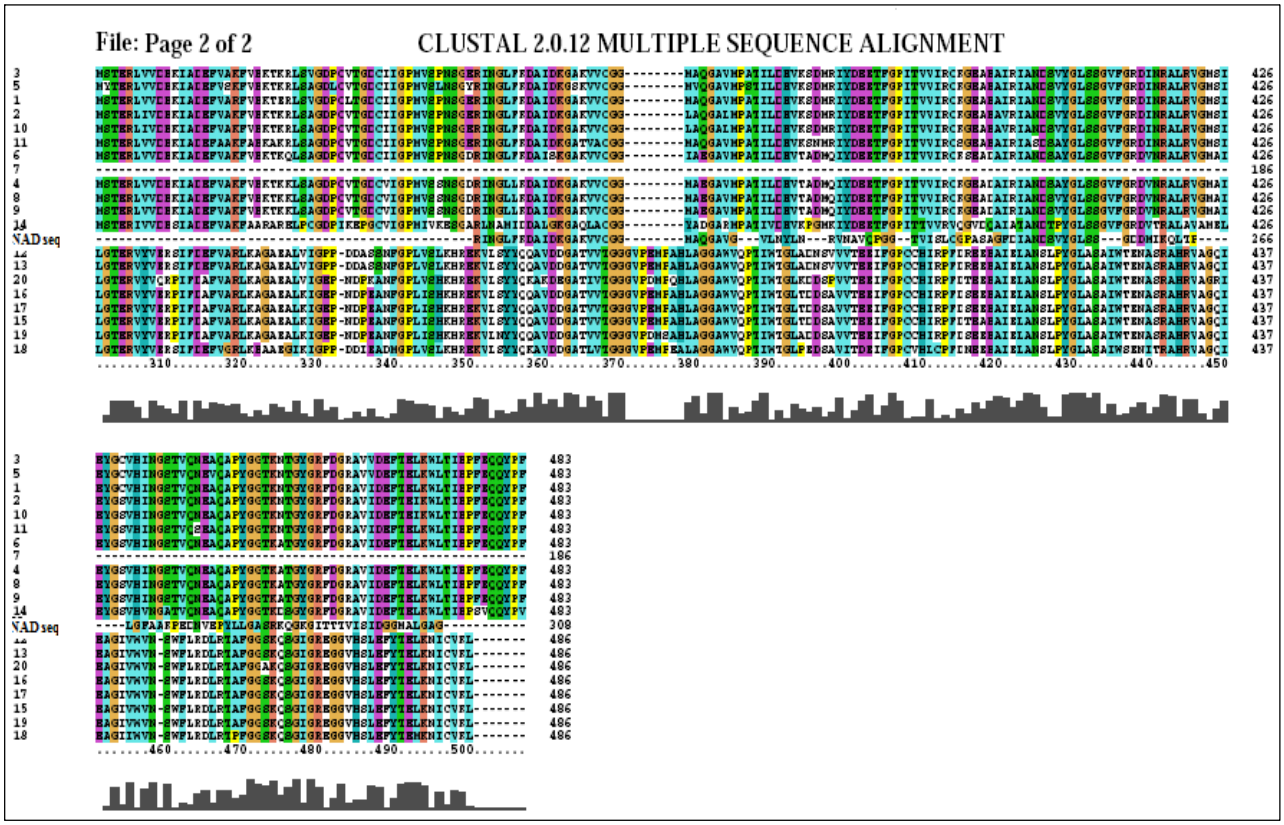

Fig. 4.26 CLUSTALX alignment of predicted peptide sequence seq (1) from *Pseudomonas putida* G7 with similar peptide sequences; gi|90576583|ref|YP_534825.1| salicylaldehyde dehydrogenase NahF [Pseudomonas putida](**1**); gi|32469901|ref|NP_863075.1| salicyladehyde dehydrogenase [Pseudomonas putida] (**2**); gi|2189974|dbj|BAA20394.1| dehydrogenase [Pseudomonas putida] (**3**); gi|254028646|gb|ACT53252.1| salicylaldehyde dehydrogenase [Burkholderia sp. C3] (**4**); gi|15809675|gb|AAL07269.1| salicylaldehyde dehydrogenase [Pseudomonas fluorescens] (**5**); gi|3337416|gb|AAD12613.1| salicylaldehyde dehydrogenase [Ralstonia sp. U2] (**6**); gi|8118288|gb|AAF72979.1|AF252550_6 salicylaldehyde dehydrogenase-like protein [Comamonas testosteroni] (**7**); gi|121605378|ref|YP_982707.1| aldehyde dehydrogenase [Polaromonas naphthalenivorans CJ2] (**8**); gi|74136893|gb|AAZ93391.1| salicylaldehyde dehydrogenase [Polaromonas naphthalenivorans CJ2](**9**); gi|1255672|dbj|BAA12243.1| dehydrogenase [Pseudomonas aeruginosa] (**10**); gi|4104756|gb|AAD02139.1| salicylaldehyde dehydrogenase [Pseudomonas stutzeri] (**11**); gi|19033978|gb|AAL83661.1| 2-hydroxymuconic semialdehyde dehydrogenase [Pseudomonas putida] (**12**); gi|111116464|ref|YP_709348.1| 2-hydroxymuconic semialdehyde dehydrogenase [Pseudomonas putida] (**13**); gi|171057492|ref|YP_001789841.1| aldehyde dehydrogenase [Leptothrix cholodnii SP-6] (**14**); gi|3293056|dbj|BAA31265.1| 2-hydroxymuconic semialdehyde dehydrogenase [Pseudomonas stutzeri] (**15**); gi|4104767|gb|AAD02149.1| hydroxymuconic semialdehyde dehydrogenase [Pseudomonas stutzeri] (**16**); gi|37220706|gb|AAQ89676.1| hydoroxymuconic semialdehyde dehydrogenase [Pseudomonas putida] (**17**); gi|149375513|ref|ZP_01893283.1| 2-Hydroxymuconic semialdehyde dehydrogenase [Marinobacter algicola DG893] (**18**); gi|47078060|gb|AAT09777.1| XylG [Pseudomonas sp. ST41] (**19**); gi|226943016|ref|YP_002798089.1| 2-hydroxymuconic semi-aldehyde dehydrogenase [Azotobacter vinelandii DJ] (**20**); NAD seq from *Pseudomonas putida* G7(query sequence). Asterisks (‘*’) above the aligned sequences identical residues in all sequences. Positions with colons (‘:’) contain a residue of the strongly conserved groups in all sequences, and periods (‘.’) indicate weakly conserved groups in all sequences.

4.3.6 Catalytic properties of the limonin degrading enzyme

The limonin utilization by the purified enzyme was conclusively demonstrated from HPLC results. The chromatograms revealed the substrate retention time to be 9.3 minutes; a reduction in peak following catalysis by the purified dehydrogenase was observed. A biotransformation was evidenced from the appearance of two new peaks at retention times of 15.9 and 25.2 minutes (Fig. 4.27). The peak area of 66% of standard limonin in the medium, following reaction with the purified enzyme of *P. putida* G7 resulted in reduction in peak area to 9.07%, which corresponded to 76% of limonin reduction. However, a complete disappearance of limonin peak was not observed due to the presence of residual limonin in the medium. These results indicated a strong role of the dehydrogenase for limonin utilization.

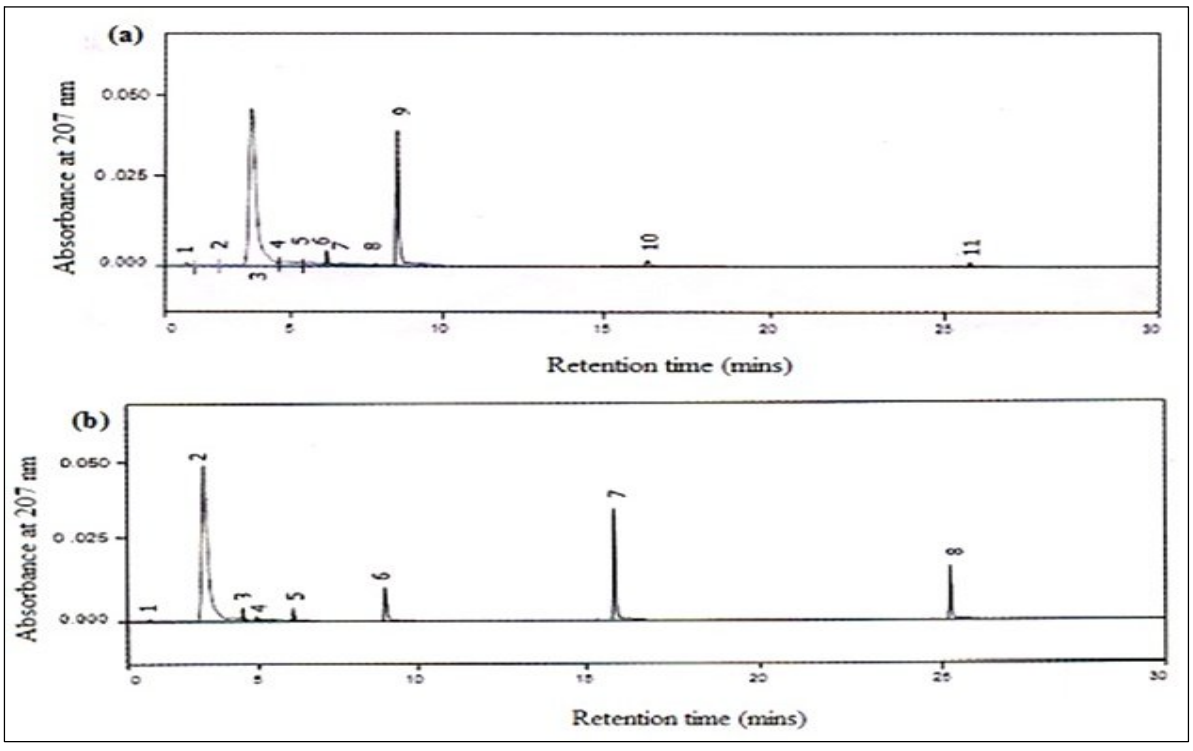

Fig. 4.27 (a) HPLC chromatogram of standard limonin (90µg/ml) and (b) chromatograms of standard limonin (90µg/ml) utilization by purified enzyme of *Pseudomonas putida* G7, using an acetonitrile/deionised water (32:68) with a flow rate 0.9 ml/min and an injection volume of 20 µl

The Kinetic parameters - maximum reaction velocity (V_{max}) and apparent Michaelis constant (K_M) were determined for purified periplasmic enzyme with respect to the limonin at 35°C by Lineweaver–Burk plot. Under optimal conditions (35ºC, pH 8.5), limonin utilization activity exhibited Michaelis–Menten type kinetics (Fig. 4.28), The Michaelis constant (K_M) measured for limonin was 4.5µM and V_{max} was found to be 8µmoles/min. At 35ºC the purified enzyme resulted in 76% degradation (Fig. 4.29a) followed by a steady state at pH 8, at lower pH values of 3-5 degradation was relatively less (Fig. 4.29b), indicating that utilization of limonin was maximum at alkaline pH 8. The purified enzyme exhibited no activity at temperatures higher than 65°C. The following activities were observed over a temperature range of 10°C - 70°C (Fig. 4.29c). In all the above cases optimal activity was attained at 35ºC in the presence of NAD^+. The ability of the periplasmic enzyme to catalyze different substrates (at an optimum pH of 7.0), was examined thereafter.

The purified dehydrogenase exhibited broad substrate specificities and catalyzed the oxidation of salicylaldehyde, 5-chlorosalicylaldehyde, *m*-nitrobenzaldehyde, *o*-methoxybenzaldehyde, formaldehyde, and glutaraldehyde. However, the relative rates at which the substituted analogs were transformed differed considerably (Table 4.12). The enzyme displayed the greatest activity for Limonin followed by salicylaldehyde; the derivatives of salicylaldehyde, 5-chlorosalicylaldehyde and m-nitrobenzaldehyde were also transformed at high rates. A variety of enzyme inhibitors was tested for their ability to inhibit the limonin biotransforming activity (Table 4.13). Addition of 1 $x10^{-3}$ EDTA did not reduce the activity whereas $HgCl_2$, SDS, $CoCl_2$ and NaN_3 reduced the enzyme activity respectively indicating the possibility that sulfhydryl group(s) may be required for activity. Divalent ions; Ca, Mg, Mn did not result in reduction of activity.

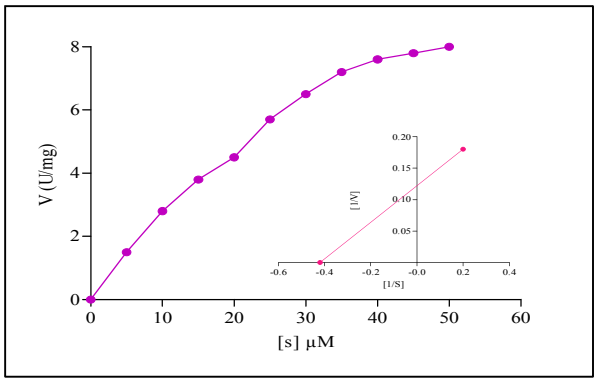

Fig. 4.28 Michaelis constant (K_M) for purified periplamic enzyme of *P. putida* G7 with respect to limonin (substrate) by Lineweaver–Burk plot at optimal conditions (35°C, pH 8.5)

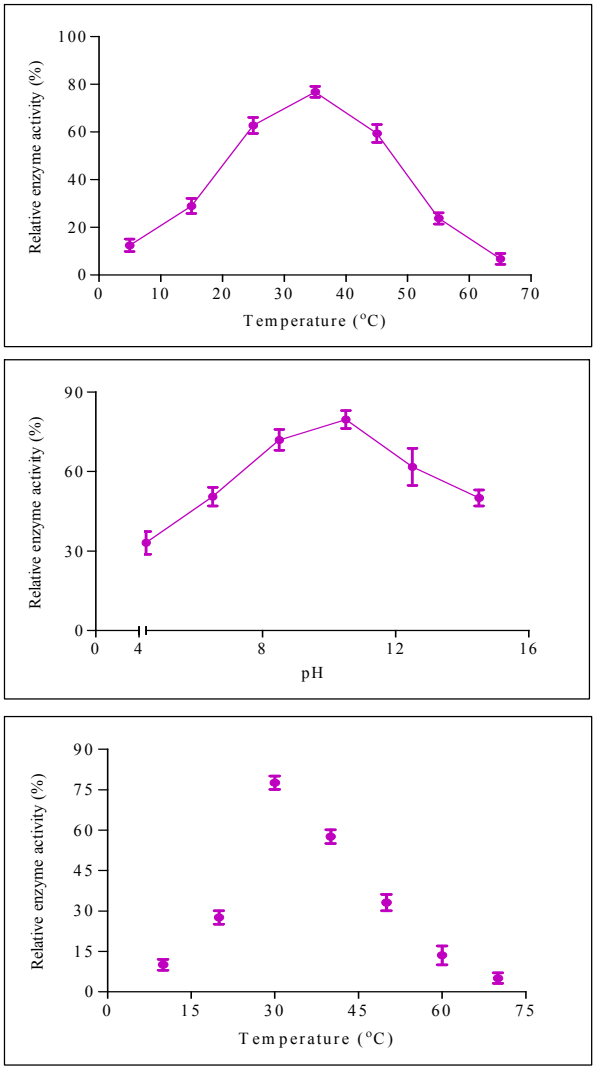

Fig. 4.29 Kinetic parameters of periplasmic dehydrogenase catalyzing limonin (a) temperature, (b) pH, and (c) its thermal stability; [a)]Values are mean of three replicates

Table 4.12 Substrate specificity of the purified enzyme

Substrate	Relative activity (%)
Limonin	100[a](±0.02)
m-nitrobenzaldehyde	23 [a](±0.07)
Salicylaldehyde	96.4 [a](±0.05)
5-chlorosalicylaldehyde	64 [a](±0.02)
Glutaraldehyde	1.8 [a](±0.03)
Formaldehyde	2.5 [a](±0.02)
o-methoxybenzaldehyde	1.5 [a](±0.01)

[a]Activities were obtained according to the standard procedure with the substrate concentration of 200 µmol/L and expressed as the percentage of the maximum activity detected (100%)

Table 4.13 Effect of inhibitors and metal ions on periplasmic dehydrogenase

Effector	Conc (mM)	Relative activity*
None	-----	100%(±0.07)
EDTA	10	100%(±0.03)
SDS	1	25%(±0.01)
NaN_3	1	ND[a](±0.05)
$HgCl_2$	1	ND[a](±0.03)
$CaCl_2$	1	100%(±0.04)
$MgCl_2$	1	100%(±0.01)
$MnCl_2$	1	98.8%(±0.07)
$CoCl_2$	1	40.2%(±0.02)

* 100% activity with limonin as substrate; [a]ND: not detected; [b] Activities were assayed according to standard procedures with the purified enzyme in the presence of various metal ions with a final concentration of 1-10 mmol/L and expressed as relative activity, as the percentage of the activity detected without metal ions (100%)

4.3.7 Identification of limonin biotransformed product

Thin Layer chromatography

It was desirable to examine the products following utilization of limonin. Thin layer chromatography is an important initial procedure for identification of biotransformed product and has been used in earlier studies for investigating degradation/utilization of limonin. The aliquots of enzyme utilizing limonin were examined at regular intervals by resolving on TLC plates along with references available commercially. Ehrlich's reagent was used to develop and detect the spots on the TLC plates: the Ehrlich test constitutes a good evidence for the presence of a furan ring in the substrate, a characteristic of limonoids, the latter produce characteristic yellowish orange spots with this reagent. R_f values were calculated for the spots and were compared with the references (Table 4.14). The neutral and acidic fractions of juice serum extracts were analyzed and results were similar to that of results obtained by analysis of 0 h culture grown in minimal media containing juice.

The neutral fraction showed three spots (one spot with R_f value of 0.54 had the same mobility to that of the standard limonin) and only one spot could be detected in acidic fraction. The neutral fraction of utilized sample resulted with a very faint spot as compared to the intense spot for standard limonin. The absence of any other spot in the neutral fraction indicated that the metabolites formed after transformation of limonin not to be present in the neutral fractions. However, when acidic fraction of the above sample was analyzed one spot was detected having R_f values similar to defuran limonin, and very faint bands of deoxylimonin, deoxylimonoic acid and 17- Dehydrolimonoate A-ring lactone. The defuran formation is shown in Fig.4.30.

Table 4.14 R_f values of the biotransformed products of limonin

Sample	Fractions	Benzene-ethanol-water-acetic acid (200:47:15:1)
Standard limonin		0.81[a]
Utilization standard limonin	Neutral fraction (Dichloromethane)	0.50 0.71
	Acidic fraction (Ethyl acetate)	0.20[c] 0.83[b] 0.41[d]
Juice serum	Neutral fraction (Dichloromethane)	0.82[a] 0.5 0.39
	Acidic fraction (Ethyl acetate)	0.87
Juice serum (Utilization limonin)	Neutral fraction (Dichloromethane)	0.52 0.74
	Acidic fraction (Ethyl acetate)	0.21[c] 0.85[b] 0.43[d]

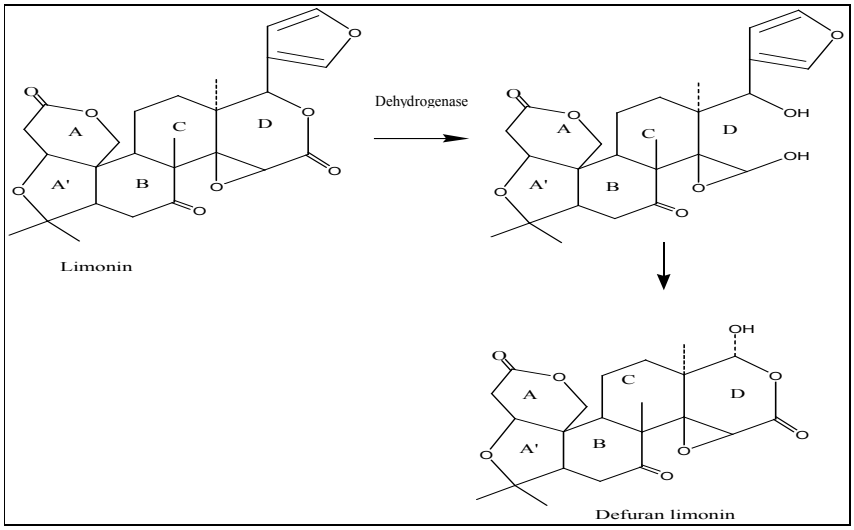

Fig. 4.30 Proposed scheme of biotransformation of limonin to defuran limonin; proposed chemical mechanism is referred in two steps: removal of defuran is facilitated by delocalization of electron on the oxygen atom of D ring lactone followed by subsequent protonation of D ring

Nuclear Magnetic Resonance(NMR) Spectroscopy

The structure of predicted biotransformed product of limonin from thin layer chromatography was confirmed by nuclear magnetic resonance (NMR) spectroscopy and the purity of the isolated limonoids was analyzed by HPLC. To elucidate the structures of the metabolites, MS, ^{1}H and ^{13}C NMR were used. The ^{1}H and ^{13}C spectra of limonin and defuran limonin with assignments of various signals are shown in Fig. 4.31a and 4.31b, respectively.

On the basis of the NMR results, the structure of the biotransformed product for limonin was tentatively identified as defuran limonin. ^{13}C NMR spectra demonstrated the signals in which "C" peaks 21, 22, 23, 4 are absent in case of defuran limonin spectra as compared to the ^{13}C NMR spectra of limonin. The "C" peak 20 in limonin spectra at position 120.0 has shifted to 170 in defuran limonin spectra. In case of ^{1}H NMR spectra the signals for "H" peaks 21, 22, 23, 15, 1 are absent in case of defuran limonin spectra. The "H" peak 17 in limonin spectra at position 5.0 have shifted before 5.0 & 4.0 in defuran limonin spectra. A new peak for 5 appeared at position 4.0 in defuran limonin spectra and absent in limonin spectra. In addition, mass spectra of the modified limonoids reported the molecular ion peak at m/z 506.2294 [M+Li]+ and 447.1145 [M- H]- for limonin and defuran limonin, respectively.

4.3.8 Antioxidant & Chemopreventive properties

Recent studies have highlighted the potential of several debitterring compounds for their bioactivity; in this regard, the antioxidant activity of limonin has been documented. Thus it was pertinent to carry out preliminary studies pertaining to bioactivity of the utilization metabolic products of limonin. A comparison to untransformed limonin was drawn in order to determine whether limonin retained its therapeutic properties upon being subjected to the microbial enzyme. The total antioxidant activities of limonin and its utilization product

(defuran limonin) was determined by scavenging ABTS radical and DPPH radical and decrease in β carotene levels. The β carotene bleaching assays revealed a decrease in

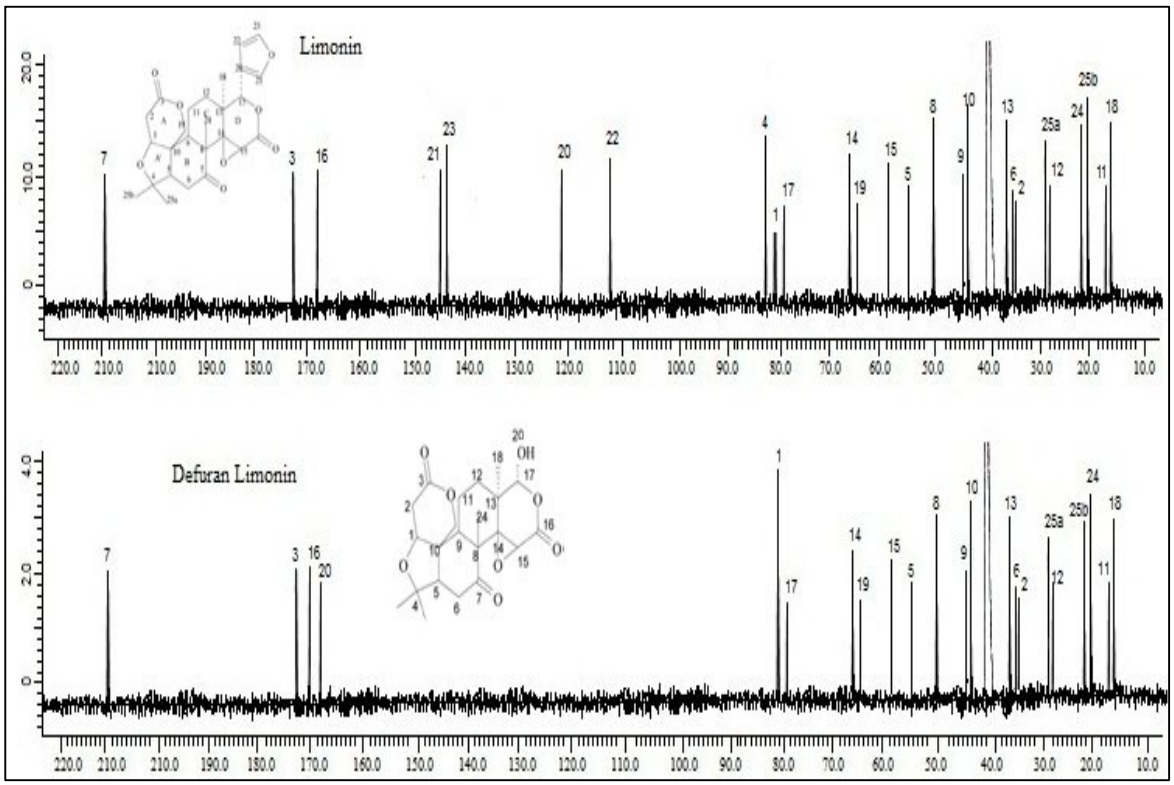

(a)

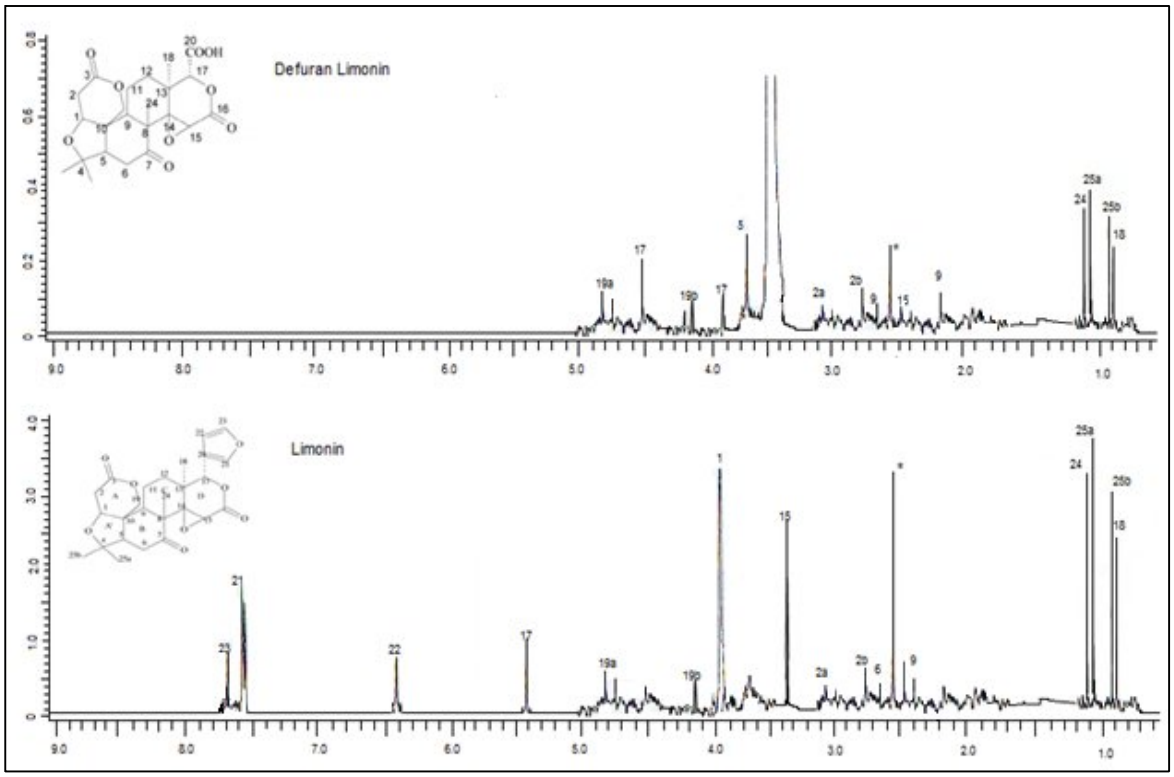

(b)

Fig. 4.31 ^{13}C (a) and ^{1}H NMR (b) spectra of biotransformed product of limonin

absorbance for up to 30% and 32% for limonin and defuran limonin (utilization product of limonin) (Fig. 4.32a). The ABTS radical reduced by 10% and 12% respectively with limonin and defuran limonin, whereas DPPH was scavenged to 13% and 11%. Superoxide radical was scavenged at a very minimal level (Fig. 4.32b). The activities of limonin and defuran limonin for the various antioxidant were approximately similar i.e. no significant changes ($p>0.05$) occurred in both DPPH, ABTS scavenging activity of limonin and defuran limonin. Thus during the enzyme mediated transformation the utilization products retained the original nutritional attributes of limonin implying the practical applicability of the enzyme for debitterring process.

(a)

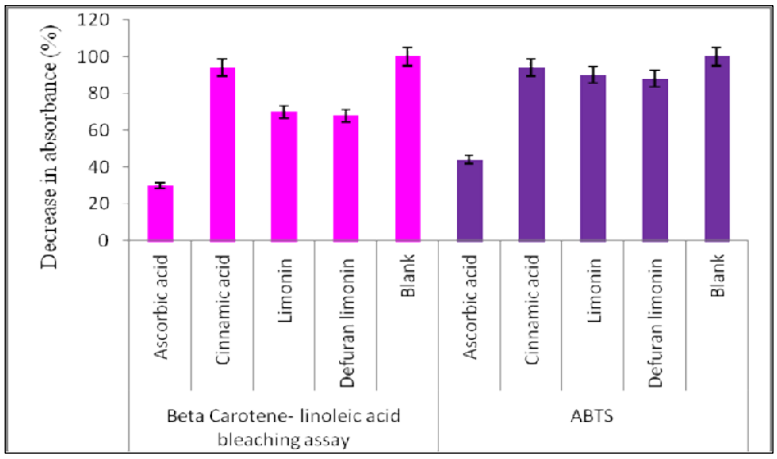

*Cinnamic acid and ascorbic acid were used as negative and positive controls respectively.

(b)

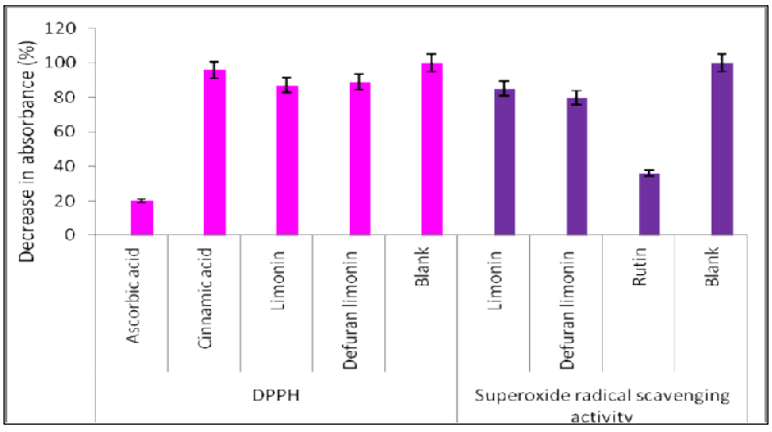

[a]Values are means ± SD, n=3, [*]Cinnamic acid and ascorbic acid were used as negative and positive controls respectively for DPPH activity. Rutin as positive control and reaction without NBT (Nitroblue tetrazolium) as negative control were used. Values are means ± SD, n=3

Fig. 4.32 Antioxidant activity of limonin and its biotransformed product determined by (a) β carotene bleaching and ABTS radical cation decolorization, (b) DPPH radical scavenging activity and superoxide radical scavenging activity

4.4 Real time application of *P. putida* G7 for debittering mandarin (citrus) juice

Since the ultimate objective of the study is to devise an approach for reducing limonin content of kinnow mandarin juices, a complete compositional analysis prior to application of *P. putida* G7 and following its application was deemed important. In order to analyze the composition, the citrus juice was extracted as described by Kola et al. 2010, and pasteurized. Pasteurization was attempted to inactivate the contaminating microbial flora and retain the inherent components of the juice. To verify whether the pasteurized juice possessed initial limonin levels as well as the nutritional components, levels of limonin were estimated in both pasteurized and unpasteurized citrus juice regularly till 12 weeks (Fig. 4.33). The limonin levels in both pasteurized and unpasteurized juices were found to be 55.63 ppm and 53.21 ppm respectively. The typical juice yield, Ascorbic acid (Vitamin C), TSS (Total soluble solids), TA (Titrable acidity) TSS/TA ratio, total sugars, microbial population, of the pasteurized and unpasteurized citrus juice are depicted in Table 4.15. An increased TSS observed with gradual increase of juice extraction might be due to hydrolysis of polysaccharides into monosaccharide and oligosaccharides. The Vitamin C content were 29.1 mg/ml and 28.7 mg/ml in both pasteurized and unpasteurized citrus juice respectively and the total juice yields of pasteurized was 30.9% and that of unpasteurized citrus juice 31.2%. These results suggested that significant ($p<0.05$) differences did not occur following pasteurization.

Kinetic studies of P. putida G7 for limonin utilization in mandarin juice

Kinetic studies are important for understanding the response of the bacterial cell towards any specific compound or carbon source. The kinetics of *P.putida* G7 was determined in mandarin juice and minimal medium with limonin as sole source of carbon. The cells

exhibited a growth rate of 0.23 h^{-1}, as much as 45% limonin utilization was noted. (Fig. 4.34); utilization of limonin was not observed during stationary phase.

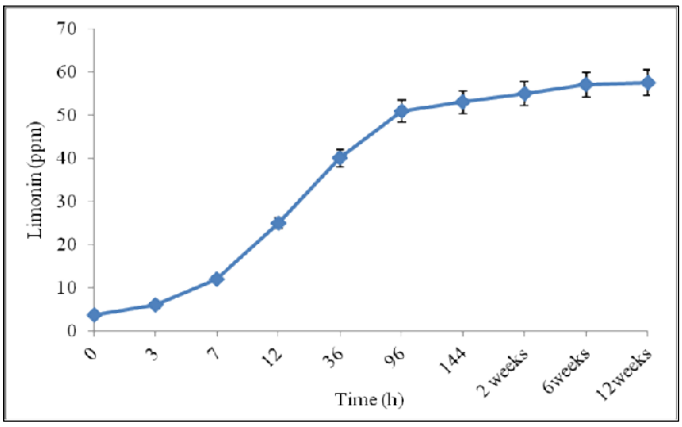

Fig. 4.33 Limonin content with ageing of juice

Table 4.15 Physiochemical properties of mandarin juice

Quality parameter	Mandarin juice (Pasteurized)	Mandarin juice (UnPasteurized)
Juice yield (%)	30.93 ± 1.07	31.2± 1.12
TSS (g L^{-1})	118.67 ± 1.31	121.67 ± 1.11
TA (g L^{-1})	61.42 ± 1.44	60.76 ± 1.05
TSS/TA ratio	1.9 ± 0.03	1.7 ± 0.05
Vitamin C (mg mL^{-1})	29.1 ± 0.41	28.7± 0.37
Total Phenolics	778 mg GAE L^{-1}	775 mg GAE L^{-1}
Total Flavonoids	53.7 mg CE L^{-1}	54.1 mg GAE L^{-1}
Total Sugars	7.6%	7.1%
Bacterial population(cfu/ml)	3	$9.1x10^3$
Yeast population(cfu/ml)	1	$4.3x10^3$
Mould population(cfu/ml)	0	$3.2x10^3$

[a]Results are expressed as means ± standard deviation of three measurements. Means followed by a different letter are significantly different.

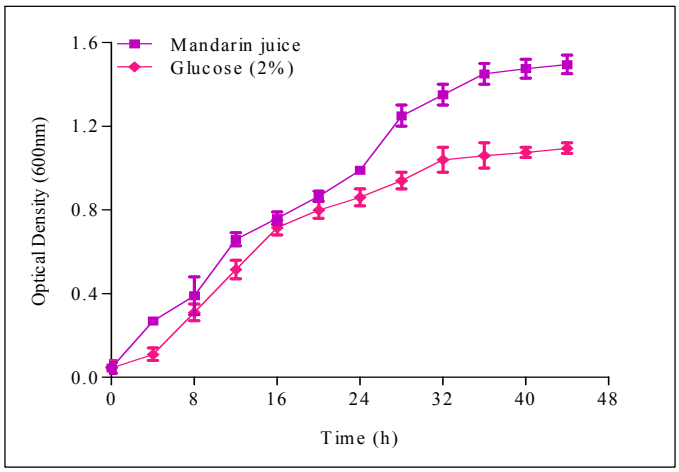

Fig. 4.34 Growth kinetics and limonin utilization profile of *P. putida* G7 in mandarin juice and in minimal medium with limonin as sole source of carbon

4.4.1 Cell immobilization of P. putida G7 to enhance limonin biotransformation

In order to efficiently immobilze bacterial cells various parameters were optimized. Among the various preliminary experiments performed for the selection of process parameters effecting limonin biotransformation in citrus juice, alginate concentration, cell load and bead diameter were screened as the most significant parameters for maximal limonin biotransformation by immobilized *P. putida* G7. Limonin in citrus juice was biotransformed upto 40% and 58% with *P. putida* G7 cells (cell load of 50 mg/ml) immobilized in agar and alginate respectively (Fig. 4.35). Biotransformation response with cell immobilized in agar (concentration of 2.5% and bead diameter of 2.0 mm) was lower i.e. 30% as compared to the cells immobilized in alginate (concentration of 3% and bead diameter of 2.5 mm) which showed a response of 57% in citrus juice (Fig. 4.36). Based on the response of conventional studies, alginate was preferred as a matrix for immobilizing *P. putida* G7 cells to direct the further studies for limonin biotransformation in citrus juices.

Statistical analysis

The combined effect or the inter-relationship of the parameters for limonin biotransformation response was observed with a face centered cube design of 2^3=8 + 6 centre points and 6 (2x3) star points which lead to a total of 20 experiments. The coded value of the selected variables is present in Table 4.16. Based on the optimization of process parameters and the experimental results (obtained from CCD and regression analysis) (Table 4.17), the relationship between the limonin biotransformation and the significant parameters (alginate concentration, cell load and bead diameter) was established in the form of a quadratic polynomial equation. The equation for the model in terms of coded factors is present in Table 4.18.

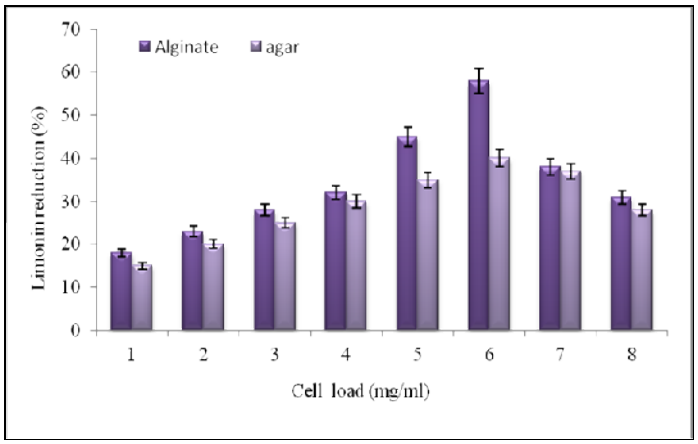

Fig. 4.35 Effect of cell load (w/v) in alginate beads on limonin reduction

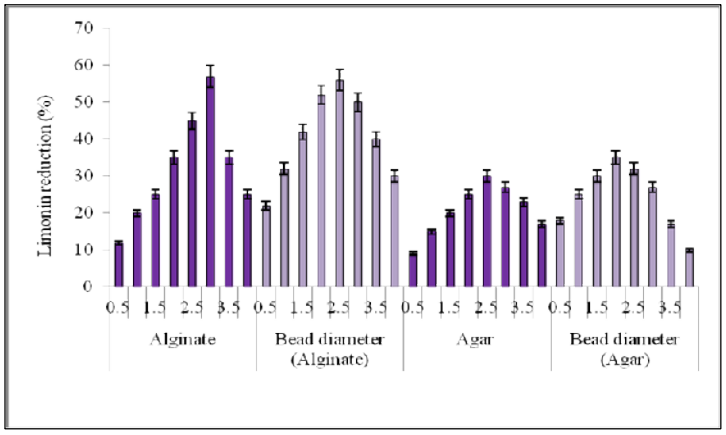

Fig. 4.36 Effect of concentration of alginate, agar and their respective bead size for immobilizing *P. puitda* G7 cells on limonin reduction

Table 4.16 Coded values of all the significant variables selected

Variables	Coded Values				
	-α	-1	0	+1	+ α
A- Alginate concentration (%, w/v)	0.32	1	2	3	3.68
B- Cell load (mg/ml)	36.5	40	45	50	53.41

C-Bead diameter (mm)	1.16	1.5	2	2.5	2.84

Table 4.17 Response surface central composite design (CCD) for limonin biotransformation

Run	A	B	C	R1-Limonin Biotransformation(%)		R2 - Stability	
				Actual	Predicted	Actual	Predicted
1	2.00	36.59	2.00	50.1	50.45	0.092	0.10
2	0.32	45.00	2.00	63.8	62.47	0.089	0.094
3	2.00	45.00	1.16	55.6	57.54	0.126	0.13
4	1.00	40.00	2.50	56	56.12	0.12	0.11
5	2.00	45.00	2.00	64.5	64.43	0.11	0.11
6	2.00	45.00	2.00	64.3	64.43	0.11	0.11
7	2.00	45.00	2.00	64.4	64.43	0.11	0.11
8	3.00	40.00	1.50	61.8	59.17	0.16	0.15
9	3.00	50.00	2.50	60.6	59.74	0.145	0.14
10	1.00	40.00	1.50	49.7	50.42	0.07	0.072
11	1.00	50.00	1.50	62.7	61.49	0.13	0.12
12	2.00	45.00	2.00	64.4	64.43	0.1	0.11
13	3.00	50.00	1.50	60.1	59.83	0.138	0.15
14	2.00	53.41	2.00	59.2	59.05	0.132	0.13
15	3.00	40.00	2.50	59.5	60.57	0.15	0.15
16	2.00	45.00	2.00	64.5	64.43	0.11	0.11
17	3.68	45.00	2.00	63.3	64.83	0.15	0.15
18	1.00	50.00	2.50	63.2	65.69	0.138	0.14
19	2.00	45.00	2.84	64	62.25	0.15	0.15
20	2.00	45.00	2.00	64.5	64.43	0.11	0.11

[a]A-Alginate concentration, B- Cell Load, C- Bead diameter, R1-Limonin Biotransformation (%), R2- Stability (O.D. 600 nm)

Table 4.18 Model equation for limonin biotransformation by *P.putida* G7

Limonin biotransformation (R1) = $+64.43 + 0.70 * A + 2.56 * B + 1.40 * C - 2.60 * A * B - 1.07 * A * C - 0.37 * B * C - 0.28 * A^2 - 3.42 * B^2 - 1.60 * C^2$

Where Y is the response value for limonin biotransformation (%), A- Alginate concentration, B- Cell Load, C- Bead diameter

The analysis of variance (ANOVA) of the model for limonin biotransformation are presented in Table 4.19. The F value (14.97) of the model signifies the significane of the model and there was only 0.01 % chance that the model F value must have occurred due to noise.

Regression analysis results has revealed R^2 (coefficient of determination, and the value more closer to 1 indicates the model fit of the experimental data) value of 0.9309, which signifies that the model was enable to explain only 7% of the total variations. The adjusted R^2 (adjusted determination coefficient) value of 0.8687 was quite high which indicates the high reliablity of the model and the quadratic polynomial equation. The values of "Prob>F" of the model far less than 0.05, indicates the significant and desirability of the model terms. The "Lack of Fit F-value" of 843.93 implies the Lack of Fit is significant. There is only a 0.01% chance that a "Lack of Fit F-value" this large could occur due to noise. "Adeq Precision" measures the signal to noise ratio (a ratio greater than 4 is desirable) and the ratio of 12.862 indicates an adequate signal. A low value of CV (coefficient of variation) of 2.76% signifies a high degree of precision and a good deal of realiablity of the experimental values. According to this model, the significant parameters A-B has shown the highest interaction effect, followed by A-C and B-C with the least interaction, for the maximal response of limonin biotransformation.

The experimental relationship between stability of the beads (response) and the three significant parameters in the coded values is presented in Table 4.17. This response is of great importance in estimating the bead scabrousness for their potential to withstand mechanical stress. The analysis of variance (ANOVA) for this model is presented in Table 4.20. The F value (14.97) of the model signifies the significane of the model and there was only 0.01% chance that the model F value must have occurred due to noise. The model equation is present in Table 4.21.

Regression analysis results presenting the R^2 (coefficient of determination) and adjusted R^2 (adjusted determination coefficient) values of 0.9253 and 0.8581 respectively, was quite high which indicates the high reliablity of the model and the quadratic polynomial equation. The values of "Prob>F" of the model far less than 0.05, indicates the significant and desirability

of the model terms. The "Lack of Fit F-value" of 5.31 implies the Lack of Fit is significant and the corresponding 0.01% chance that a "Lack of Fit F-value" this large could occur due to noise. "Adeq Precision" ratio value of 12.683 indicates an adequate signal which signifies a high degree of precision with a good deal of reliablity of the experimental values. According to this model, the significant varibales A-B has shown the highest interaction effect, followed by A-C and B-C with the least interaction, for the maximal response of high stability of the alginate beads.

Table 4.19 Analysis of variance (ANOVA) for limonin biotransformation

Source	Sum of squares	df	Mean square	F value	p-value Prob>F	
Model	379.49	9	42.17	14.97	0.0001	significant
A-Alginate concewntration (%)	6.69	1	6.69	2.38	0.1543	
B-Cell load (%)	89.21	1	89.21	31.67	0.0002	
C-Bead diameter (mm)	26.79	1	26.79	9.51	0.0116	
AB	54.08	1	54.08	19.20	0.0014	
AC	9.24	1	9.24	3.28	0.1001	
BC	1.12	1	1.12	0.40	0.5416	
A^2	1.09	1	1.09	0.39	0.5476	
B^2	168.74	1	168.74	59.91	<0.0001	
C^2	36.94	1	36.94	13.12	0.0047	
Residual	28.16	10	2.82			
Lack of Fit	28.13	5	5.63	843.93	< 0.0001	significant
Pure Error	0.033	5	6.667E-003			
Cor Total	407.66	19				

Table 4.20 Analysis of variance (ANOVA) for stability

Source	Sum of squares	df	Mean square	F value	p-value Prob>F	
Model	0.010	9	1.157E-003	13.76	0.0002	significant
A-Alginate conc. (%)	*4.133E-003*	*1*	*4.133E-003*	*49.16*	*< 0.0001*	
B-Cell load ( )	*1.024E-003*	*1*	*1.024E-003*	*12.18*	*0.0058*	
C-Bead diameter (mm)	*6.659E-004*	*1*	*6.659E-004*	*7.92*	*0.0183*	
AB	*1.378E-003*	*1*	*1.378E-003*	*16.39*	0.0023	

AC	*4.651E-004*	*1*	*4.651E-004*	*5.53*	0.0405	
BC	*7.812E-005*	*1*	*7.812E-005*	*0.93*	0.3578	
A^2	*5.289E-004*	*1*	*5.289E-004*	*6.29*	0.0310	
B^2	*1.672E-004*	*1*	*1.672E-004*	*1.99*	0.1888	
C^2	*2.288E-003*	*1*	*2.288E-003*	*27.21*	0.0004	
Residual	8.407E-004	10	8.407E-005			
Lack of Fit	*7.074E-004*	*5*	*1.415E-004*	*5.31*	*0.045*	significant
Pure Error	*1.333E-004*	*5*	*2.667E-005*			
Cor Total	0.011	19				

Table 4.21 Model equation for limonin biotransformation by *P.putida* G7 with optimum levels of significant variables in minimal medium

Stability (R2) = +0.11 +0.017*A + 8.660E - 003*B + 6.983E-003*C - 0.013*A*B - 7.625E-003*A*C -3.125E-003*B*C + 6.058E-003*A^2 +3.407E - 003* B^2 + 0.013*C^2
Where Y is the response value for limonin biotransformation (%), A- Alginate concentration, B- Cell Load, C- Bead diameter

RSM analysis

The response model developed was further represented in the form of contour plots for a better understanding of the interaction among the three significant parameters and for the detection of the optimum level of each parameter for a maximum response. The contours plot showed the interaction of two independent parameters when the third parameter is fixed at zero (Fig 4.37 a-c), which represents the limonin biotransformation response. Limonin biotransformation increases moderately with increasing alginate concentration from 2% to 3% (w/v), with a high increase in cell load results in high biotransformation (Fig. 4.37 a). Fig. 4.37 b demonstrates that response increases moderately with increase in bead diameter and alginate concentration. An increased response was observed with increase in cell load, and bead diameter (Fig. 4.37c).

The contours for stability with regard to the significant parameters of alginate concentration, cell load, and bead diameter are presented in Fig. 4.38 a-c. Fig. 4.38a shows that higher stability could be obtained at a moderate alginate concentration and low cell load. Fig. 4.38b

indictates that stability increases with an increased bead diameter and at a moderate alginate concentration. Low cell load and a moderate bead diameter directs towards an increased response for stability (Fig. 4.38c).

Validation of the model

The experimental model was validated by considering both activity and stability for a high limonin biotransformation and low OD600 nm responses, with the help of the regression equation. The experimental reactions (100 ml Erlenmeyer flask containing 50 ml citrus juice)

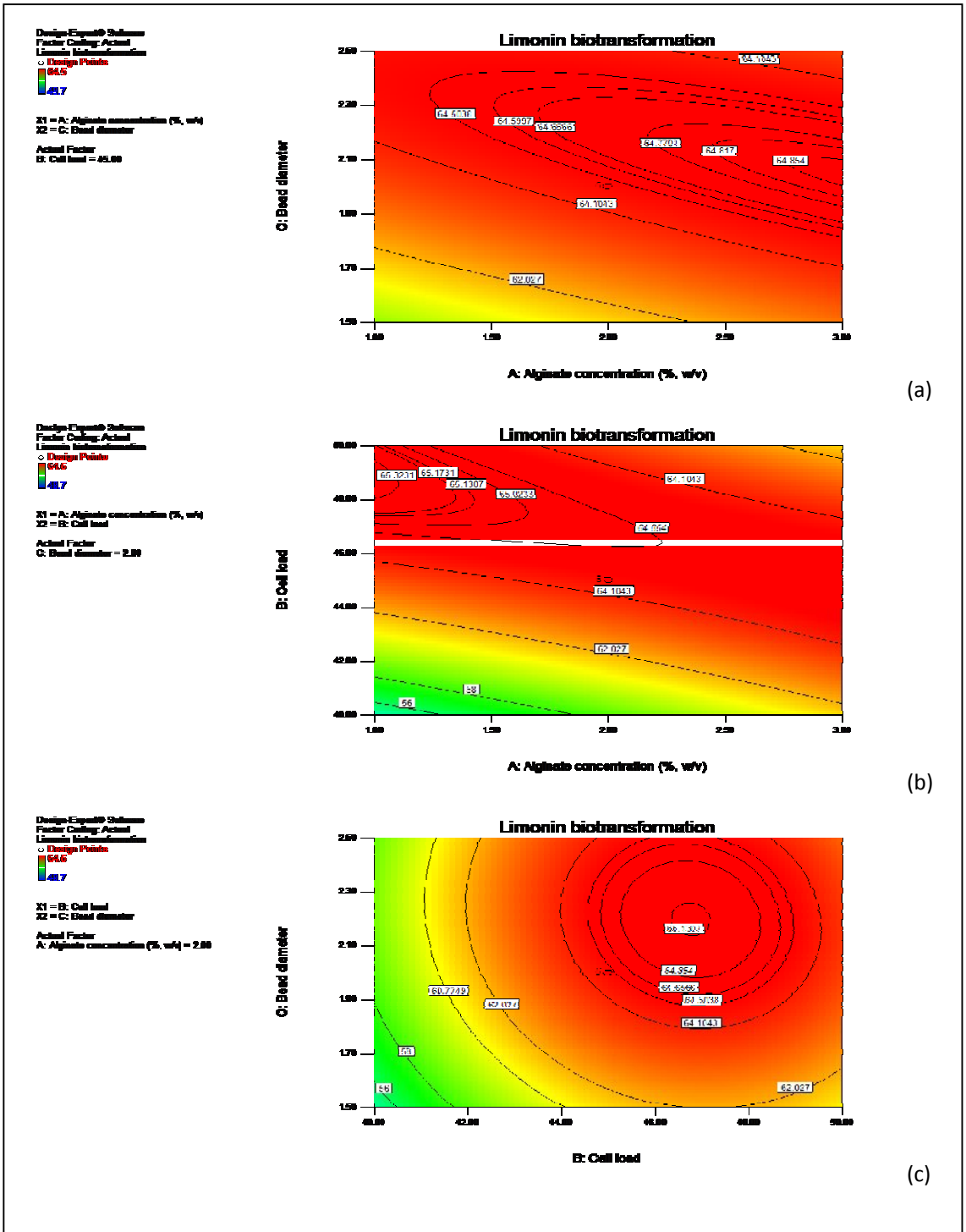

Fig. 4.37 Contour plots showing the combined effects of the significant variables for whole cell immobilization in terms of limonin bioconversion; (a) Interaction effect between alginate concentration and bead diameter (b) alginate concentration and cell load; (c) interaction effect between cell load and bead diameter

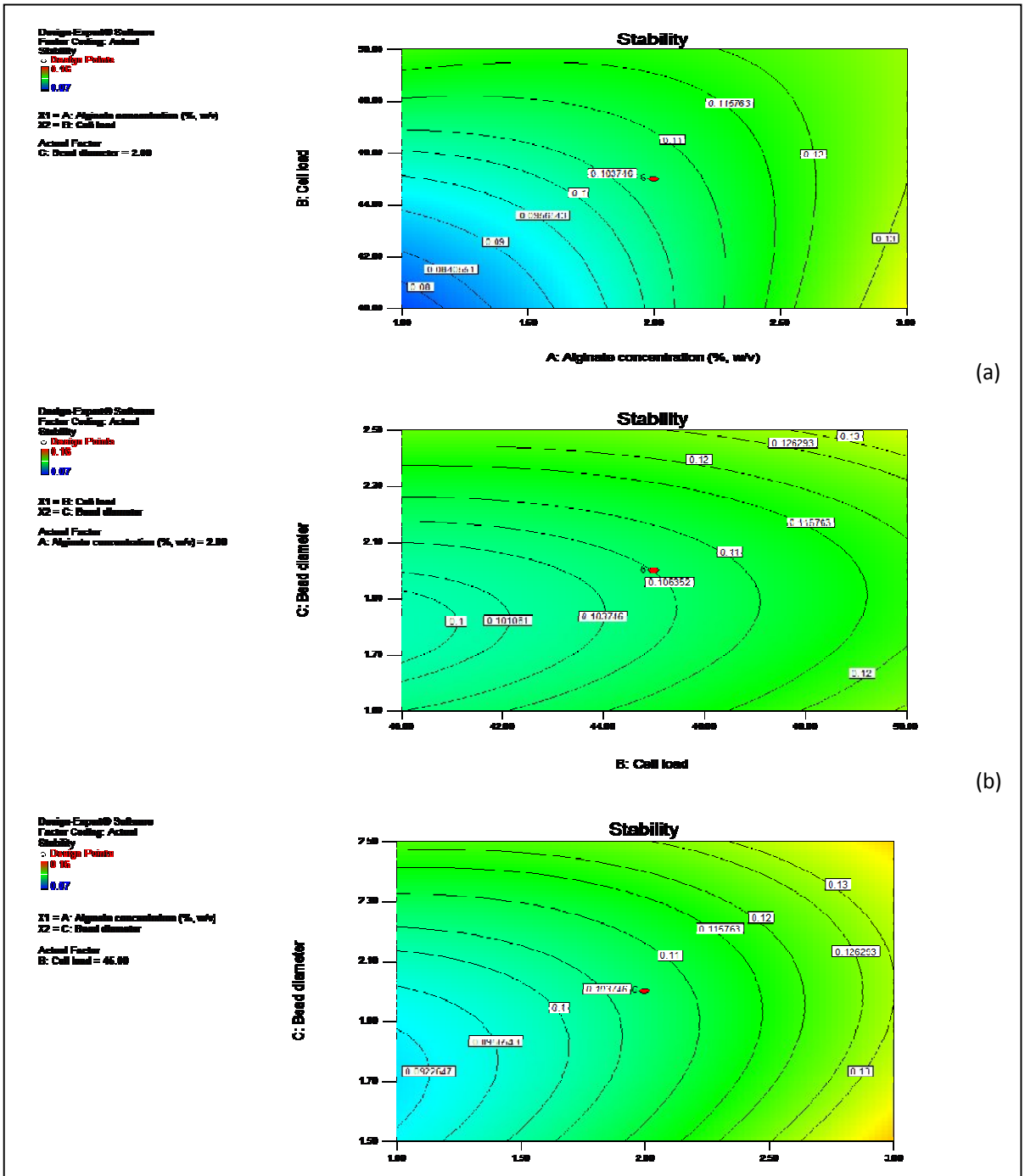

Fig. 4.38 Contour plots showing the combined effects of the significant variables for bead stability in terms of limonin bioconversion; (a) Interaction effect between alginate concentration and cell load (b) alginate concentration and bead diameter; (c) interaction effect between alginate concentration and bead diameter

with immobilized cells for the maximum response included an alginate concentration of 2%, a cell load of 47.2 g/l, and a bead diameter of 2.1 mm. The predicted values for the maximum response of limonin biotransformation and stability giving these conditions were 65.1% and 0.094 respectively. The experiments were conducted in triplicates and maximum response with all the optimized conditions were 65.8% and 0.97 OD.

Reusability and stability of immobilized cell

The reusability of the immobilized cells *P. putida* G7 was compared with free cells (20 beads, equivalent to 47 mg/ml cells and free cells - 47 mg/ml cells), for the evaluation of limonin biotransformation under the optimized parameters, at the original pH of citrus juice (4 pH) and at 35°C. The immobilized bacterial cells and free cells were evaluated for their biotransformation potential in successive cycles. After each cycle the alginate beads were filtered and the free cells were collected by centrifugation, washed with saline and phosphate buffer and were then reused for limonin biotransformation in the next set of citrus juice. All the reactions conditions were kept constant for every batch cycle. The biotransformation reaction was carried out for 3 hr and the bioconversion during each cycle by immobilized and free cells is presented in Fig. 4.39. The results depict a faster bioconversion and high reusability (till 8th cycle) of immobilized cells as compared to free cells (till 5^{th} cycle).

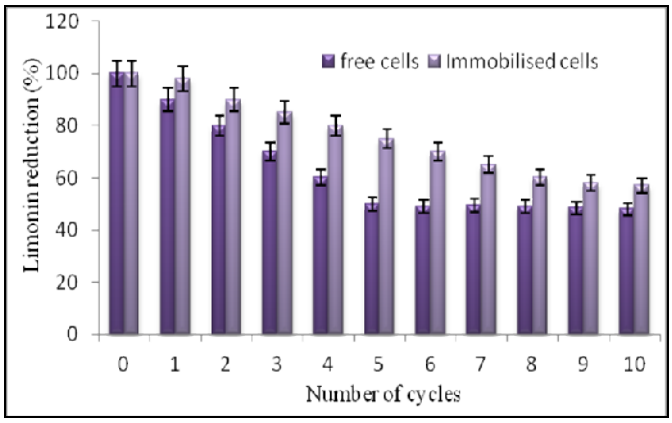

Fig. 4.39 Reusability and stability of free and immobilized cells of *P. putida* G7 for limonin biotransformation

4.4.2 Permeabilization of whole cells

The limonin utilization trend by whole cells as well as limonin utilization by purified enzyme prompted for processes which could substantially enhance enzyme substrate interaction. To this end, cell permeabilization a simple and effective technique have been advocated in several biotechnological processes in recent times. Whole cell permeabilization of *Pseudomonas putida* G7, Na_2EDTA proved to be the most potential permeabilizing agent as compared to the other permeabilizing agents like organic solvents (toluene, chloroform, benzene, hexane), 1% for the detergents (CTAB, SDS, Triton X-100) and proteases. The potentiality was expressed in terms of limonin utilization activity, which was found to be the maximum when 1 µM of Na_2EDTA was used as permeabilizing agent. The results on the effect of different methods of permeabilization of *P. putida* G7 cells on reduction of limonin were shown in Fig. 4.40. The incubation of cells for a period of 10 minutes were considered as optimum since viability (monitored by periodically plating appropriately diluted aliquots onto Nutrient agar plates; results not shown) and enzyme activity were lost when cells were incubated beyond the given time. Permeabilization with Na_2EDTA enhanced the enzyme activity up to 11.8 folds compared to the normal cells, within 3 hours. The SEM and TEM profiles of cells permeabilized Na_2EDTA are presented in Fig. 4.41 & 4.42**,** which

demonstrates the effect of permeabilizing agent on the cell wall as compared to the unpermeabilzed counterpart (control).

Limonin utilization kinetics by free permeabilized cells

Limonin utilization by the permeabilized cells of *P. putida* G7 were insignificant ($p<0.05$) in comparison to the unpermeabilized cells of *P. putida* G7 (Table 4.22). The limonin utilization by the permeabilzed cells in M63 medium as well as in mandarin juice (containing equivalent quantities of limonin) revealed a similar trend, though a difference in utilization rates were observed (70% and 50% respectively). Permeabilized biomass of 1g dry weight was

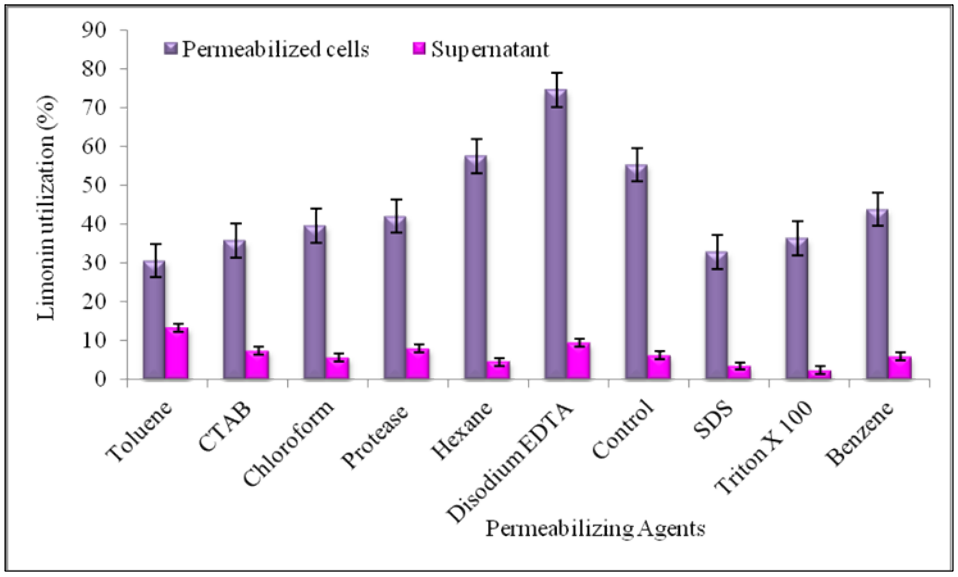

Fig. 4.40 Comparison of different permeabilization methods to evaluate the reduction in limonin by *P. putida* G7. The reactions with the various methods were incubated for 1 hour at 37°C, 200 rpm. Limonin estimation was performed at 35°C. Results are mean of three independent replicates

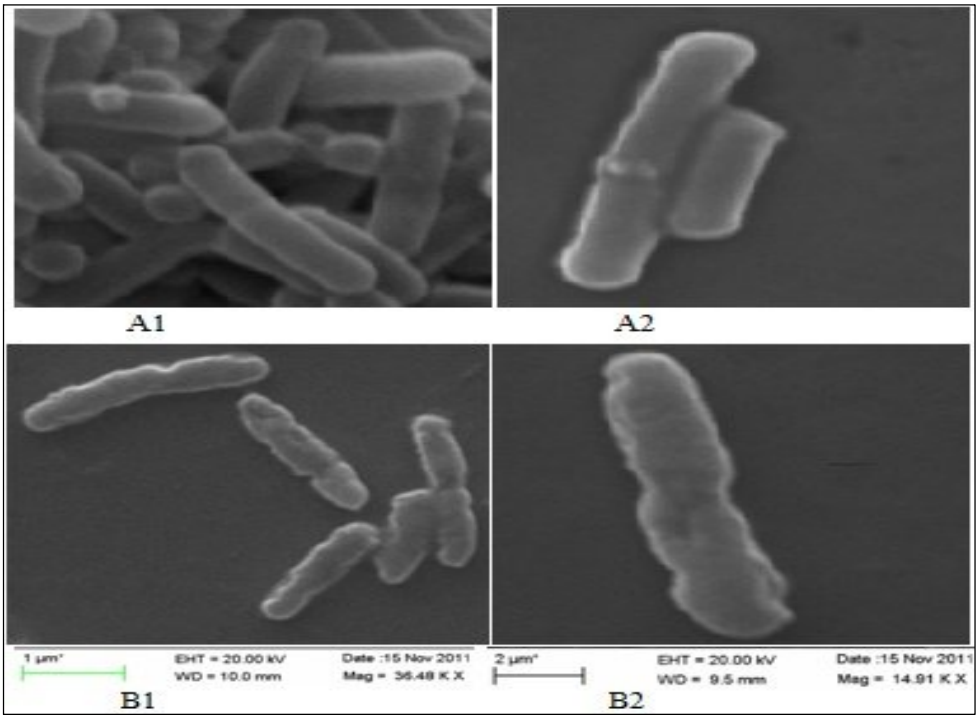

Fig. 4.41 Scanning Electron Micrograph of *P. putida* G7 after whole cell permeabilization; A1 and A2 shows the whole cell(s) before treatment (unpermeabilized cells); and B1and B2 shows the cell(s) (unpermeabilized cells) after treatment with disodium EDTA

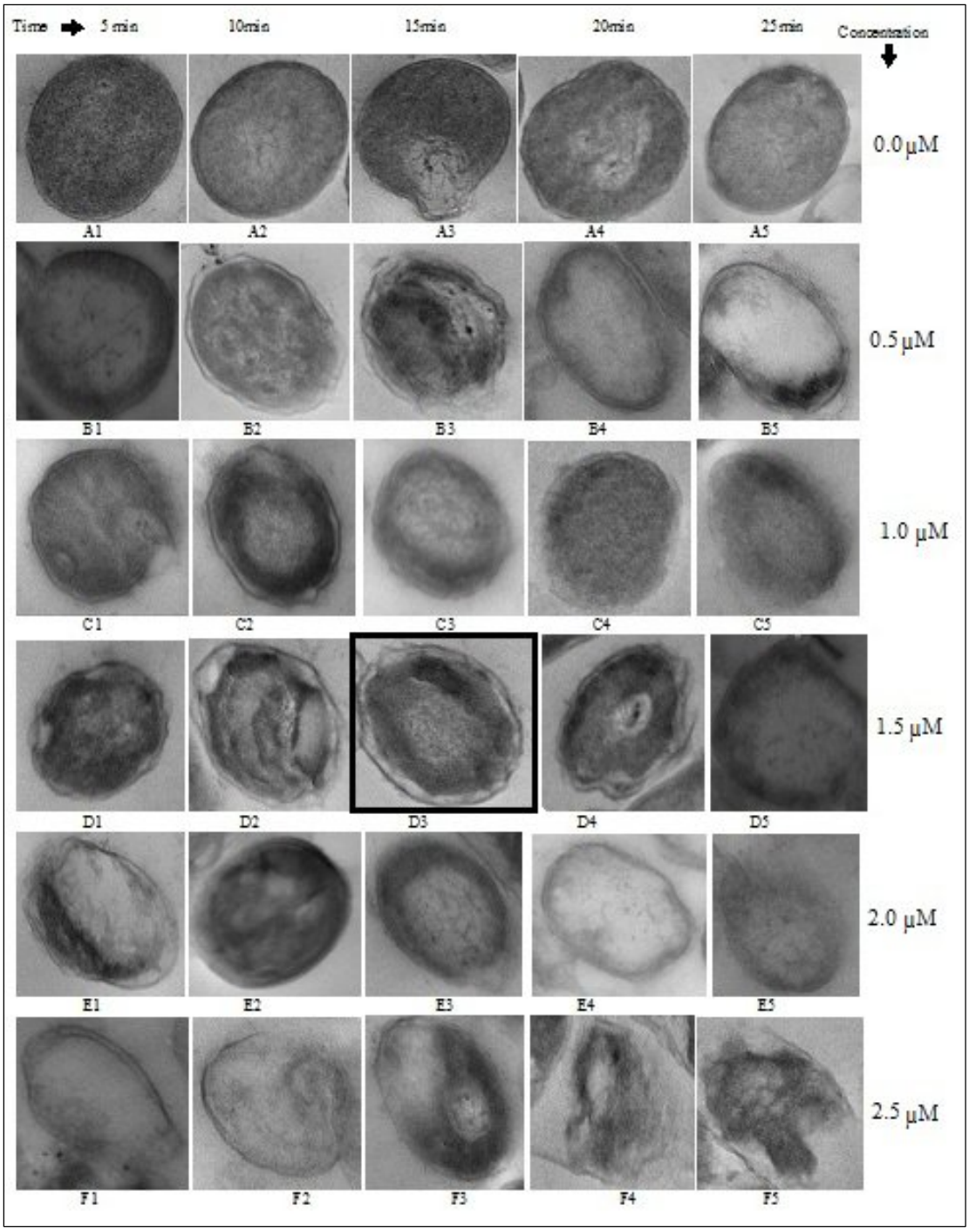

Fig. 4.42 Transmission Electron Micrograph of permeabilized cells for optimization of permeabilization process; cells were permeabilized with a EDTA concentration range of 0.5 µM – 2.5 µM and incubated at a time interval of 5 min – 25 min respectively; permeabilized cell (D3) was the most optimum condition for permeabilization which showed the maximum enzyme activity for limonin bioconversion

considered optimum in terms of limonin utilization, whereas increasing biomass concentration did not lead to higher utilization rate.

Performance of dialysis membrane entrapped permeabilized cells

The performance of limonin utilization was studied in an experimental set up shown in Fig. 4.43, where the permeabilized cells of *P. putida* G7 were entrapped inside dialysis membrane. The efficiency of the reduction of limonin was examined both in minimal medium and in mandarin juice comprising of equivalent amounts of limonin. The transformation of limonin by the permeabilized cells was found to be higher in the minimal medium containing pure limonin than that observed in the mandarin juice (i.e. 76.45% and 73.23% respectively). The maximum reduction was achieved within 180 minutes of incubation of permeabilized cells inside the dialysis sac. No reduction was observed thereafter (Fig. 4.44), whether the reduction of limonin was solely due to utilization, was evaluated by estimating limonin within the sac with or without cells. Limonin was not detected inside the dialysis sac during experiments, also the empty dialysis sacs incubated in juice for a similar time span indicated that removal of limonin was not due to adsorption (Fig. 4.44).

Table 4.22 Limonin utilization by permeabilized and unpermeabilized cells of *P. putida* G7

	Mandarin juice		M 63 minimal medium *	
Biomass (/g drywt)	**Unpermeabilised**	**Permeabilised**	**Unpermeabilised**	**Permeabilised**
0.5	22.97(±0.04)	46.59(±0.03)	36.23(±0.05)	65.89(±0.03)
1.0	50.71(±0.05)	68.67(±0.04)	54.68(±0.04)	70.88(±0.05)
2.0	51.08(±0.03)	69.01(±0.02)	55.09(±0.04)	71.01(±0.06)

[a]Unpasteurized mandarin juice and M63 medium (200ml volume with limonin concentrations in a range of 50 µg/ml) were treated with permeabilized and unpermeabilized cells, incubated at 30°C for 6 hours, for limonin utilization

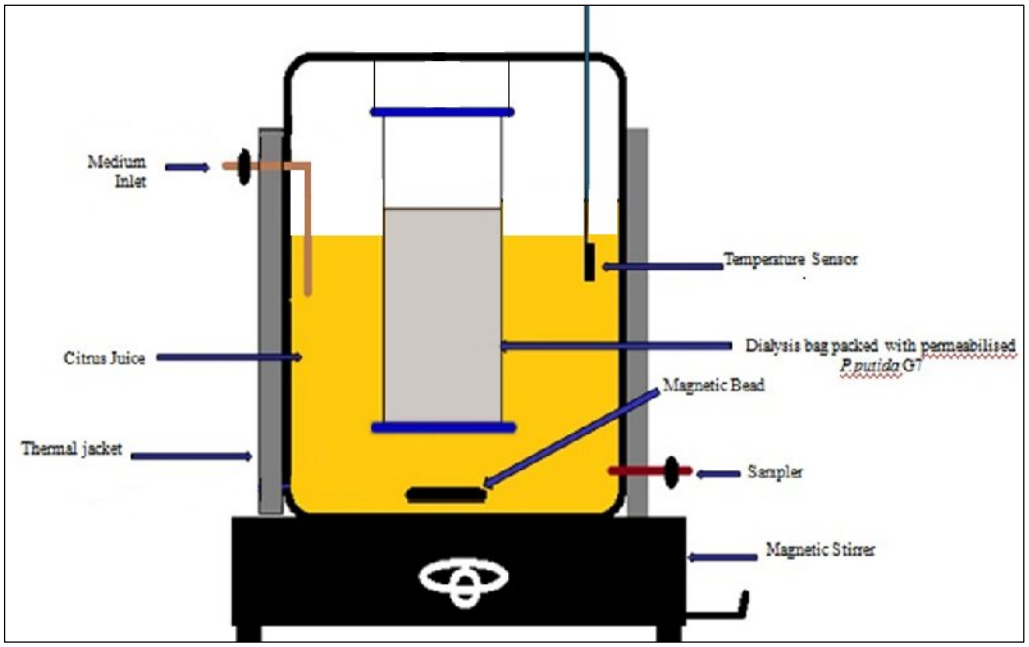

Fig. 4.43 Experimental setup for the study of limonin utilization by the dialysis membrane entrapped permeabilized *P. putida* G7. Volume of the mandarin juice in the vessel was 200ml; temperature was monitored using temperature controller

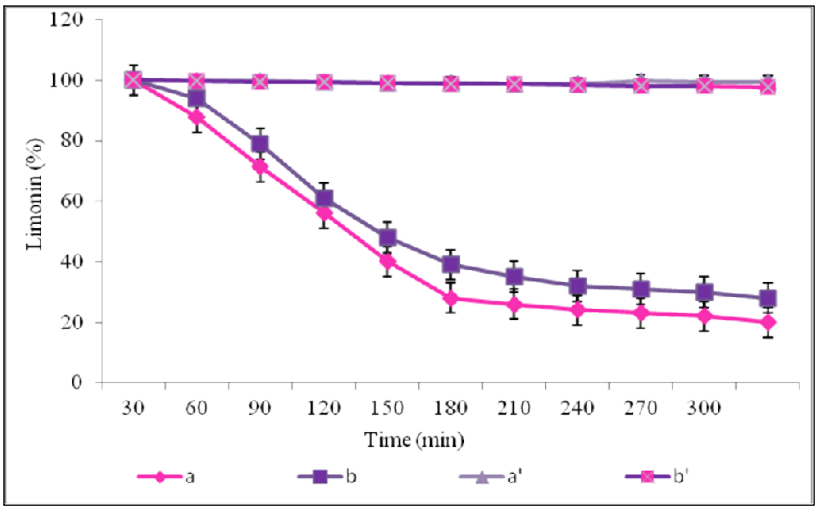

Fig. 4.44 Limonin utilization kinetics by permeabilized entrapped cells in minimal medium (M63) supplemented with equivalent amounts of (a) limonin, (b), mandarin juice, (a') Adsorbed limonin in empty dialysis sac in M63 minimal medium and (b') Adsorbed limonin in empty dialysis sac in Mandarin juice. Results are mean of three independent replicates

Evaluation of limonin content by HPLC

To authenticate limonin utilization, HPLC was used for estimating the residual limonin levels. A prominent peak, at a retention time of 9.3 minutes was obtained for standard limonin (Fig. 4.45a). The utilization was evidenced from the appearance of two new peaks at retention times of 15.9 and 25.2 minutes (Fig. 4.45b). The area under the curve that represented limonin peak was reduced in the utilization sample. As illustrated in Fig. 4.46, compared to the peak area of 62% and 66% of respective controls of juice serum and standard limonin in the medium, the utilization resulted in reduction in peak area to 19.08% and 8.23% respectively. However, a complete disappearance of limonin peak was not observed due to the residual limonin in the medium and these limonin levels (<5ppm) were far less than the sensorial property of the consumer. Further, in Fig. 4.46, the peak areas 39.64 % and 27.03% corresponded to utilization of limonin by the unpermeabilised free cells in juice serum and in medium containing standard limonin respectively. The entrapped permeabilized *P. putida* G7 cells stored in PBS at room temperature and 30°C for 45 days exhibited no loss in its limonin removal efficiency for subsequent 8 batch cycles (Fig. 4.47) and a decline was observed thereafter, probably due to inactivation of the enzyme. These results indicated the stability of the enzymes and hence reusability of permeabilized cells. The dialysis entrapment method thus proved to be quite effective for removing limonin.

Response surface modeling for maximum limonin bioconversion

Response surface methodology (RSM) with central composite rotatable design (CCRD) was chosen to optimize the significant variables (Na_2EDTA concentration, pH, time duration and temperature) for permeabilisation of *P. putida* G7 cells. The coded levels for independent variables are presented in Table 4.23. The mean predicted and experimental bioconversion activity are presented as a response, as detected by central composite rotatable design experiments (Table 4.24).

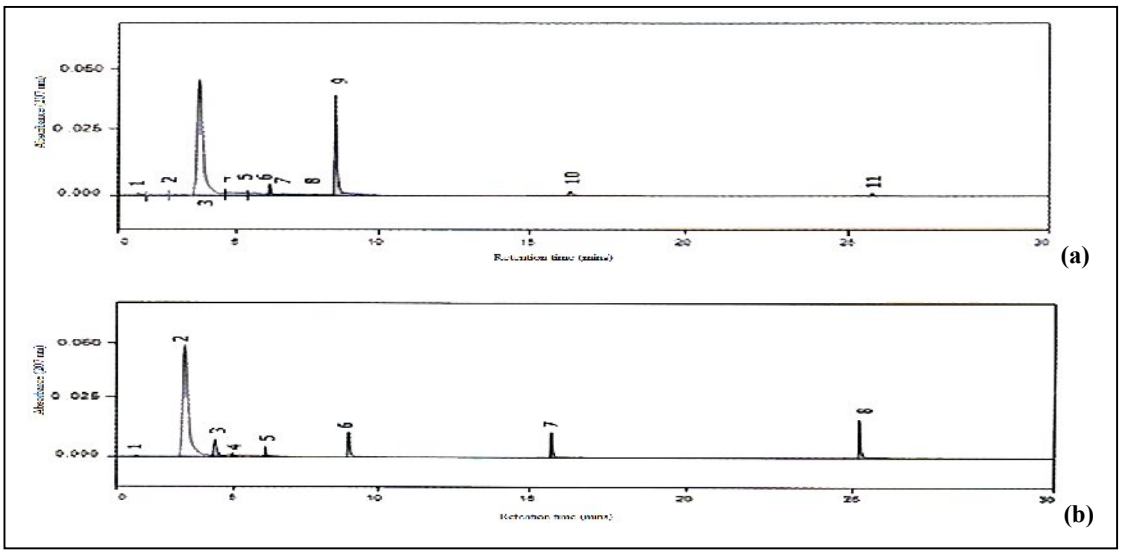

Fig. 4.45 (a) HPLC chromatogram of standard limonin (90µg/ml) and (b) chromatogram of standard limonin (90µg/ml) utilization by permeabilised cells of *P. putida* G7, using an acetonitrile/deionised water (32:68) with a flow rate 0.9 ml/min and an injection volume of 20 µl

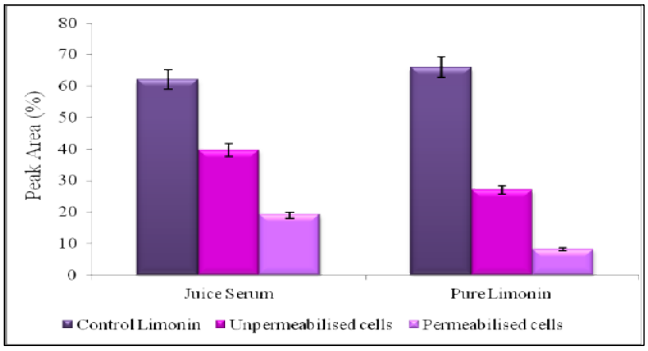

Fig. 4.46 Comparison of limonin utilization using permeabilised and unpermeabilised cells of *Pseudomonas putida* G7 in standard limonin and mandarin juice by HPLC in terms of peak area (%) for residual limonin

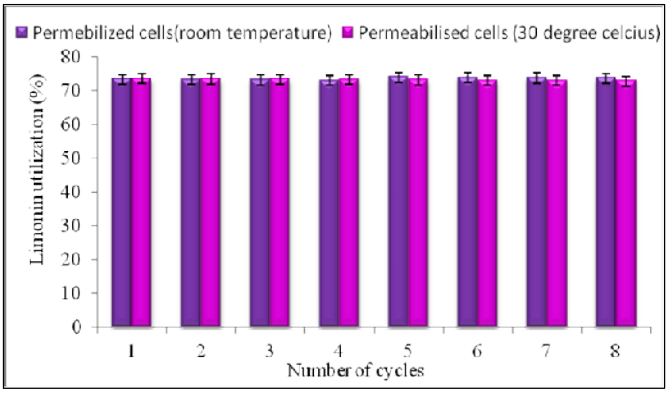

Fig. 4.47 Reusability and stability of permeabilised *P. putida* G7; Limonin utilization by permeabilised *P. putida* G7 cells stored at 4^0C and 30^0C in phosphate buffer for 45 days. Results are mean of three independent replicates

Table 4.23 Levels of variables tested in central composite rotatable design (CCRD)

Variables		Coded Levels				
		-2	-1	0	+1	+2
A	Na_2EDTA (µM)	0.5	1	1.5	2	2.5
B	Time duration (mins)	5	10	15	20	25
C	Temperature (°C)	12	20	28	37	45
D	pH	2	4.0	8.0	9.0	12

Table 4.24 Design matrix prepared using CCRD of RSM

Runs	Coded Values				Actual value	Predicted value
Runs	A	B	C	D	Limonin utilization (%)	
1	1.00	-1.00	-1.00	-1.00	67.19	67.63
2	0.00	0.00	0.00	0.00	76.71	75.82
3	-1.00	-1.00	1.00	-1.00	65.72	66.41
4	-2.00	0.00	0.00	0.00	68.66	68.86
5	-1.00	-1.00	1.00	1.00	69.42	69.49
6	2.00	0.00	0.00	0.00	70.89	70.72
7	0.00	0.00	0.00	0.00	76.71	75.82
8	-1.00	1.00	-1.00	1.00	72.36	71.94
9	1.00	-1.00	1.00	1.00	70.02	69.99
10	0.00	-2.00	0.00	0.00	71.49	71.22
11	0.00	0.00	0.00	0.00	76.71	75.82
12	0.00	0.00	0.00	2.00	72.96	72.44
13	0.00	0.00	0.00	0.00	76.71	75.82
14	0.00	0.00	0.00	0.00	76.71	75.82
15	-1.00	1.00	1.00	1.00	75.19	74.30
16	1.00	-1.00	1.00	-1.00	76.66	75.52
17	-1.00	-1.00	-1.00	1.00	69.71	69.66
18	-1.00	1.00	-1.00	-1.00	71.18	72.11
19	1.00	1.00	-1.00	1.00	69.71	69.66
20	0.00	2.00	0.00	0.00	71.18	72.11
21	0.00	0.00	0.00	0.00	76.71	75.82
22	-1.00	1.00	1.00	-1.00	71.95	73.62
23	0.00	0.00	2.00	0.00	68.98	67.98
24	1.00	-1.00	-1.00	1.00	71.13	71.13
25	-1.00	-1.00	-1.00	-1.00	70.31	70.31
26	1.00	1.00	1.00	-1.00	71.13	71.13
27	1.00	1.00	-1.00	-1.00	70.31	70.31
28	0.00	0.00	-2.00	0.00	70.31	70.31
29	0.00	0.00	0.00	-2.00	70.11	70.11
30	1.00	1.00	1.00	1.00	71.13	71.13

[a] A,B,C,D are the coded values for the significant variables - Na2EDTA concentration, time duration, temperature, pH, respectively;
[b] All the responses in the 30 runs were performed in triplicates. The calculated values were significant ($p < 0.001$).

The ANOVA results demonstrate that the regression is highly significant (at 99% confidence level) and presents an excellent determination coefficient ($R^2 = 0.904$). This meant that 90.4% variability in the observed data could be explained by polynomial equation. The second order regression equation obtained after the analysis of variance (ANOVA) provided the levels of bioconversion activity as a function of values of the Na_2EDTA (1.5µM) for time duration (15 min) at temperature (28°C), and pH (8.0) (Table 4.25). The final estimative response model equation in terms of limonin bio conversion (Y) was:

Limonin bioconversion (Y) = +76.71 +0.61* A+0.62* B+1.55* C+1.78* D+0.060* A * B+0.078 * A * C+3.44 * A * D +0.098 * B * C +3.43* B * D +3.39 * C * D+0.14 * A^2 +0.14 * B^2+0.058 * C^2 +0.32 * D^2;
[a]Where A, B,C and D are the coded values for Na_2EDTA (A) time duration (B) temperature (C), pH (D).

According to ANOVA of the model for activity of limonin utilization indicates that the "F" value of 11.58 and values of "Prob > F" less than 0.0500 infers that the model was significant. The R^2 value of 0.904, closer to 1 denotes a very high significance of the model. A higher reliability of the experiment is usually indicated by lower value of coefficient of variation (CV) i.e 1.65 which indicates that the experiments performed were reliable. The "Adequate Precision" measures the signal to noise ratio and a ratio greater than 4 is desirable. The ratio of 14.118 indicates an adequate signal and indicates that this model can be used to navigate the design space.

The obtained responses from the CCRD were fitted to a second order polynomial equation to explain the dependence of catalysis of limonin on the optimization of the significant variables for permeabilization of *P. putida* G7 (Fig. 4.48 a-c). As shown in Fig. 4.48a the highest value of limonin bioconversion activity was obtained when the cells were exposed to a concentration of 1.5 µm Na_2EDTA for 15mins. The optimum operating conditions of temperature and pH for effective permeabilization was 28^oC and 8 respectively. The response surface plotted in Fig. 4.48b, between Na_2EDTA concentration and temperature and the trend of the surface plot of temperature versus time in Fig. 4.48c depicted the similar activity of

Table 4.25 Analysis of variance (ANOVA) of the experimental results of CCD

Variables	Coefficient Estimation	Sum of Square	Standard Error	df	F-value	p-value
Model	76.71	1245.25	0.078	17	11.58	0.001
A	0.61	23.36	0.014	1	1.098	0.032
B	0.62	24.51	0.014	1	1,083	0.025
C	1.55	41.28	0.014	1	3.078	0.013
D	1.78	42.64	0.014	1	4.002	0.125
AB	0.060	7.39	0.017	1	0.003	0.004
AC	0.078	8.91	0.017	1	0.004	0.012
AD	3.44	215.78	0.017	1	6.005	0.022
BC	0.098	9.36	0.017	1	0.007	0.009
BD	3.43	211.57	0.017	1	5.005	0.006
CD	0.39	201.38	0.017	1	5.006	0.007
A^2	0.14	17.56	0.010	1	1.030	0.153
B^2	0.14	17.56	0.010	1	1.030	0.318
C^2	0.058	21.56	0.010	1	1.007	0.125
D^2	0.32	19.89	0.010	1	0.810	0.431

[a] A,B,C,D are the coded values for the significant variables - Na_2EDTA concentration, time duration, temperature, pH, respectively

limonin bioconversion. In fact, the close interaction of temperature and pH with time was quite evident. Thus, the response shown was based on the interaction of the significant variables. The predicted response was aproximately 75.82% when the significant variables were taken at "0" level, whereas the experimental response (based on the best predicted combinations of significant variables showing maximum response in CCRD) was approximately 76.71%, confirming the validity of the model.

Performance of permeabilized cells

The performance of permeabilized cells of *P. putida* G7 (permeabilized under optimized conditions) for limonin bioconversion was studied by using entrapped permeabilized cells in a dialysis based bioreactor. For evaluating the efficiency of limonin reduction, its level was monitored in two model solutions; minimal medium (M63) with limonin as the substrate and in citrus juice with equivalent limonin content. Limonin bioconversion peaked typically at three hours, following which further reduction was not observed (Fig. 4.49). In citrus juices, 76.71% of limonin removal was achieved within 150 mins. Further, the ability of entrapped permeabilized cells was compared with the efficiency of the purified enzyme by HPLC. A

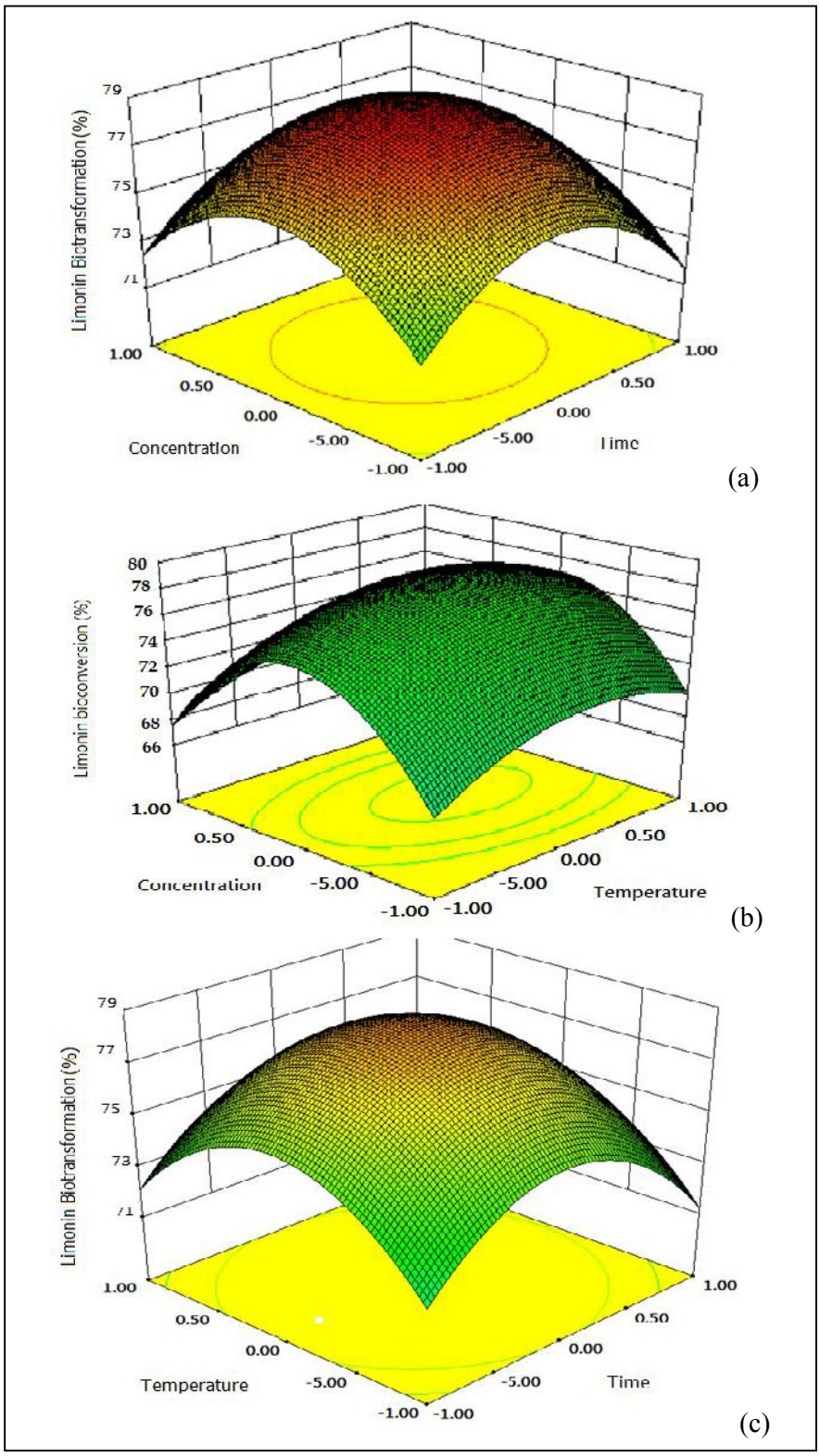

Fig. 4.48 (a-c) Response surface plots showing the combined effects of the significant variables in terms of Limonin bioconversion using permeabilized cells (a) Interaction effect between concentration and time (b) interaction effect between concentration and temperature ; (c) interaction effect between time versus temperature

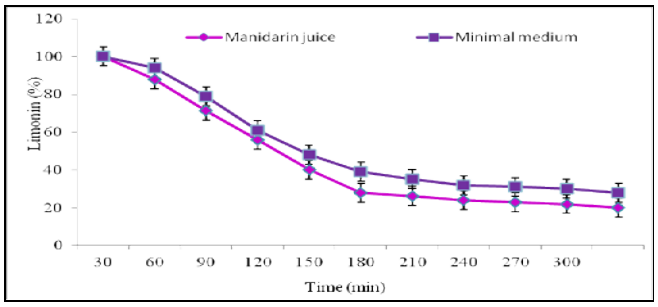

Fig. 4.49 Limonin bioconversion kinetics by permeabilized entrapped cells in juice and in minimal medium M63 supplemented with equivalent amounts of limonin. Results are mean of three independent replicates

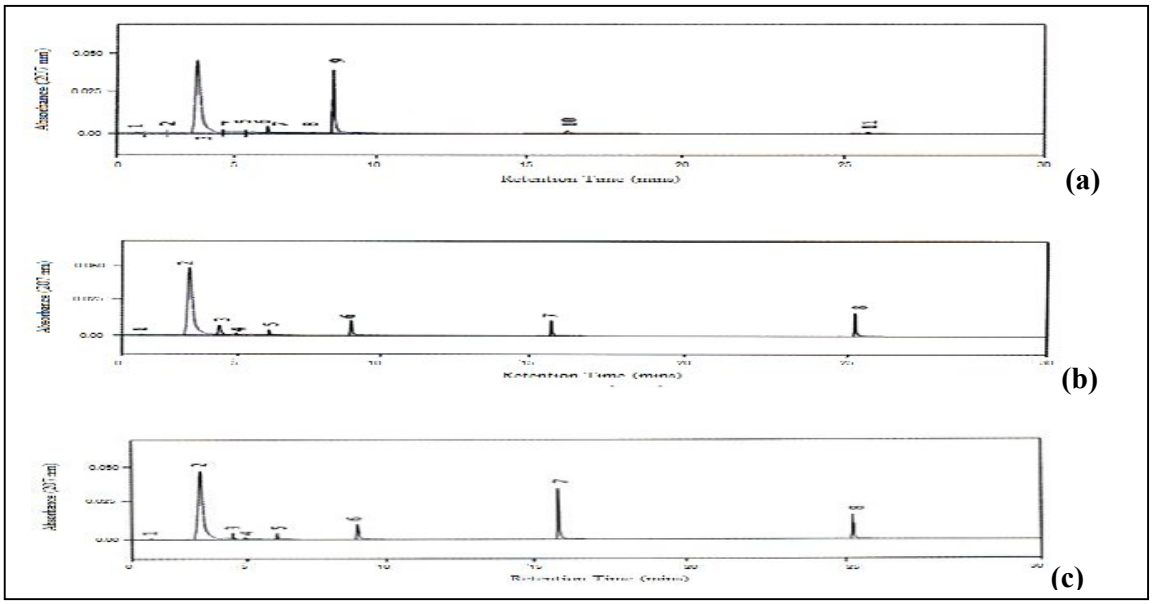

Fig. 4.50 (a) HPLC chromatogram of standard limonin (90µg/ml), (b) chromatograms of standard limonin (90µg/ml) utilization by permeabilised cells and purified enzyme (c) of *P. putida* G7, using an acetonitrile/deionised water (32:68) with a flow rate 0.9 ml/min and an injection volume of 20 µl

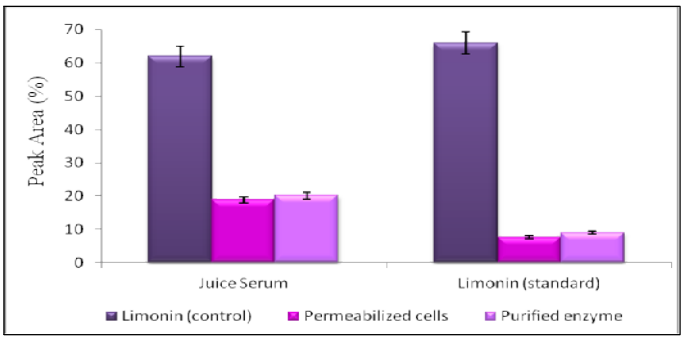

Fig. 4.51 Comparison of limonin bioconversion efficiency in two model solutions (standard limonin and juice sample with same limonin content) using cells of *P. putida* G7 permeabilised with Na_2EDTA under specified conditions and the purified enzyme. The results are explained in terms of peak area (%) for residual limonin by HPLC

prominent peak, at a retention time of 9.3 minutes was obtained with standard limonin (Fig. 4.50a). The peak area that represented limonin was reduced following utilization and appearance of two new peaks at retention times of 15.9 and 25.2 minutes were observed (Fig. 4.50b,c). As illustrated in Fig. 4.51, the peak area of 62% and 66% represented limonin in two respective model solutions of juice serum and standard limonin in the medium.A reduction in peak area to 9.07% and 7.09% was evidenced from the HPLC profile obtained after utilization by purified enzyme and the entrapped permeabilized cells respectively. The same reduced the corresponding peak area to 18.08% and 17.08% in the juice medium with the equivalent limonin content. Thus, in both the model solutions i.e. of juice serum and standard limonin in the minimal medium, the permeabilized cells proved to be equally efficient in biotransforming limonin as that of the purified enzyme.

Zymography

Zymography is a routine electrophoretic technique to identify proteolytic activities in polyacrylamide gels under non denaturing conditions. This method could be a simple yet crucial for noting functionality of enzymes. Thus it was adopted to detect the functionality of the enzyme in permeabilized cells. Immersion of gels in a suspension containing 375 mM Tris-HCl (pH- 8.8), 0.5 mM NADH, and 2 mM disodium limonoate and exposure to UV light allowed visualization of a band of yellow fluorescence (due to NADH) after few minutes,

the activity of the dehydrogenase over 8 cycles is shown in Fig. 4.52. Intensity of spots decreased significantly following 8th batch cycle, indicating loss of enzyme activity.

Western immunoblotting

In order to authenticate the above observations, western blotting was performed using the *P. putida* cell lysates from each batch cyce. The 26 kDa polypeptide of permeabilized cell lysates obtained during each batch cycle cross-reacted with monospecific anti-LDase antibodies raised against LDase from *Rhodococcus fasciens* (Fig. 4.53) indicating the

integrity as well as authenticity of the *P. putida* dehydrogenase during the batch cycle. The results also confirmed the predominant role of the enzyme for limonin utilization.

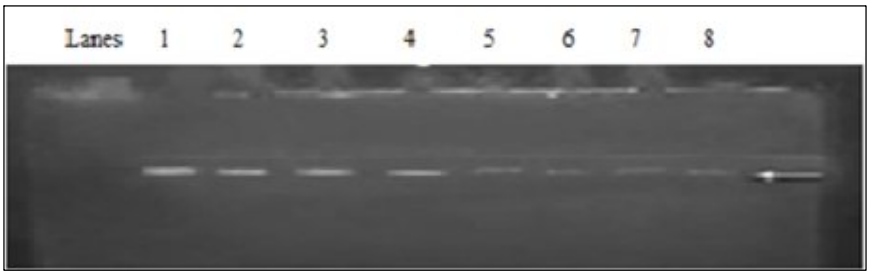

Fig. 4.52 Zymogram showing the intensity of dehydrogenase activity in permeabilized cells (A) Lane 1-8: Permeabilised cell extracts from batch cycles 1-8

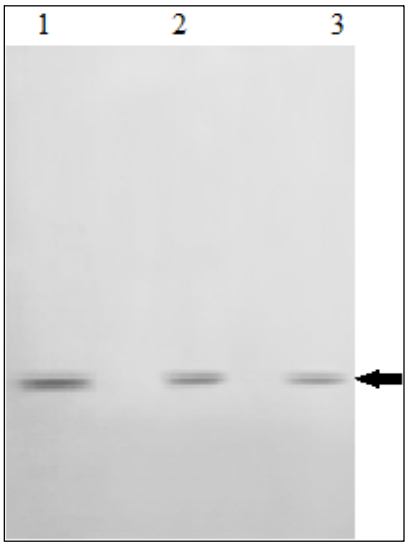

Fig. 4.53 Western blots showing LDase signal of permeabilised cells fractions of *P. putida* G7 from batch cycles 1, 4 and 8 in Lanes 1, 2, 3 respectively

Chapter4

Results

4.1 Physiological insights for limonin utilization by *Pseudomonas putida* G7

4.1.1 Metabolic fingerprint for carbon source(s)

Members of Pseudomonas species have been ascribed to possess the capability of utilizing a wide gamut of carbon sources. Thus, a profile of carbon utilization is helpful in elucidating the metabolic versatility of the members. Fig. 4.1 shows a differential utilization profile of variable carbon sources in microtitre plate with TTC. The differential intensity of the color signified the bacterial growth with respect to the carbon source utilized. The *P. putida* G7 tested on 95 different carbon sources utilized 82 of the carbon sources, suggesting its metabolic robustness. The high specific growth rate of 0.62 h^{-1} was observed for glucose as carbon source (Fig. 4.2). The ability of *P. putida* G7 cells to utilize limonin as sole carbon source was demonstrated by an increase in cell density and a proportionate reduction of limonin from the medium; approximately 54% of limonin was metabolized by *P. putida* G7 in 48 h, appreciable limonin was utilized during the log phase of growth. The cells exhibited a lag time of approximately 1 h and exhibited a specific growth rate (μ) of 0.43 h^{-1} suggesting a slow utilization of the triterpenoid.

Both acetonitrile and chloroform, which have been commonly used in earlier studies, were examined for their effect on the growth of *P. putida* G7. Amongst acetonitrile (2%) and chloroform (1.5%), acetontrile supported cell viability to a tune of 98%. Attempts to make the cells more adaptable to organic solvent and thus increased limonin utilization were successful. In cells precultivated in acetonitrile the lag phase was shortened notably as compared to freshly inoculated cells and exhibited a higher specific growth rate of 0.43 h^{-1} in comparison to the untreated cells (specific growth rate of 0.25 h^{-1}).

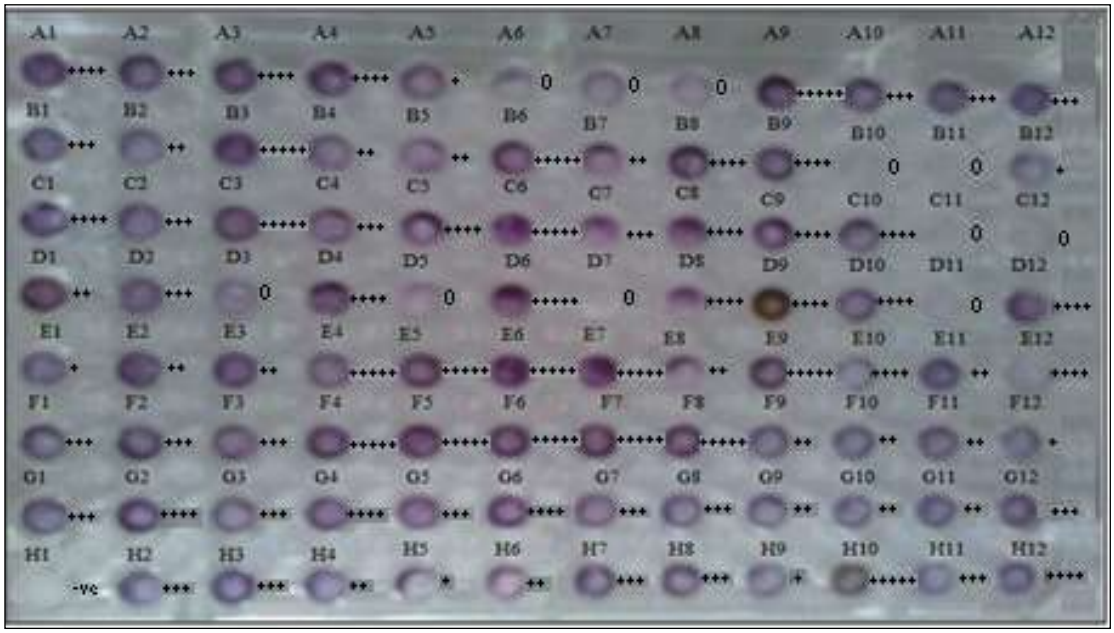

Fig. 4.1 Different carbon source(s) utilization profile of *P. putida* G7

(A1-Water, A2-α-Cyclodextrin, A3-Dextrin, A4-Glycogen, A5-Tween 40, **A6-Tween 80, A7-N-Acetyl-D-Galactosamine, A8-N-Acetyl-D-Glucosamine,** A9-Adonitol, A10-L-Arabinose, A11-D-Arabitol, A12-D-Cellobiose, B1-i-Erythritol, B2-D-Fucose, B3-L-Fructose, B4-D-Galactose, B5-Gentiobiose, B6-α-D-Glucose, B7-m-Inositol, B8-α-D-Lactose, B9-Lactulose, **B10-Maltose, B11- D-Mannitol,** B12- D-Mannose, C1- D-Melibiose, C2-β-Methyl-D-Glucoside, C3- D-Psicose, C4-D-Raffinose, C5-L-Rhamnose, C6-D-Sorbitol, C7-Sucrose, fdC8-D-Trehalose, C9-Turanose, C10-Xylitol**, C11-Pyruvic Acid Methyl Ester, C12-Succinic Acid Mono-Methyl-Ester**, D1-Acetic Acid, D2-Cis-Aconitic Acid, **D3-Citric Acid,** D4-Formic Acid, **D5-D-Galactonic Acid Lactone,** D6-D-Galacturonic Acid**, D7-D-Gluconic Acid,** D8-D-Glucosaminic Acid, D9-D-Glucuronic Acid, D10-α-Hydroxybutyric Acid, **D11-β-Hydroxybutyric Acid,** D12-γ-Hydroxybutyric Acid, E1-p-Hydroxy Phenylacetic Acid, E2-Itaconic Acid, E3-α-Keto Butyric Acid, E4- α-Keto Glutaric Acid, E5-α-Keto Valeric Acid, E6-D,L-Lactic Acid, E7-Malonic Acid, E8- Propionic Acid, E9-Quinic Acid, E10-D-Saccharic Acid, E11-Sebacic Acid, E12-Succinic Acid, F1-Bromosuccinic Acid, F2-Succinamic Acid, F3-Glucuronamide, F4-L-Alaninamide, F5-D-Alanine, F6-L-Alanine, F7-L-Alanylglycine, F8-L-Asparagine, F9-L-Aspartic Acid, F10-L-Glutamic Acid, F11-Glycyl-LAspartic Acid, F12-Glycyl-LGlutamic Acid, G1-L-Histidine, G2-Hydroxy-LProline, G3-L-Leucine, G4- L-Ornithine, G5- L Phenylalanine, G6-L-Proline, G7-L-Pyroglutamic Acid, G8-D-Serine, G9-L-Serine, G10-L-Threonine, G11-D,L-Carnitine, G12-γ-Amino Butyric Acid, **H1-Urocanic Acid,** H2-Inosine, H3-Uridine, H4-Thymidine, H5-Phenyethylamine, H6- Putrescine, H7-2-Aminoethanol, H8-2,3-Butanediol, H9-Glycerol, H10-D,L-α-Glycerol Phosphate, H11-α-D-Glucose-1-Phosphate, H12-D-Glucose-6-Phosphate)

*Differential growth score for variable carbon sources ([a] -vc = negative control ; +vc = positive control ; +++++ = excellent growth in glucose (standard),++++ = very good growth; +++ = average growth; ++ = less growth; + = poor growth; 0 = no growth

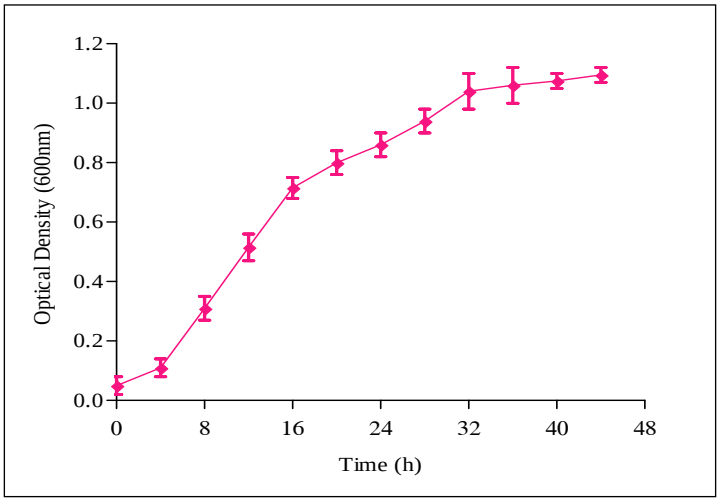

Fig. 4.2 Growth kinetics of *P. putida* G7 for utilizing glucose

4.1.2 Effect of Limonin concentration

Few if any earlier studies have examined the effect of limonin concentrations on growth of microorganisms; this is important for understanding both the tolerance and utilization at different concentrations. It was deemed necessary to examine a range of limonin concentrations on cell growth and subsequent utilization. A concentration of 50 µg/ml of limonin indicated adequacy in terms of specific growth rate of 0.43 h^{-1} and reduction in limonin level within 36 h; higher limonin concentrations were not favorable for cell growth as well as limonin utilization (Fig. 4.3). The residual limonin levels were estimated by HPLC. The chromatograms revealed the substrate retention time to be 9.3 minutes; a reduction in peak following utilization by the *P. putida* G7 cells was observed. The limonin was utilized and converted to metabolites which appeared as two new peaks at retention times of 15.9 and 25.2 minutes (Fig. 4.4) respectively. The limonin levels were reduced to a peak area of 46.4% this corresponded to reduction of initial levels of limonin by 55.2%.

4.1.3 Effect of pH

The effect of pH range 5.0 - 9.0 on the growth and limonin utilization of *P. putida* was determined. Optimal pH was considered the one which afforded maximum bacterial growth and limonin utilization in 48h (Fig. 4.5). Low pH impeded growth and limonin utilization. Significant reduction in limonin levels was however observed in the pH range of 7 to 9; the cells exhibited a maximum specific growth rate of 0.40 h^{-1} when the initial pH was adjusted to 8. The *P. putida* strain lacked both growth and limonin utilization at pH values above 8.

4.1.4 Effect of Temperature

Temperature is a prerequisite for growth and thus important for conferring optimal metabolism to bacterial cells. To determine the influence of temperature on the growth and limonin metabolism, growth and limonin levels were monitored over a temperature

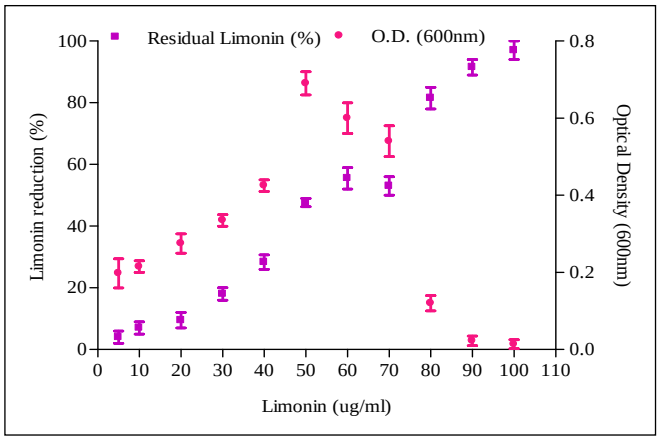

Fig. 4.3 Effect of limonin concentration

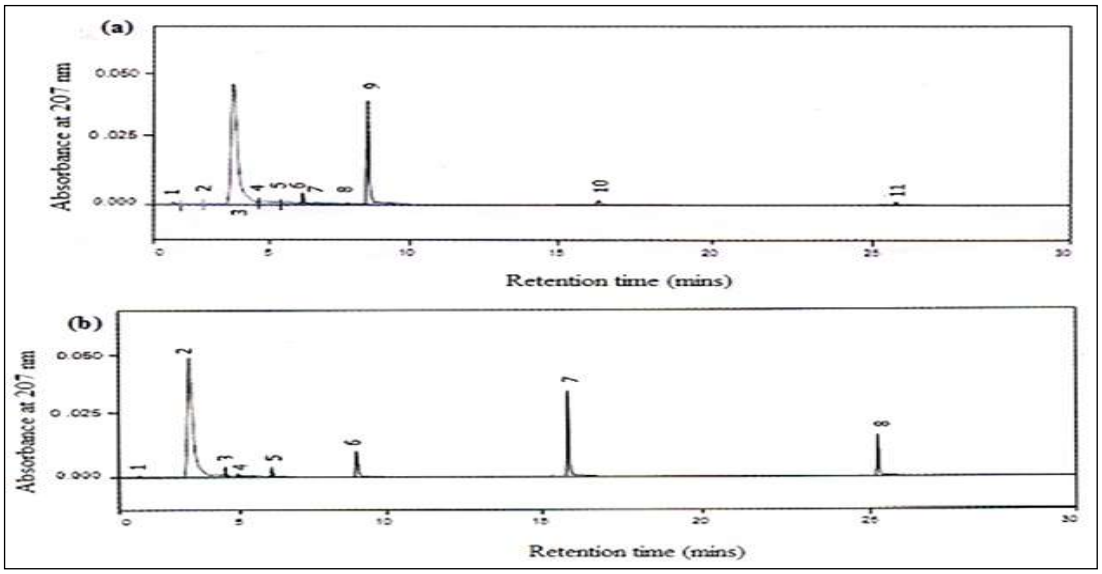

Fig. 4.4 (a) HPLC chromatograms of standard limonin (50µg/ml) and (b) chromatograms of standard limonin (90µg/ml) utilized by *P. putida* G7, using an acetonitrile/deionised water (32:68) with a flow rate 0.9 ml/min and an injection volume of 20 µl

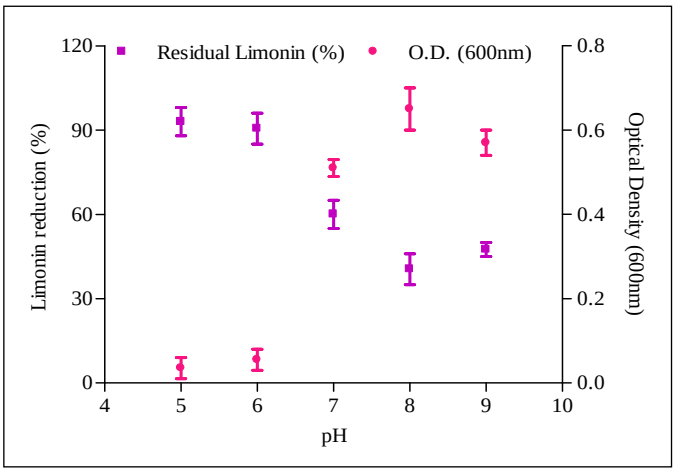

Fig. 4.5 Effect of pH on growth and limonin utilization ability of *P.putida G7*

range 20^{O}C- 35^{O}C (Fig. 4.6). Maximal growth was observed at 30^{O}C, at lower and high temperatures, the *P.putida* G7 cells lacked appreciable growth. Limonin utilized could be correlated to these observations.

4.1.5 Effect of Agitation

Agitation regulates the oxygen concentration and helps uniform exposure of bacterial cells to medium nutrients. However higher agitation speeds may mechanically damage cellular integrity, therefore it was desirable to optimize the most suited agitation speed for *P. putida* G7. Both maximal growth and limonin utilization ooccurred (53.5%) when the cells were incubated at an rpm of 120. At higher agitation speed (200 rpm and more) increase in growth (specific growth rate $0.41h^{-1}$) with an early induction of stationary phase was observed but limonin utilization was lower. Microscopic observation of cells agitated at higher speeds exhibited gross disruption. A comparison of the temperature, pH optima and corresponding specific growth rate and limonin utilization with reported limonin degrading strains revealed a higher utlization of limonin within a shorter time period. This corroborated with a higher specific growth rate of the strain as well. A comparison of various microorganisms utilizing limonin at various cultural parameters is shown in Table 4.1.

4.1.6 Statistical optimization of cultural parameters for maximal limonin utilization

The combined effect or the inter-relationship of the selected cultural parameters for limonin utilization response was observed with response surface methodology with central composite design in a face centred cube design of 2^3=8 + 6 centre points and 6 (2x3) star points which lead to a total of 20 experiments. The coded values of the significant variables are presented in Table 4.2. Based on the optimization of process parameters and the experimental results (obtained from CCD and regression analysis) (Table 4.3), the relationship between the limonin utilization and the significant parameters (A- limonin concentration, B- temperature, C- pH) was established in the form of a quadratic polynomial equation. The analysis of

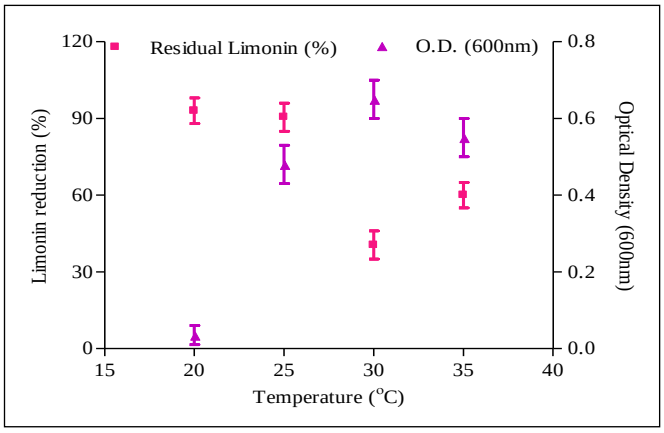

Fig. 4.6 Effect of temperature on growth and limonin utilization ability of *P.putida G7*

Table 4.1 Comparision of limonin utilization potential of different bacterial strains with their specific growth rate and physiological conditions

Microorganisms	Temperature (°C)	pH	Limonin utilization (%)	Time	Specific growth rate (h^{-1})
Arthrobacter globiformis	30	3.5	28	56	0.22
Pseudomonas 321-18	30	7	45	54	0.33
Bacterium 342-152-1	37	7.5	36	60	0.25
Acinetobactor sp	35	4	42	72	0.31
Corynebacterium fascians	37	8	41	70	0.29
Rhodococcus facians	37	4.5	48	62	0.37
P. putida G7	30	8	54	48	0.43

*Data collected from literature references (Hasegawa et al. 1972; 1974; 1975; 1981; 1985; Manjon et al. 1989)

Table 4.2 Coded values of all the significant variables

Variables	Coded Values				
	-α	-1	0	+1	+ α
A-Limonin (µg/ml)	9.77	20	35	50	60.23
B- Temperature (°C)	16.59	20	25	30	33.41
C- pH	2.63	4	6	8	9.36

variance for this model is present in Table 4.4. The F value (43.08) of the model signifies the significance of the model and there was only 0.01 % chance that the model F value must have occurred due to noise. Regression analysis results has revealed R^2 (coefficient of determination, and the value more closer to 1 indicates the model fit of the experimental data) value of 0.9748, which signified the strength of the model and predicted a better response along with the enability of the model to explain only 2.52% of the total variations. The predicted R^2 of 0.78978 was in reasonable agreement with the adjusted R^2 (adjusted determination coefficient) value of 0.9522, which indicates the high reliability of the model and the quadratic polynomial equation. The statistical analysis also allowed us to determine the contribution of experimental factors (signals) in comparison to noise, where the signal should be fairly large in comparison to noise. The "adequate precision" which measures the signal to noise ratio (a ratio greater than 4 is desirable) and the ratio of 25.041 indicates an adequate signal. The values of "Prob>F" of the model far less than 0.05, indicates the significant and desirability of the model terms. The Fisher's "*F*" test of the model for limonin utilization response shows that fitted second order response surface model is significant i.e. 43.08425 (p= <0.0001). The parameters A, B, C (*p*= <0.0001) were significant and a significant interaction was observed among the parametrs AC & BC followed by AB, for the maximal response of limonin utilization (R1).The "Lack of Fit F-value" of 102.74 implies that the Lack of Fit is significant. There is only a 0.01% chance that this large "Lack of Fit F-value" could occur due to noise. A low value of CV (coefficient of variation) of 11.61% signifies a high degree of precision and a good deal of reliability of the experimental values. Values greater than 0.1 indicates the model terms are not significant. The equation for the model in terms of coded factors was determined as explained in Table 4.5.

The response model was developed further represented in the form of contour plots for a better understanding of the interaction among the three significant parameters and for the

Table 4.3 Response surface central composite design (CCD) and experimental limonin utilization

Run	A-Limonin (ug/ml)	B-Temperature (°C)	C-pH	Limonin Utilization (%) Actual	Predicted
1	35	25	2.63	7	5.17
2	35	25	6	30	29.97
3	50	20	8	37	37.29
4	35	33.40	6	33	30.22
5	35	25	6	30	29.97
6	60.22	25	6	40	39.67
7	35	25	9.36	50	52.54
8	35	25	6	30	29.97
9	20	20	8	31	25.72
10	35	25	6	30	29.97
11	9.77	25	6	20	21.04
12	35	16.59	6	8	11.49
13	50	20	4	12	9.13
14	35	25	6	30	29.97
15	20	20	4	10	11.55
16	35	25	6	30	29.97
17	20	30	8	35	37.35
18	50	30	4	15	19.76
19	50	30	8	64	61.93
20	20	30	4	10	9.192

Table 4.4 Analysis of variance (ANOVA) for Response Surface Quadratic Model

Source	Sum of squares	df	Mean square	F -value	p-value Prob>F
Model	3984.054	9	442.6727	43.08425	< 0.0001 significant
A-Limonin	418.8946	*1*	418.8946	40.76999	< 0.0001
B- Temperature (°C)	423.4368	*1*	423.4368	41.21207	< 0.0001
C- pH	2708.227	*1*	2708.227	263.5851	< 0.0001
AB	84.5	*1*	84.5	8.224179	0.0167
AC	98	*1*	98	9.538101	0.0115
BC	98	*1*	98	9.538101	0.0115
A^2	0.262112	*1*	0.262112	0.025511	0.8763
B^2	149.7837	*1*	149.7837	14.57808	0.0034
C^2	2.253845	*1*	2.253845	0.219361	0.6496
Residual	102.7458	10	10.27458		
Lack of Fit	102.7458	*5*	20.54916		
Pure Error	0	5	0		
Cor Total	4086.8	19			

Table 4.5 Equation for the response surface model for limonin utilization

Final Equation in Terms of Actual Factors:
Limonin utilization (%) = -21.53654 -1.45607 * Limonin +3.94477* Temperature -4.60588 * pH +0.043333 * Limonin * Temperature +0.11667 * Limonin * pH +0.35000 * Temperature * pH +5.99390 E-004 * Limonin^2 -0.12896 * Temperature^2 -0.098867 * pH^2
Final Equation in Terms of coded factors:
Limonin utilization (%) = +29.98 +5.54 * A + 5.57 * B +14.08 * C +3.25 * A * B +3.50 * A * C +3.50 * B * C +0.13 * A^2 -3.22 * B^2 -0.40 * C^2

detection of the optimum level of each parameter for a maximum response. The contours plot showed the interaction of two independent parameters when the third parameter is fixed at zero (Fig 4.7 a-c), which represents the limonin utilization response. It is observed that if the contour is elliptical, the mutual interaction between the two factors is significant; or else if it is circular, the mutual interaction effect is non-significant. As shown in Fig. 4.7a the highest value of limonin utilization was obtained when the cells were grown at pH 8 with a limonin concentration of 50µg/ml over a time period of 36 h. The optimum operating conditions of pH (8) and temperature (30°C) was observed for effective response of limonin utilization (Fig. 4.7b). The response surface plotted in Fig. 4.7c, between temperature (30°C) and pH (8), depicted a higher activity of limonin utilization. Among the three significant variables A (limonin concentration), B (temperature) and C (pH); BC and AC exhibited the highest interaction which was most significant, followed by an interaction between BC. The experimental response for limonin utilization by *P. puitda* G7 was 64% when a limonin concentration of 50µg/ml was chosen as substrate and incubation carried out at 27.6°C and pH 8.

Thus, the response shown was based on the interaction of the significant variables. The close associations of the predicted and actual response were approximately 61.93% and 64% and signified the validity of the model.

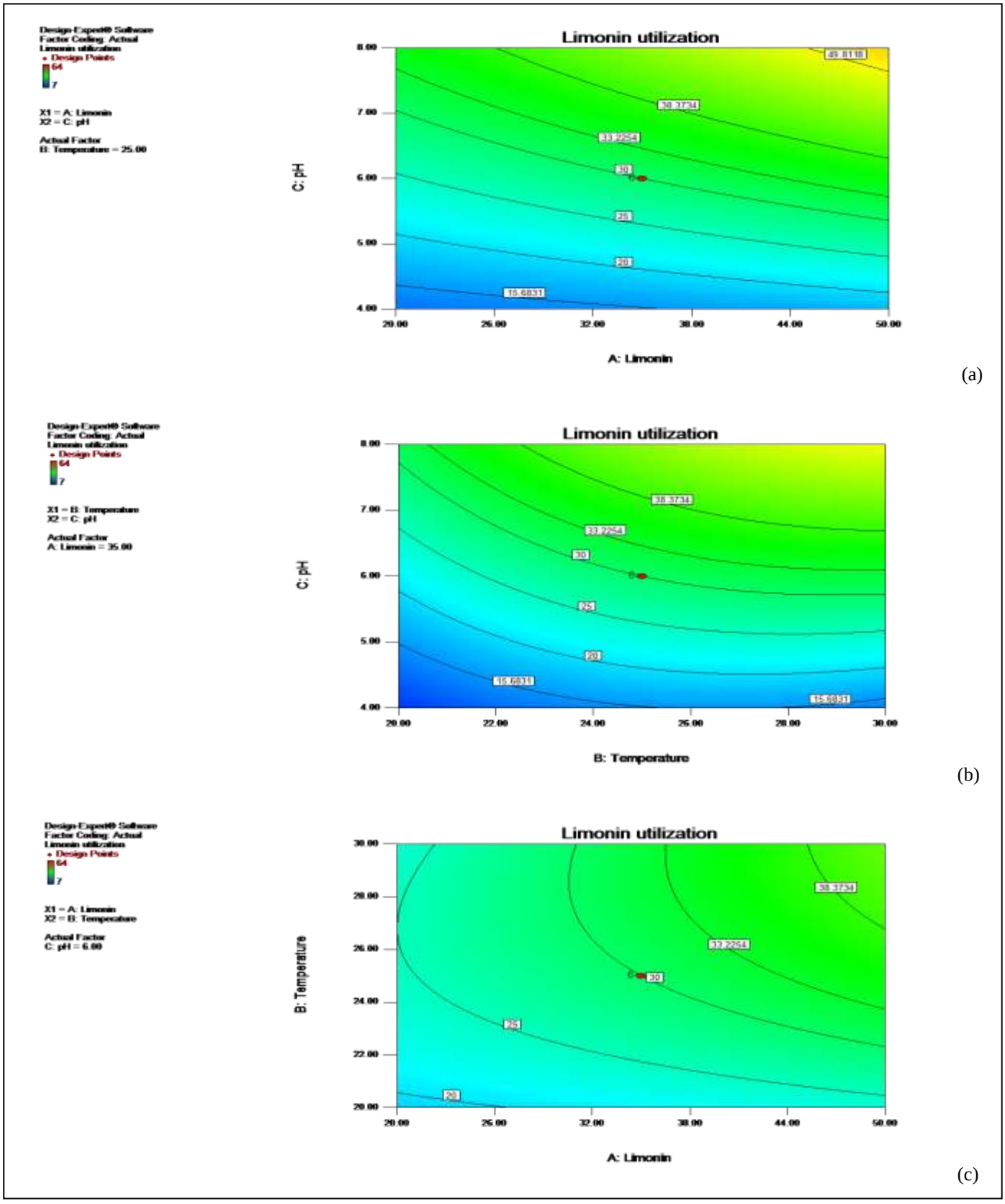

Fig. 4.7 Contour plots for limonin utilization by *P. putida* G7 in minimal medium depicting the interaction of significant factors (a) Interaction effect between limonin concentration and pH (b) Interaction effect between temperature and pH ; (c) interaction effect between limonin concentration and temperature

4.2 Genetic studies of *Pseudomonas putida G7* associated with limonin utilization

The most direct way to establish the function of a gene is by mutation. Insertional mutagenesis provides a short cut to isolating the gene in question without recourse to linkage mapping and the assembly of large clone contigs. Here the phenotype generated by transposon Tn5 insertion is absence of limonin utilizing ability (lim^-) in *P. putida* G7 because the insertion element had disrupted the corresponding gene, which means that the gene's sequence will flank the insertion site. Further a PCR based technique referred as inverse PCR was used for isolation of flanking sequence using different pair of primers that anneals to the transposon ends and detects the gene at the flanking sites to detect the disrupted gene. Where the genomic DNA from a lim^- mutant was cleaved with a restriction enzyme and self-circularized. PCR amplification was then carried out using primers that specifically anneal to the insertion transposon element but point outward rather than inward. In a circular DNA molecule, this will result in the amplification of sequences flanking the insert.

4.2.1 Transposon Tn5 insertional mutagenesis

Random Tn*5* transposon mutagenesis was accomplished for generation of a mutant library by mobilizing the suicide vector pGS9 (which harbored Tn5 transposon) from *E. coli* JB110 to generate mutants in *P. Putida G7*. A Tn5 transposition of 10^{-2} to 10^{-3} per cell generation occurred in *P. putida* G7. The total library consisted of >1,850 randomly picked mutants without discriminating by colony morphology or size. The mutants were arrayed in 96-well plates for phenotypic screening based on limonin utilization (Fig. 4.8). The color developed with TTC differentially depicted the growth in limonin. Those putative mutants were selected for further screening which did not turn up the formazan precipitates. This indicated absence of growth or inability to utilize limonin as the carbon source due to disruption by insertion of Tn5. Finally a stable mutant was selected and it was designated as *P. putida* strain lim A^- mutant.

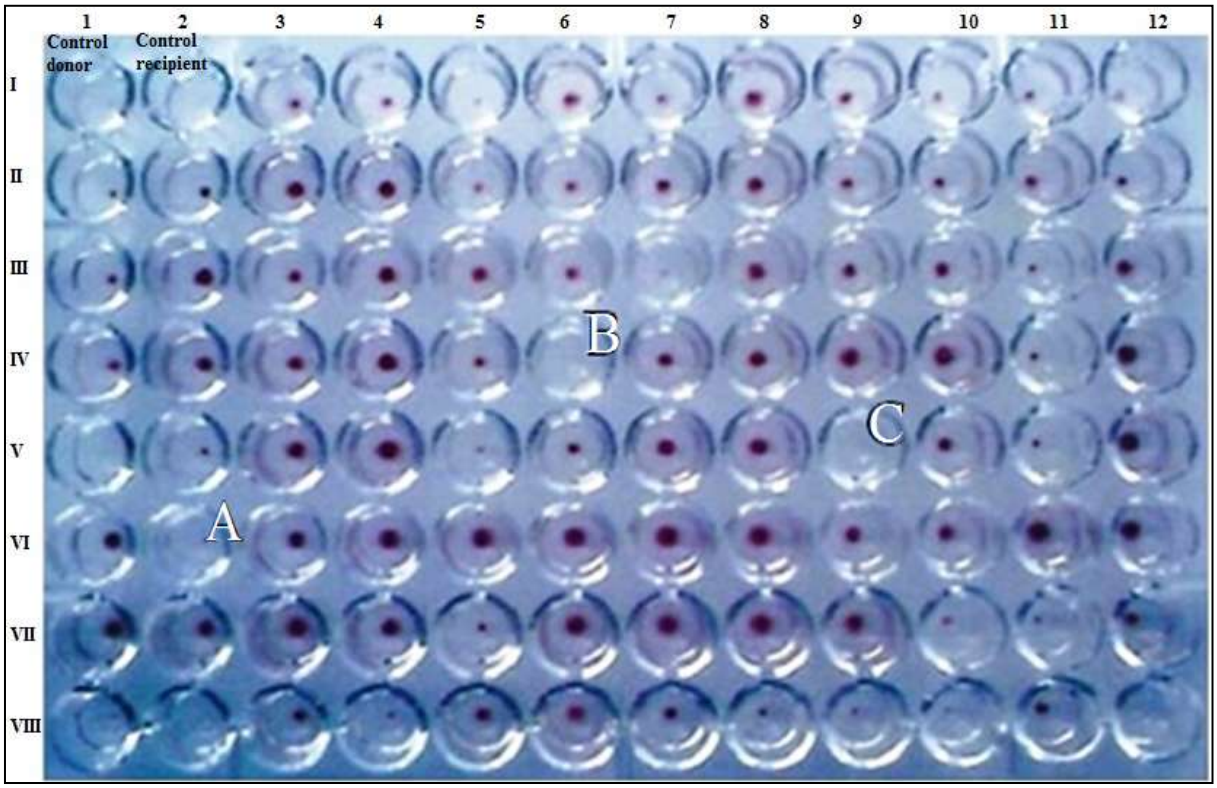

Fig. 4.8 Screening of mutant library generated by transposon mutagenesis for putative lim⁻ phenotypes; The three wells marked as A,B,C were the phenotypic mutants (unable to utilize limonin as carbon source), selected on the basis of absence of development of red precipitates of formazan as an indicator of growth

4.2.2 Detection of Tn5 in lim⁻A mutant

The transposition of Tn5 in the chromosome of *P. putida* G7 was confirmed by amplification of Tn5. The 625bp fragment based on IS50 element of Tn5 was amplified by PCR and amplification was positive in lim⁻ A mutant (Fig 4.9). No amplification was observed in the wild type *P. putida*.

4.2.3 Size approximation of Tn5 by Southern Hybridization

A highly sensitive Tn5 probe labelled with DIG-dUTP (as a visible marker) was generated and confirmed by resolution on a 0.8% agarose gel, where it showed less mobility as compared to the control (unlabelled Tn5) (Fig. 4.10). The genomic DNA of *P. putida* G7 (wild), lim⁻ A mutant and pGS9 plasmid DNA of *E.coli* (JB110) were isolated and digested with restriction enzymes Eco R1 and Hpa 1 (Fig. 4.11). The gel adhered with the digested profile of the target samples was denatured and unsterilized with various respective buffers followed by blotting the DNA profiles on the nitrocellulose membrane. The probe was employed for the detection of the copy number of Tn5 target sequence by hybridization. A visible signal for the target DNA sequence was immunodetected and documented. Fig. 4.12 showed no signal for *P. putida* G7 (wild), A signal was visible at 5.8kb in genomic DNA profile of *P. putida* G7 lim⁻ A. Also plasmid pGS9 of *E.coli* - JB110 was used as one of the controls for detecting the Tn5 signal.

4.2.4 Cloning and detection of the Tn5 flanking region

A high throughput inverse PCR approach was employed to detect the gene loci in lim⁻ A mutant. The gene sequence at the Tn5 flanking site was mapped by locating Tn5 insertion in the various restricted endonuclease digests of the lim⁻A mutant. The restriction fragments of variable restriction enzymes (Sal1, Bam H1, Bgl11, Not 1, Hpa1) were when circularized by ligation, gave various amplicons of varied sizes, with the respective primers (Fig. 4.13). Approximately, 18 amplicons corresponded to the variable circularized DNA were resulted

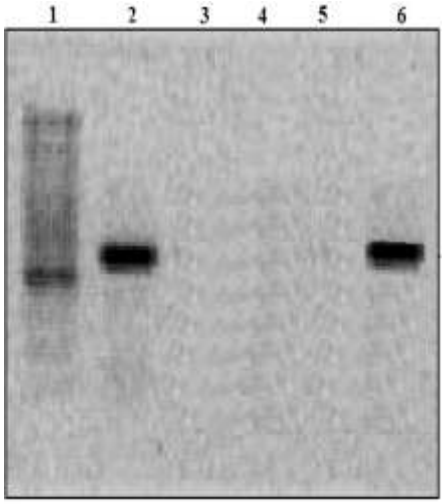

Fig. 4.9 Confirmation of Tn5 insertion in *P. putida* G7 by PCR amplification; Lane1: Molecular weight marker (100bp ladder); Lane2: Presence of Tn5 amplicon in Tn5 transconjugant "A" (Lim$^-$ mutant); Lane3,4: Absence of Tn5 amplification in Tn5 transconjugant B & C; Lane5: Absence of Tn5 amplification in *P. putida* G7 (wild type) (-ve control); Lane 6: Presence of Tn5 amplification in pGS9 plasmid (+ve control)

Fig. 4.10 DIG labeled Tn5 probe generated by PCR amplification; Lane 1: 100 bp Molecular weight marker; Lane2: Unlabelled control Tn5 probe; Lane3: DIG labeled Tn5 probe

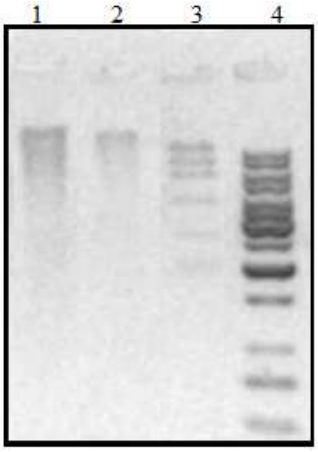

Fig. 4.11 Restriction digestion profile of *P. putida* G7 lim$^-$ A mutant; Lane 1: Eco R1 digested DNA sample of wild type of *P. putida* G7; Lane 2: Eco R1 digested DNA of lim$^-$ A mutant of *P. putida* G7; Lane 3: Hpa1 digested products of pGS9 plasmid; Lane4: 1 Kb DNA molecular weight marker

Fig. 4.12 Immunodetection of Tn5 insertion in lim⁻ A mutant of *P. putida* G7; Lane 1- Negative control (wild type of *P.putida* G7); Lane 2- lim⁻ A mutant confirms the presence of signal for Tn5; Lane 3- Positive control (suicidal vector pGS9 containing Tn5 of strain JB110)

Fig. 4.13 Gene amplification at the insertion sites of Tn5 by Inverse PCR in lim⁻ A mutant of *P. putida* G7; Lane1- three amplicons of Bam HI restriction digested product; Lane 2- three amplicons of Not 1 restriction digested product; Lane 3- four amplicons of Sal I restriction digested product; Lane 4- four amplicons of Bgl III restriction digested product; Lane 5- four amplicons of Hpa I restriction digested product; Lane 6- 1kb ladder

as a result of inverse PCR (Table 4.6). The amplicons were extracted and purified, cloned in the pGEM-T Easy vector system and transformed into *E.coli* (DH5α). A clone library was formed and nearly 215 clones were selected from the transformed colonies (corresponding to the various restriction enzymes) on IPTG/X-gal plates and were sequenced.

4.2.5 Sequence Analysis and gene identification

The clones sequences obtained were multaligned and restriction mapped. The deduced gene sequence had shown similarity with various chromosomal streches of variable identical restriction pattern, when identified using blast-n, blast-p and NCBI ORF finder bioinformatic tools. Of the various clones sequences, 9 clones had shown ORF'S which had similarities with partial genes sequences or with hypothetical genes (Table 4.7). One of the larger fragments of clones Sal 1 of 1.206 kb (Accession: BankIt1523539) had shown an ORF1 (tnA) with a putative function for a gltS glutamate transporter from its 78-846 position. ORF2 (tnB) has also shown an ORF with a similar putative function of gltS Sodium/glutamate symport carrier protein, from 677-967 position in the Sal 1 fragment. The physical map of the gene sequence and its translated protein sequence has been predicted by a Dnadynamo software as presented in Fig. 4.14. This revealed that the Tn5 insertion must have deactivated the glutamate transporter gene due to which the bacterial cell were unable to utilize limonin. Thus the gene sequence derived from the flanking region of Th5 only 2 ORF's are proposed to be the participants of the gene corresponding to limonin utilization/uptake on the basis of the sequence homologies and the effect of mutation. ORF1 (tnA) and ORF2 (tnB) showed a similarity with the ORF's of glutamate symporter/transporters located on the membranes of *E. coli* K12, MG1655 an *E. coli* CFT073 respectively. Disruption of this membranous protein was response for the inability of lim^- mutant of *P. putida* G7 to uptake and utilize limonin as the carbon source.

Table 4.6 Amplicons generated by Inverse PCR

E.coli strain /pGEMT Vector	Genotype	
	Restriction digested	Insert
Δ1/S1	Sal 1	560bp
Δ2/S2		730bp
Δ3/S3		1.3kb
Δ4/S4	Bam H1	450bp
Δ5/Bm1		493bp
Δ6/Bm2		684bp
Δ7/Bm3		1.12kb
Δ8/Bg1	Bgl 11	480bp
Δ9/Bg2		651bp
Δ10/Bg3		1.2kb
Δ11/Bg4	Not 1	550bp
Δ12/No1		538bp
Δ13/No2		854bp
Δ14/No3		630bp
Δ15/Hp1	Hpa 1	850 bp
Δ16/Hp2		750bp
Δ17/Hp3		954bp
Δ18/Hp4		325bp

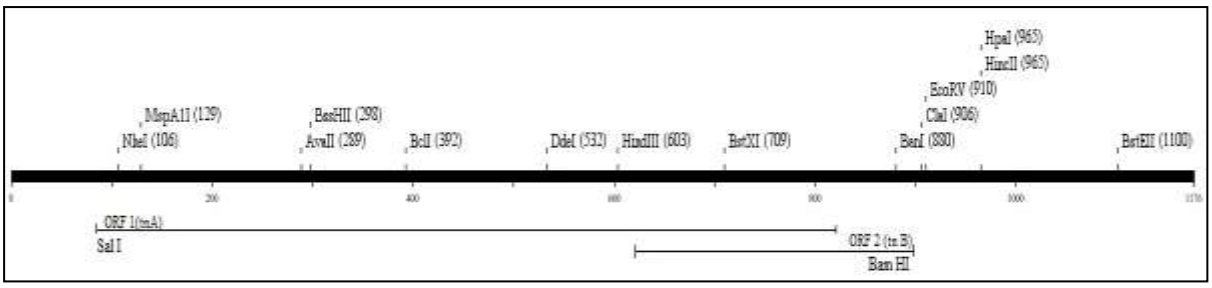

Fig. 4.14 Position of essential ORF's and the restriction map of the gene associated with limonin utilization

Table 4.7 Features of the ORF'S encoded in the 1.1 76kb DNA region from Lim⁻ A mutant of *P. putida* G7

ORF	Position	Identity %	Putative function	Organism	Accession no
ORF 1 (tnA)	79-846	98	gltS glutamate transporter	*Escherichia coli str. K-12 substr. MG1655*	NP_418110.1
ORF2 **(tnB)**	677-967	99	gltS Sodium/glutamate symport carrier protein	*Escherichia coli CFT073*	YP_002384972.1
ORF4 **(tnD)**	547-7 44	44	ECU08_0210 SEC31-like protein involved in vesicular transport from ER to golgi	*Encephalitozoon cuniculi GB-M1*	NP_597151.1
ORF5 **(tnE)**	930-1175	41	hypothetical protein B2_07867	Bacteroides sp. 2_1_7	ZP_05285934.1
ORF6 **(tnF)**	434-1051	39	CIMG_04173 hypothetical protein	*Coccidioides immitis RS*	XP_001244732.1
ORF7 (tnG)	74-316	100	ytfM hypothetical protein	*Shigella dysenteriae Sd197*	YP_405829.1
ORF8 (tnH)	22-261	26	BVU_0689 serine acetyltransferase	*Bacteroides vulgatus ATCC 8482*	YP_001298017.1
ORF10 (tnJ)	406-546	43	lysA diaminopimelate decarboxylase	*Shigella dysenteriae Sd197*	YP_404563.1
ORF12 (tnL)	500-616	52	CTU_34270 hypothetical protein	*Cronobacter turicensis z3032*	YP_003211790.1

4.2.6 Detection of Gltase activity in lim⁻ A mutant

The deactivation of the glutamate symporter gene due to Tn5 insertion was further confirmed by detecting the variation in the glutamate uptake of (50 µg/ml, as carbon source) potential of the lim⁻A mutant and wild type of *P. putida* G7. The spectrophotometric analysis when done for the detection of glutamate levels at O.D. 450 nm, showed a reduction in the absorbance (which corresponds to the reduction in the glutamate concentration of 15% in 30 min) after the incubation of the wild type cells of *P. putida* G7. This shows that the undisrupted glutamate symorter in wild type corresponded to the uptake of glutamate (as the carbon source). Whereas the lim⁻ A mutant of *P. putida* G7 showed an insignificant 1-2% ($p<0.05$) reduction in absorbance. This revealed that the lim⁻ A mutant which was unable to utilize limonin was also unable to uptake glutamate as the carbon source.

4.2.7 Chemotaxis for limonin by P. putida G7

Though motility is essential for gram negative bacteria, however it is important to understand whether the bacterial cells actually chemotax towards the compound of interest i.e. limonin. The *P. putida* G7 cells (Fig. 4.15), placed on one end of the filter paper and observed at regular intervals, exhibited positive motility on the filter paper by utilizing limonin present and reducing the TTC present into red color formazan. The observations indicated that *P.putida* G7 cells could utilize limonin, when present as sole carbon source.

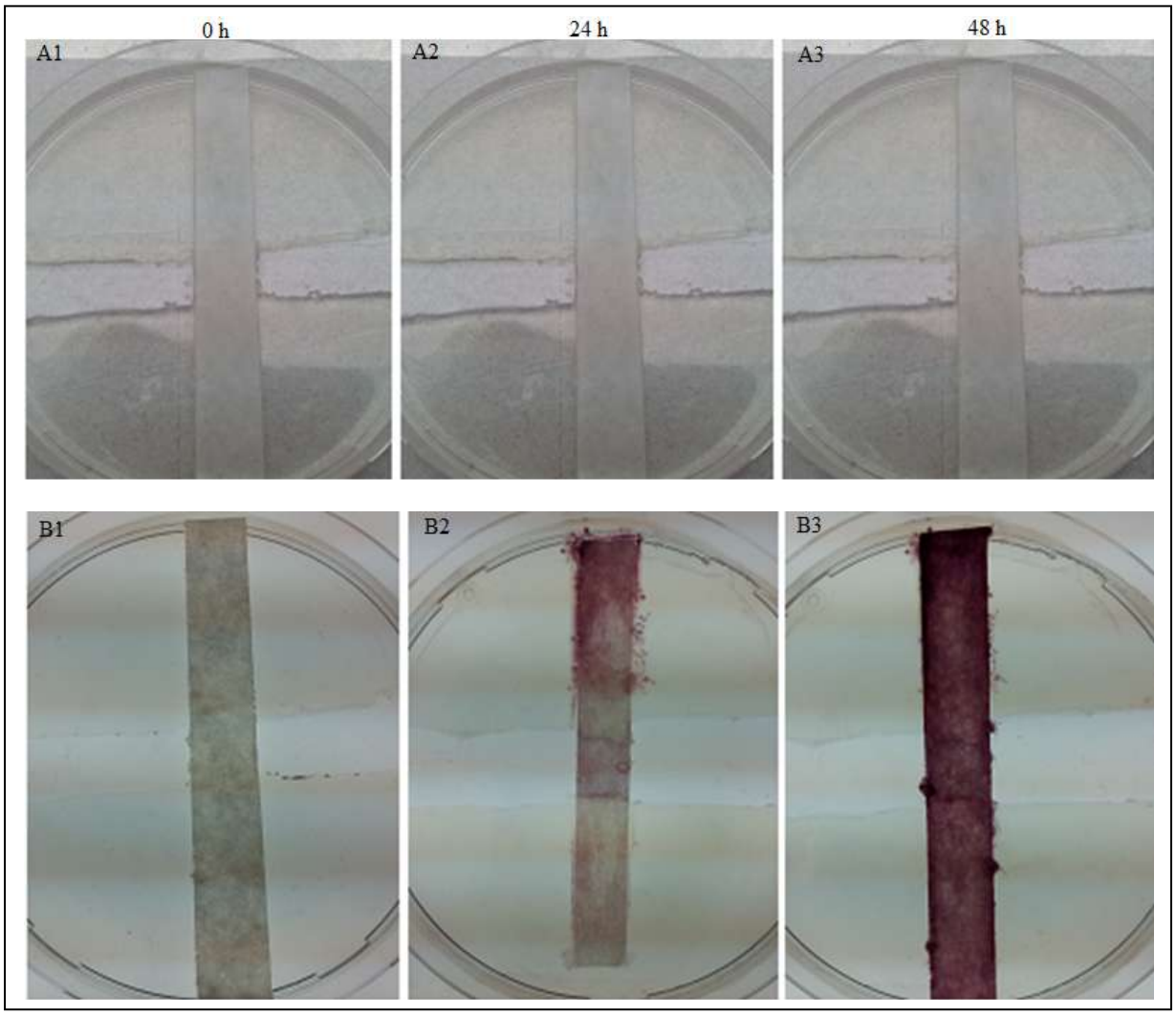

Fig. 4.15 Chemotaxis of *P. putida* G7 cells for chemo-attractant limonin; Growth was observed for *P. putida* G7 in B2 and B3, by red color due to TTC, which confirmed the mobility of cells to utilize limonin across the well. Absence of motility was observed in A2 and A3 which explained the inability of *E. coli* Dh5α to utilize limonin as cabon source

4.2.8 Role of NAH plasmid of *P. putida* G7 in Limonin biotransformation

As evident form the foregoing studies, that identity of the genes responsible for limonin bioconversion remained elusive. Therefore it was anticipated that the NAH plasmid responsible for naphthalene degradation in *P. putida* G7 might offer clues for characterizing limonin degrading genes. Plasmid curing was therefore attempted to examine whether cured strains retained the ability to utilize limonin. Prior to curing studies the plasmid characteristics were examined in a preliminary study.

Detection and molecular weight determination of plasmid in P. putida G7

The slow mobility of the purified plasmid DNA indicated its large size; comparison to the lambda marker suggested its size to be more than 23kb lambda marker (Fig. 4.16). The ability of *P. putida* to metabolize naphthalene signified its identity as low copy number NAH plasmids with size varying between 60-100kb. For obtaining a genetic fingerprint, the plasmid was subjected to restriction digestion and resolved on agarose gel. The profile of digested fragments was used to determine the molecular weight using the Mol Match program. The plasmid had a molecular weight of approximately 83 kb.

Plasmid curing

The role of plasmid borne structural gene(s) implicated in limonin utilization was determined by curing the wild type strain of its indigenous NAH plasmid. Among the various curing agents mitomycin C proved to be most efficient (Table 4.8). The number of viable cells was plotted as a function of mitomycin C (Fig. 4.17). A killing rate of 94.7% (±1.2, n=6) was observed in the presence of 20 μg/ml mitomycin C. Such a rate was considered sufficiently high for screening the remaining viable cells (5.3%) for plasmid loss. These cells were further grown and approximately 1600 colonies were screened in terms of their ability to utilize naphthalene and limonin as sole carbon and energy sources.

Fig. 4.16 Profile of plasmid of *P. putida G7*, Lane 1: Plasmid DNA, Lane 2: 1 Kb marker

Table 4.8 Effect of different curing agents on their ability of curing plasmid from *P. putida* G7

Curing agent	Sub inhibitory concentration	Total number of colonies examined	Colonies with lost plasmid	Frequency of curing (%)
Ethidium Bromide	80 µg/ml	952	0	0
SDS	0.1 g/ml	683	0	0
Elevated temperature	45°C	875	0	0
Mitomycin C	20 µg/ml	1600	4	2.47%

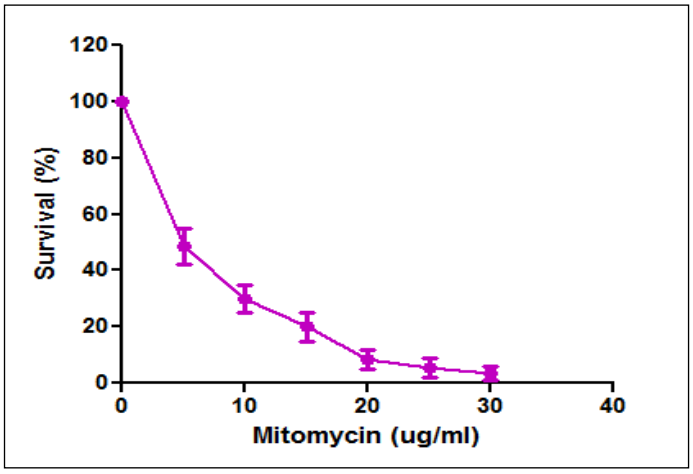

Fig. 4.17 Survival curve of *P. putida* G7 as function of mitomycin C

Amongst these four colonies, *viz*. PpC1–PpC4 were observed which did not reduce it to formazan (red color indicator) i.e. did showing their inability to utilize limonin as a carbon source as compared to the wild type. Similarly, no growth was observed in the presence of naphthalene vapors even after 24 h (Table 4.9). However in two (PpC2, PpC4) colonies, very faint growth was observed after 48 h. All the four suspected cured derivatives were analyzed for plasmid loss; however only one of the four strains (PpC1) showed the presence of plasmid (Fig. 4.18). Among the four suspected cured derivatives (PpC1-PpC4); only PpC3 was confirmed as a true cured strain (PpC3) as evidenced by loss of plasmid, and failure to grow on naphthalene and limonin as a sole carbon source. The other two cured strains viz. PpC2 and PpC4 appeared to have had the plasmid integrated into the genome, as evidenced by the absence of plasmid. PpC1 was essentially a mutant, as the strain harbored the plasmid, but lost the ability to grow on naphthalene for one reason or another. A curing frequency with a mean of 4×10^{-4} i.e 1 per cell 1.6×10^{2}, (n=6), was calculated.

Confirmation of plasmid encoded ndo gene by amplification

The plasmid encoded *ndo* gene (one of the gene responsible for naphthalene degradation) was ensured in the four suspected cured derivatives. The *ndo* gene specific primers resulted an amplification of 640 bp, which confirmed the presence of *ndo* gene in wild type and in two cured strains, viz. PpC2, PpC4. Absence of *ndo* specific amplification confirmed the absence of plasmid in PpC1 or PpC3 (Fig. 4.19).

Verification of cured strain and confirmation of plasmid encoded limonin utilization

The plasmid-encoded function for limonin utilization was verified in the PpC3 cured strain of *P. putida* G7. The strategy employed was to check the recuperation of the limonin utilization function after transmitting the indigenous plasmid from the donor wild type to the cured strain. The transconjugants obtained regained their potential to utilize naphthalene and limonin as a sole carbon and energy with a physical presence of plasmid (Fig. 4.20).

Table 4.9 Characteristic profile of four cured mutants

Putative cured derivatives	Growth on naphthalene (After 24 hrs)	Presence of ndo gene	Growth in limonin	Plasmid
PpC1	-	-	-	visible
PpC2	-	+	-	not visible
PpC3	-	-	-	not visible
PpC4	-	+	-	not visible

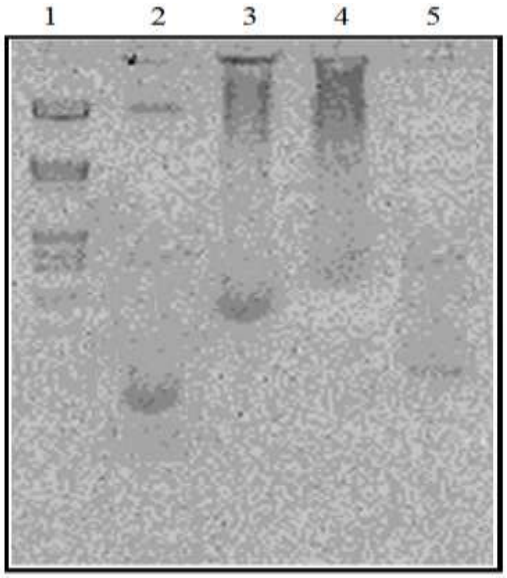

Fig.4.18 Plasmid detection in the cured derivatives of *P. putida* G7; Lane 1: 23kb ladder as marker Lane 2: Presence of plasmid in PpC1 cured strain Lane 3-5: Absence of plasmid in PpC2, PpC3, PpC4 cured derivatives

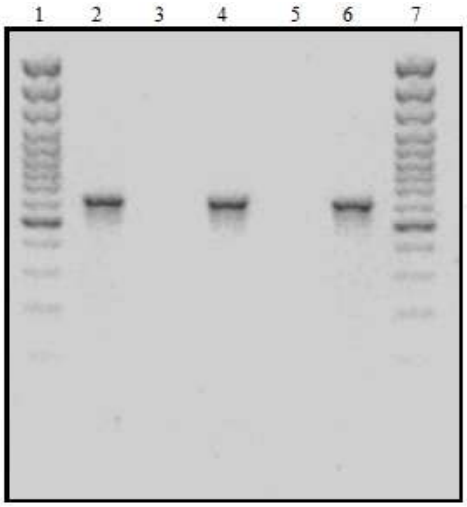

Fig. 4.19 Confirmation of plasmid encoded ndo gene located on NAH7 plasmid by amplification; Lane 1, 100 bp ladder, Lane 2,4,6, presence of ndo gene (640 bp fragment) in wild-type *P. putida* G7, PpC2 & PpC4 respectively; Lane 3& 5, absence of ndo gene in PpC1& PpC3 derivatives respectively, Lane 7, 100 bp molecular weight marker

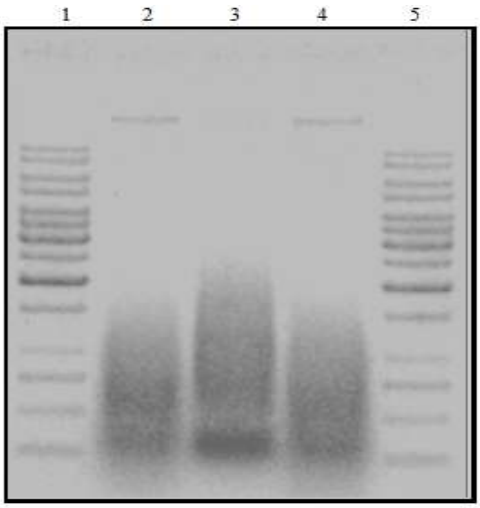

Fig. 4.20 Detection of plasmid DNA in the transconjugants screened; Lane 1: 1Kb molecular size marker, Lane 2: plasmid DNA of *P. putida* G7 (wild-type), Lane 3: Absence of plasmid in the cured strain, Lane 4: presence of plasmid DNA after conjugal transfer into cured derivative (transconjugant); Lane 5: 1 Kb molecular size marker

4.3 Biochemical attributes of limonin biotransformation

A complete understanding of the biochemical mechanism for limonin utilization by *P.putida* G7 can provide valuable insights and enable effective approaches for reducing limonin mediated bitterness in kinnow mandarin juices. Thus, the biochemical mechanism(s) of *P. putida* regarding its limonin utilization was studied. Comparison was drawn to its Tn5 mutant, which has lost its ability to utilize limonin as sole carbon source.

4.3.1 Limonin utilization kinetics by P. putida in minimal medium

Standard limonin was used as sole carbon source in minimal medium for studying limonin utilization by the wild type and mutant *P. putida*. The residual limonin level at each phase of growth was estimated for up to 50 hours. An overall reduction in initial limonin levels by 64% within 48 hours of growth was observed; the mutant survived but failed to grow (Fig. 4.21).

4.3.2 *Cellular locus of enzyme of P. putida G7*

The cell extracts of wild type and its mutant (PpC3) obtained by ultrasonic disruption were assayed for limonin degradation. A decrease in absorbance observed over time could be correlated with a proportionate decline in limonin levels; the final limonin content decreased by 03.4% (Table 4.10). A similar trend was not observed in case of cell extracts obtained from PpC3 mutant. In parallel experiments cell fractions were heat inactivated and treated with proteinase K and assayed for limonin degradation, however, initial levels of limonin did not decline in these cases. The observations indicated the involvement of enzyme for limonin degradation. Further, the cell proteins of both wild type and mutant *P. putida* cells resolved on SDS-PAGE revealed the absence of two polypeptides of molecular weight 43 KDa and 14 KDa (Fig. 4.22) suggesting a possible role of these polypeptides in limonin degradation. The cellular locus of the limonin degrading enzyme was ascertained by isolating the periplasmic, spheroplast fractions of *P. putida*. Limonin degradation assays conducted with

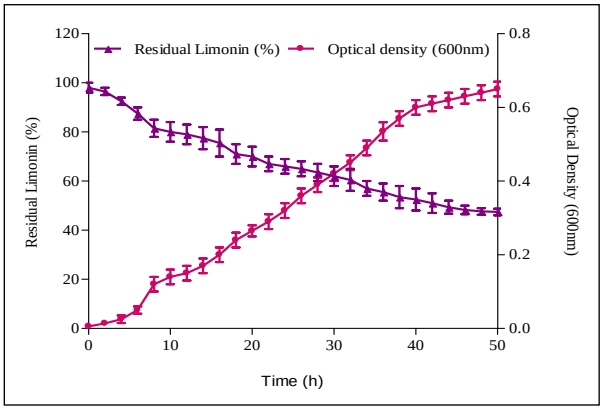

Fig. 4.21 Growth and limonin utilization profile of *P. putida* G7 in minimal medium

Table 4.10 Limonin utilization by various cellular fractions

Various cell fractions	*P. putida* (wild)	Cured *P. putida* (PpC3)
Cell free extracts	03.4%	ND
Periplasmic fraction	76.3%	ND
Spheroplast fraction	02.8%	ND

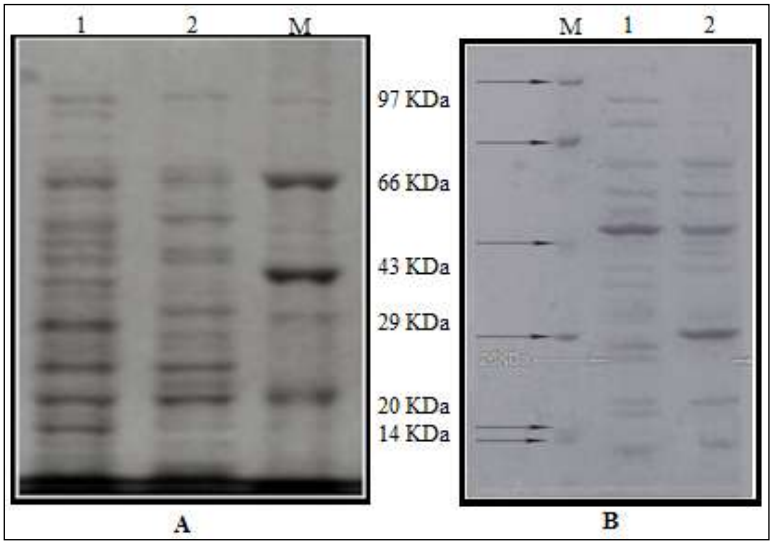

Fig. 4.22 SDS-PAGE profile for (a) cell free extract proteins of wild type of *P. putida* G7 and its PpC3 mutant; [Lane 1: Cell free extracts of wild type of *P. putida* G7; Lane 2: Cell free extracts of *P. putida* G7 (PpC3 mutant); Lane 3: Molecular weight marker]; **and (b) periplasmic fraction proteins of wild type of *P. putida* G7 and its PpC3 mutant [**Lane 1: Molecular weight marker; Lane 2: Periplasmic fraction of wild type of *P. putida* G7; Lane 3: Periplasmic fraction of *P. putida* G7 (PpC3 mutant)]

the periplasmic fraction exhibited a decline in limonin content by up to 76.3% (Table 4.10). In comparison, the periplasmic extracts of PpC3 mutant showed no change in the limonin concentration. The periplasmic fractions of both wild type and mutant *P. putida* cells were resolved on SDS- PAGE. The PpC3 mutant lacked at least five polypeptides - 22 KDa, 26 KDa, 38 KDa, 72 KDa and 89 KDa in comparison to its wild type counterpart (Fig. 4.22).

To examine whether spheroplast fractions retained limonin degrading activity, both wild type and PpC3 spheroplast fractions were assayed. Results indicated a reduction in limonin levels by 02.8% (Table 4.10). No decline in initial limonin level was detectable in case of PpC3 mutant. The requirement of cofactors was examined by extensively dialyzing the periplasmic fraction and re-assaying for limonin degradation in separate combinations comparing-dialyzate and retentate, retentate alone and retentate with NAD. The conversion of NAD to NADH was concomitant in retentate added with NAD; a five fold higher reduction in the limonin content was observed. These results suggested the requirement of the cofactor NAD for the limonin biotransforming enzyme.

4.3.3 Purification of limonin degrading enzyme

Since the limonin degrading activity was primarily obtained in the periplasmic fraction, purification was attempted in order to further characterize the enzyme. To achieve purification, the periplasmic fraction was subjected to a number of steps including gel filtration, hydroxyapatite, anion exchange and finally Mono Q (Table 4.11) to obtain 26-fold purification of the enzyme with an overall yield of 26%. SDS–PAGE of the purified enzyme revealed a single distinct band of a molecular mass of 26 kDa (Fig. 4.23), implying the integrity and purity of the purified enzyme. The molecular mass of the native enzyme was 26 kDa, indicating the enzyme to be a monomer.

4.434 Immunoblotting and Zymography

To determine whether the limonin degrading enzyme is homologous to other previously reported enzymes having similar function, the 26 kDa polypeptide was cross-reacted with monospecific anti-LDase antibodies raised against *A. globiformis* Limonin dehydrogenase. Cross reaction of the *P. putida* enzyme to that of *A. globiformis* could be clearly demonstrated (Fig. 4.24). To elucidate the nature of the enzyme, activity staining assay was carried out. The 26kDa band showed a strong fluorescence under UV light upon incubation with limonin (Fig. 4.25) suggesting a "dehydrogenase" nature of the enzyme.

4.3.5 Peptide mass fingerprinting

To further characterize the limonin degrading enzyme, purified enzyme was subjected to peptide mass fingerprinting. The MASCOT and Pro Found searches indicated this protein to be homologous to Salicylaldehyde dehydrogenase (DoxF, SaliADH, EC=1.2.1.65) involved in the upper naphthalene catabolic pathway of Pseudomonas strain C18. The salicylaldehyde dehydrogenase possessed 48% of amino acid identity (53% similarity) to DoxF from Pseudomonas C18, with alignment coverage of 82%. Similar results were obtained when the predicted peptide sequence was analyzed by BLAST (p), followed by an analysis of similar peptide sequences clustal alignment of the various sequences (Fig. 4.26). The conserved domains on the sequence from amino acid residues 65-190 were similar with aldehyde dehydrogenase super family (ALDH-SF) of NAD (P) dependent enzymes. The amino acid residues from 220-308 shows a similarity with the NADB Rossmann super family that shares Rossmann-fold NAD(P)H/NAD(P)(+) binding (NADB) domain. The NADB domain is found in numerous dehydrogenases of metabolic pathways such as glycolysis and many other redox enzymes. The proteins in this family comprise a second domain in addition to the NADB domain, which is responsible for specifically binding a substrate and catalyzing a particular

enzymatic reaction. The sequence of the limonin dehydrogenase has been submitted in Uniprot KB, the accession number of the protein is P86808.

Table 4.11 Purification profile of periplasmic limonin dehydrogenase of *P. putida* G7

Purification Step	Total protein (mg)	Specific activity ($IUmg^{-1}$)	Purification (fold)	Yield (%)
A- Periplasmic extract	300 (±0.06)	5.6(±0.02)	1(±0.03)	100(±0.03)
B- Gel filtration	130(±0.07)	9.9(±0.05)	1.8(±0.02)	78(±0.02)
C-Hydroxyapatite	32 (±0.02)	25(±0.03)	4.5(±0.03)	48(±0.01)
D-Anion exchange	6.5(±0.02)	110(±0.01)	20(±0.02)	43(±0.02)
E-Mono Q	3.0(±0.01)	145(±0.04)	26(±0.01)	26(±0.03)

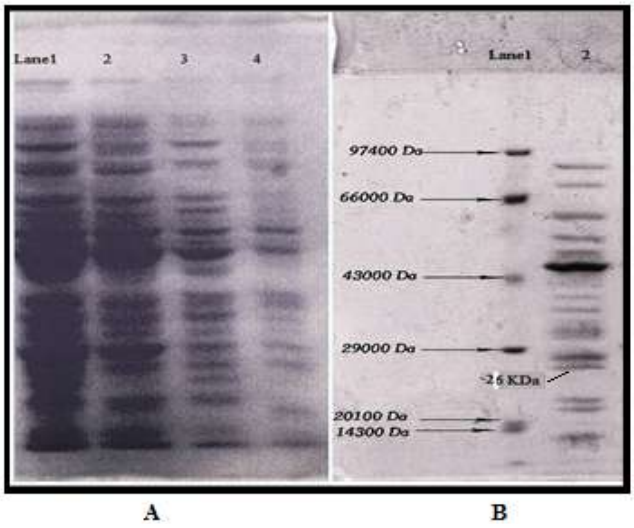

Fig. 4.23 SDS PAGE of periplasmic extract of *P. putida* G7; (A) Lanes 1-4, shows the protein profile of the periplasmic enzyme during various purification steps (B) shows the SDS-PAGE of the purified periplasmic enzyme, Lane1: Molecular markers; Lane2:Purified limonin dehydrogenase of *P.putida* G7

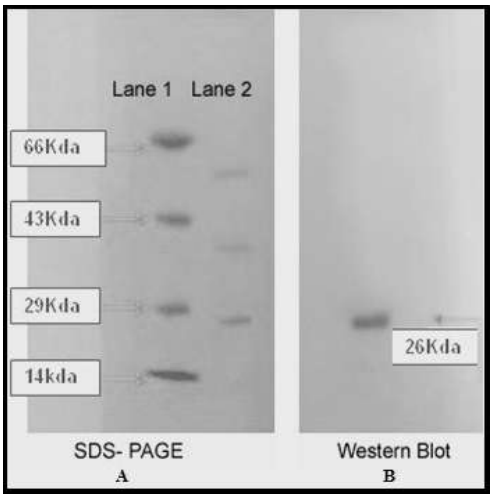

Fig. 4.24 Western blot analysis of the limonin degrading enzyme of *P. putida* G7 (A) SDS PAGE [Lane1: Molecular weight marker, Lane 2: Purified periplasmic fraction of *P. putida* G7] and (B) Western blot analysis of purified periplasmic fraction

Fig. 4.25 Zymogram of LDase activity; a single band of protein corresponds to *in situ* assay for LDase activity

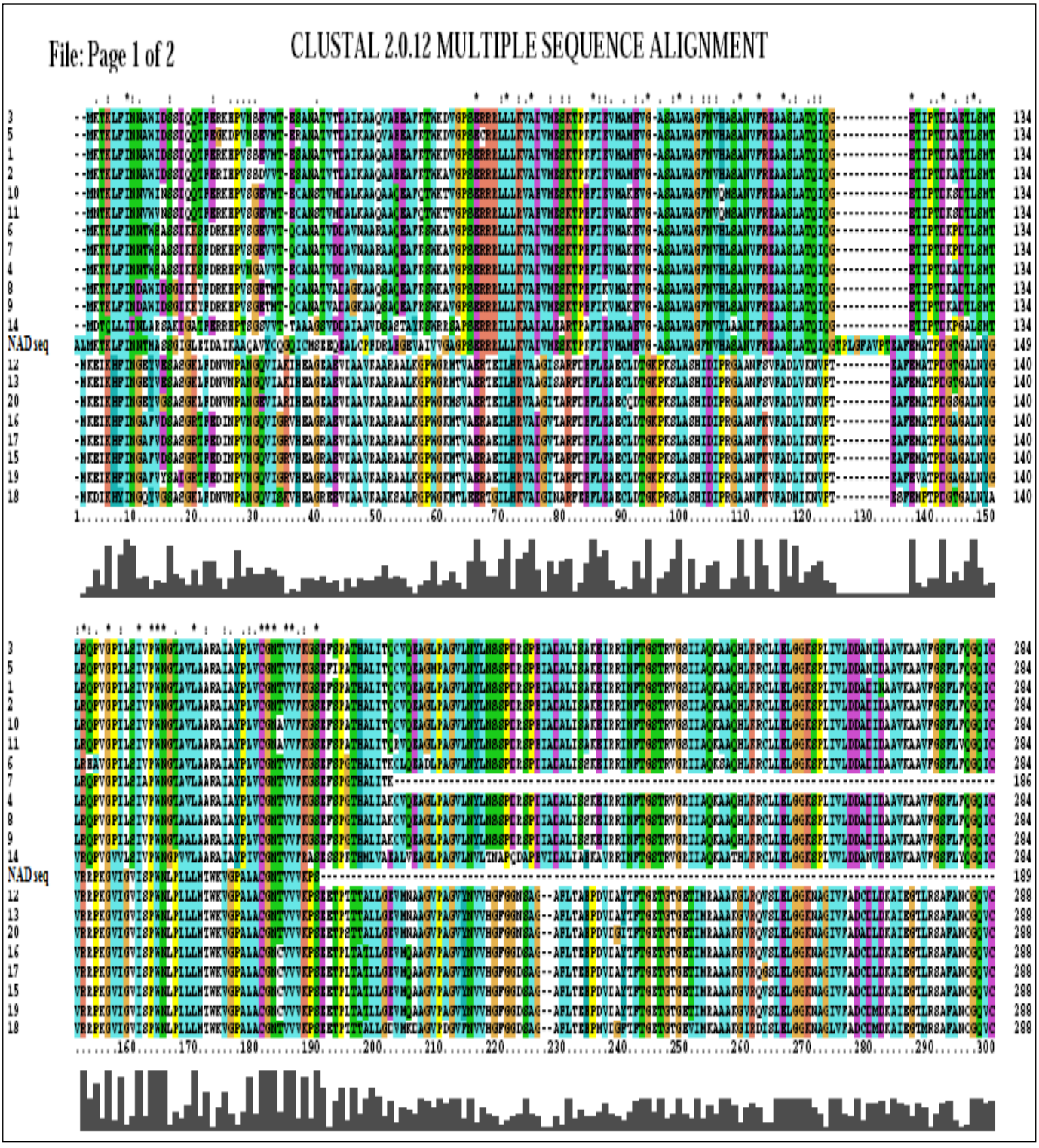
File: Page 1 of 2
CLUSTAL 2.0.12 MULTIPLE SEQUENCE ALIGNMENT
NADseq

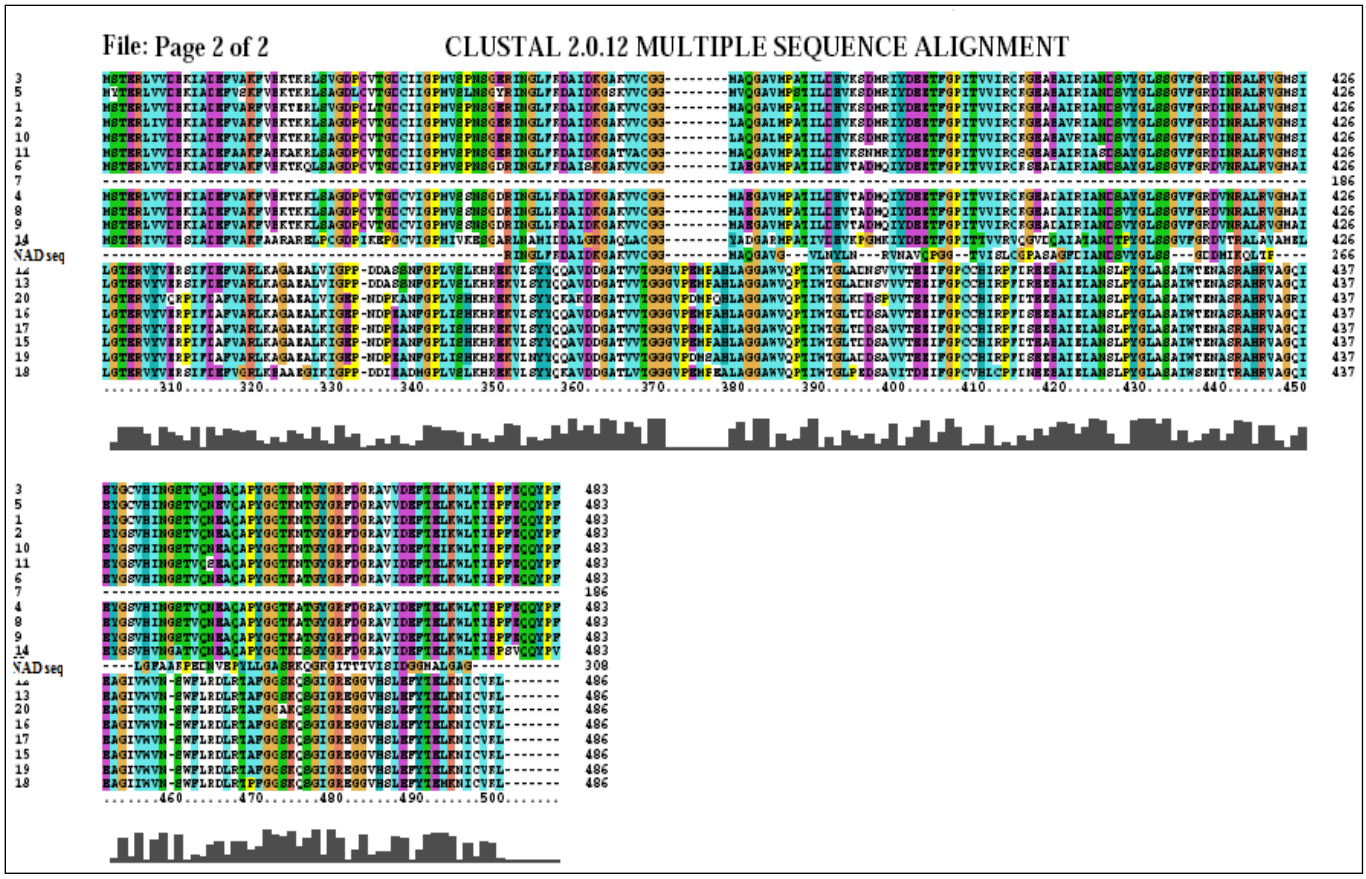

Fig. 4.26 CLUSTALX alignment of predicted peptide sequence seq (1) from *Pseudomonas putida* G7 with similar peptide sequences; gi|90576583|ref|YP_534825.1| salicylaldehyde dehydrogenase NahF [Pseudomonas putida](**1**); gi|32469901|ref|NP_863075.1| salicyladehyde dehydrogenase [Pseudomonas putida] (**2**); gi|2189974|dbj|BAA20394.1| dehydrogenase [Pseudomonas putida] (**3**); gi|254028646|gb|ACT53252.1| salicylaldehyde dehydrogenase [Burkholderia sp. C3] (**4**); gi|15809675|gb|AAL07269.1| salicylaldehyde dehydrogenase [Pseudomonas fluorescens] (**5**); gi|3337416|gb|AAD12613.1| salicylaldehyde dehydrogenase [Ralstonia sp. U2] (**6**); gi|8118288|gb|AAF72979.1|AF252550_6 salicylaldehyde dehydrogenase-like protein [Comamonas testosteroni] (**7**); gi|121605378|ref|YP_982707.1| aldehyde dehydrogenase [Polaromonas naphthalenivorans CJ2] (**8**); gi|74136893|gb|AAZ93391.1| salicylaldehyde dehydrogenase [Polaromonas naphthalenivorans CJ2](**9**); gi|1255672|dbj|BAA12243.1| dehydrogenase [Pseudomonas aeruginosa] (**10**); gi|4104756|gb|AAD02139.1| salicylaldehyde dehydrogenase [Pseudomonas stutzeri] (**11**); gi|19033978|gb|AAL83661.1| 2-hydroxymuconic semialdehyde dehydrogenase [Pseudomonas putida] (**12**); gi|111116464|ref|YP_709348.1| 2-hydroxymuconic semialdehyde dehydrogenase [Pseudomonas putida] (**13**); gi|171057492|ref|YP_001789841.1| aldehyde dehydrogenase [Leptothrix cholodnii SP-6] (**14**); gi|3293056|dbj|BAA31265.1| 2-hydroxymuconic semialdehyde dehydrogenase [Pseudomonas stutzeri] (**15**); gi|4104767|gb|AAD02149.1| hydroxymuconic semialdehyde dehydrogenase [Pseudomonas stutzeri] (**16**); gi|37220706|gb|AAQ89676.1| hydoroxymuconic semialdehyde dehydrogenase [Pseudomonas putida] (**17**); gi|149375513|ref|ZP_01893283.1| 2-Hydroxymuconic semialdehyde dehydrogenase [Marinobacter algicola DG893] (**18**); gi|47078060|gb|AAT09777.1| XylG [Pseudomonas sp. ST41] (**19**); gi|226943016|ref|YP_002798089.1| 2-hydroxymuconic semi-aldehyde dehydrogenase [Azotobacter vinelandii DJ] (**20**); NAD seq from *Pseudomonas putida* G7(query sequence). Asterisks (‘*’) above the aligned sequences identical residues in all sequences. Positions with colons (‘:’) contain a residue of the strongly conserved groups in all sequences, and periods (‘.’) indicate weakly conserved groups in all sequences.

4.3.6 Catalytic properties of the limonin degrading enzyme

The limonin utilization by the purified enzyme was conclusively demonstrated from HPLC results. The chromatograms revealed the substrate retention time to be 9.3 minutes; a reduction in peak following catalysis by the purified dehydrogenase was observed. A biotransformation was evidenced from the appearance of two new peaks at retention times of 15.9 and 25.2 minutes (Fig. 4.27). The peak area of 66% of standard limonin in the medium, following reaction with the purified enzyme of *P. putida* G7 resulted in reduction in peak area to 9.07%, which corresponded to 76% of limonin reduction. However, a complete disappearance of limonin peak was not observed due to the presence of residual limonin in the medium. These results indicated a strong role of the dehydrogenase for limonin utilization.

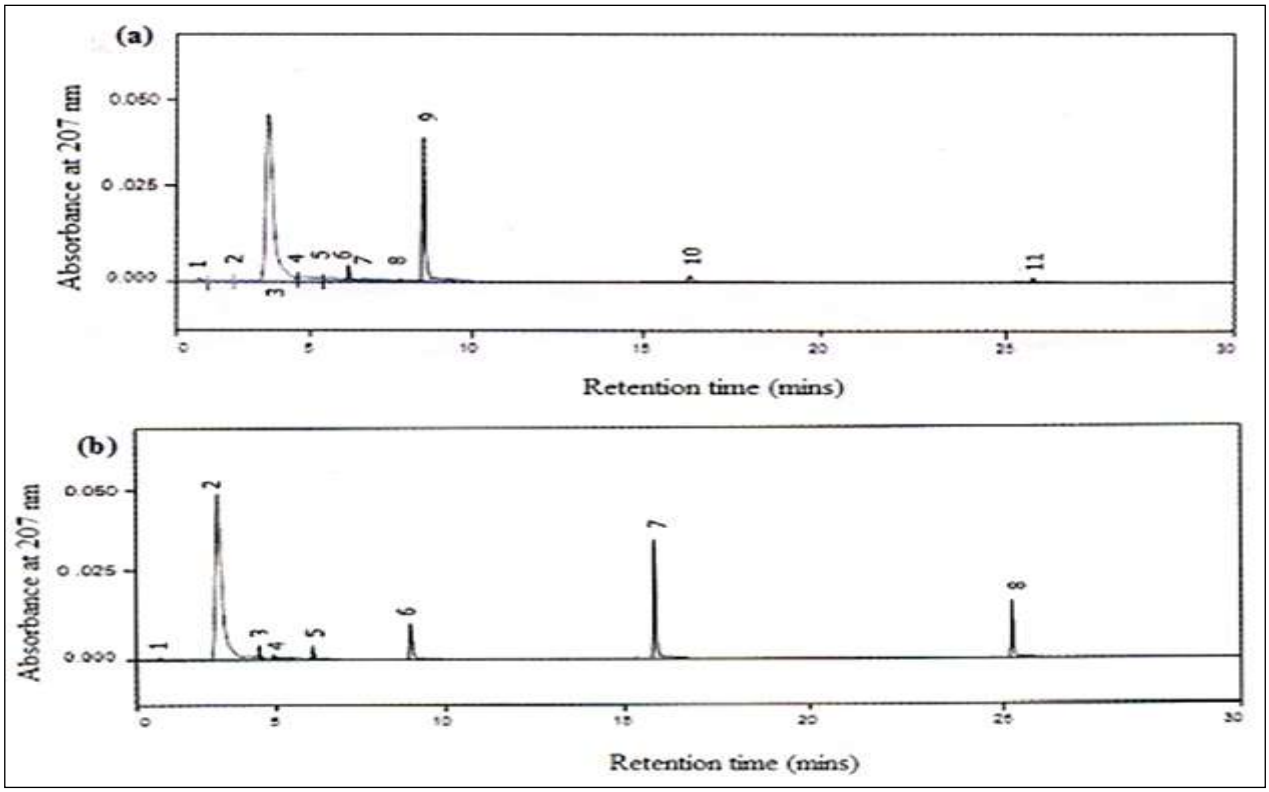

Fig. 4.27 (a) HPLC chromatogram of standard limonin (90µg/ml) and (b) chromatograms of standard limonin (90µg/ml) utilization by purified enzyme of *Pseudomonas putida* G7, using an acetonitrile/deionised water (32:68) with a flow rate 0.9 ml/min and an injection volume of 20 µl

The Kinetic parameters - maximum reaction velocity (V_{max}) and apparent Michaelis constant (K_M) were determined for purified periplasmic enzyme with respect to the limonin at 35°C by Lineweaver–Burk plot. Under optimal conditions (35ºC, pH 8.5), limonin utilization activity exhibited Michaelis–Menten type kinetics (Fig. 4.28), The Michaelis constant (K_M) measured for limonin was 4.5µM and V_{max} was found to be 8µmoles/min. At 35ºC the purified enzyme resulted in 76% degradation (Fig. 4.29a) followed by a steady state at pH 8, at lower pH values of 3-5 degradation was relatively less (Fig. 4.29b), indicating that utilization of limonin was maximum at alkaline pH 8. The purified enzyme exhibited no activity at temperatures higher than 65°C. The following activities were observed over a temperature range of 10°C - 70°C (Fig. 4.29c). In all the above cases optimal activity was attained at 35ºC in the presence of NAD^+. The ability of the periplasmic enzyme to catalyze different substrates (at an optimum pH of 7.0), was examined thereafter.

The purified dehydrogenase exhibited broad substrate specificities and catalyzed the oxidation of salicylaldehyde, 5-chlorosalicylaldehyde, *m*-nitrobenzaldehyde, *o*-methoxybenzaldehyde, formaldehyde, and glutaraldehyde. However, the relative rates at which the substituted analogs were transformed differed considerably (Table 4.12). The enzyme displayed the greatest activity for Limonin followed by salicylaldehyde; the derivatives of salicylaldehyde, 5-chlorosalicylaldehyde and m-nitrobenzaldehyde were also transformed at high rates. A variety of enzyme inhibitors was tested for their ability to inhibit the limonin biotransforming activity (Table 4.13). Addition of 1 $x10^{-3}$ EDTA did not reduce the activity whereas $HgCl_2$, SDS, $CoCl_2$ and NaN_3 reduced the enzyme activity respectively indicating the possibility that sulfhydryl group(s) may be required for activity. Divalent ions; Ca, Mg, Mn did not result in reduction of activity.

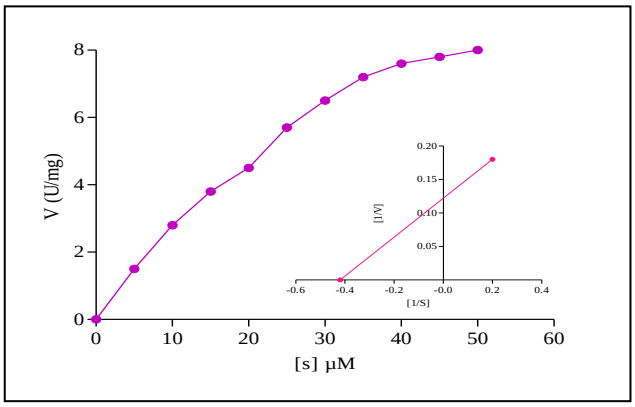

Fig. 4.28 Michaelis constant (K_M) for purified periplamic enzyme of *P. putida* G7 with respect to limonin (substrate) by Lineweaver–Burk plot at optimal conditions (35˚C, pH 8.5)

(a)

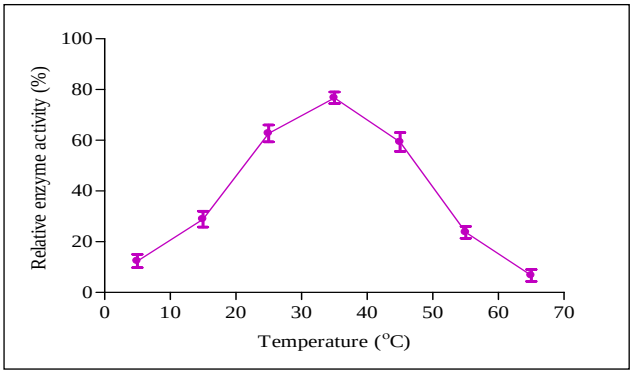

(b)

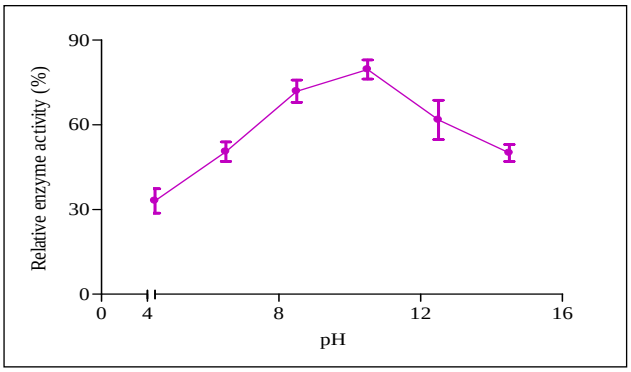

(c)

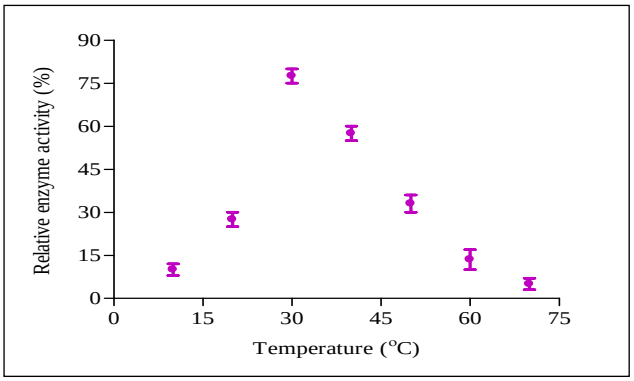

Fig. 4.29 Kinetic parameters of periplasmic dehydrogenase catalyzing limonin (a) temperature, (b) pH, and (c) its thermal stability; [a)]Values are mean of three replicates

Table 4.12 Substrate specificity of the purified enzyme

Substrate	Relative activity (%)
Limonin	100[a](±0.02)
m-nitrobenzaldehyde	23 [a](±0.07)
Salicylaldehyde	96.4 [a](±0.05)
5-chlorosalicylaldehyde	64 [a](±0.02)
Glutaraldehyde	1.8 [a](±0.03)
Formaldehyde	2.5 [a](±0.02)
***o*-methoxybenzaldehyde**	1.5 [a](±0.01)

[a]Activities were obtained according to the standard procedure with the substrate concentration of 200 µmol/L and expressed as the percentage of the maximum activity detected (100%)

Table 4.13 Effect of inhibitors and metal ions on periplasmic dehydrogenase

Effector	Conc (mM)	Relative activity*
None	-----	100%(±0.07)
EDTA	10	100%(±0.03)
SDS	1	25%(±0.01)
NaN_3	1	ND[a](±0.05)
$HgCl_2$	1	ND[a](±0.03)
$CaCl_2$	1	100%(±0.04)
$MgCl_2$	1	100%(±0.01)
$MnCl_2$	1	98.8%(±0.07)
$CoCl_2$	1	40.2%(±0.02)

* 100% activity with limonin as substrate; [a]ND: not detected; [b)] Activities were assayed according to standard procedures with the purified enzyme in the presence of various metal ions with a final concentration of 1-10 mmol/L and expressed as relative activity, as the percentage of the activity detected without metal ions (100%)

4.3.7 Identification of limonin biotransformed product

Thin Layer chromatography

It was desirable to examine the products following utilization of limonin. Thin layer chromatography is an important initial procedure for identification of biotransformed product and has been used in earlier studies for investigating degradation/utilization of limonin. The aliquots of enzyme utilizing limonin were examined at regular intervals by resolving on TLC plates along with references available commercially. Ehrlich's reagent was used to develop and detect the spots on the TLC plates: the Ehrlich test constitutes a good evidence for the presence of a furan ring in the substrate, a characteristic of limonoids, the latter produce characteristic yellowish orange spots with this reagent. R_f values were calculated for the spots and were compared with the references (Table 4.14). The neutral and acidic fractions of juice serum extracts were analyzed and results were similar to that of results obtained by analysis of 0 h culture grown in minimal media containing juice.

The neutral fraction showed three spots (one spot with R_f value of 0.54 had the same mobility to that of the standard limonin) and only one spot could be detected in acidic fraction. The neutral fraction of utilized sample resulted with a very faint spot as compared to the intense spot for standard limonin. The absence of any other spot in the neutral fraction indicated that the metabolites formed after transformation of limonin not to be present in the neutral fractions. However, when acidic fraction of the above sample was analyzed one spot was detected having R_f values similar to defuran limonin, and very faint bands of deoxylimonin, deoxylimonoic acid and 17- Dehydrolimonoate A-ring lactone. The defuran formation is shown in Fig.4.30.

Table 4.14 R_f values of the biotransformed products of limonin

Sample	Fractions	Benzene-ethanol-water-acetic acid (200:47:15:1)
Standard limonin		0.81[a]
Utilization standard limonin	Neutral fraction (Dichloromethane)	0.50 0.71
	Acidic fraction (Ethyl acetate)	0.20[c] 0.83[b] 0.41[d]
Juice serum	Neutral fraction (Dichloromethane)	0.82[a] 0.5 0.39
	Acidic fraction (Ethyl acetate)	0.87
Juice serum (Utilization limonin)	Neutral fraction (Dichloromethane)	0.52 0.74
	Acidic fraction (Ethyl acetate)	0.21[c] 0.85[b] 0.43[d]

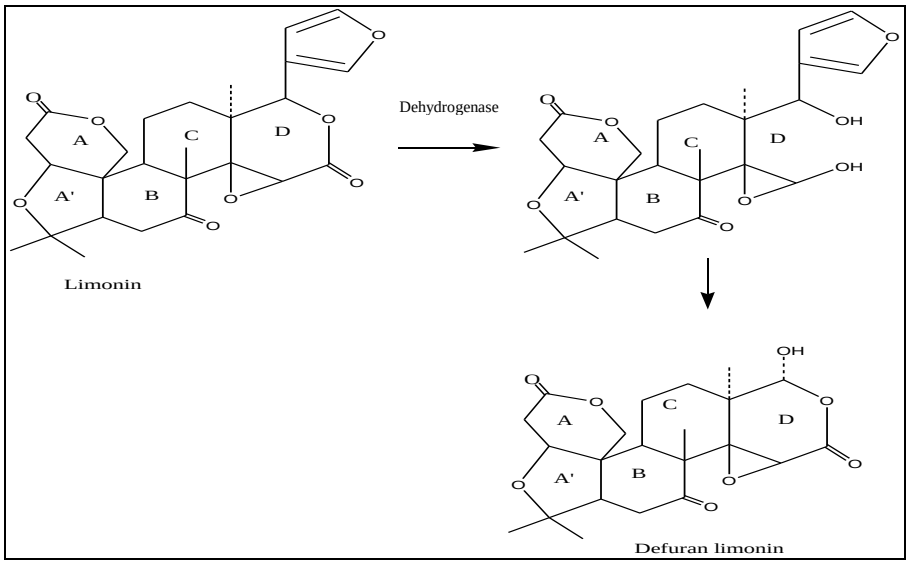

Fig. 4.30 Proposed scheme of biotransformation of limonin to defuran limonin; proposed chemical mechanism is referred in two steps: removal of defuran is facilitated by delocalization of electron on the oxygen atom of D ring lactone followed by subsequent protonation of D ring

Nuclear Magnetic Resonance(NMR) Spectroscopy

The structure of predicted biotransformed product of limonin from thin layer chromatography was confirmed by nuclear magnetic resonance (NMR) spectroscopy and the purity of the isolated limonoids was analyzed by HPLC. To elucidate the structures of the metabolites, MS, ^{1}H and ^{13}C NMR were used. The ^{1}H and ^{13}C spectra of limonin and defuran limonin with assignments of various signals are shown in Fig. 4.31a and 4.31b, respectively.

On the basis of the NMR results, the structure of the biotransformed product for limonin was tentatively identified as defuran limonin. ^{13}C NMR spectra demonstrated the signals in which "C" peaks 21, 22, 23, 4 are absent in case of defuran limonin spectra as compared to the ^{13}C NMR spectra of limonin. The "C" peak 20 in limonin spectra at position 120.0 has shifted to 170 in defuran limonin spectra. In case of ^{1}H NMR spectra the signals for "H" peaks 21, 22, 23, 15, 1 are absent in case of defuran limonin spectra. The "H" peak 17 in limonin spectra at position 5.0 have shifted before 5.0 & 4.0 in defuran limonin spectra. A new peak for 5 appeared at position 4.0 in defuran limonin spectra and absent in limonin spectra. In addition, mass spectra of the modified limonoids reported the molecular ion peak at m/z 506.2294 [M+Li]+ and 447.1145 [M- H]- for limonin and defuran limonin, respectively.

4.3.8 Antioxidant & Chemopreventive properties

Recent studies have highlighted the potential of several debitterring compounds for their bioactivity; in this regard, the antioxidant activity of limonin has been documented. Thus it was pertinent to carry out preliminary studies pertaining to bioactivity of the utilization metabolic products of limonin. A comparison to untransformed limonin was drawn in order to determine whether limonin retained its therapeutic properties upon being subjected to the microbial enzyme. The total antioxidant activities of limonin and its utilization product (defuran limonin) was determined by scavenging ABTS radical and DPPH radical and decrease in β carotene levels. The β carotene bleaching assays revealed a decrease in

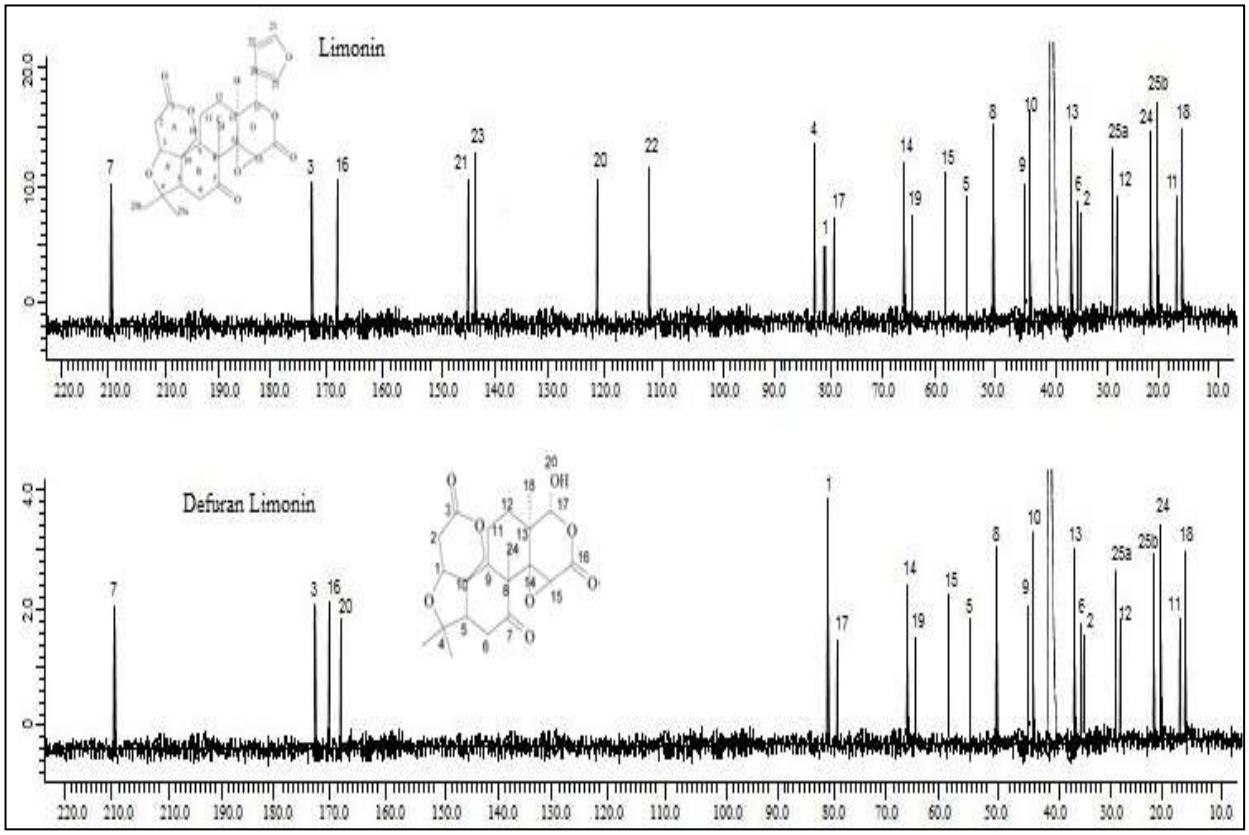

(a)

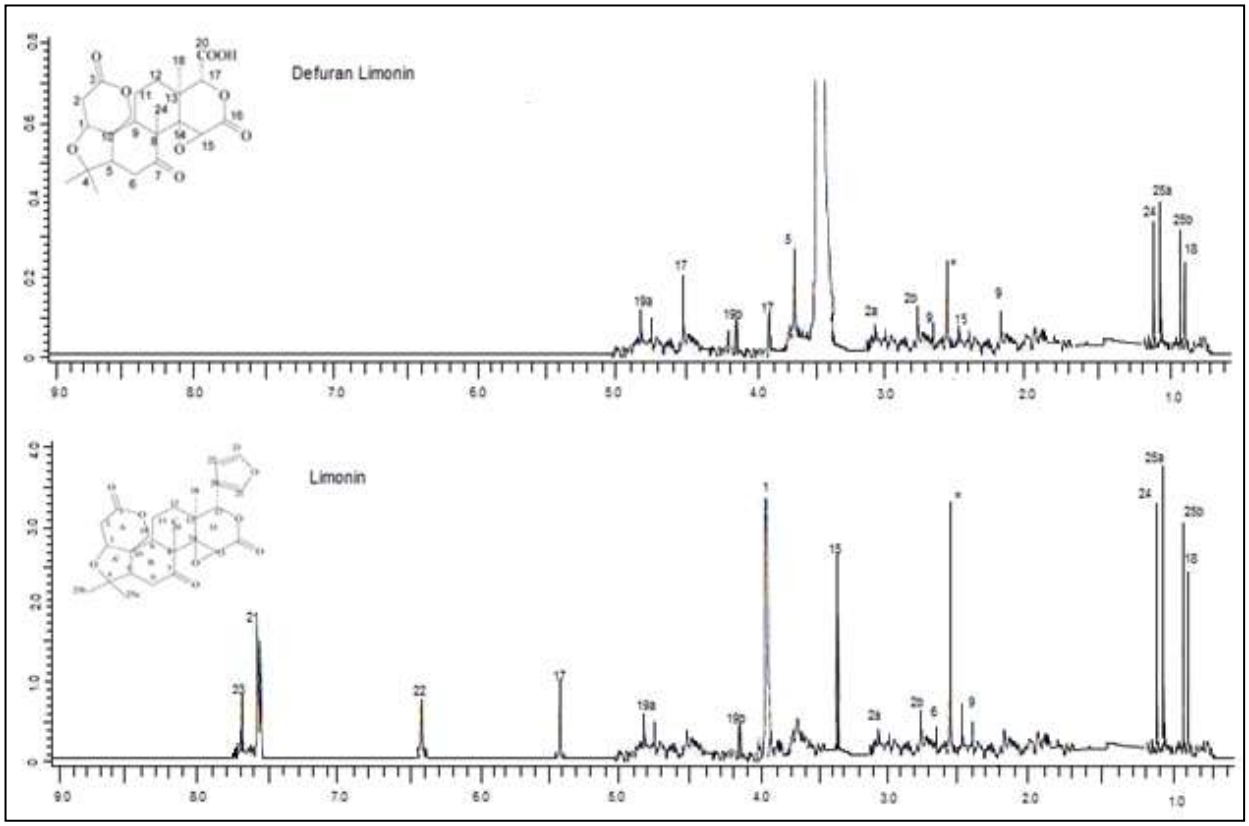

(b)

Fig. 4.31 ^{13}C (a) and ^{1}H NMR (b) spectra of biotransformed product of limonin

absorbance for up to 30% and 32% for limonin and defuran limonin (utilization product of limonin) (Fig. 4.32a). The ABTS radical reduced by 10% and 12% respectively with limonin and defuran limonin, whereas DPPH was scavenged to 13% and 11%. Superoxide radical was simulated at a very minimal level (Fig. 4.32b). The activities of limonin and defuran limonin for the various antioxidant were approximately similar i.e. no significant changes ($p>0.05$) occurred in both DPPH, ABTS scavenging activity of limonin and defuran limonin. Thus, during the enzyme mediated transformation the utilization products retained the original nutritional attributes of limonin implying the practical applicability of the enzyme for debitterring process.

(a)

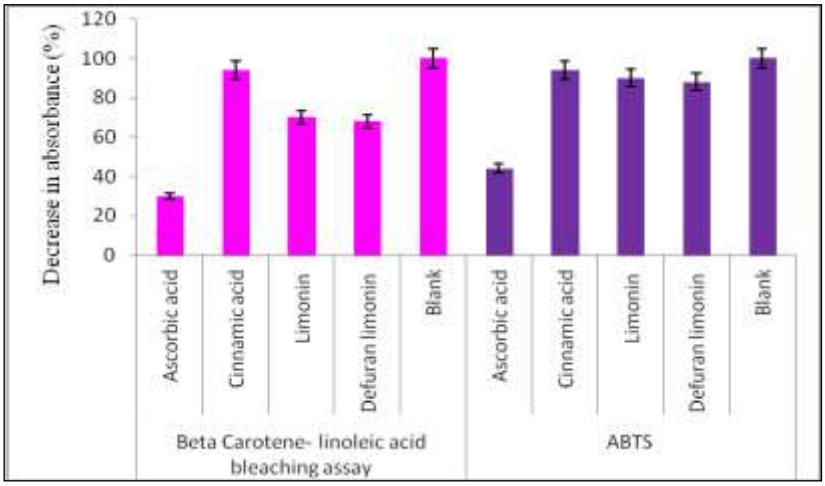

*Cinnamic acid and ascorbic acid were used as negative and positive controls respectively.

(b)

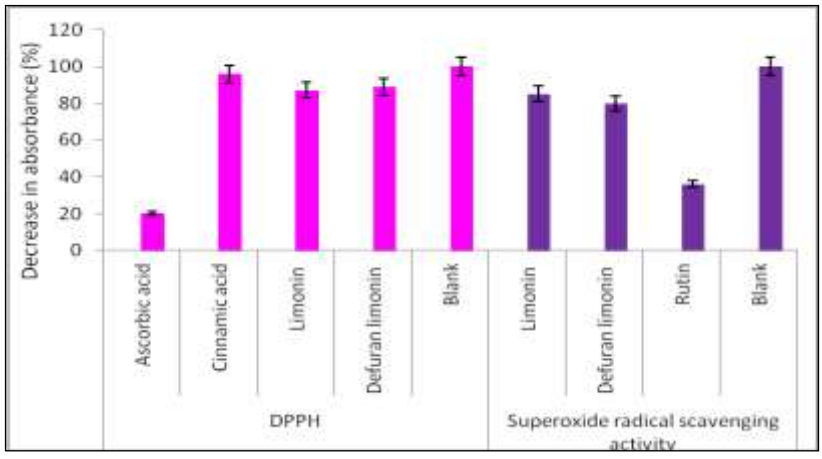

[a]Values are means ± SD, n=3, *Cinnamic acid and ascorbic acid were used as negative and positive controls respectively for DPPH activity. Rutin as positive control and reaction without NBT (Nitroblue tetrazolium) as negative control were used. Values are means ± SD, n=3

Fig. 4.32 Antioxidant activity of limonin and its biotransformed product determined by (a) β carotene bleaching and ABTS radical cation decolorization, (b) DPPH radical scavenging activity and superoxide radical scavenging simulation

4.4 Real time application of *P. putida* G7 for debittering mandarin (citrus) juice

Since the ultimate objective of the study is to devise an approach for reducing limonin content of kinnow mandarin juices, a complete compositional analysis prior to application of *P. putida* G7 and following its application was deemed important. In order to analyze the composition, the citrus juice was extracted as described by Kola et al. 2010, and pasteurized. Pasteurization was attempted to inactivate the contaminating microbial flora and retain the inherent components of the juice. To verify whether the pasteurized juice possessed initial limonin levels as well as the nutritional components, levels of limonin were estimated in both pasteurized and unpasteurized citrus juice regularly till 12 weeks (Fig. 4.33). The limonin levels in both pasteurized and unpasteurized juices were found to be 55.63 ppm and 53.21 ppm respectively. The typical juice yield, Ascorbic acid (Vitamin C), TSS (Total soluble solids), TA (Titrable acidity) TSS/TA ratio, total sugars, microbial population, of the pasteurized and unpasteurized citrus juice are depicted in Table 4.15. An increased TSS observed with gradual increase of juice extraction might be due to hydrolysis of polysaccharides into monosaccharide and oligosaccharides. The Vitamin C content were 29.1 mg/ml and 28.7 mg/ml in both pasteurized and unpasteurized citrus juice respectively and the total juice yields of pasteurized was 30.9% and that of unpasteurized citrus juice 31.2%. These results suggested that significant ($p<0.05$) differences did not occur following pasteurization.

Kinetic studies of P. putida G7 for limonin utilization in mandarin juice

Kinetic studies are important for understanding the response of the bacterial cell towards any specific compound or carbon source. The kinetics of *P.putida* G7 was determined in mandarin juice and minimal medium with limonin as sole source of carbon. The cells exhibited a specific growth rate of 0.23 h^{-1}, as much as 45% limonin utilization was noted. (Fig. 4.34); utilization of limonin was not observed during stationary phase.

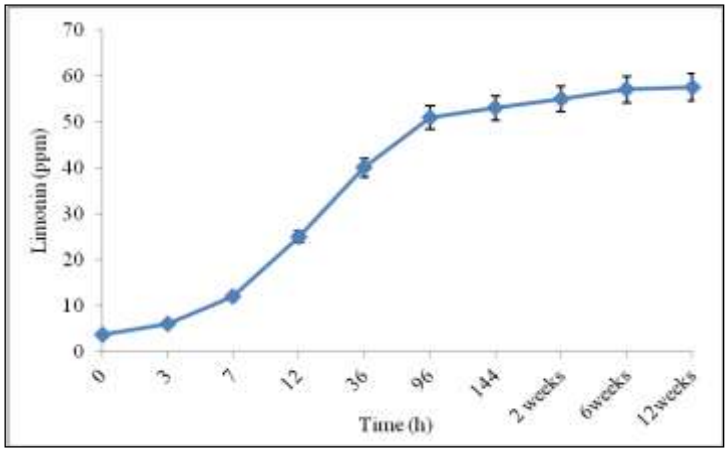

Fig. 4.33 Limonin content with ageing of juice

Table 4.15 Physiochemical properties of mandarin juice

Quality parameter	Mandarin juice (Pasteurized)	Mandarin juice (UnPasteurized)
Juice yield (%)	30.93 ± 1.07	31.2± 1.12
TSS (g L^{-1})	118.67 ± 1.31	121.67 ± 1.11
TA (g L^{-1})	61.42 ± 1.44	60.76 ± 1.05
TSS/TA ratio	1.9 ± 0.03	1.7 ± 0.05
Vitamin C (mg mL^{-1})	29.1 ± 0.41	28.7± 0.37
Total Phenolics	778 mg GAE L^{-1}	775 mg GAE L^{-1}
Total Flavonoids	53.7 mg CE L^{-1}	54.1 mg GAE L^{-1}
Total Sugars	7.6%	7.1%
Bacterial population(cfu/ml)	3	$9.1x10^3$
Yeast population(cfu/ml)	1	$4.3x10^3$
Mould population(cfu/ml)	0	$3.2x10^3$

[a]Results are expressed as means ± standard deviation of three measurements. Means followed by a different letter are significantly different.

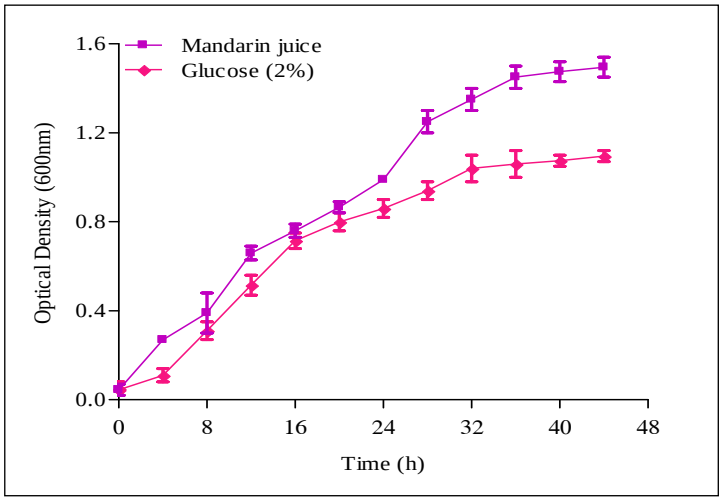

Fig. 4.34 Growth kinetics and limonin utilization profile of *P. putida* G7 in mandarin juice and in minimal medium with limonin as sole source of carbon

4.4.1 Cell immobilization of P. putida G7 to enhance limonin biotransformation

In order to efficiently immobilize bacterial cells various parameters were optimized. Among the various preliminary experiments performed for the selection of process parameters effecting limonin biotransformation in citrus juice, alginate concentration, cell load and bead diameter were screened as the most significant parameters for maximal limonin biotransformation by immobilized *P. putida* G7. Limonin in citrus juice was biotransformed upto 40% and 58% with *P. putida* G7 cells (cell load of 50 mg/ml) immobilized in agar and alginate respectively (Fig. 4.35). Biotransformation response with cell immobilized in agar (concentration of 2.5% and bead diameter of 2.0 mm) was lower i.e. 30% as compared to the cells immobilized in alginate (concentration of 3% and bead diameter of 2.5 mm) which showed a response of 57% in citrus juice (Fig. 4.36). Based on the response of conventional studies, alginate was preferred as a matrix for immobilizing *P. putida* G7 cells to direct the further studies for limonin biotransformation in citrus juices.

Statistical analysis

The combined effect or the inter-relationship of the parameters for limonin biotransformation response was observed with a face centered cube design of 2^3=8 + 6 centre points and 6 (2x3) star points which lead to a total of 20 experiments. The coded value of the selected variables is present in Table 4.16. Based on the optimization of process parameters and the experimental results (obtained from CCD and regression analysis) (Table 4.17), the relationship between the limonin biotransformation and the significant parameters (alginate concentration, cell load and bead diameter) was established in the form of a quadratic polynomial equation. The equation for the model in terms of coded factors is present in Table 4.18.

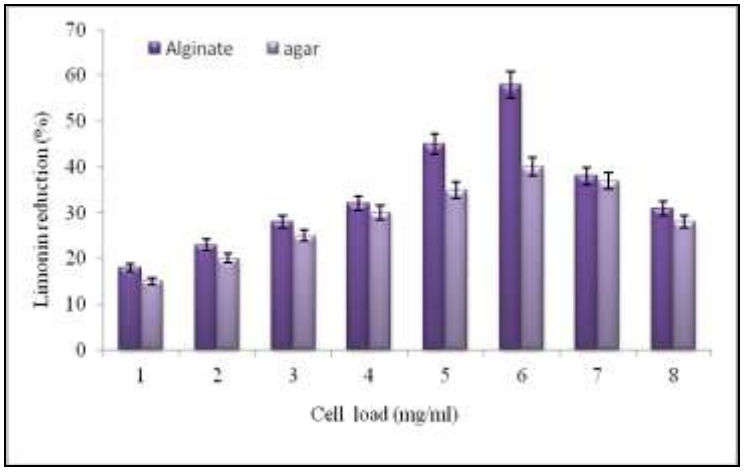

Fig. 4.35 Effect of cell load (w/v) in alginate beads on limonin reduction

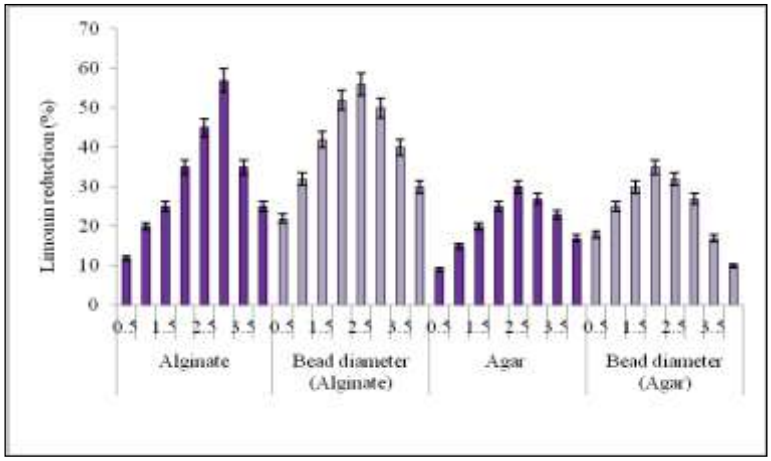

Fig. 4.36 Effect of concentration of alginate, agar and their respective bead size for immobilizing *P. puitda* G7 cells on limonin reduction

Table 4.16 Coded values of all the significant variables selected

Variables	Coded Values				
	-α	-1	0	+1	+ α
A- Alginate concentration (%, w/v)	0.32	1	2	3	3.68
B- Cell load (mg/ml)	36.5	40	45	50	53.41
C-Bead diameter (mm)	1.16	1.5	2	2.5	2.84

Table 4.17 Response surface central composite design (CCD) for limonin biotransformation

Run	A	B	C	R1-Limonin Biotransformation(%)		R2 - Stability	
				Actual	Predicted	Actual	Predicted
1	2.00	36.59	2.00	50.1	50.45	0.092	0.10
2	0.32	45.00	2.00	63.8	62.47	0.089	0.094
3	2.00	45.00	1.16	55.6	57.54	0.126	0.13
4	1.00	40.00	2.50	56	56.12	0.12	0.11
5	2.00	45.00	2.00	64.5	64.43	0.11	0.11
6	2.00	45.00	2.00	64.3	64.43	0.11	0.11
7	2.00	45.00	2.00	64.4	64.43	0.11	0.11
8	3.00	40.00	1.50	61.8	59.17	0.16	0.15
9	3.00	50.00	2.50	60.6	59.74	0.145	0.14
10	1.00	40.00	1.50	49.7	50.42	0.07	0.072
11	1.00	50.00	1.50	62.7	61.49	0.13	0.12
12	2.00	45.00	2.00	64.4	64.43	0.1	0.11
13	3.00	50.00	1.50	60.1	59.83	0.138	0.15
14	2.00	53.41	2.00	59.2	59.05	0.132	0.13
15	3.00	40.00	2.50	59.5	60.57	0.15	0.15
16	2.00	45.00	2.00	64.5	64.43	0.11	0.11
17	3.68	45.00	2.00	63.3	64.83	0.15	0.15
18	1.00	50.00	2.50	63.2	65.69	0.138	0.14
19	2.00	45.00	2.84	64	62.25	0.15	0.15
20	2.00	45.00	2.00	64.5	64.43	0.11	0.11

[a]A-Alginate concentration, B- Cell Load, C- Bead diameter, R1-Limonin Biotransformation (%), R2- Stability (O.D. 600 nm)

Table 4.18 Model equation for limonin biotransformation by *P.putida* G7

Limonin biotransformation (R1) = $+64.43 + 0.70 * A + 2.56 * B + 1.40 * C - 2.60 * A * B - 1.07 * A * C - 0.37 * B * C - 0.28 * A^2 - 3.42 * B^2 - 1.60 * C^2$

Where Y is the response value for limonin biotransformation (%), A- Alginate concentration, B- Cell Load, C- Bead diameter

The analysis of variance (ANOVA) of the model for limonin biotransformation are presented in Table 4.19. The F value (14.97) of the model signifies the significane of the model and there was only 0.01 % chance that the model F value must have occurred due to noise. Regression analysis results has revealed R^2 (coefficient of determination, and the value more closer to 1 indicates the model fit of the experimental data) value of 0.9309, which signifies that the model was enable to explain only 7% of the total variations. The adjusted R^2 (adjusted determination coefficient) value of 0.8687 was quite high which indicates the high reliablity of the model and the quadratic polynomial equation. The values of "Prob>F" of the model far less than 0.05, indicates the significant and desirability of the model terms. The "Lack of Fit F-value" of 843.93 implies the Lack of Fit is significant. There is only a 0.01%

chance that a "Lack of Fit F-value" this large could occur due to noise. "Adeq Precision" measures the signal to noise ratio (a ratio greater than 4 is desirable) and the ratio of 12.862 indicates an adequate signal. A low value of CV (coefficient of variation) of 2.76% signifies a high degree of precision and a good deal of realiablity of the experimental values. According to this model, the significant parameters A-B has shown the highest interaction effect, followed by A-C and B-C with the least interaction, for the maximal response of limonin biotransformation.

The experimental relationship between stability of the beads (response) and the three significant parameters in the coded values is presented in Table 4.17. This response is of great importance in estimating the bead scabrousness for their potential to withstand mechanical stress. The analysis of variance (ANOVA) for this model is presented in Table 4.20. The F value (14.97) of the model signifies the significane of the model and there was only 0.01% chance that the model F value must have occurred due to noise. The model equation is present in Table 4.21.

Regression analysis results presenting the R^2 (coefficient of determination) and adjusted R^2 (adjusted determination coefficient) values of 0.9253 and 0.8581 respectively, was quite high which indicates the high reliablity of the model and the quadratic polynomial equation. The values of “Prob>F” of the model far less than 0.05, indicates the significant and desirability of the model terms. The "Lack of Fit F-value" of 5.31 implies the Lack of Fit is significant and the corresponding 0.01% chance that a "Lack of Fit F-value" this large could occur due to noise. "Adeq Precision" ratio value of 12.683 indicates an adequate signal which signifies a high degree of precision with a good deal of reliablity of the experimental values. According to this model, the significant varibales A-B has shown the highest interaction effect, followed by A-C and B-C with the least interaction, for the maximal response of high stability of the alginate beads.

Table 4.19 Analysis of variance (ANOVA) for limonin biotransformation

Source	Sum of squares	df	Mean square	F value	p-value Prob>F	
Model	379.49	9	42.17	14.97	0.0001	significant
A-Alginate concewntration (%)	6.69	1	6.69	2.38	0.1543	
B-Cell load (%)	89.21	1	89.21	31.67	0.0002	
C-Bead diameter (mm)	26.79	1	26.79	9.51	0.0116	
AB	54.08	1	54.08	19.20	0.0014	
AC	9.24	1	9.24	3.28	0.1001	
BC	1.12	1	1.12	0.40	0.5416	
A^2	1.09	1	1.09	0.39	0.5476	
B^2	168.74	1	168.74	59.91	<0.0001	
C^2	36.94	1	36.94	13.12	0.0047	
Residual	28.16	10	2.82			
Lack of Fit	28.13	5	5.63	843.93	< 0.0001	significant
Pure Error	0.033	5	6.667E-003			
Cor Total	407.66	19				

Table 4.20 Analysis of variance (ANOVA) for stability

Source	Sum of squares	df	Mean square	F value	p-value Prob>F	
Model	0.010	9	1.157E-003	13.76	0.0002	significant
A-Alginate conc. (%)	*4.133E-003*	*1*	*4.133E-003*	*49.16*	*< 0.0001*	
B-Cell load ( )	*1.024E-003*	*1*	*1.024E-003*	*12.18*	*0.0058*	
C-Bead diameter (mm)	*6.659E-004*	*1*	*6.659E-004*	*7.92*	*0.0183*	
AB	*1.378E-003*	*1*	*1.378E-003*	*16.39*	0.0023	
AC	*4.651E-004*	*1*	*4.651E-004*	*5.53*	0.0405	
BC	*7.812E-005*	*1*	*7.812E-005*	*0.93*	0.3578	
A^2	*5.289E-004*	*1*	*5.289E-004*	*6.29*	0.0310	
B^2	*1.672E-004*	*1*	*1.672E-004*	*1.99*	0.1888	
C^2	*2.288E-003*	*1*	*2.288E-003*	*27.21*	0.0004	
Residual	8.407E-004	10	8.407E-005			
Lack of Fit	*7.074E-004*	*5*	*1.415E-004*	*5.31*	*0.045*	significant
Pure Error	*1.333E-004*	*5*	*2.667E-005*			
Cor Total	0.011	19				

Table 4.21 Model equation for limonin biotransformation by *P.putida* G7 with optimum levels of significant variables in minimal medium

Stability (R2) = +0.11 +0.017*A + 8.660E - 003*B + 6.983E-003*C - 0.013*A*B - 7.625E-003*A*C -3.125E-003*B*C + 6.058E-003*A^2 +3.407E - 003* B^2 + 0.013*C^2
Where Y is the response value for limonin biotransformation (%), A- Alginate concentration, B- Cell Load, C- Bead diameter

RSM analysis

The response model developed was further represented in the form of contour plots for a better understanding of the interaction among the three significant parameters and for the detection of the optimum level of each parameter for a maximum response. The contours plot showed the interaction of two independent parameters when the third parameter is fixed at zero (Fig 4.37 a-c), which represents the limonin biotransformation response. Limonin biotransformation increases moderately with increasing alginate concentration from 2% to 3% (w/v), with a high increase in cell load results in high biotransformation (Fig. 4.37 a). Fig. 4.37 b demonstrates that response increases moderately with increase in bead diameter and alginate concentration. An increased response was observed with increase in cell load, and bead diameter (Fig. 4.37c).

The contours for stability with regard to the significant parameters of alginate concentration, cell load, and bead diameter are presented in Fig. 4.38 a-c. Fig. 4.38a shows that higher stability could be obtained at a moderate alginate concentration and low cell load. Fig. 4.38b indictates that stability increases with an increased bead diameter and at a moderate alginate concentration. Low cell load and a moderate bead diameter directs towards an increased response for stability (Fig. 4.38c).

Validation of the model

The experimental model was validated by considering both activity and stability for a high limonin biotransformation and low OD600 nm responses, with the help of the regression equation. The experimental reactions (100 ml Erlenmeyer flask containing 50 ml citrus juice)

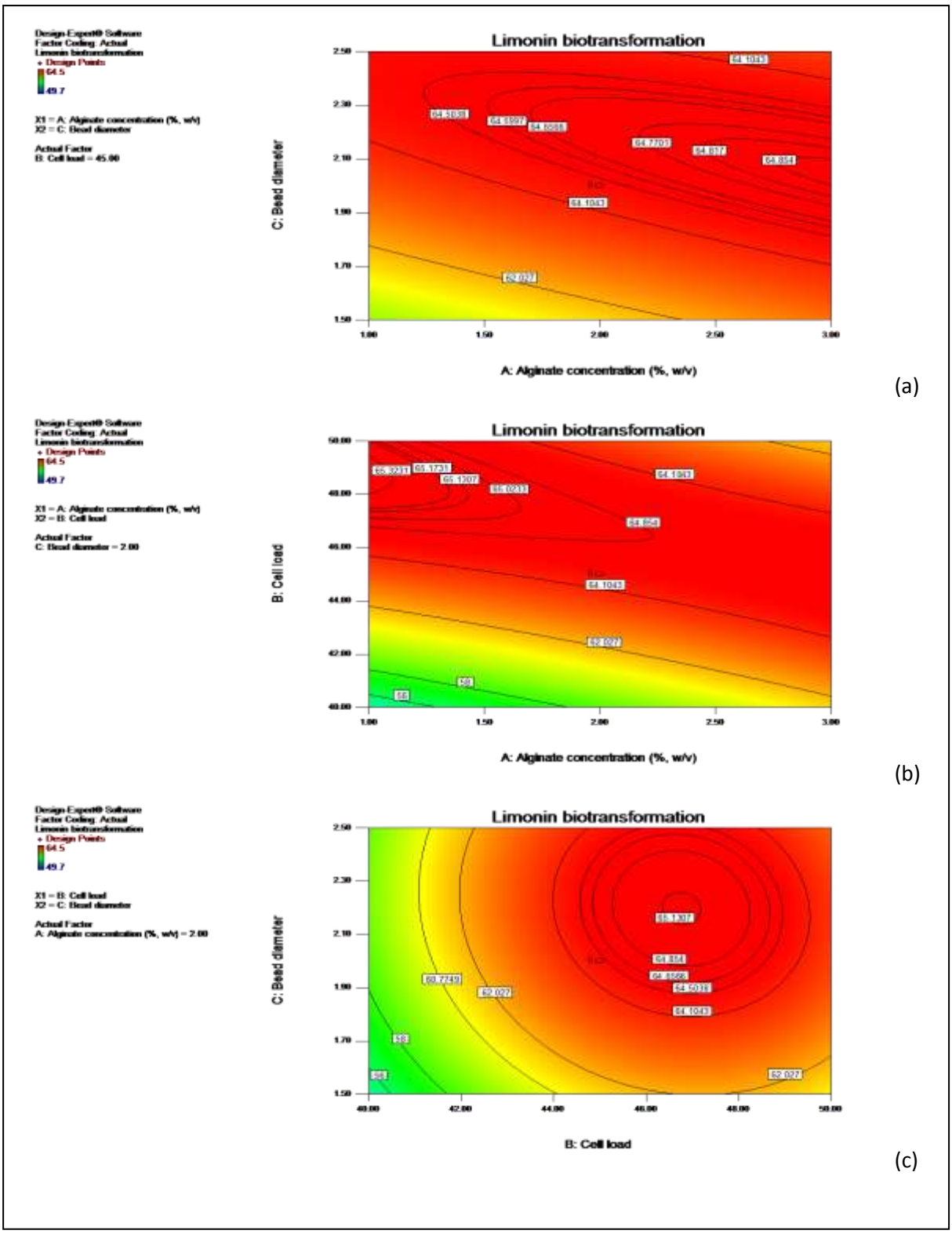

Fig. 4.37 Contour plots showing the combined effects of the significant variables for whole cell immobilization in terms of limonin bioconversion; (a) Interaction effect between alginate concentration and bead diameter (b) alginate concentration and cell load; (c) interaction effect between cell load and bead diameter

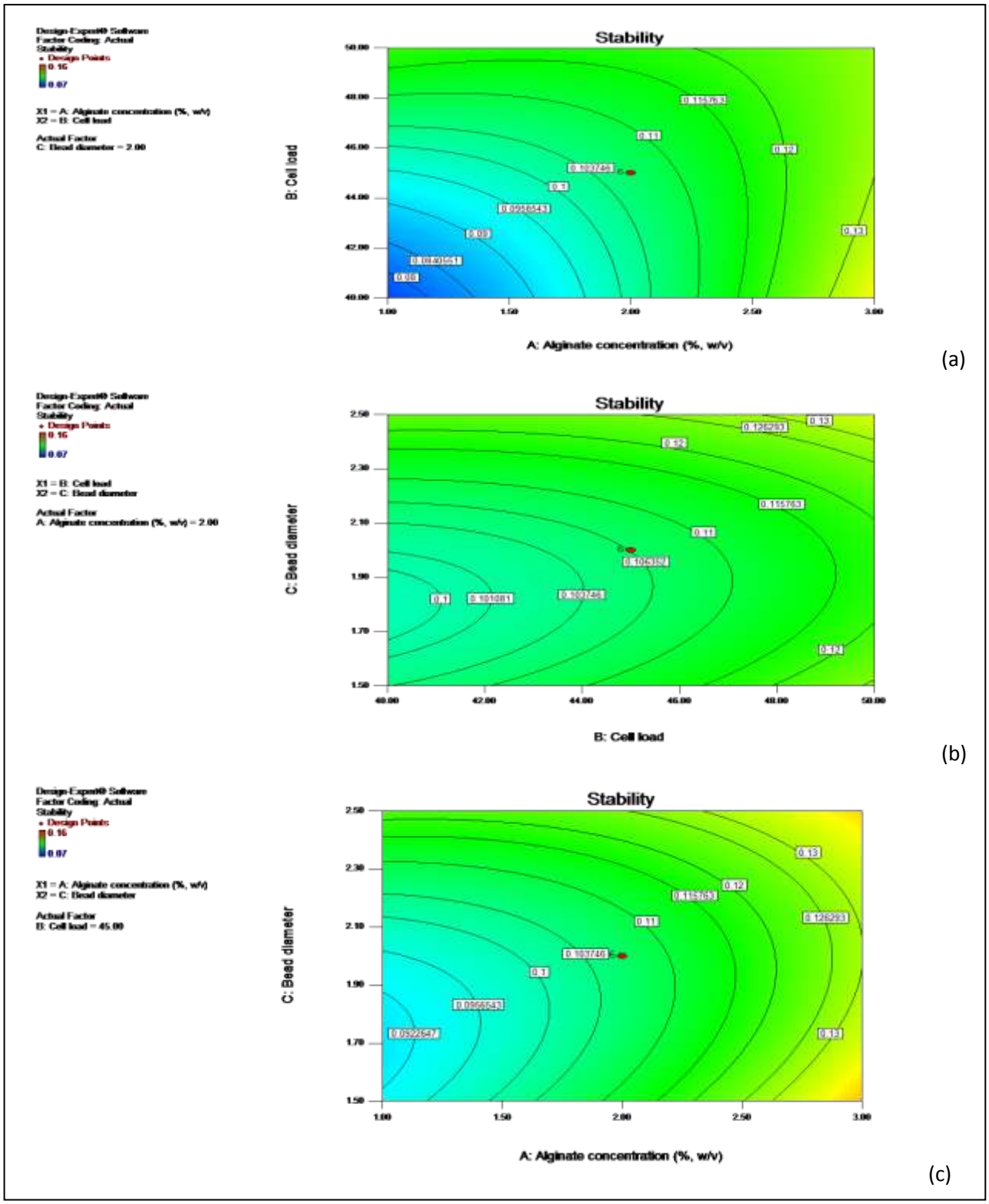

Fig. 4.38 Contour plots showing the combined effects of the significant variables for bead stability in terms of limonin bioconversion; (a) Interaction effect between alginate concentration and cell load (b) alginate concentration and bead diameter; (c) interaction effect between alginate concentration and bead diameter

with immobilized cells for the maximum response included an alginate concentration of 2%, a cell load of 47.2 g/l, and a bead diameter of 2.1 mm. The predicted values for the maximum response of limonin biotransformation and stability giving these conditions were 65.1% and 0.094 respectively. The experiments were conducted in triplicates and maximum response with all the optimized conditions were 65.8% and 0.97 OD.

Reusability and stability of immobilized cell

The reusability of the immobilized cells *P. putida* G7 was compared with free cells (20 beads, equivalent to 47 mg/ml cells and free cells - 47 mg/ml cells), for the evaluation of limonin biotransformation under the optimized parameters, at the original pH of citrus juice (4 pH) and at 35°C. The immobilized bacterial cells and free cells were evaluated for their biotransformation potential in successive cycles. After each cycle the alginate beads were filtered and the free cells were collected by centrifugation, washed with saline and phosphate buffer and were then reused for limonin biotransformation in the next set of citrus juice. All the reactions conditions were kept constant for every batch cycle. The biotransformation reaction was carried out for 3 hr and the bioconversion during each cycle by immobilized and free cells is presented in Fig. 4.39. The results depict a faster bioconversion and high reusability (till 8th cycle) of immobilized cells as compared to free cells (till 5th cycle).

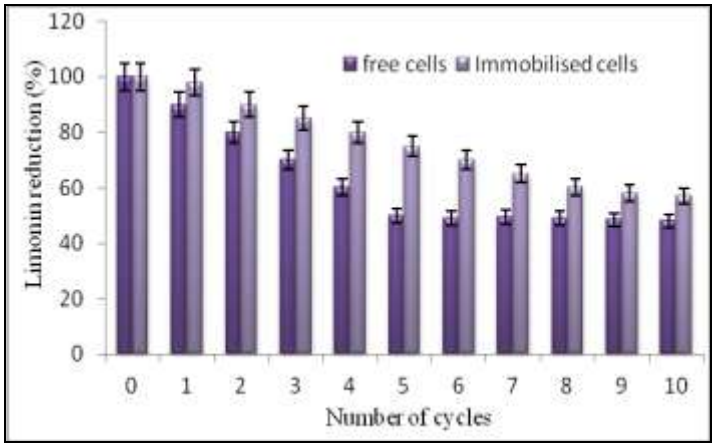

Fig. 4.39 Reusability and stability of free and immobilized cells of *P. putida* G7 for limonin biotransformation

4.4.2 Permeabilization of whole cells

The limonin utilization trend by whole cells as well as limonin utilization by purified enzyme prompted for processes which could substantially enhance enzyme substrate interaction. To this end, cell permeabilization a simple and effective technique has been advocated in several biotechnological processes in recent times. Whole cell permeabilization of *Pseudomonas putida* G7, Na_2EDTA proved to be the most potential permeabilizing agent as compared to the other permeabilizing agents like organic solvents (toluene, chloroform, benzene, hexane) (Kieboom et al. 1998; Halan et al. 2011), 1% for the detergents (CTAB, SDS, Triton X-100) and proteases. The potentiality was expressed in terms of limonin utilization activity, which was found to be the maximum when 1 µM of Na_2EDTA was used as permeabilizing agent. The results on the effect of different methods of permeabilization of *P. putida* G7 cells on reduction of limonin were shown in Fig. 4.40. The incubation of cells for a period of 10 minutes were considered as optimum since viability (monitored by periodically plating appropriately diluted aliquots onto Nutrient agar plates; results not shown) and enzyme activity were lost when cells were incubated beyond the given time. Permeabilization with Na_2EDTA enhanced the enzyme activity up to 11.8 folds compared to the normal cells, within 3 hours. The SEM and TEM profiles of cells permeabilized Na_2EDTA are presented in Fig. 4.41 & 4.42**,** which demonstrates the effect of permeabilizing agent on the cell wall as compared to the unpermeabilzed counterpart (control).

Limonin utilization kinetics by free permeabilized cells

Limonin utilization by the permeabilized cells of *P. putida* G7 were insignificant ($p<0.05$) in comparison to the unpermeabilized cells of *P. putida* G7 (Table 4.22). The limonin utilization by the permeabilzed cells in M63 medium as well as in mandarin juice (containing equivalent quantities of limonin) revealed a similar trend, though a difference in utilization rates were observed (70% and 50% respectively). Permeabilized biomass of 1g dry weight was

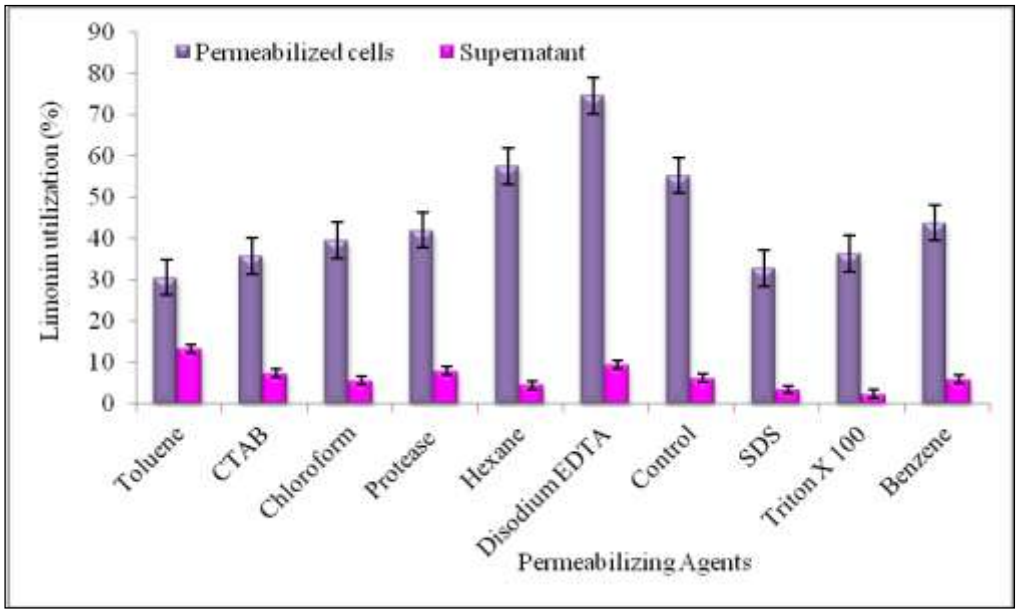

Fig. 4.40 Comparison of different permeabilization methods to evaluate the reduction in limonin by *P. putida* G7. The reactions with the various methods were incubated for 1 hour at 37°C, 200 rpm. Limonin estimation was performed at 35°C. Results are mean of three independent replicates

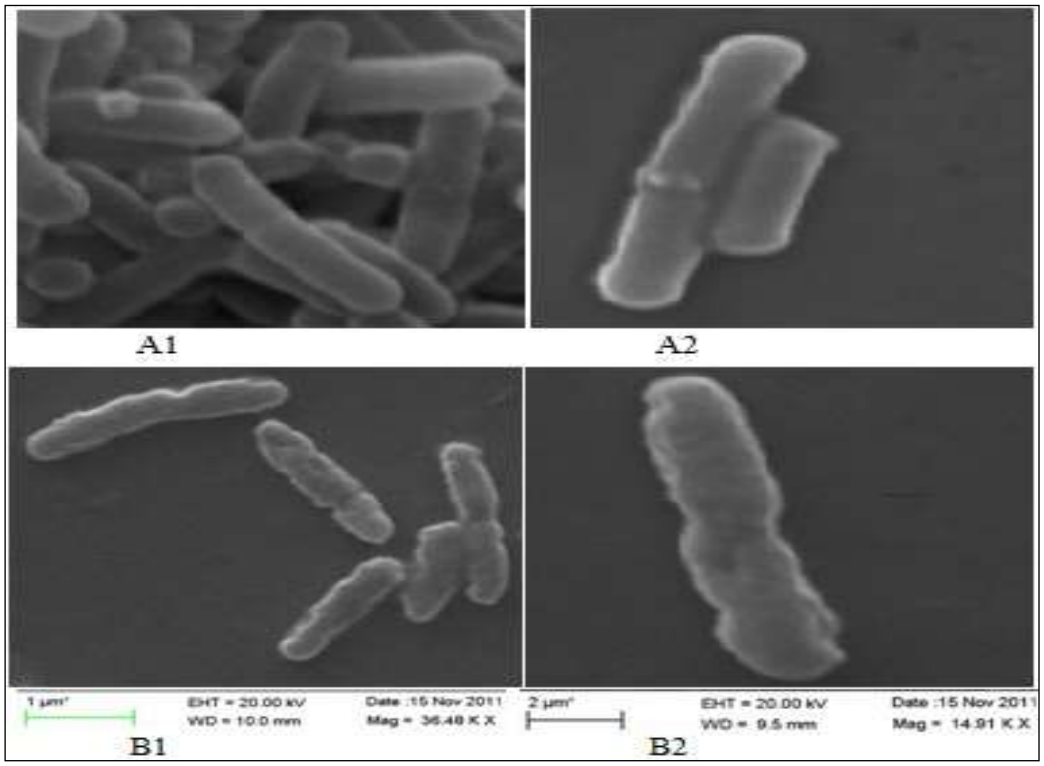

Fig. 4.41 Scanning Electron Micrograph of *P. putida* G7 after whole cell permeabilization; A1 and A2 shows the whole cell(s) before treatment (unpermeabilized cells); and B1and B2 shows the cell(s) (unpermeabilized cells) after treatment with disodium EDTA

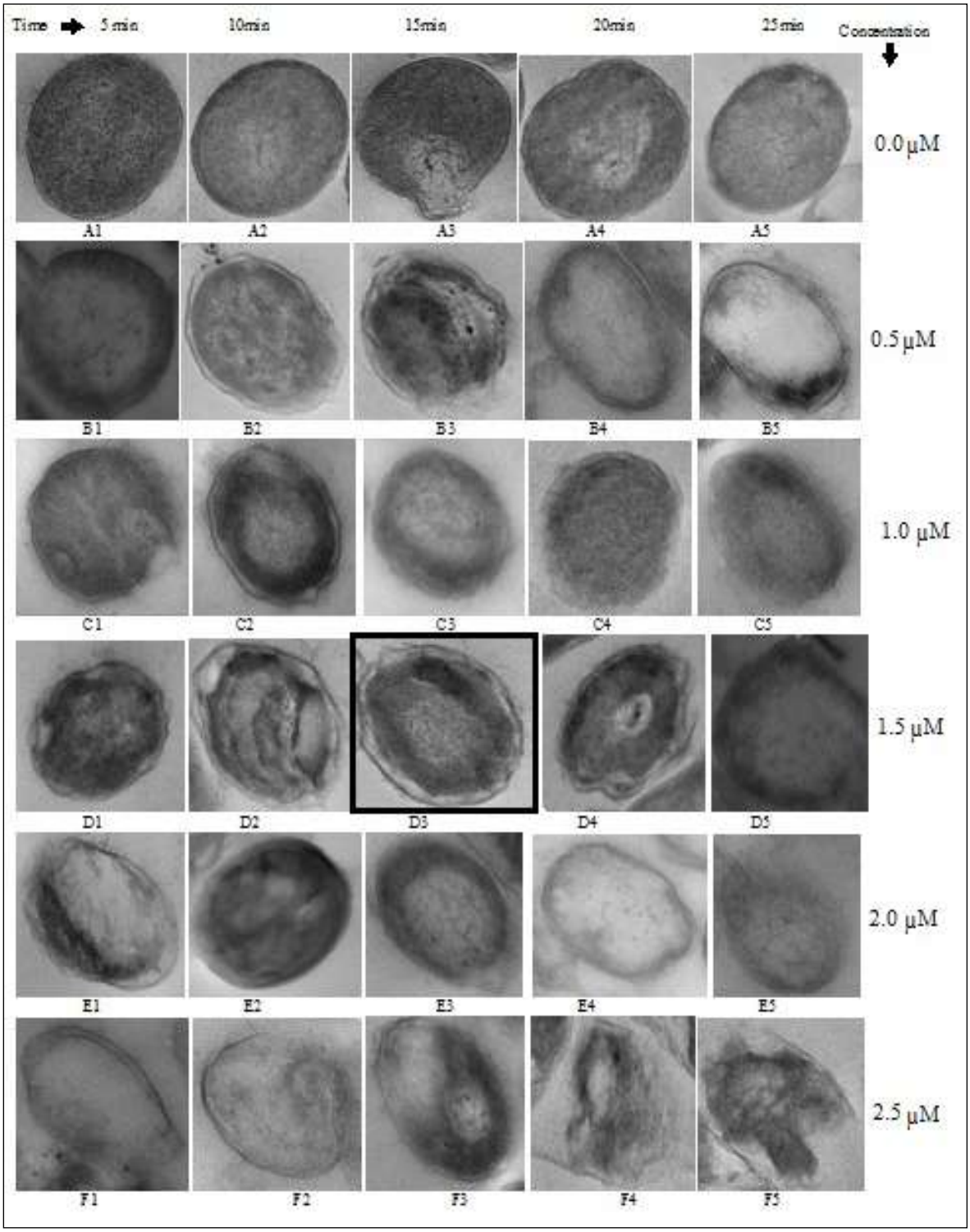

Fig. 4.42 Transmission Electron Micrograph of permeabilized cells for optimization of permeabilization process; cells were permeabilized with a EDTA concentration range of 0.5 µM – 2.5 µM and incubated at a time interval of 5 min – 25 min respectively; permeabilized cell (D3) was the most optimum condition for permeabilization which showed the maximum enzyme activity for limonin bioconversion

considered optimum in terms of limonin utilization, whereas increasing biomass concentration did not lead to higher utilization rate.

Performance of dialysis membrane entrapped permeabilized cells

The performance of limonin utilization was studied in an experimental set up shown in Fig. 4.43, where the permeabilized cells of *P. putida* G7 were entrapped inside dialysis membrane. The efficiency of the reduction of limonin was examined both in minimal medium and in mandarin juice comprising of equivalent amounts of limonin. The transformation of limonin by the permeabilized cells was found to be higher in the minimal medium containing pure limonin than that observed in the mandarin juice (i.e. 76.45% and 73.23% respectively). The maximum reduction was achieved within 180 minutes of incubation of permeabilized cells inside the dialysis sac. No reduction was observed thereafter (Fig. 4.44), whether the reduction of limonin was solely due to utilization, was evaluated by estimating limonin within the sac with or without cells. Limonin was not detected inside the dialysis sac during experiments, also the empty dialysis sacs incubated in juice for a similar time span indicated that removal of limonin was not due to adsorption (Fig. 4.44).

Table 4.22 Limonin utilization by permeabilized and unpermeabilized cells of *P. putida* G7

	Mandarin juice		M 63 minimal medium *	
Biomass (/g drywt)	**Unpermeabilised**	**Permeabilised**	**Unpermeabilised**	**Permeabilised**
0.5	22.97(±0.04)	46.59(±0.03)	36.23(±0.05)	65.89(±0.03)
1.0	50.71(±0.05)	68.67(±0.04)	54.68(±0.04)	70.88(±0.05)
2.0	51.08(±0.03)	69.01(±0.02)	55.09(±0.04)	71.01(±0.06)

[a]Unpasteurized mandarin juice and M63 medium (200ml volume with limonin concentrations in a range of 50 µg/ml) were treated with permeabilized and unpermeabilized cells, incubated at 30°C for 6 hours, for limonin utilization

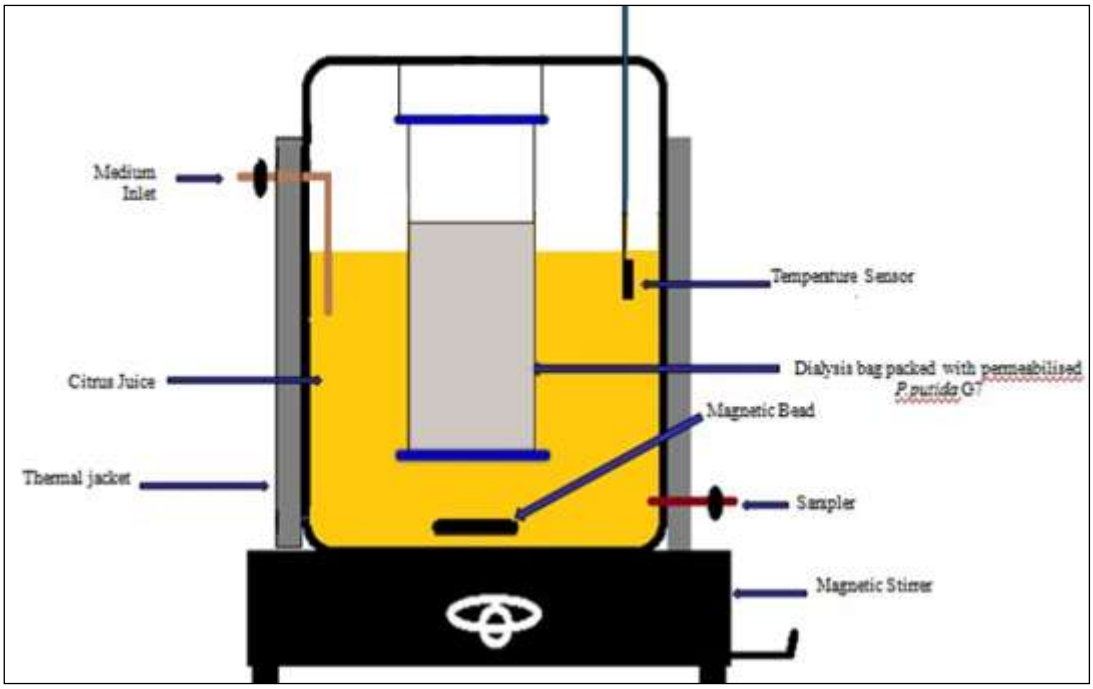

Fig. 4.43 Experimental setup for the study of limonin utilization by the dialysis membrane entrapped permeabilized *P. putida* G7. Volume of the mandarin juice in the vessel was 200ml; temperature was monitored using temperature controller

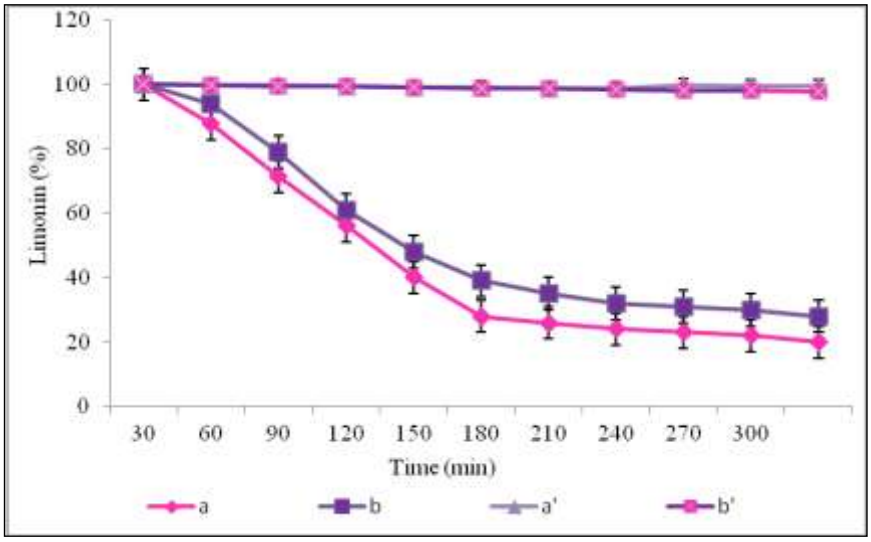

Fig. 4.44 Limonin utilization kinetics by permeabilized entrapped cells in minimal medium (M63) supplemented with equivalent amounts of (a) limonin, (b), mandarin juice, (a') Adsorbed limonin in empty dialysis sac in M63 minimal medium and (b') Adsorbed limonin in empty dialysis sac in Mandarin juice. Results are mean of three independent replicates

Evaluation of limonin content by HPLC

To authenticate limonin utilization, HPLC was used for estimating the residual limonin levels. A prominent peak, at a retention time of 9.3 minutes was obtained for standard limonin (Fig. 4.45a). The utilization was evidenced from the appearance of two new peaks at retention times of 15.9 and 25.2 minutes (Fig. 4.45b). The area under the curve that represented limonin peak was reduced in the utilization sample. As illustrated in Fig. 4.46, compared to the peak area of 62% and 66% of respective controls of juice serum and standard limonin in the medium, the utilization resulted in reduction in peak area to 19.08% and 8.23% respectively. However, a complete disappearance of limonin peak was not observed due to the residual limonin in the medium and these limonin levels (<5ppm) were far less than the sensorial property of the consumer. Further, in Fig. 4.46, the peak areas 39.64 % and 27.03% corresponded to utilization of limonin by the unpermeabilised free cells in juice serum and in medium containing standard limonin respectively. The entrapped permeabilized *P. putida* G7 cells stored in PBS at room temperature and 30°C for 45 days exhibited no loss in its limonin removal efficiency for subsequent 8 batch cycles (Fig. 4.47) and a decline was observed thereafter, probably due to inactivation of the enzyme. These results indicated the stability of the enzymes and hence reusability of permeabilized cells. The dialysis entrapment method thus proved to be quite effective for removing limonin.

Response surface modeling for maximum limonin bioconversion

Response surface methodology (RSM) with central composite rotatable design (CCRD) was chosen to optimize the significant variables (Na_2EDTA concentration, pH, time duration and temperature) for permeabilisation of *P. putida* G7 cells. The coded levels for independent variables are presented in Table 4.23. The mean predicted and experimental bioconversion activity are presented as a response, as detected by central composite rotatable design experiments (Table 4.24).

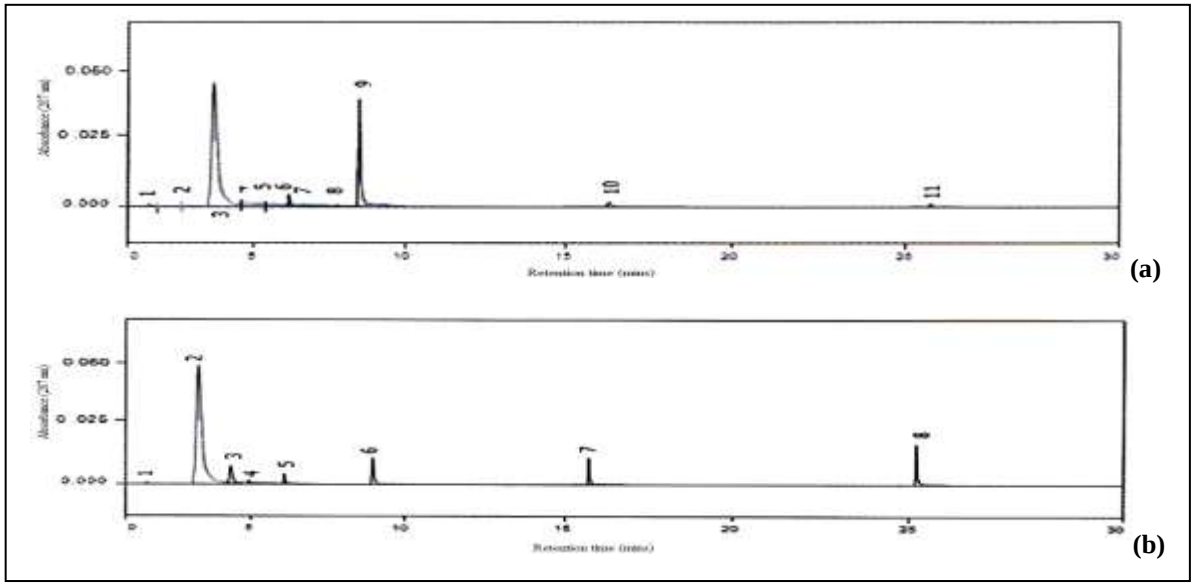

Fig. 4.45 (a) HPLC chromatogram of standard limonin (90µg/ml) and (b) chromatogram of standard limonin (90µg/ml) utilization by permeabilised cells of *P. putida* G7, using an acetonitrile/deionised water (32:68) with a flow rate 0.9 ml/min and an injection volume of 20 µl

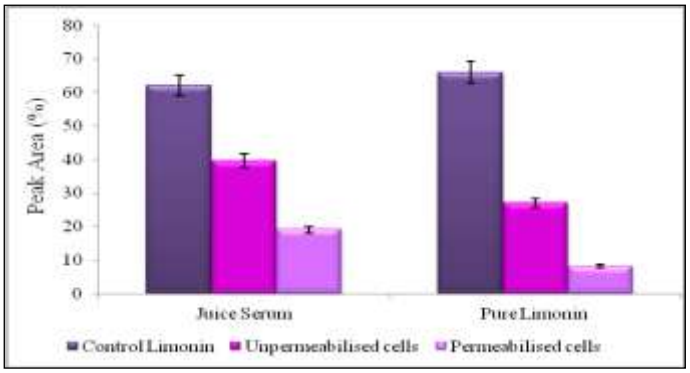

Fig. 4.46 Comparison of limonin utilization using permeabilised and unpermeabilised cells of *Pseudomonas putida* G7 in standard limonin and mandarin juice by HPLC in terms of peak area (%) for residual limonin

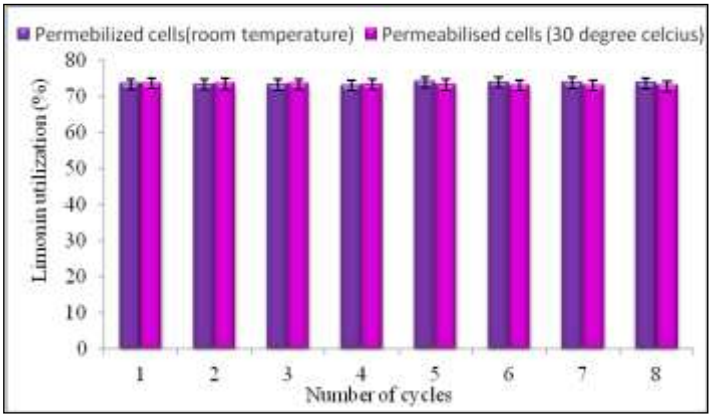

Fig. 4.47 Reusability and stability of permeabilised *P. putida* G7; Limonin utilization by permeabilised *P. putida* G7 cells stored at 4^0C and 30^0C in phosphate buffer for 45 days. Results are mean of three independent replicates

Table 4.23 Levels of variables tested in central composite rotatable design (CCRD)

Variables		Coded Levels				
		-2	-1	0	+1	+2
A	Na_2EDTA (µM)	0.5	1	1.5	2	2.5
B	Time duration (mins)	5	10	15	20	25
C	Temperature (°C)	12	20	28	37	45
D	pH	2	4.0	8.0	9.0	12

Table 4.24 Design matrix prepared using CCRD of RSM

Runs	Coded Values				Actual value	Predicted value
Runs	A	B	C	D	Limonin utilization (%)	
1	1.00	-1.00	-1.00	-1.00	67.19	67.63
2	0.00	0.00	0.00	0.00	76.71	75.82
3	-1.00	-1.00	1.00	-1.00	65.72	66.41
4	-2.00	0.00	0.00	0.00	68.66	68.86
5	-1.00	-1.00	1.00	1.00	69.42	69.49
6	2.00	0.00	0.00	0.00	70.89	70.72
7	0.00	0.00	0.00	0.00	76.71	75.82
8	-1.00	1.00	-1.00	1.00	72.36	71.94
9	1.00	-1.00	1.00	1.00	70.02	69.99
10	0.00	-2.00	0.00	0.00	71.49	71.22
11	0.00	0.00	0.00	0.00	76.71	75.82
12	0.00	0.00	0.00	2.00	72.96	72.44
13	0.00	0.00	0.00	0.00	76.71	75.82
14	0.00	0.00	0.00	0.00	76.71	75.82
15	-1.00	1.00	1.00	1.00	75.19	74.30
16	1.00	-1.00	1.00	-1.00	76.66	75.52
17	-1.00	-1.00	-1.00	1.00	69.71	69.66
18	-1.00	1.00	-1.00	-1.00	71.18	72.11
19	1.00	1.00	-1.00	1.00	69.71	69.66
20	0.00	2.00	0.00	0.00	71.18	72.11
21	0.00	0.00	0.00	0.00	76.71	75.82
22	-1.00	1.00	1.00	-1.00	71.95	73.62
23	0.00	0.00	2.00	0.00	68.98	67.98
24	1.00	-1.00	-1.00	1.00	71.13	71.13
25	-1.00	-1.00	-1.00	-1.00	70.31	70.31
26	1.00	1.00	1.00	-1.00	71.13	71.13
27	1.00	1.00	-1.00	-1.00	70.31	70.31
28	0.00	0.00	-2.00	0.00	70.31	70.31
29	0.00	0.00	0.00	-2.00	70.11	70.11
30	1.00	1.00	1.00	1.00	71.13	71.13

[a] A,B,C,D are the coded values for the significant variables - Na2EDTA concentration, time duration, temperature, pH, respectively;
[b] All the responses in the 30 runs were performed in triplicates. The calculated values were significant ($p < 0.001$).

The ANOVA results demonstrate that the regression is highly significant (at 99% confidence level) and presents an excellent determination coefficient (R^2 = 0.904). This meant that 90.4% variability in the observed data could be explained by polynomial equation. The second order regression equation obtained after the analysis of variance (ANOVA) provided the levels of bioconversion activity as a function of values of the Na_2EDTA (1.5µM) for time duration (15 min) at temperature (28°C), and pH (8.0) (Table 4.25). The final estimative response model equation in terms of limonin bio conversion (Y) was:

Limonin bioconversion (Y) = +76.71 +0.61* A+0.62* B+1.55* C+1.78* D+0.060* A * B+0.078 * A * C+3.44 * A * D +0.098 * B * C +3.43* B * D +3.39 * C * D+0.14 * A^2 +0.14 * B^2+0.058 * C^2 +0.32 * D^2;
[a]Where A, B,C and D are the coded values for Na_2EDTA (A) time duration (B) temperature (C), pH (D).

According to ANOVA of the model for activity of limonin utilization indicates that the "F" value of 11.58 and values of "Prob > F" less than 0.0500 infers that the model was significant. The R^2 value of 0.904, closer to 1 denotes a very high significance of the model. A higher reliability of the experiment is usually indicated by lower value of coefficient of variation (CV) i.e 1.65 which indicates that the experiments performed were reliable. The "Adequate Precision" measures the signal to noise ratio and a ratio greater than 4 is desirable. The ratio of 14.118 indicates an adequate signal and indicates that this model can be used to navigate the design space.

The obtained responses from the CCRD were fitted to a second order polynomial equation to explain the dependence of catalysis of limonin on the optimization of the significant variables for permeabilization of *P. putida* G7 (Fig. 4.48 a-c). As shown in Fig. 4.48a the highest value of limonin bioconversion activity was obtained when the cells were exposed to a concentration of 1.5 µm Na_2EDTA for 15mins. The optimum operating conditions of temperature and pH for effective permeabilization was 28^oC and 8 respectively. The response surface plotted in Fig. 4.48b, between Na_2EDTA concentration and temperature and the trend of the surface plot of temperature versus time in Fig. 4.48c depicted the similar activity of

Table 4.25 Analysis of variance (ANOVA) of the experimental results of CCD

Variables	Coefficient Estimation	Sum of Square	Standard Error	df	F-value	p-value
Model	76.71	1245.25	0.078	17	11.58	0.001
A	0.61	23.36	0.014	1	1.098	0.032
B	0.62	24.51	0.014	1	1,083	0.025
C	1.55	41.28	0.014	1	3.078	0.013
D	1.78	42.64	0.014	1	4.002	0.125
AB	0.060	7.39	0.017	1	0.003	0.004
AC	0.078	8.91	0.017	1	0.004	0.012
AD	3.44	215.78	0.017	1	6.005	0.022
BC	0.098	9.36	0.017	1	0.007	0.009
BD	3.43	211.57	0.017	1	5.005	0.006
CD	0.39	201.38	0.017	1	5.006	0.007
A^2	0.14	17.56	0.010	1	1.030	0.153
B^2	0.14	17.56	0.010	1	1.030	0.318
C^2	0.058	21.56	0.010	1	1.007	0.125
D^2	0.32	19.89	0.010	1	0.810	0.431

[a] A,B,C,D are the coded values for the significant variables - Na_2EDTA concentration, time duration, temperature, pH, respectively

limonin bioconversion. In fact, the close interaction of temperature and pH with time was quite evident. Thus, the response shown was based on the interaction of the significant variables. The predicted response was aproximately 75.82% when the significant variables were taken at "0" level, whereas the experimental response (based on the best predicted combinations of significant variables showing maximum response in CCRD) was approximately 76.71%, confirming the validity of the model.

Performance of permeabilized cells

The performance of permeabilized cells of *P. putida* G7 (permeabilized under optimized conditions) for limonin bioconversion was studied by using entrapped permeabilized cells in a dialysis based bioreactor. For evaluating the efficiency of limonin reduction, its level was monitored in two model solutions; minimal medium (M63) with limonin as the substrate and in citrus juice with equivalent limonin content. Limonin bioconversion peaked typically at three hours, following which further reduction was not observed (Fig. 4.49). In citrus juices, 76.71% of limonin removal was achieved within 150 mins. Further, the ability of entrapped permeabilized cells was compared with the efficiency of the purified enzyme by HPLC. A

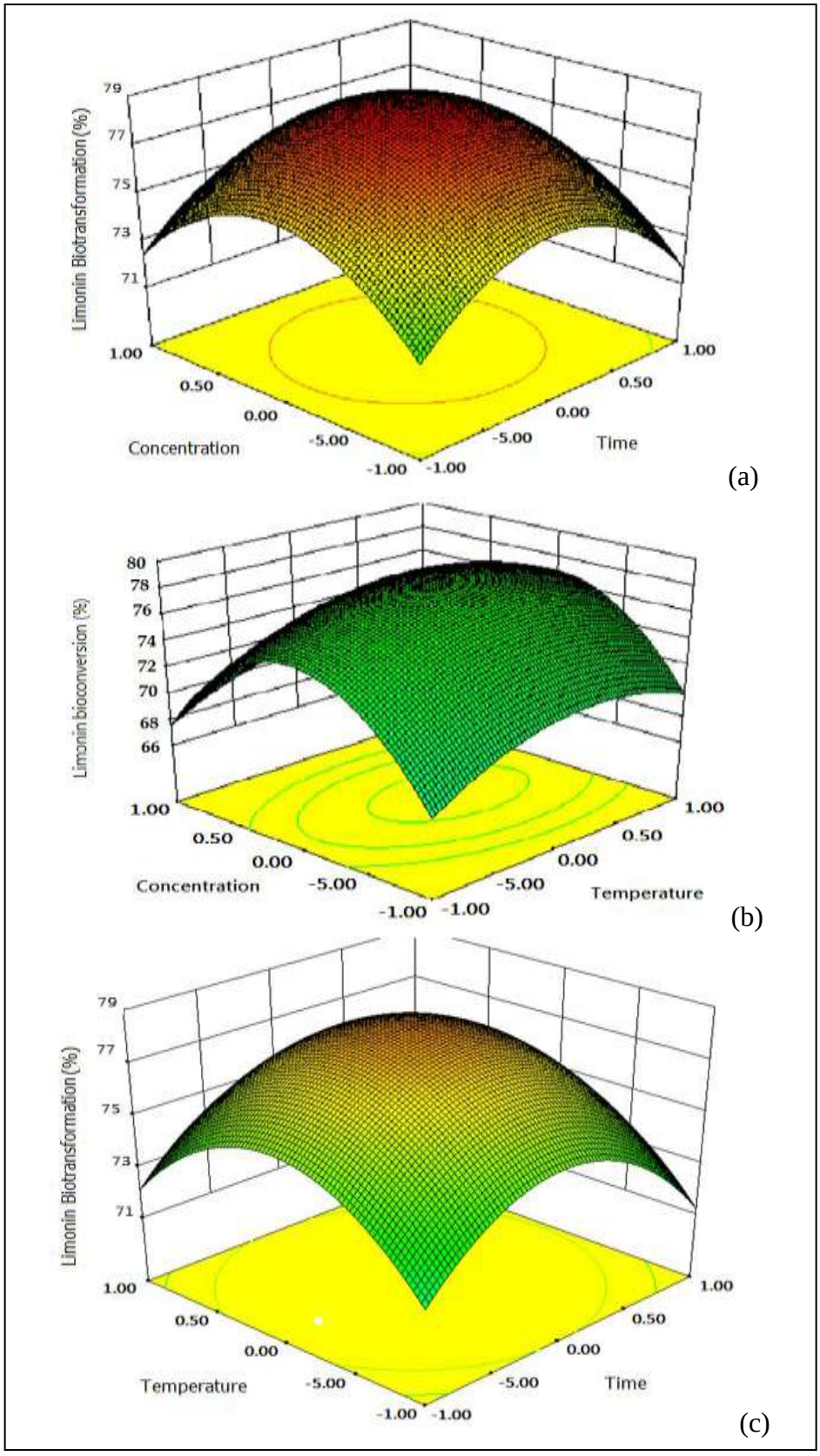

Fig. 4.48 (a-c) Response surface plots showing the combined effects of the significant variables in terms of Limonin bioconversion using permeabilized cells (a) Interaction effect between concentration and time (b) interaction effect between concentration and temperature ; (c) interaction effect between time versus temperature

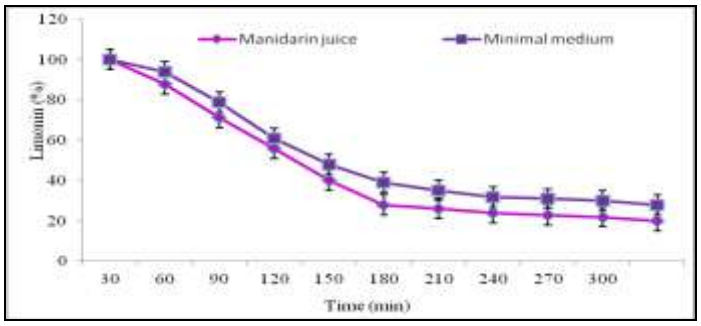

Fig. 4.49 Limonin bioconversion kinetics by permeabilized entrapped cells in juice and in minimal medium M63 supplemented with equivalent amounts of limonin. Results are mean of three independent replicates

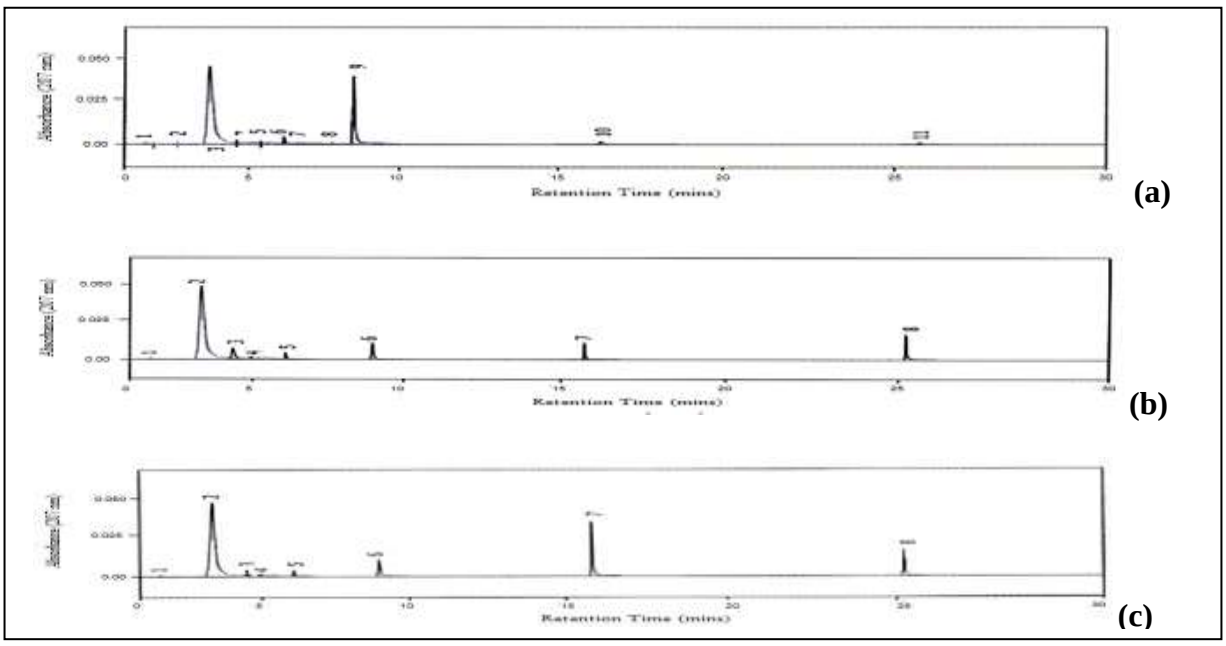

Fig. 4.50 (a) HPLC chromatogram of standard limonin (90µg/ml), (b) chromatograms of standard limonin (90µg/ml) utilization by permeabilised cells and purified enzyme (c) of *P. putida* G7, using an acetonitrile/deionised water (32:68) with a flow rate 0.9 ml/min and an injection volume of 20 µl

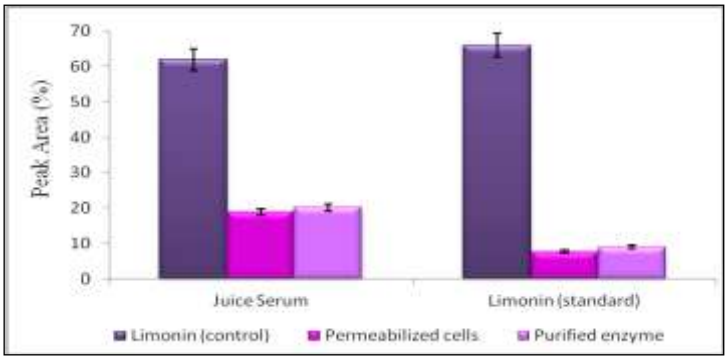

Fig. 4.51 Comparison of limonin bioconversion efficiency in two model solutions (standard limonin and juice sample with same limonin content) using cells of *P. putida* G7 permeabilised with Na_2EDTA under specified conditions and the purified enzyme. The results are explained in terms of peak area (%) for residual limonin by HPLC

prominent peak, at a retention time of 9.3 minutes was obtained with standard limonin (Fig. 4.50a). The peak area that represented limonin was reduced following utilization and appearance of two new peaks at retention times of 15.9 and 25.2 minutes were observed (Fig. 4.50b,c). As illustrated in Fig. 4.51, the peak area of 62% and 66% represented limonin in two respective model solutions of juice serum and standard limonin in the medium.A reduction in peak area to 9.07% and 7.09% was evidenced from the HPLC profile obtained after utilization by purified enzyme and the entrapped permeabilized cells respectively. The same reduced the corresponding peak area to 18.08% and 17.08% in the juice medium with the equivalent limonin content. Thus, in both the model solutions i.e. of juice serum and standard limonin in the minimal medium, the permeabilized cells proved to be equally efficient in biotransforming limonin as that of the purified enzyme.

Zymography

Zymography is a routine electrophoretic technique to identify proteolytic activities in polyacrylamide gels under non denaturing conditions. This method could be a simple yet crucial for noting functionality of enzymes. Thus it was adopted to detect the functionality of the enzyme in permeabilized cells. Immersion of gels in a suspension containing 375 mM Tris-HCl (pH- 8.8), 0.5 mM NADH, and 2 mM disodium limonoate and exposure to UV light allowed visualization of a band of yellow fluorescence (due to NADH) after few minutes,

the activity of the dehydrogenase over 8 cycles is shown in Fig. 4.52. Intensity of spots decreased significantly following 8th batch cycle, indicating loss of enzyme activity.

Western immunoblotting

In order to authenticate the above observations, western blotting was performed using the *P. putida* cell lysates from each batch cyce. The 26 kDa polypeptide of permeabilized cell lysates obtained during each batch cycle cross-reacted with monospecific anti-LDase antibodies raised against LDase from *Rhodococcus fasciens* (Fig. 4.53) indicating the

integrity as well as authenticity of the *P. putida* dehydrogenase during the batch cycle. The results also confirmed the predominant role of the enzyme for limonin utilization.

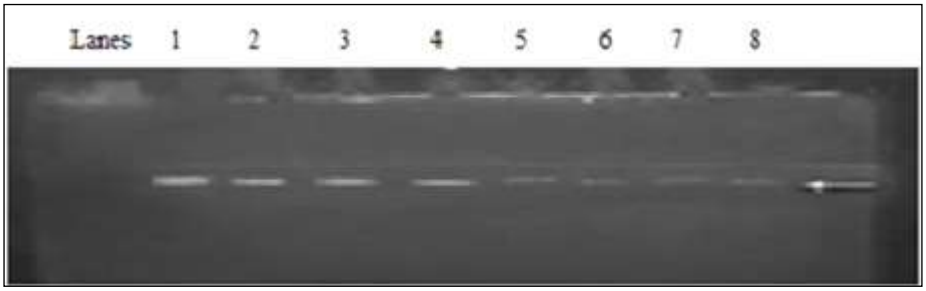

Fig. 4.52 Zymogram showing the intensity of dehydrogenase activity in permeabilized cells (A) Lane 1-8: Permeabilised cell extracts from batch cycles 1-8

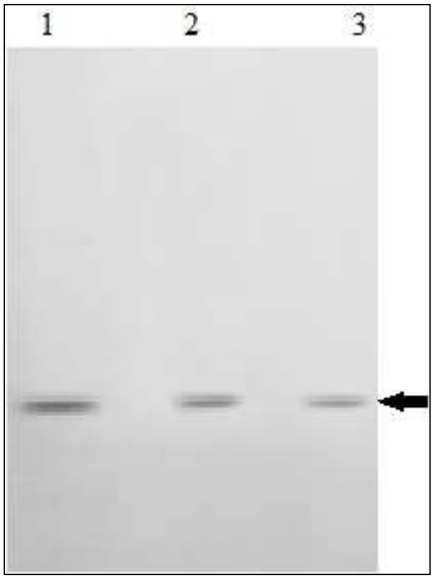

Fig. 4.53 Western blots showing LDase signal of permeabilised cells fractions of *P. putida* G7 from batch cycles 1, 4 and 8 in Lanes 1, 2, 3 respectively

Chapter5

Discussion

A cornerstone of biotechnology is the use of microorganisms for the efficient production of chemicals and bioconversions; *Pseudomonas putida* is an archetype of such microbes due to its metabolic versatility and amenability to genetic modifications. These features as well as the Recognized as Safe (GRAS certified) provide means to investigate the metabolic potential of the *P. putida* as attractive agents for biocatalysts and open up avenues for the development of new biotechnological applications. Thus far, an effective biotechnological method using microbial biocatalysts for bioconversion of limonin, the bitter triterpenoid in citrus juices, has remained elusive. The structural resemblance of triterpenoids to naphthalene degradation by *P. putida* G7 served as cues for exploiting this strain for in depth studies for limonin degradation with a view to harness this strain for debiterring citrus juices.

The utilization of limonin by *P. putida* were demonstrated by reduction of the, 2,3,5 triphenyl tetrazolium dye (TTC) by cells in media supplemented with limonin as sole source of carbon. Development of redox sensitive dyes such as TTC and incorporation of these dyes into microtiter plates has allowed for rapid profiling of sole source carbon utilization by bacterial isolates (Tang et al. 1998). Colour formation in micro plate wells is based on the conversion of the redox sensitive tetrazolium dye which is reduced during respiratory activity, and accumulates as insoluble formazan inside active cells.

Further evidence was obtained through growth and viability of cells in minimal medium containing limonin as sole source of carbon. The tolerance of the strain towards acetonitrile overruled the inhibitory effects of this solvent used for dissolution of pure limonin. Solvent tolerant strains of *Pseudomonas* have been reported to produce high quantities of phospholipids in their cell envelope leading to a consequent thickening of the cell envelope, thereby protecting the cells from toxic effects of solvents. A similar reason may be presumed for the observed solvent tolerance in case of *P.putida* G7 strain as well. Notable limonin utilization occurred at the exponential phase of growth but declined thereafter when the cells

entered stationary phase suggesting the role of extracellular metabolites in impeding limonin utilization (Furukawa and Chakrabarty, 1982; Chauhan and Jain, 2000; Thakur et al. 2001) when the cells reached stationary phase. It is also possible that enzyme(s) responsible for limonin metabolism are synthesized only during log phase. The decrease in activity following maximum activity could also be due to several reasons such as increasing concentration of an inhibitor, exhaustion of an activator, or even some proteolysis of the enzyme (Panesar et al. 2010).

The efficacy of *P. putida* G7 for limonin utilization/consumption was reflected by high specific growth rate and low residual limonin within a reasonably short time period of 48 hours. Earlier reported microorganisms exhibited lower specific growth rates, low limonin utilization and higher incubation time (Hasegawa et al. 1972; 74; 75; 81; 83; 1989). Since limonin utilization was linked to growing cells, a presumptive examination of cultural parameters responsible for cell growth was imperative and revealed that temperature, pH, inoculum size and agitation to be crucial however in order to accurately understand the interactions and contributions of each for the utilization, response surface methodology (RSM) was applied. Response Surface Methodology (RSM) was recently used for modelling bioconversion and optimization reaction conditions by *Acinetobacter calcocaeticus* as a function of temperature (23–37°C) and limonin content (Ribeiro et al. 2003). In this study the application of RSM contributed in elucidating the interdependency of culture pH, inoculum size and limonin concentrations.

Observations from physiological studies were encouraging for investigating the genetic mechanism involved in limonin utilization by the *P. putida* G7 strain. Insights in elucidating the responsible genes in limonin degrading bacterial strains reported earlier are not available thus it was envisaged that results would may contribute in the current understanding of evolution of pathways for microbial triterpenoid metabolism. Besides attempts in future may

be made to metabolically improve the inherent metabolic potential of the strain. An elegant approach for such studies is to analyze mutants incapacitated to limonin utilization. Transposons are the most versatile tools for the genetic analysis of bacteria (Berg, Berg and Groissman, 1989). Transposon mutagenesis provides complete disruption of the mutated gene. The resulting mutant phenotype can be genetically linked to a selectable marker such as solvent or antibiotic tolerance, (deLorenzo & Timmis, 1994). The advantage of transposon mutagenesis for the study of a metabolic pathway is principally when there is little information regarding the genetic locus of the genes involved, i.e. when very few intermediary metabolites, metabolic steps and enzymes have been identified. Although authentic mutants of *P. putida* defective in limonin metabolism were obtained from these experiments, a convincible identity of genes responsible for limonin degradation could not be arrived at since no homologous gene sequences corresponding to metabolic enzymes were observed. Interestingly, analysis of the clones indicated strong homology to the glutamate symporter genes. Results obtained from glutamate uptake assays and motility experiments (in semisolid media with limonin as sole source of carbon) confirmed the inability of the mutant clones for glutamate uptake and chemotaxis towards limonin. Recent studies indicate that in *Pseudomonas putida* KT2440, glutamate and aspartate are selectively transported by an ABC transporter. The operon *aat* coding for this transporter depends on s54, an alternative sigma factor typically involved in the transcription of genes related to nitrogen metabolism (Singh et al, 2008; Sonawane et al., 2006). More recently, Trembley and Deziel (2010) showed that the glutamate symporters are induced at the swarming tip of *Pseudomonas aeruginosa*. In bacteria, glutamate serves as the general amino group donor for amino acid and nucleotide biosynthesis, and may also act as a source of carbon and nitrogen under nitrogen limiting conditions. Though a strong involvement of the glutamate symporter in limonin catabolism may be suggested in case of *P. putida*, the precise role of this symporter during limonin

metabolism is obscure at present and requires detailed study. The observations from above studies however were not effective for arriving at a conclusive identity of limonin catabolic genes. Since napthalene degradation by *P.putida* G7 is mediated by the NAH plasmid, it was logical to examine the involvement of this plasmid for limonin catabolism.

Plasmid curing studies were carried out with several curing agents of which mitomycin C proved to be successful; the cured strains lacked the ability to metabolize limonin. However the low copy number and the large molecular size of the plasmid made it extremely difficult to carry out detailed analysis of the limonin catabolic genes. Though inconclusive these observations signified clearly the involvement of the *nah* plasmid in limonin catabolism by *P.putida* G7. The observations from both genetic and physiological studies suggested a definitive pattern of limonin utilization necessitated characterization of the biochemical principle implicated for limonin degradation. The cured counterparts of *P.putida* devoid of limonin metabolism were used throughout for comparison. Whole cell extracts of wild type *P.putida* G7 possessed notable limonin degrading ability. Extensively dialyzed and concentrated culture supernatants lacked limonin degradation suggesting the involvement of an intracellular biochemical principle. An analysis with whole cell extracts revealed typical limonin degradation kinetics, inactivation to heat and protease treatment signifying the biochemical principle as an enzyme. A comparison of limonin degradation by whole cell extracts, periplasmic fractions and spheroplasts indicated significant activity in the periplasmic fractions; the spheroplast fractions lacked such an activity whereas whole cell extracts had equivalent limonin degrading activity. A periplasmic location of the putative limonin degrading enzyme was thus established. To date, several periplasmically located hydrolytic enzymes have been reported in gram-negative bacteria. These enzymes degrade complex molecules to simpler forms suitable for transport across the inner membrane and subsequent metabolism (Gerngross et al. 1993). Besides, a wide variety of specialized

transport systems responsible for transit of molecules through the outer membrane permeability barrier has been demonstrated in *Pseudomonas* species (Cho and Cronan, 1995). It is possible that a localization of limonin biotransforming enzyme in *P. putida* G7 in the periplasmic space, with its catalytic site exposed to the external environment, may offer a unique arrangement- that enables the cells to metabolize limonin with ease.

To elucidate the enzyme characteristics, enzyme purification were attempted from periplasmic fractions initially with gel filtration. Gel filtration appears to be an excellent and gentle technique to avoid inactivation of enzymes during purification (Scopes, 1987). It is a non denaturing separation technique, based on hydrodynamic volume and molecular size of the protein facilitates complete recovery of enzymes (Lillehoj and Malik, 1989). Though gel filtration resulted in enzyme separation as a single peak, with the enzyme yield of 78 % only 1.8 fold purity was obtained, hydroxyapatite did not result in significant purity. Therefore anion exchange and finally Mono Q columns were used. This process simplified the complications in further purification steps and resulted in high resolution of separation with 26 fold purification with a specific activity of 145 U/mg protein. Limonin dehydrogenase from *Arthrobacter*, *Pseudomonas*, and *R. fascians* has been partially purified by using a procedure which includes chromatography (Suhayda et al. 1995; Brewster et al. 1976; Puri et al. 2002). In fact the LDase from *A. globiformis* was purified to homogeneity by using affinity and ion exchange chromatography and more recently purification for *R. fascians* has been reported where two applications of Mono Q FPLC were highly resolving and produced marked increases in specific activity of LDase. In general, poor stability and low amounts of intracellular quantities of enzyme have complicated the purification process in most cases. The purity of *P.putida* limonin degrading enzyme was confirmed by SDS-PAGE where a single band indicated a homogeneous preparation. The molecular weight of the enzyme under denaturing condition was estimated to be 26 kDa. Immunoblotting experiments confirmed

homology of this enzyme with limonin dehydrogenase from *Arthrobacter globiformis*. LDases from *A. globiformis* (Suhayda et al. 1995) and *R. fascians* (Humanes et al. 1997) has been purified to homogeneity and appear to be similar with values around 120,000 and 30,000 Da respectively; $NH_{2=}$ terminal sequence of the two characterized LDases reveal a significant degree of homology (Humanes et al. 1997). The cross reaction of the 26kDa polypeptide with anti-LDase antibody indicated homology of this polypeptide with that of LDase raised against *R. fasciens* LDase. The pH characteristics of the purified enzyme indicated a requirement of alkaline pH for optimal limonin degradation. The effect of pH on the enzyme activity is determined by the nature of the amino acids at the active site, which undergoes protonation and deprotonation, and by the conformational changes induced by the ionization of the amino acids. Enzymes are very sensitive to changes in pH and they function best over a very limited range, with a definite pH optimum (Sabu et al. 2005; Tan 2011) The pH dependent degradation of limonin (at pH 8) observed in this study showed similarity to LDases characterized from *A globiformis*, *Pseudomonas* and *R. fasciencs* also possessed optimal activity at alkaline pH. Any change in pH affects the protein structure and a decline in enzyme activity beyond the optimum pH could be due to enzyme inactivation or its instability. Enzyme activity was lost above at temperature of 65^0C and was maximal at 35^0C. Requirement of NAD was a prerequisite for the activity of purified enzyme, as was reflected by highest limonin degradation upon addition of the cofactor as well as zymographic results of the native purified enzyme. These observations were similar to earlier reported LDases which required either NADP or NAD as cofactors for limonin catalysis (Humanes et al, 1997).

Metals act as cofactors that help enzymes to express their full catalytic activities. Most of the enzymes require the presence of metal ions for the expression of their catalytic activity and consequently metal ion activation of enzyme reaction assumes importance in industrial

biocatalysis towards achieving maximal catalytic efficiency. At low concentration, metal ions act as cofactors of many enzymes, thereby increasing the catalytic activity of the enzyme, whereas at high concentrations the catalytic activity is reduced. This may be due to the partial denaturation of the enzyme by the presence of excessive free ions in the enzyme extract.

As evident from the results metal ions like Hg^{2+} and Co^{2+}, inhibited the enzyme activity. The inhibitory effect of heavy metal ions is well documented in the literature (Vallieeb and Ulmer, 1972). Hg^{2+} may interact with -SH and S-S groups of proteins in a multitude of systems thereby causing conformational changes in proteins. It is known that ions of mercury react with protein thiol groups (converting them to mercaptides) and also react with histidine and tryptophan residues; moreover, by the action of mercury, the disulfide bond could also be hydrolytically degraded. Thus the role of sulfhydryl group(s) for activity was evident. Further, the decreased activity in the presence of divalent cations could be due to the nonspecific binding or aggregation of the enzyme (Kar et al. 2003). On the other hand, divalent ions; Cu, Ca, Mg, Mn, Zn did not result in reduction or enhancement of the *P.putida* enzyme activity. Stimulation of activity by Zn ions on enzymes from *Arthrobacter* and *Pseudomonas* species (Brewster et al. 1976; Hasegawa et al. 1973) has been reported, no effect of this cation was observed for *R.fasciens* LDase. In fact, Mn and Mg partially inactivated LDase from *R. fascians*, while the enzyme was completely inactivated by Cu.

Kinetic studies performed for purified *P.putida* limonin degrading enzyme using limonin as the substrate indicated similar results to those reported for Limonoate dehydrogenase (LDase) in *R. fasciens* NRRL-1069 (Puri et al. 2002). A comparison of the catalytic efficiency (ratio of Vmax to Km) indicated *R. fasciens* LDase to be high by around 6 times than *P. putida* Limonin degrading enzyme, no affinity was observed with LARL. This is in contrast to the observations with LDase characterized from *R. fasciens* where the catalytic efficiency of LDase was clearly higher for LARL, which has been described as the

physiological substrate for the enzyme (Puri et al. 2002). Based on the results of *In situ* assay under non denaturing conditions the dehydrogenase nature of the limonin degrading enzyme was confirmed. Further evidence of the enzyme identity to salicyldehyde dehydrogenase was obtained from its peptide mass fingerprints; the results corroborated the observed affinity of the purified enzyme to salicyladehyde. The structural basis for the emergence of extended biotransforming ability of enzymes has been reported in *Pseudomonas* sp., (Ganguli and Tripathi 2001) moreover the plasticity of the active site and adaptability of several enzymes to new substrates have been documented (Alves et al. 2002). It appears that the highly oxygenated heterocyclic triterpenoid, limonin, due primarily to its structural resemblance with that of polycyclic aromatic hydrocarbons, may possess such metabolic potential. It is postulated that many degraders of aromatics could be involved in the degradation of plant phytochemicals which is massively distributed in the environment and which consists of many polymeric aromatic moieties. This idea coincides with the fact that a number of catabolic genes involved in the degradation of aromatic compounds share a common ancestry.

The principal product of limonin catalysis by *P. putida* G7 was identified as Defuran limonin, which is similar in structure to limonin except the absence of the furan ring. The furan ring in limonin can be considered as a possible target for initial enzymes of the naphthalene catabolic pathway. Generally, furan is considered to be aromatic because one of the lone pairs of electrons on the oxygen atom is delocalized into the ring, creating a 4n+2 aromatic system similar to benzene. Thus, removal of furan may be the first step in biotransformation of limonin by the microrganism. Subsequent protonation of the D- ring lactone to a structure similar to salicylaldehyde thereafter enables further catabolism by the salicylaldehyde dehydrogenase. Previous reports have indicated Pseudomonas-sp. 321-18 to metabolize limonoate through the deoxylimonin pathway, with dedoxylimonin as major catalytic

product. For another effective limonin degrading strain, *Arthrobacter globiformis*, limonoate appeared to be metabolized only through the 17-dehydrolimonoate pathway and the characterized Limonoate dehydrogenase enzyme converted the precursor of bitter limonin, limonoate A-ring lactone, to nonbitter 17-dehydrolimonoate A-ring lactone.

However in order to conclusively establish the mechanism studies further physical studies with the purified enzyme is required and was beyond the scope of the thesis. The beneficial contribution of bitter components in citrus juices especially limonoids on human health and their biological activities especially on cancer prevention, heart and Alzheimer's disease (Shibu et al. 2005) have been demonstrated extensively based on cell culture and animal studies (Ejaz et al. 2006; Bayazit et al. 2010). Thus it was desirable to examine whether bioconversion of limonin led to a loss of the intrinsic health beneficial attributes. The antioxidant activity of limonin prior to bioconversion was analyzed and compared to the purified catalytic product defuran limonin. Moreover recent findings (Perez et al. 2009) have furnished evidence of furan moiety for the induction of the phase II detoxifying enzyme glutathione S-transferase (GST) and NAD(P)H: quinone reductase (QR); both these enzymes have significant role in protecting cells against toxic and neoplastic effects of xenobiotics as well as cytotoxicity. In this study the antioxidant activities of enzyme debittered mandarin juices did not differ significantly from those observed prior to enzyme treatment. This suggested the nutritional adequacy as well as possible therapeutic effects of debittered juices due to the presence of defuran limonin.

Although advantageous, attempts to apply limonin utilizing microorganisms as a possible citrus-juice-debittering biocatalyst have been unsuccessful primarily due to the lack of an effective, economical biocatalyst (Canovas et al. 1998; Verma et al. 2010). The only microorganism considered potential for commercial processes is *R. fascians*. The behavior of free and immobilized *R. fascians* cells within batch and continuous reactors in the presence of

synthetic citrus juices and under the conditions characteristic of processing citrus juices has been studied extensively. Besides immobilization of *R. fasciens* in K-carragenan, polyacrylamide and polyurethane foam has been reported. Though suitability of polyurethane foam as solid support because of its high structural stability and biomass retention capability was suggested in these studies, possibility of using polyurethane foam immobilized cells in actual citrus juice was not explored. A significant factor, from a process point of view, was to achieve good contact between the substrate, limonin and the enzyme, use of purified enzyme in this regard is not economically advantageous. Therefore a whole cell biocatalyst based process may assure viability under real time conditions. However, it was observed that the whole cell stability was an important criterion for impeded limonin bioconversion during batch culture studies even though the culture variables were adequately optimized using RSM, since effective limonin utilization by whole cells of *P. putida* was observed only during log phase. Immobilization of whole microbial cells has been extensively employed as a non invasive, simple method for restricting cellular growth yet retaining the vital biochemical processes. Besides firsthand information regarding behavior of the cultures over time regarding its desired activity may be obtained by immobilized whole cells. In view of these entrapment of *P. putida* in a few commonly available matrices were attempted and the limonin degradation studied in batch cultures. An adequate combination of the process parameters such as bead diameter, cellular load and alginate concentration identified by RSM, resulted in a faster bioconversion and high reusability (till 8th cycle) of immobilized cells. These observations imply that immobilization afforded a significant protection to the cells against the external environment (low pH, essential oils) in juice for a better performance. The enhanced limonin bioconversion of 65% achieved in 3 hours by alginate entrapped *P. putida* cells is noteworthy when compared to other immobilizing matrices used so far (high limonin bioconversion time i.e 50-60 h) (Canovas et al. 1998) for limonoid

degrading bacterial strains. However, the bioconversion rate declined over subsequent uses presumably on account of low enzyme activity or diffusional restriction due to impermeability of cellular membrane. The decreasing efficiency of alginate entrapped *P.putida* cells during subsequent uses may also be attributed to the deposition of juice solids around the alginate beads and the degeneration of entrapped *P. putida* biomass.

Therefore further attempts were directed towards alleviating permeability limitations. Permeabilization of whole cells offer an attractive proposition of enhancing catalysis, thus varied permeabilization procedures were attempted in *P. putida* G7 using toluene, chloroform-detergent, hexane and proteinase K; EDTA, lysozyme etc.

Highest limonin biotransformation was achieved with Na_2EDTA lysozyme permeabilized cells; which acted as a chelating agent by confiscating divalent cations of Ca^{2+}, Mg^{2+} where the latter stabilizes the outer membrane structure by bonding the lipopolysaccharides to each other and thus creating a hydrophobic pathway for channeling of certain substances. Tris-EDTA has been reported to potentiate the activity of bacterial cell wall degrading agents (e.g., lysozyme, nisin) (Kumar et al. 2008). Once these cations are removed from the EDTA, the lipopolysaccharides are detached, resulting in perforations in areas of the outer walls (Siso et al. 1992). The process of permeabilization rendered better contact between enzyme and substrate thereby enhancing limonin catalysis. The optimal permeabilization of the cells enabled retention of cofactors, especially NADH for functioning of the dehydrogenase affording stability to the biocatalytic process. The availability of cofactors in whole cells is deemed crucial for operability of dehydrogenase based biotransformations. It has been claimed that permeabilized whole cells have an advantage over more pure enzyme preparations due to increased stability (maintained by the intracellular environment); the low specific activity of the desired enzyme needs to be compensated. This intrinsic disadvantage of low specific activity of the desired enzyme was compensated by immobilization or

entrapment of the permeabilized cells (Cheng et al. 2006). A similar decrease in enzyme activity of free permeabilized cells was observed, which prompted entrapment of the cells in a suitable matrix. Dialysis membrane based entrapment of biomass being a simple, effective method (Ganguli et al. 2002) was adopted for assessing limonin biotransformation in mandarin juice.

The results of Response surface methodology (RSM) with central composite rotatable design (CCRD) signified the ability of *P. putida* to biotransform limonin under all tested conditions. The findings indicated that application of RSM to the evolution of enhancement in limonin bioconversion had R2 value closer to 1. The lower value of coefficient of variation (CV), the "Adequate Precision", denotes a higher reliability of the experiments and a very high significance of the model (Venil et al. 2009; Kaur and Satyanarayan, 2010). Upon optimization of the significant variables for permeabilization of *P. putida* G7, the surface plots helped a better understanding of the interactions of the significant variables and thus enabled the determination of the optimal level of each variable for maximizing limonin bioconversion. Permeabilized whole cell biocatalysts are generally not mechanically stable, to afford mechanical stability entrapment methods have been suggested. An earlier study applied dialysis membrane for entrapping whole cells of *Acinetobacter* sp for limonin reduction in orange juices (Vaks and Lifshtiz, 1981). Though entrapment of whole cells had resulted in slightly higher rate of limonin conversion the operation time seemed to be too long which is an impeding factor for practical feasibility. In the present study, entrapment of permeabilized *P. putida* G7 cells in dialysis membranes was attempted. Results of limonin bioconversion obtained directly in kinnow mandarin juices in batch culture experiments indicated enhanced lowering of initial limonin levels and a shortened bioconversion time. These observations implied the role of dialysis membranes in affording stability to the permeabilized whole cells enabling a substantial increase in enzyme – substrate interaction

which resulted in an enhanced limonin bioconversion rate. In the recent past, the feasibility of Immobilized permeabilized whole cell biocatalysts have been extensively explored in several bioprocesses with promising results (Naglak et al. 1990; Lee et al. 2004). Juice samples treated with permeabilized, entrapped whole cells of *P. putida* possessed very low levels of limonin corelatable to the reduction in bitterness (Soares & Hotchkiss, 1998). Since, residual limonin levels in the treated citrus juice remained far below the threshold limit of bitterness for humans, a sensorial acceptance by consumers of the treated juices may be anticipated.

The dialysis membrane entrapped permeabilzed *P. putida* cells retained both viability and enzyme activity which may be attributed to a better protection against the acidic pH of the mandarin juice. In fact, enhanced protection against external pH in whole bacterial cells possessing debitterring enzymes has been reported in earlier studies (Iborra et al. 1994). Though insignificant, the lower rates of limonin biotransformation observed while treating juice may be attributed either due to restriction in the diffusion of limonin or components of the juice (like essential oils) leading to a possible loss of enzyme activity (Verma et al. 2010). The entrapped, permeabilized cells stored over a period of 45 days at room temperature and 30^0C in phosphate buffered saline retained its enzyme activity. Furthermore, the stored permeabilized cells could be reused for at least 8 batch cycles without significant loss of enzyme activity. Studies with both intact and immobilized (k-carragenaan, polyacrylamide and polyurethane foam) cells of *R. fascians* have limitations in terms of biocatalyst reuse for commercial processes. In order to confirm the integrity of the limonin biotransforming dehydrogenase in the permeabilized cells during biotransformation, a zymogram method was used. This method was adopted to detect the functionality of the enzyme in permeabilized cells during the batch cycles. Limonin dehydrogenase concentration in the permeabilized cells could be correlated to the trace intensity of the precipitate using a calibration curve established with purified enzyme from *P.putida* G7. The dialysis membrane may be

important in compensating biocatalyst reuse by overcoming diffusion limitations typical of gel entrapment (Kumar et al. 2008; Ganguli et al. 2002; Swaisgood 1991). Therefore, the enhanced limonin biotransformation by permeabilzed *P. putida* G7 cells, their operational and storage stability upon entrapment in dialysis membranes are important prerequisites for an industrial biocatalyst.

To summarize, this study attempted to elucidate the physiology, genetics and biochemical mechanisms for limonin bioconversion by *P. putida* G7. The results obtained were successfully applied for developing a feasible debiterring strategy for mandarin juices. The nutritional profile of the enzymatically debiterred mandarin juices remained unaltered, suggesting consumer acceptability.

CONCLUSIONS

In summary, the work aimed at examining the following objectives:

- Physiological and biochemical characterization of *Pseudomonas putida G7* in biotransformation of limonin
- Molecular studies and real time application of *P. putida* G7 for limonin biotransformation

Conclusions

- Limonin, the bitter triterpenoid in citrus juices, could be utilized as sole source of carbon and energy by *P. putida* G7. Optimization of cultural parameters enabled 64% biotransformation by *P. putida* in minimal medium containing limonin (50 µg/ml), at pH 8 and temperature 30°C over 48 h. It was inferred that *P. puitda* G7 may possess biochemical mechanisms adequate for catalyzing limonin and subsequent conversion to non-bitter metabolic products and subsequently debittering of mandarin juice.
- Transposon mutagenesis revealed the essential genes of *P. putida G7* for limonin biotransformation. Among 1,800 transconjugants screened, three mutants incapacitated of limonin utilization as the sole carbon source and one strain of *P. putida* Lim^- A mutant was the desired mutant. A high throughput inverse PCR method was employed to detect the essential genes on the flanking regions of Tn5 transposon insertion site in *P. putida* G7, which are responsible for limonin biotransformation.

  The molecular characterization and identification of one of the unknown genes suggested the imperative role of membranous glutamate symporter in limonin biotransformation

- *P. putida* G7 harbors a single and large NAH plasmid of size of approximately ~80kb, present in low copy number and encodes for naphthalene oxidative enzymes. Plasmid curing studies established a possible role of indigenous NAH plasmid for limonin utilization by *P. puitda* G7.
- A periplasmically located enzyme responsible for biotransformation of limonin was identified in *P. putida* G7. The pH and temperature optima of the enzyme were 8.5 and 35°C respectively and the K_M value for limonin was 4.5μM. The dehydrogenase a monomer of MW 26kDa, converted limonin to defuran limonin. The dehydrogenase, exhibited high substrate specificity to limonin followed by salycyldehyde; peptide mass fingerprinting analysis of the enzyme revealed 48% of amino acid identity (53% similarity) to DoxF from *Pseudomonas* C18, with an alignment coverage of 82, involved in the upper naphthalene catabolic pathway of *Pseudomonas* C18. A potential involvement of this novel isofunctional dehydrogenase in biotransformation of limonin is suggested.
- The biocatalytic activity of periplasmic dehydrogenase of *P. putida* G7 strain for limonin was enhanced when whole cells were permeabilized with Na_2EDTA (1μM) and lysozyme. Permeabilised cells (1g dry weight) entrapped in dialysis membrane could biotransform 73.67% of limonin in mandarin juices in a single batch cycle of 3 hours.
- A dialysis based bioreactor was optimized using the permeabilized cells of *P. putida* G7. Permeabilization of cells was statistically optimized with Response Surface Methodology and Central Composite Design to enhance the limonin biocatalysis in citrus juice. The optimum operating conditions for the permeabilization process were Na_2EDTA concentration (1.5 μM), permeabilization treatment time of 15 mins and temperature

28°C at pH 8. Validation experiments carried out under selected conditions demonstrated an enhanced dehydrogenase activity by reducing the limonin to 76.71% within 150 minutes. Permeabilized cells stored for 45 days in phosphate buffered saline, at room temperature and 30°C, retained enzyme activity and were reusable for up to 8 batch cycles for limonin reduction. This study suggested the potential of permeabilized *P. putida* G7 cells for limonin biotransformation.

Based on the understanding developed for the catabolic abilities, enzyme(s) and gene(s) in *Pseudomonas putida* G7 with possible involvement in the process of limonin bioconversion a dialysis membrane based bioreactor was developed by employing the permeabilized *Pseudomonas putida* G7. Overall the outcomes of this study contributed in developing a holistic insight of limonin bioconversion mechanism of *P. putida*. The results of this study can substantially improve currently available debiterring strategies for mandarin juices.

REFERENCES

Abbasi S, Zandi P, Mirbagheri E. (2005) Quantitation of limonin in Iranian orange juice concentrates using high performance liquid chromatography and spectrophotometric methods. Euro Food Res and Technol 221, 202-207

Albach RF, Redman GH, Lime BJ (1981) Limonin, Content of Juice from Marrs and Hamlin Oranges [*Citrus sinensis* (L.) Osbeck] J Agric Food Chem 29, 313-315

Albano MA, Arroyo J, Eisenstein BI, Engleberg NC (1992) phoA gene fusions in *Legionella pneumophila* generated in vivo using a new transposon, MudphoA. Mol Microbiol 6, 1829-1839

Aletor VA, Adeogun OA (1995) Nutrient and antinutrient components of some tropical leafy vegetables. Food Chem 53, 375-379

Aliero BL (2003) Larvaecidal effects of aqueous extracts of*Azadirachta indica* (neem) on the larvae of*Anopheles* mosquito. African J Biotechnol 2, 325-327

Alves R, Chaleil RA, Sternberg MJ (2002) Evolution of Enzymes in Metabolism: a Networking Perspective. J Mol Bio 320, 751-770

Ames GFL, Prody C, Kusm S (1984) Simple, rapid, and quantitative release of periplasmic proteins by chloroform. J Bact 160, 1181-1183

Arnott S, Davie AW, Robertson JM, Sim GA, Watson DG (1960) The structure of limonin. Experientia 16, 49–51

Austen RA, Dunn NW (1980) Regulation of the Plasmid-specified Naphthalene Catabolic Pathway of *Pseudornonas putida*. J Gen Microbiol 117, 521-528

Azzolina BA, Yuan X, Anderson MS, El-Sherbeini M (2001) The cell wall and cell division gene cluster in the Mra operon of *Pseudomonas aeruginosa*: cloning, production, and purification of active enzymes. Prot Expr Purif 21, 393-400

Babu PSR, Panda T (1991) Studies on improved techniques for immobilizing and stabilizing penicillin amidase associated with *E. Coli* cells. Enz Microbial Tech 13, 676–682

Bansal-Mutalik R, Gaikar VG (2003) Cell permeabilization for extraction of penicillin acylase from *Escherichia coli* by reverse micellar solution. Enzyme Microb Technol 32, 14–26

Barmore CR, Fisher JF, Feller PJ, Rouseff RL (1986) Reduction of bitterness and tartness in grapefruit juice with florisil. J Food Sci 51, 415-419

Bayazit V, Konar V (2010) Biochemical and Physiological Evaluations of Limonoids as Potential Cancer Destroyers. J Animal Vet Adv 9, 1099-1107

Bennett RD (1971) Acidic limonoids of grapefruit seeds. Phytochem 10, 3065-3068

Bennett RD and Hasegawa S (1982) 7a-Oxygenated limonoids from Rutaceae. Phytochem 21, 2349-2354

Berg DE (1989) Transposon Tn5. In Mobile DNA (Berg, D. E. & Howe, M. M., eds), American Society for Microbiol, Washington, DC, 185-210

Berg CM, Berg DE, Groisman EA (1989) Transposable Elements and the Genetic Engineering of Bacteria in Mobile DNA. eds Berg D. E., HoweM. M. (American Society for Microbiology, Washington, D.C.) pp 879–925

Bernal V, Gonzalez-Veracruz M, Canovas M, Iborra JL (2007) Plasmid maintenance and physiology of a genetically engineered *Escherichia coli* strain during continuous L-carnitine production. Biotechnol Lett 29, 1549–1556

Bernay S (1841) Limonin. Ananlen 24, 317

Bethesda Research Laboratories (1986) BRL pUC host: *E. coli* DH5α competent cells. Focus 8 2, 9.

Bhasin A, Goryshin IY, Steiniger-White M, York D, Reznikoff WS (2000) Characterization of a Tn5 Pre-cleavage Synaptic Complex. J Mol Biol 302, 49-63

Birgisson H, Wheat JO, Hreggvidsson GO, Kristjansson JK, Mattiasson B (2007) Immobilization of a recombinant *Escherichia coli* producing a thermostable a-L-rhamnosidase: creation of a bioreactor for hydrolyses of naringin. Enz Microbiol Technol 40, 1181–1187

Bourhy P, Louvel H, I Saint Girons, Picardeau M (2005) Random insertional mutagenesis of *Leptospira interrogans*, the agent of leptospirosis, using a mariner transposon. J Bacteriol 187, 3255-3258

Bradford MM (1976) A rapid and sensitive method for the quantitation of microgram quantities of protein utilizing the principle of protein-dye binding. Anal Biochem 72, 248-254

Breedveld MW, Zevenhuizen LP, Zehnder AJB (1992) Synthesis of cyclic β-1,2-glucans by *Rhizobium leguminosarum* Biovar trifolii TA-1: factors influencing excretion. J Bacteriol 174, 6336–6342

Brewster LC, Hasegawa S, Maier VP (1976) Bitterness Prevention in Citrus Juices. Comparative Activities and abilities of the Limonate Dehydrogenases from *Pseudomonas* and *Arthrobacter*. J Agric Food Chem 24, 21-24

Burman LG, Nurudstrom K, Bloom GD (1972) Murein and the outer penetration barrier of *Escherichia coli K-12, Proteus mirubilis* and *Pseudomonus aeruginosa*. J Bacteriol 11, 1364–1374

Busto MD, Garcıa-Tramontın KE, Ortega N, Perez-Mateos M (2006) Preparation and properties of an immobilized *pectinlyase* for the treatment of fruit juices. Biores Technol 97, 1477–1483

Butterfield YS, Marra MA, Asano JK, Chan SY, Guin R, et al (2002) An efficient strategy for large-scale high-throughput transposon-mediated sequencing of cDNA clones. Nucleic Acids Res 30, 2460–2468

Canovas M, Garcia-Cases L and Iborra J (1998) Limonin consumption at acidic pH values and absence of aeration by *Rhodococcus fascians* cells in batch and immobilized continuous systems. Enz Microbial Technol 22, 111–116

Canovas M, Garcia-Cases L, Iborra J (1998) Limonin consumption at acidic pH values and absence of aeration by *Rhodococcus fascians* cells in batch and immobilized continuous systems. Enz Microbial Technol 22, 111–116

Canovas M, Garcia-cases L, Iborra JL (1996) pH influence on the consumption of limonin species by *Rhodococcus fascians* cells. Biotechnol Lett 18, 423-428

Cánovas M, García-Cases L, Iborra JL (1997) Shifts in metabolism and morphology of *Rhodococcus fascians* when debittering synthetic citrus juices in the absence of aeration. Biotechnol Lett 19, 1181–1184

Cavonas M, Torroglosa T, Kleber H, Iborra JL (2003) Effect of salt stress on crotonobetaine and D-carnitine biotransformation of L-carnitine by resting cells of *Escherichia coli*. J Basic Microbiol 43, 259–268

Cetinus SA, Oztop HN (2003) Immobilization of catalase into chemically crosslinked chitosan beads. Enzyme and Microbial Technology 32, 889–894

Chandler BV, Kefford JF (1968) Removal of limonin from bitter orange juice. J Sci Food Agric 19, 83-87

Chatterjee T and Bhattacharya DK (2001) Biotransformation of limonene by *Psuedomonas putida*. App Microbiol Biotechnol 55, 541-546

Chauhan K, Trivedi UB, Patel KC (2006) Application of response surface methodology for optimization of lactic acid production using date juice. J Microbiol Biotechnol 16, 1410–1415

Chen S, Songkumarn P, Liu J, Wang GL (2009) A Versatile Zero Background T-Vector System for Gene Cloning and Functional Genomics. Plant Physiol 150, 1111–1121

Cheng S, Dongzhi W, Song Q, Zhao X (2006) Immobilization of Permeabilized Whole Cell Penicillin G Acylase from *Alcaligenes faecalis* Using Pore Matrix Cross linked with Glutaraldehyde. Biotechnol Lett 28, 1129-1133

Chidambara Murthy KN, Jayaprakasha GK, Kumar V, Rathore KS, Patil BS (2011) Citrus limonin and its glucoside inhibit colon adenocarcinoma cell proliferation through apoptosis. J Agric Food Chem 59, 2314-2323

Chisti Y, Moo-Young M (1986) Disruption of microbial cells for in-tracellular products. Enz Microb Technol 8, 194-204

Cho H, Cronan JE Jr (1995) Defective export of a periplasmic enzyme disrupts regulation of fatty acid synthesis. J Biol Chem 270, 4216-4219

Chowdary GV, Divakar S, Prapulla SG (2002) Modelling on isoamyl isovalerate synthesis from *Rhizomucor miehei* lipase in organic media: optimization studies. W J Microbiol Biotechnol 18, 179–185

Colegio OR, Griffin TJ, Grindley NDF, Gala´n JE (2001) In vitro transposition system for efficient generation of random mutants of *Campylobacter jejuni*. J Bacteriol 183, 2384–2388

Comfort NC (2001) From controlling elements to transposons: Barbara McClintock and the Nobel Prize. Trends Biochem Sci 26, 454–457

Das AK, Cohen PTH, Barford D (1998) The structure of the tetratricopeptide repeats of protein phosphatase 5: implications for TPR-mediated protein-protein interactions. EMBO J 17, 1192-1199

De Bont JAM (1998) Solvent-tolerant bacteria in biocatalysis. Trends Biotechnol 16, 493–499

DeLorenzo V, Timmis, KN (1994). Analysis and Construction of Stable Phenotypes in Gram-negative Bacteria with Tn*5* and Tn*10*-derived Mini-Transposons. Methods Enzymol 235, 386–405

Denome SA, Stanley DC, Olson ES, Young KD (1993) Metabolism of dibenzothiophene and naphthalene in *Pseudomonas* strains: complete DNA sequence of an upper naphthalene catabolic pathway. J Bacteriol 175, 6890-6901

Devakumar C, Dev S (1996) Chemistry ed. by Randhawa NS, Parmar BS, Neem Research and Development, Soci of Pesticide Sci New Delhi, India, 63-99

Dewanto V, Wu X, Adom KK, Liu RH (2002) Thermal processing enhances the nutritional value of tomatoes by increasing total antioxidant activity. J Agric Food Chem 50, 3010–3014

Dreyer DL (1965) Citrus bitter principles. III. Isolation of deacetylnomilin and deoxylimonin. Org Chem 30, 749-751

Dreyer DL (1965) Citrus bitter principles-II. Application of NMR to structural and stereochemical problems. Tetrahed 21, 75-87

Dubois M, Gilles KA, Hamilton JK, Rebers PA, Smith F (1956) Colorimetric method for determination of sugars and related substances. Anal Chem 28, 350-356

Dunn NW, Gunsalus IC (1973) Transmissible plasmid coding early enzymes of naphthalene oxidation in *Pseudomonas putida.* J Bacteriol 114, 974-979

Dupont C, Clarke AJ (1991) In-vitro synthesis and O acetylation of peptidoglycan by permeabilized cells of *Proteus mirabilis*. J Bacteriol 3, 4618–4624

Dwevedi A, Singh AK, Singh DP, Srivastava ON, Kayastha AM (2009) Lactose nano-probe optimized using response surface methodology. Biosen Bioelec 25, 784-790

Eaton RW (1994) Organization and evolution of naphthalene catabolic pathways: sequence of the DNA encoding 2-hydroxychromene-2-carboxylate hydratase-aldolase from the NAH7 plasmid. J Bacteriol 176, 7757-7762

Ejaz S, Ejaz A, Matsuda K, Lim CW (2006) Limonoids as Cancer Chemopreventive Agents. J Sci Food Agric 86, 339–345

Emerson OH (1949) The bitter principle of navel oranges. Food Technol. (Chicago, IL) 3, 243-250

Ensley BD, Ratzkin BJ, Osslund TD, Simon MJ (1983) Expression of naphthalene oxidation genes in *Escherichia coli* results in the biosynthesis of indigo. Sci 222, 167-169

Femandez E, Couture R, Rouseff RL, Chen CS, Barros S (1992) Evaluation of ultrafiltration and adsorption to debitter grapefruit juice and grapefruit pulp wash. J Food Sci 57, 664-669

Foght JM, Westlake DW (1996) Transposon and spontaneous deletion mutants of plasmid-borne genes encoding polycyclic aromatic degradation by a strain of *Pseudomonas fluorescens*. Biodegradation 7, 353-366

Fong CH, Hasegawa S, Coggins CW Jr, Atkins DR, Miyake M (1992) Contents of limonoids and limonin 17-B-D-glucopyranoside in fruit tissue of valencia orange during fruit growth and maturation. J Agric Food Chem 40, 1178–118

Fontanille P, Larroche C (2003) Optimization of isonovalal production from α-pinene oxide using permeabilized cells of *Pseudomonas rhodesiae* CIP 107491. Appl Microbiol Biotechnol 60, 534–540

Ganguli A, Tripathi AK (2001) Inducible Periplasmic Chromate Reductase Activity in a Tannery Isolated *Pseudomonas* sp. J Microbiol Biotechnol 11, 23-29

Ganguli A, Tripathi AK (2002) Bioremediation of toxic chromium from electroplating effluent by chromate reducing *Pseudomonas aeruginosa* A2Chr in two bioreactors. Appl Microbiol Biotechnol 58, 416-420

Gerngross UT, Romaniec MPM, Kobayashi T, Huskisson NS, Demain AL (1993) Sequencing of a Clostridium Thermo- cellum gene (+A) Encoding the Cellulosomal SL-Protein Reveals an Unusual Degree of Internal Homology. Mol Microbiol 8, 325-334

Ghosh M, Ganguli A, Mallik M (2006) Evidence of Indigenous NAH Plasmid of Naphthalene Degrading *Pseudomonas putida* PpG7 Strain Implicated in Limonin Degradation. J Microbiol 44, 473-479

Gisby PE, Rao KK, Hall DD (1987) Entrapment techniques for chloroplasts, cyanobacteria and hydrogenases. Meth Enzymol 135, 440–454

Gohel V, Jiwan D, Vyas P, Chatpar HS (2005) Statistical optimization of chitinase production by *Pantoea dispersa* to enhance degradation of crustacean chitin waste. J Microbiol Biotechnol 15, 197–201

Goldstein L, Lifshitz A and Skolovsky M (1971) Water insoluble derivatives of naringinase. Int J Biochem 10, 448-453

Golovleva LA, Zaborina O, Pertsova R, Baskunov B, Schurukhin Y, Kuzmin S (1992) Degradation of polychlorinated phenols by *Streptomyces rochei*. Biodegradation 2, 201-208

Gorinstein S, Haruenkit R, Park YS, Jung ST, Zachwieja Z, Jastrzebski Z (2004b) Bioactive compounds and antioxidant potential in fresh and dried Jaffal (R) sweeties, a new kind of citrus fruit. J Sci Food Agric 84, 1459-1463

Gray MG and Olson AC (1981) Hydrolysis of high levels of naringin in grapefruit juice using a hollow fibre naringinase reactor. J Agric Food Chem 29, 1298

Griffin TJ 4th, Parsons L, Leschziner AE, DeVost J, Derbyshire KM, Grindley ND (1999) In vitro transposition of Tn*552*: a tool for DNA sequencing and mutagenesis. Nucleic Acids Res 27, 3859–3865

Griffith FP (1969) Process for Reactivating Polyamides Resin Used in Debittering Citrus Juice. U.S. Patent 3463763

Grimm AC, Harwood CS (1997) Chemotaxis of *Pseudomonas* sp. to the polyaromatic hydrocarbon naphthalene. Appl Environ Microbiol 63, 4111-4115

Grimm AC, Harwood CS (1999) NahY, a catabolic plasmid-encoded receptor required for chemotaxis of *Pseudomonas putida* to the aromatic hydrocarbon naphthalene. J Bacteriol 181, 3310-3316

Guadagni DG, Maier VP, Turnbaugh JG (1973) Effects of some citrus constituents on taste thresholds for limonin and naringin bitterness. J Sci Food Agric 24, 1277–1288

Guthrie N, Hasegawa S, Manners GD, Carroll KK, Berhow MA, Hasegawa S, Manners GD (2000) Inhibition of human breast cancer cells by citrus limonoids. In Citrus Limonoids: Functional chemicals in agriculture and foods; Berhow, MA, Hasegawa S, Manners GD, Eds.; American Chem Soci: Washington, DC, 758, 164–174

Guthrie N, Kurowska EM, Manners G, Hasegawa S, White D, Freeman D (2002) Inhibition of human breast cancer cell growth by citrus limonoids. FASEB J 16, A999

Haiau LT, Lee WC, Wang FS (1997) Immobilization of whole-cell penicillin G acylase by entrapping within polymethacrylamide beads. Appl Biochem Biotech 62, 303–315

Halan B, Schmid A and Buehler K (2011) Real-Time Solvent Tolerance Analysis of Pseudomonas sp. Strain VLB120 C Catalytic Biofilms, Appl and Environmen Microbiol, 77, 1563–1571

Hamer L, DeZwaan TM, Montenegro-Chamorro MV, Frank SA, Hamer JE (2001) Recent advances in large-scale transposon mutagenesis. Curr Opin Chem Biol 5, 67–73

Hasagawa S, Maier VP (1983) Solutions to limonin bitterness problem of citrus juices. J Food Technol 131, 73-77

Hasegawa S (1976) Metabolism of Iimonoids. Limonin D-ring lactone hydrolase activity in *Pseudomonas.* Agric Food Chem 24, 24-26

Hasegawa S, King AD (1983) A species of bacterium producing constitutive enzymes for limonoid metabolism. J Agric Food Chem 31, 807

Hasegawa S, Bennett RD, Vincent PM (1972) Metabolism of limonin and limonate by microorganisms: the conversion to non-bitter compounds. J Agric Food Chem 20, 435

Hasegawa S, Bennett RD, Herman Z, Fong Chi H, Ou P (1989) Limonoid Glucosides in Citrus. Phytochem 28, 1717–1720

Hasegawa S, Bennett RD, Maier VP, King AD (1972) Limonate dehydrogenase from *Arthrobacter globiformis.* J Agric Food Chem 20, 1031

Hasegawa S, Berhow MA, Manner GD (2000) Citrus limonoids research: An overview. In M. A. Berhow, S. Hasegawa, & G. D. Manners (Eds.), Citrus limonoids: Functional chemicals in agriculture and foods. ACS symp series 758, 1–8

Hasegawa S, Brewster LC, Maier VP (1973) Use of Limonate Dehydrogenase of *Arthrobacter globiformis* for the Pevention or Removal of Limonin Bitterness in Citrus Products. J Food Sci 38, 1153-1155

Hasegawa S, Dillberger AM and Choi GY (1984) Metabolism of Iimonoids: conversion of nomilin to obacunone in *Corynebacterium fascians.* Agric Food Chem 32, 457-459

Hasegawa S, Fong Chi H, Herman Z, Miyake M (1992) Glucosides of limonoids. In Flavor precursors; Teranish R, Takeoka GR, Matthias G, Eds, American Chemical Society: Washington DC 490, 88–97

Hasegawa S, Herman Z and Au P (1986) Metabolism of limonoids: nomilin to nomilinate in *Citrus limon.* Phytochem 25, 542-543

Hasegawa S, Kim KS (1975) Biochemistry of limonoids. A new limonoid debittering enzyme. Abstracts, Citrus Research Conference, Pasadena, CA, December 16, 1975

Hasegawa S, Maier VP (1990) Biochemistry of limnoids in citrus juice bitter principles and biochemical debittering processes. In R.L. Rouseff (ed.), Bitterness in Foods and Bev. Elsevier, New York, NY, U.S.A, 293-308

Hasegawa S, Miyake M (1996) Biochemistry and biological functions of citrus limonoids. Food Rev Int 12, 413-435

Hasegawa S, Ou P, Fong Chi H, Herman Z, Coggins CW Jr, Atkins DR (1991) Changes in the limonate-A-ring lactone and limonin 17-B-D-glucopyranoside content of navel oranges during fruit growth and maturation. J Agric Food Chem 39, 262–265

Hasegawa S, Patel MN and Snyder RC (1982) Reduction of limonin bitterness in navel orange juice serum with bacterial cells immobilized in acrylamide gel. J Agric Food Chem 30, 509-511

Hasegawa S, Pelton VA and Bennett RD (1983) Metabolism of limonoids by *Arthrobacter globiformis* II: basis for practical means of reducing the limonin content of orange juice by immobilized cells. Agric Food Chem 31, 1002-1004

Hasegawa S, Vandercook CE, Choi GY, Herman Z, and Ou P (1985) Limonoid debittering of citrus juices sera by immobilized cells of *Corynebacterium fascians.* J Food Sci 50, 330

Hasegawa S, Yokoyama H and Hoagland JE (1977) Inhibition of limonoid biosynthesis in leaves of *Citrus limon.* Phytochem 16, 1083-1085

Hawagawa S, Maier VP, and King AD., Jr (1974) Isolation of new limonate dehydrogenase from *Pseudomonas.* J Agric Food Chem 22, 523

Hayes F (2003) Transposon-based strategies for microbial functional genomics and proteomics. Annu Rev Genet 37, 3-29

Hewtter DJ, Wang HY (1986) Protein released from chemically permeabilised *Escherichia coli*. J.A. Asenjo, J. Hong (Eds.), Seperation, Recovery and Purification in Biotechnology, ACS Symposium Series 314 American Chem Soci 2-8

Higby RH (1938) The bitter constituents of navel and Valencia oranges. J Amer Chem Soc 60, 3013-3018

Huijberts GNM, Eggink G (1996) Production of poly (3-hydroxyalkanoates) by *Pseudomonas putida* KT2442 in continuous cultures. Appl Microbiol Biotechnol 46, 233–239

Humanes L, Lopez-Ruiz A, Merin MT, Roldan JM, Diez J (1997). Purification and Characterization of Limonoate Dehydrogenase from *Rhodococcus fascians.* Appl Environ Microbiol 63, 3385-3389

Iborra JL, Manjon A, Canovas M, Lozano P, Martınez C (1994) Continuous Limonin Degradation by Immobilized *Rhodococcus fascians* Cells in K-carragenaan. Appl Microbiol Biotechnol 41, 487–493

Isoai A, Kimura H, Reichert A, Schorgendorfer K, Nikaido K, Tohda H, Giga-Hama Y, Mutoh N, Kumagai H (2002) Production of D-amino acid oxidase (DAO) of *Trigonopsis variabilis* in *Schizosaccharomyces* pombe and the characterization of biocatalysis prepared with recombinant cells. Biotechnol Bioeng 80, 22–32

Jackman JE, Raetz CR, Fierke CA (2001) Site-directed mutagenesis of the bacterial metalloamidase UDP-(3-O-acyl)-N-acetylglucosamine deacetylase (LpxC). Identification of the zinc binding site. Biochem 40, 514-523

Jayaprakasha GK, Patil BS (2007) In vitro evaluation of the antioxidant activities in fruit extracts from citron and blood orange. Food Chem 101, 410–418

Jimeno A, Manjon A, Canvos M and Iborra JL (1987) Use of naringinase immobilized on glycophase coated porous glass for fruit juice debittering. Process Biochem 22, 13

Johnsen AR, Wick LY, Harms H (2005) Principles of microbial PAH degradation in soil. Environ. Poll 133, 71-84

Johnson RL, Chandler BV (1988) Absorptive removal of bitter principles and titrable acid from citrus juices. Food Technol 45, 130-136

Jourdan PS, Mansell RL, Oliver DG, Weiler EW (1984) Competitive solid phase enzyme linked immunoassay for the quantification of limonin in citrus juices. Anal Biochem 138, 19-23

Kado CI, Liu ST (1981) Rapid Procedure for Detection and Isolation of Large and Small plasmids. J Bact (145) 1365-1373

Kanaly RA, Harayama S (2000) Biodegradation of high-molecular weight polycyclic aromatic hydrocarbons by bacteria. J. Bacteriol 182, 2059-2067

Kanaly RA, Harayama S (2010) Advances in the field of high-molecular weight polycyclic aromatic hydrocarbon biodegradation by bacteria. Microbiol Biotechol 3, 132-164

Kar B, Banerjee R, Bhattacharyya BC (2003) Effect of Additives on the Behavioural Properties of Tannin acyl hydrolase. Process Biochem 38, 1285-1293

Karel SF, Libicki SB, Robertson CR (1985) The immobilization of whole cells: engineering principles. Chemical Eng Sci 40, 1321–1354

Kaur P, Satyanarayana T (2010) Improvement in cell-bound phytase activity of *Pichia anomala* by permeabilization and applicability of permeabilized cells in soyamilk dephytinization. J Appl Microbiol 108, 2041-2049

Kefford JF (1959) The chemical constituents of citrus fruits. Adv Food Res 9, 285-292

Kieboom J, Jonathan J, Dennis S, Jan AM de Bont, and Gerben J, Zylstra S (1998) Identification and Molecular Characterization of an Efflux Pump Involved in Pseudomonas putida S12 Solvent Tolerance, J Biolo Chem 273, 85–91

Kim SY, Kim RH, Huh TL, Park JW (2001) α-Phenyl-N-t-butylnitrone protects oxidative damage to HepG2 cells. J Biochem Mol Biol 34, 43-46

Kimball DA (1987) Debittering of citrus juices using supercritical carbon dioxide. J Food Sci 52, 481-487

Kimball DA, Norman SI (1990) Processing effects during commercial debittering of California navel orange juice. J Agric Food Chem 38, 1396–1400

Kinsella JE, Frankel EN, German JB, Kanner J (1993) Possible Mechanisms for the Protective Role of Antioxidants in Wine and Plant Foods. Food Technol 47, 85-89

Kiyohara H, Nagao K (1978) The catabolism of phenanthrene and naphthalene by bacteria. J Gen Microbiol 105, 69-75

Kiyohara H, Torigoe S, Kaida N, Asaki T, Iida T, Hayashi H, Takizawa N (1994). Cloning and characterization of a chromosomal gene cluster, pah, that encodes the upper pathway for phenanthrene and naphthalene utilization by *Pseudomonas putida* OUS82. J Bacteriol 176, 2439-2443

Kola O, Kaya C, Duran H, Altan A (2010) Removal of limonin bitterness by treatment of ion exchange and adsorbent resins, Food Sci Biotechnol 19, 411-416

Konno A, Miyawaki M, Toda J, Wada T, Yasumatsu K (1982) Bitterness reduction of naringin and limonin by 0-cyclodextrin polymer. Agric Biol Chem 46, 2203-2209

Krasaekoopt W, Bhandari B, Deeth H (2003) Evaluation of encapsulation techniques for probiotics for yogurt. Int Dairy J 13, 3-13

Kumar SS, Kundu S, Pakshirajan K, Dasu VV (2008) Cephalosporins Determination with a Novel Microbial Biosensor Based on Permeabilized *Pseudomonas aeruginosa*, Whole Cells. Appl Biochem Biotechnol 151, 653-664

Kunamneni A, Kumar KS, Singh S (2005) Response surface methodological approach to optimize the nutritional parameters for enhanced production of -amylase in solid state fermentation by *Thermomyces lanuginosus*. Afric J Biotechnol 4, 708-716

Kurkela S, Lehvaslaiho H, Palva ET, Teeri TH (1988) Cloning, nucleotide sequence, and characterization of genes encoding naphthalene dioxygenase of *Pseudomonas putida* strain NCIB9816. Gene 73, 355-362

Laemmli UK (1970) Cleavage of structural proteins during the assembly of the head of bacteriophage T4. Nature 227, 680-685

Lam LKT, Hasegawa S, Bergstrom C, Lam SH and Kenney P (2000) Limonin and nomilin inhibitoryeffects on chemical induced tumorgenesis. In Citrus Limonoids: Functional chemicals inagriculture and foods; Berhow, M. A., Hasegawa, S., Manners, G. D., Eds.; American Chemical Society: Washington DC, 2000; Vol. 758, 185–200.

Lam LKT, Li Y, Hasegawa S (1989) Effects of citrus limonoids on glutathione S-transferase activity in mice. J Agric Food Chem 37, 878–880

Lee WC, Yusof S, Hamid NSA, Baharin BS (2006) Optimizing conditions for enzymatic clarification of banana juice using response surface methodology (RSM). J Food Eng 73, 55–63

Lee YJ, Kim CS, Oh DK (2004) Lactulose production by β−galactosidase in permeabilized cells of *Kluyveromyces lactis*. Appl Microbiol Biotechnol 64, 787–793

Lillehoj EP, Malik VS (1989) Protein purification. Adv Biochem Eng Biotechnol 40, 19-71

Lim JS, Park MC, Lee JH, Park SW, Kim SW (2005) Optimization of culture medium and conditions for neo-fructo oligosaccharides production by *Penicillium citrinum*. Eur Food Res Technol 221, 639–644

Liu L, Whalen W, Das A, Berg CM (1987) Rapid sequencing of cloned DNA using a transposon for bidirectional priming: sequence of the *Escherichia coli* K-12 *avtA* gene. Nucleic Acids Res 15, 9461–9469

Liu Y, Hama H, Fujita Y, Kondo A, Inoue Y, Kimura A, Fukuda H (1999) Production of S-lactoylglutathione by high activity whole cell biocatalysts prepared by permeabilization of recombinant *Saccharomyces cerevisiae* with alcohols. Biotechnol Bioeng 64, 54–60

Lorenzo H. Chen, Thomas O. Baldwin (1989) Random and Site-Directed Mutagenesis of *Bacterial Luciferase*: Investigation of the Aldehyde Binding Site Biochemistry 28, 2684-2689

Lowry OH, Rosenbrough NJ, Farr AL, Randall RJ (1951) Protein measurement with the Folin Phenol Reagent. J Biol CHem 193, 265-275

Maekawa T, Yanagihara K, Ohtsubo E (1996) A cell-free system of Tn*3* transposition and transposition immunity. Genes Cells 1, 1007–1016

Maier VP, Bennett RD, Hasegawa S (1977) Limonin and other limonoids. In citrus Science and Technology, Nagy S, Shaw P, Velduis MK, Avi Publishing, Westport CT 1, 335-396

Maier VP, Beverly GD (1968) Limonin monolactone, the nonbitter precursor responsible for delayed bitterness in certain citrus juices. J Food Sci 33, 488-492

Maier VP, Brewster LC, Hsu AC (1973) Ethylene accelerated limonoids metabolism in citrus fruits: a process for reducing juice bitterness. J Agric Food Chem 21, 490-497

Maier VP, Hasegawa S and Hera E (1969) Limonin D-ring lactone hydrolase. A new enzyme from Citrus seeds. Phytochem 8, 405-407

Maier VP, Hasegawa S, Bennett RD, Echols LC (1980) Limonin andlimonoids. Chemistry, biochemistry and juice bitterness. In Citrus nutrition and quality; Nagy, S., Attaway, J. A., Eds.; American Chem Soci: Washington, DC 143, 63–82

Maier VP, Margileth DA (1969) Limonoic acid A-ring lactone, a new limonin derivative in citrus. Phytochem 8, 243-248

Maniatis T, Fritsch EF, Sambrook J (1982) Molecular cloning, a laboratory manual (Cold Spring Harbor: Cold Spring Harbor Laboratory, NY

Manjon A, Bastida J, Romero C, Jimeno A and Iborra, JL (1985) Immobilization of naringinase on glycophase coated porous glass beads. Biotech Lett 7, 487-492

Manjon A, Iborra JL and Martinez-Madrid C (1991) pH control of limonin debittering with entrapped *Rhodococcus fascians* cells. Appl Microbiol Biotechnol 35,176

Manners GD (2005) The feasability of colorimetric analysis for the determination of freeze impacted citrus quality; California Citrus Research Board: Visalia, CA, 1-8

Manners GD (2007) Citrus Limonoids: Analysis, Bioactivity, and Biomedical Prospects. J Agric Food Chem 55, 8285–8294

Manners GD, Hasegawa S, Barnett RD, Wong RY (2000) LC–MS and NMR techniques for the analysis and characterization of citrus limonoids. In Berhow MA, Hasegawa S, Manners GD (Eds.), Citrus limonoids: Functional chemicals in agriculture and foods. ACS symposium series 758, 40–59

Manoil C (2000) Tagging exported proteins using *Escherichia coli* alkaline phosphatase gene fusions. Methods Enzymol 326, 35–47

Mansell RL, Weiler EW (1980) Radioimmunoassay for the determination of limonin in Citrus. Phytochem 19, 1403-1407

Martinez-Madrid C, Manjon A and Iborra JL (1989) Degradation of limonin by entrapped *Rhodococcus fascians* cells. Biotechnol Lett 2, 653-259

Marwaha SS, Puri M, Bhullar M and Kothari RM (1994) Optimization of process parameters for debittering kinnow fruit juice. Enzyme Microb Technol 16, 723-725

Matsumoto T, Takahash S, Kaieda M, Ueda M, Tanaka A, Fukuda H, Kondo A (2001) Yeast whole-cell biocatalyst constructed by intracellular overproduction of *Rhizopus oryzae* lipase is applicable to biodiesel fuel production. Appl Microbiol Biotechnol 57, 515–520

Mei JM, Nourbakhsh F, Ford CW, Holden DW (1997) Identification of *Staphylococcus aureus* virulence genes in a murine model of bacteraemia using signaturetagged mutagenesis. Mol Microbiol 26, 399–407

Menn F, Bruce M, Gary A, Sayler S (1993) NAH Plasmid-Mediated Catabolism of Anthracene and Phenanthrene to Naphthoic Acids. App Env Microbiol 59, 1938-1942

Methogo RM, Dufresne-Martin G, Leclerc P, Leduc R, Klarskov K (2005) Mass Spectrometric Peptide Fingerprinting of Proteins after Western Blotting on Polyvinylidene Fluoride and Enhanced Chemiluminescence Detection. J Proteo Res 4, 2216-2224

Miller EG, Record MT, Binnie WH, Hasegawa S (2000) Limonoid glucosides: Systemic effects on oral carcinogenesis. In Phytochemicals and Phytopharmaceuticals; Shahidi, F., Ho, C., Eds.; AOAC Press: Champaign IL 95–105

Miller GL (1959) Use of Dinitrosalicylic Acid Reagent for Determination of Reducing Sugar Anal Chem 31, 426–428

Moore ERB, Tindall BJ, Martins Dos Santos VAP, Pieper DH, Ramos JL, Palleroni NJ **(**2006**)** Nonmedical: *Pseudomonas* The Prokaryotes. *Proteobacteria:* Gamma subclass 6, 646–703.

Mosqueda G, Ramos-Gonzalez MI, Ramos JL (1999) Toluene metabolism by the solvent-tolerant *Pseudomonas putida* DOT-T1 strain, and its role in solvent impermeabilization**.** Gene**,** 232, 69–76

Muraji M, Taniguchi H, Tatebe W, Berg H (1999) Examination of the relationship between parameters to determine electropermeability of *Saccharomyces cerecisiae*. Bioelectrochem Bioenerg 48, 485–488

Murthy MSRC, Swaminathan T, Rakshit SK, Kosugi Y (2000) Statistical optimization of lipase catalyzed hydrolysis of methyl oleate by response surface methodology. Bioproc Bioeng 22, 35–39

Naglak TJ, Bettewar DJ, Wang HY (1990) Chemical Permeabilization of Cells for Intracellular Product Release. Separation Processes in Biotechnol Assenjo, 177-196

Neidhardt FC, Ingraham JL, Schaechter M (1990) Physiology of the bacterial cell. Sinauer Associates, Sunderland, MA

Nikaido H (1994) Prevention of drug access to bacterial targets: permeability barriers and active efflux. Science 264, 382–389

Obayori OS, Ilori MO, Adebusoye SA, Oyetibo GO, Amund OO (2008) Pyrene-degradation potentials of *Pseudomonas* species isolated from polluted tropical soils. W J Microbiol Biotechnol 24, 2639-2646

Olson AC, Gray GM and Guadagni DG (1979) Naringin bitterness of grapefruit juice debittered with naringinase immobilized in a hollow fibre. J Food Sci 44, 1358

Oluwafemi S, Lateef O, Salam B (2010) Degradation of polycyclic aromatic hydrocarbons: Role of plasmids. Sci Res Ess 5, 4093-4106

Ono M, Tosa T and Chibata I (1978) Preparation and properties of immobilized naringinase using tannin aminohexyl cellulose. Agric Biol Chem 42, 1847

Panesar PS, Panesar R, Singh B (2009) Application of response surface methodology in the optimization of process parameters for the production of kinnow wine. Nat Prod Rad 8, 366-373

Parales RE, Bruce NC, Schmid A, Wackett LP (2002) Biodegradation, biotransformation and biocatalysis (B3). Appl Environ Microbiol 68, 4699-4709

Patil BS, Yu J, Dandekar DV, Toledo RT, Singh RK, Pike LM (2006) Citrus bioactive limonoids and flavonoids extraction by supercritical fluids. In Potential health benefits of citrus; Patil BS, Turner ND, Miller ED, Brodbelt JS, Eds, American Chemical Society: Washington DC 936, 18–33

Perez JL, Jayaprakasha GK, Valdivia V, Munoz D, Dandekar DV, Ahmad H, Patil BS (2009) Limonin Methoxylation Influences the Induction of Glutathione S-Transferase and Quinone Reductase. J Agric Food Chem 57, 5279–5286

Perkins JB, Youngman PJ (1986) Construction and properties of Tn*917-lac*, a transposon derivative that mediates transcriptional gene fusions in *Bacillus subtilis*. Proc Natl Acad Sci USA 83, 140–44

Phadtare S, Vinod VP, Wadgaonkar PP, Rao M, Sastry M (2004) Free-standing nano gold membranes as scaffolds for enzyme immobilization. Langmuir 20, 3717–3723

Plessas S, Bekatorou A, Kanellaki M, Psarianos C, Koutinas A (2005) Cells immobilized in a starch–gluten–milk matrix usable for food production. Food Chem 89, 175–179

Polard P, Ton-Hoang B, Haren L, Betermier M, Walczak R, Chandler M (1996) IS*911*-mediated transpositional recombination in vitro. J Mol Biol 264, 68–81

Potumarthi R, Subhaker C, Pavani A (2008) Evaluation of various parameters of calcium alginate immobilization method for enhanced alkaline protease production by *Bacillus licheniformis* NCIM-2042 using statistical methods. Bioresour Technol 99, 1776-1786

Poulose, SM, Harris ED, Patil BS (2005) Citrus Limonoids Induce Apoptosis in Human Neuroblastoma Cells and Have Radical Scavenging Activity, J Nutr 135, 870-877

Premi BR, Lal BB and Joshi VK (1995) Efficacy of various techniques for removing bitter principles in Kinnow juice. J Food Sci Technol 32, 332-335

Premi BR, Lal BB, Joshi VK (1994) Distribution pattern of bittering principles in Kinnow fruit. J Food Sci Technol 31, 140-144

Prescott LM, Harley JP, Klein DA (2002) Microbiol 5th edn McGraw–Hill, New York

Pun A (1984) Preparation and Properties of Citrus Juices, Concentrates and Dried Powders which are reduced in bitterness. U.S. Patent 4439458

Puri M (1993) Immobilized Enzyme Technology for Clarification and Debittering of Citrus Fruit Juice with Special Reference to Kinnows. Ph.D. thesis, Punjabi University, Patiala, India.

Puri M, Kaur L and Marwa SS (2002) Partial Purification and Characterization of Limonate Dehydrogenase from *Rhodococcus facians* for the Degradation of Limonin. J Microbiol Biotechnol 12, 669-673

Puri M, Marwaha SS, Kothari RM, Kennedy JF (1996) Biochemical basis of bitterness in citrus fruit juices and biotech approaches for debittering. Cri Rev Biotechnol 16, 145-155

Raissi S (2009) Developing new processes and optimizing performance using response surface methodology. W Acad Sci Eng Technol 49, 1039–1042

Rathi P, Goswami VK, Sahai V, Gupta R (2002) Response surface methodology for improving production of hyperthermostable lipase from *Burkholderia cepacia*. J Appl Microbiol 93, 930–936

Ratnam BVV, Rao SS, Rao MD, Rao MN, Ayyanna C (2005) Optimization of medium constituents and fermentation conditions for the production of ethanol from palmyra jaggery using response surface methodology. W J Microbiol Biotechnol 21, 399–404

Re R, Pellegrini N, Proteggente A, Pannala A, Yang M, Rice-Evans C (1999) Antioxidant activity applying an improved ABTS radical cation decolorizing assay. Free rad in biol Med 26, 1231-1237

Reznikoff WS (2003) Tn*5* as a model for understanding DNA transposition. Mol Microbiol 47, 1199–1206

Reznikoff WS (2008) Transposon Tn5. Annu Rev Genet 42, 269-286

Rheinwald JG, Chakrabarty AM, Gunsalus IC (1973) A transmissible plasmid controlling camphor oxidation in *Pseudomonas putida.* Proceedings of the National Academy of Sciences of the United States of America 70, 885-889

Ribeiro MHL, Afonso C, Vila-Real HJ, Alfaia AJ, Ferreira L (2010) Contribution of response surface methodology to the modeling of naringin hydrolysis by naringinase Ca- alginate beads under high pressure. LWT Food Sci Technol 43, 482–487

Ribeiro MHL, Silveira D, Ferreira-Dias S (2003) Response surface modelling of the consumption of bitter compounds from orange juice by *Acinetobacter calcoaceticus.* J Mol Catalysis B-Enzymatic 21, 81–88

Rouseff RL, Fisher J F, 1980 Determination of limonin and limonoides in citrus juice by HPLC. Anal Biochem 52, 1228

Rouseff RL. (1990) Bitterness in food products: an overview. In: Rouoseff RL, ed. Bitterness in foods and beverages. Develop in Food Sci 25, Amsterdam: Elsevier, 1–14

S. Gough, M. Deshpande, M. Scher & J.P.N. Rosazza (2001) Permeabilization of *Pichia pastoris* for glycolate oxidase activity. Biotechnol Lett 23, 1535–1537

Sabu A, Kiran GS, Pandey A (2005). Purification and Characterization of Tannin acyl hydrolase from Aspergillus niger ATCC 16620. Food Technol. Biotechnol. 43, 133-138

Saidani M (2003) Cubic millimeter power inductor fabricated in batch-type wafer technology J Microelectromech Syst 12, 172–8

Sambrook J, Russell D (2001) Molecular Cloning A Laboratory Manual, 3rd Edition. Cold Spring Harbor Laboratory Press

Sanseverino J, Applegate BM, King JMH, Sayler GS (1993) Plasmid mediated mineralization of naphthalene phenanthrene and anthracene. Appl Environ Microbiol 59, 1931-1937

Sawabe A, Morita M, Kiso T, Kishine H, Ohtsubo Y, Minematsu T, Matsubara Y, Okamoto T (1999) Isolation and characterization of new limonoid glycosides from Citrus unshiu peels. Carbohydr Res 315, 142–147

Scopes, Robert K, Protein purification: Principles and practice, 1987, Springer-Verlag (New York), 2nd edition, 329

Shaw PE, Tatum JH and Wilson CW (1984) Improved flavour of navel orange and grapefruit juices by removal of bitter component with cyclodentrin polymer. J Agric Food Chem 32, 832

Shaw PE, Wilson CW (1983) Debittering citrus juices with P-cyclodextrin polymer. J Food Sci 48, 646-451

Shevchenko Y, Bouffard GG, Butterfield YS, Blakesley RW, Hartley JL, et al (2002) Systematic sequencing of cDNA clones using the transposon Tn*5*. Nucleic Acids Res 30, 2469–2477

Shinjoh M, Tomiyama N, Asakura A, Hoshino T (1995) Cloning and nucleotide sequencing of the membrane-bound L-sorbosone dehydrogenase gene of *Acetobacter liquefaciens* IFO 12258 and its expression in *Gluconobacter oxydans*. Appl Environ Microbiol 61**,** 413–420

Silveira MM, Jonas R (2002) The biotechnological production of sorbitol. Appl Microbiol Biotechnol 59, 400–409

Simon MJ, Osslund TD, Saunders R, Ensley BD, Suggs S, Harcourt A, Suen WC, Cruden DL, Gibson DT, Zylstra GJ (1993) Sequence of genes encoding naphthalene dioxygenase in *Pseudomonas putida* strains G7 and NCIB 9816–4. Gene 127, 31-37

Singh AK, Bhattacharyya PM, Pakrasi HB (2008) Identification of an Atypical Membrane Protein Involved in the Formation of Potein Disulfide Bonds in Oxygenic Photosynthetic Organisms. J Biol Chem 283, 15762-15770

Singh AK, Elvitigala T, Bhattacharyya PM, Aurora R, Ghosh B, Pakrasi HB (2008) Integration of Carbon and Nitrogen Metabolism with Energy Production is Crucial to Light Acclimation in the *Cyanobacterium Synechocystis*. Plant Physiol 148, 467-478

Siso MIG, Cerdan E, Picos MAF, Ramil E, Belmonte ER, Torres AR (1992) Permeabilization of *Kluyveromyces lactis cells* for milk whey saccharification: a comparison of different treatments. Biotechnol Tech 6, 289-393

Soares NFF, Hotchkiss, JHN (1998) Aringinase Immobilization in Packaging Films for Reducing Naringin Concentration in Grapefruit Juice. J Food Sci 63-71

Sonawane AM, Singh B, Rohm KH (2006) The AauR–AauS Two-Component System Regulates Uptake and Metabolism of Acidic Amino Acids in *Pseudomonas putida*. Appl Environ Microbiol 72, 6569–6577

Steinbuchel A (2001**)** Perspectives for biotechnological production and utilization of biopolymers: metabolic engineering of polyhydroxyalkanoate biosynthesis pathways as a successful example. Macromol Biosci 1, 1–24

Suhayda CG, Omura, M, Hasegawa S (1995) Limonoate dehydrogenase from *Arthrobacter globiformis*: Characteristics of the Native Enzyme and its N-terminal Sequence. *Phytochem.* 40, 17–20

Sun C, Chen K, Chen Y, Chen Q (2005) Contents and antioxidant capacity of limonin and nomilin in different tissues of citrus fruit of four cultivars during fruit growth and maturation. Food Chem 93, 599-605

Swaisgood HE (1991) Immobilized Enzymes: Application to Bioprocessing of Food. Food Enzymol 2, 309-341

Taghvaei M, Khezre-Barati S, Jalilv F, Nemat-Gorgani M (2000) Adsorptive immobilization of erythrocyte membrane. J Biotechnol 81, 107–112

Tang YW, Ellis NM, Hopkins MK, Dodge DE, Persing DH (1998) Comparison of Phenotypic and Genotypic Techniques of Identification of Unusual Aerobic Pathogenic Gram Negative Bacilli. J Clini Microbiol 3674-3679

Tapingkae W, Parkin KL, Tanasupawat S, Kruenate J, Benjakul S, Visessanguan W (2010) Whole cell immobilisation of *Natrinema gari* BCC 24369 for histamine degradation. Food Chem 120, 842-849

Tian QG, Miller EG, Ahmad H, Tang LL, Patil BS (2001) Differential inhibition of human cancer cell proliferation by citrus limonoids. Nutri Cancer-An Int J, 40, 180–184

Timmis K (2001) *Pseudomonas putida* :a cosmopolitan par excellence. Environ Microbiol 4, 779-781

Tremblay J, Deziel J (2010) Gene Expression in *Pseudomonas aeruginosa* Swarming Motility. BMC Genomics 11, 587-593

Tsen HW, Tsai SY and Yu GJ (1989) Fibre entrapment of naringinase from Penicillium sp. and application to fruit juice debittering. J Ferm Technol 67, 186-193

Tsen HY **(**1984) Factors affecting the inactivation of naringinase immobilized on chitin during debittering of fruit juice. J Ferm Technol 62, 263-275

Tsen HY and Yu GK (1991) Limonin and naringin removal from grapefruit juice with naringinase entrapped in cellulose macetate fibres. J Food Sci 56, 31-38

Upadhya R, Nagajyothi, Bhat SG (2000) Stabilization of D-amino caid oxidase and catalase in permeabilized *Rhodotorula gracilis* cells and its application for the preparation of α-ketoacids. Biotechnol Bioeng 68, 430–436

Vaara M (1993) Antibiotic-supersusceptible mutants of *Escherichia coli* and *Salmonella typhimurium*. Antimicrob Agents Chemother 37, 2255–2260

Vaara M, Nurminen M (1999) Outer membrane permeability barrier in *Escherichia coli* mutants that are defective in the late acyltransferases of lipid A biosynthesis. Antimicrob Agents Chemother 43, 1459–1462

Vaks B, Lifshitz A (1981) Debittering of Orange juice by bacteria which degrade limonin. J Agric Food Chem 29, 1258-1261

Valley LB, Ulmer DD (1972) Biochemical Effects of Mercury, Cadmium and Lead Ann Rev Biochem 41, 91–128

Van der Werf MJ, Hartmans S, Van den Tweel WJJ (1995) Permeabilization and lysis of *Pseudomonas pseudoalcaligenes* cells by triton X-100 for efficient production of D-matate. Appl Microbiol Biotechnol 43, 590–594

Venil CK, Nanthakumar K, Karthikeyan K, Lakshmanaperumalsamy P (2009) Production of L-asparaginase by *Serratia marcescens* SB08: Optimization by Response Surface Methodology. Iranian J. Biotechnol 7, 10–18

Verma JP, Singh S, Shrivastava PK, Ghosh M (2010) Identification and characterization of cellular locus of limonin biotransforming enzyme in *Pseudomonas putida*. Int. J Food Sci. Tech. 45, 319-326

Wackett LP, Hershberger LCD (2001) Biocatalysis and biodegradation: microbial transformation of organic compounds. ASM Press Washington

Wagner CJ, Wilson CW and Shaw PE (1988) Reduction of grapefruit bitter components in a fluidized P-cyclodextrin polymer bed. J Food Sci 53, 516-521

Wethern M (1991) Citrus debittering with ultrafiltration/adsorption combined technology. Trans Citrus Eng Con5 ASME 37, 48-54

Widmer WW (1991) Improvements in the quantitation of limonin in citrus juice by reversed-phase HPLC. J Agric Food Chem 39, 1472-1477

Williams PA, Murray K (1974) Metabolism of benzoate and the methylbenzoates by *Pseudomonas putida* (arvilla) mt-2: evidence of the existence of TOL plasmid. J Bacteriol 120, 416-423

Wouters PC, Bos AP, Ueckert J (2001) Membrane permeabilization in relation to inactivation kinetics of *Lactobacillus* species due to pulsed electric fields. Appl Environ Microbiol 67:3092–3101

Xin C, Yin L, Guocheng D, Jian C (2005) Application of response surface methodology in medium optimization for spore production of *Coniothyrium minitans* in solid state fermentation. W J Microbiol Biotechnol 21, 593–599

Yaks B and Lifshitz A (1981) Debittering of orange juice by bacteria which degrade limonin. J Agric Food Chem 29, 1258-1261

Yang RYK, Bayraktar O, Pu HT (2003) Plant-cell bioreactors with simultaneous electro permeabilization and electrophoresis. J Biotechnol 100, 13–22

Yee TW, Prabhu NG, Jain K, Ibrahi D (2011) Process Parameters Influencing Tannase Production by *Aspergillus niger* Using Mangrove (*Rhizophora apiculata*) Bark in Solid Substrate Fermentation. African J Biotechnol 61, 13147-13154

Yen KM, Gunsalus IC (1985) Regulation of naphthalene catabolic plasmid NAH7. J Bacteriol 162, 1008-1013

Yen KM, Serdar CM (1988) Genetics of naphthalene catabolism in *Pseudomonads*. Crit Rev Microbiol 15, 247-268

Zhang S, Wang Z, Wang T, Zheng N, Li M, Lin J (2012) Optimization of central composite design-response surface methodology in ultra high pressure extraction of *Scutellaria baicalensis*. J Medi Plants Res 6, 373-378

APPENDIX I

MEDIUM COMPOSITION

1. ***Luria-Bertani (LB) medium****

Composition	Quantity (gL^{-1})
NaCl	10.0
Beef extract	5.0
Tryptone	10.0
Agar	10.0

2. ***M63 Minimal Media****

Composition	Quantity (gL^{-1})
KH_2PO_4	13 g/mL
$(NH_4)_2SO_4$	1 g/mL
$FeSO_4$	0.00005gm/mL
Adjust pH 7.2 by 1N KOH	
$MgSO_4$	1mM

3. ***LB plates with ampicillin/IPTG/X-Gal****

Make the LB plates with ampicillin as above; 100 µl of 100 mM IPTG and 20µl of 50 mg/ml X-Gal may be spread over the surface of an LB ampicillin plate and allowed to absorb for 30 minutes at 37°C prior to use

BUFFERS AND SOLUTIONS

1. *TBE buffer (10X)*

Tris-HCl	0.09 M (pH 8)
Boric acid	0.9 M
EDTA	0.02 M (pH 8)

2. *Citrate buffer (0.1M), pH 5.5*

Citric acid (0.2 M)	116.25 mL
Sodium citrate (0.2 M)	383.75 mL
Diluted to 1 L with distilled water and store 2^oC-8^oC	

3. *0.1M Phosphate buffer*

Monobasic sodium phosphate (1M)	61.5 mL
Dibasic sodium phosphate (1M)	38.5 mL
Dilute to 1 L with distilled water	

4. *Agarose gel loading dye (6X)*

Bromophenol blue	0.25%
Xylene cyanol FF	0.25%
Glycerol in water	30.0%

*Sterilized by autoclaving at 15 lbs pressure ($121^{\circ}C$) for 15 min.

5. ***Ethidium Bromide*** 0.5µg mL^{-1}

6. ***SSC 20X***

NaCl	3M
Sodium citrate	0.3 M (pH 7)

7. ***Wash buffer I***

2X SSC	
SDS	0.1%

8. ***Wash buffer II***

1X SSC	
SDS	0.1%

9. ***TE buffer 10X***

Tris-HCl	0.1 M (pH 8)
Na2EDTA	10 M (pH 8)

10. ***4x Separating gel buffer (1.5M Tris, pH 8.8)***

Tris	3g
Distilled water	100ml

11. ***4x Stacking gel buffer (0.5M Tris, pH 6.8)***

Tris	18.15g
Distilled water	100ml

12. ***2x Sample buffer***

Tris (0.5M, pH 6.8)	2.5ml
SDS (10%)	4.0ml
Glycerol (100%)	2.0ml
β-mercaptoethanol	0.8ml
Bromophenol blue (0.1%)	300µl
Distilled water (400µl)	to 10ml

13. ***Tank buffer***

Tris	6.05g
Glycine	28.80g
SDS	1.0g
Distilled water	1000ml

14. ***Genomic DNA Extraction buffer***

Sodium acetate	100 mM
Na_2EDTA	50 mM
NaCl	500 mM
SDS	1%

15. ***STET Buffer***

Sucrose	8.0% (w/v)
TritonX	100 - 0.5% (w/v)
EDTA	50.0 mM (pH 8.0)
Tris HCl	10.0 mM (pH 8.0)

16. ***E-buffer***

Tris acetate	50mM (pH 8.0)

17. ***Lysis buffer***

SDS	3%
Tris	50mM
pH was adjusted to 12.0 using 1M NaOH	

REAGENTS

1. ***Phenol Sulfuric acid solution***

Phenol	5%
Sulfuric acid (reagent grade)	96%
Sugar standards (reagent grade)	1 mg mL^{-1}

2. ***Plasmid extraction solution I (10X)***

Tris-HCl	25 mM (pH 8.0)
Glucose	50 mM
Na_2EDTA	10mM

3. ***Plasmid extraction solution II***

NaOH	5M
SDS	10%

4. ***Plasmid extraction solution III***

K-acetate	5.0 M (pH 4.5)

5. ***Agarose gel loading dye (6X)***

Bromophenol blue	0.25%
Xylene cyanol FF	0.25%
Glycerol in water	30.0%

6. ***IPTG stock solution (0.1M)***

IPTG	1.2 g

Add steril distilled water to 50 ml final volume. Filter sterilize and store at 4°C

7. ***X-Gal*** 2ml

100 mg 5-bromo-4-chloro-3-indolyl-Dgalactoside dissolve in 2ml N,N´-dimethylformamide. Cover with aluminum foil and store at 20°C

8. ***Plasmid extraction solution I (10X)***

Tris-HCl	25 mM (pH 8.0)
Glucose	50 mM
Na_2EDTA	10mM

9. ***Ribonuclease A***

Stock solution	10mg/ mL
Working solution	10-15 g/mL

Ribonuclease A is prepared in a buffer containing 100mM Tris (pH 8.0) and 15 mM NaCl. To prepare DNAse free RNAse, the solution is boiled for 10 minutes, followed by the slow cooling, then dispensed into aliquots and is stored at -20oC for further use.

10. ***Lysozyme***

Stock solution	10mg/mL
Working solution	300 - 400 mg/mL

Lysozyme was prepared freshly is water.

11. ***Acrylamide-bisacrylamide (30%)***

Acrylamide	29.2g
Bisacrylamide	0.8g
Distilled H_2O	100ml

12. ***SDS (10%)***

SDS	10g
Distilled water	100ml

13. ***Ammonium persulfate (10%)***

Ammonium persulfate	0.1g
Distilled water	1.0ml

14. ***Bromophenol blue (0.1%)***

Bromophenol blue	5mg
Distilled water	5ml

15. ***Staining solution***

Coomassie blue (R-250)	0.3g
Methanol (AR)	80ml
Glacial acetic acid	20ml
Distilled water	100ml

16. ***Destaining solution***

Acetic acid	100ml
Methanol	300ml
Distilled water	to 1L

17. ***Gel storing solution***

Acetic acid	15ml
Distilled water	to 200ml

18. ***Alkaline sodium carbonate solution***

Na_2CO_3	20g/L
NaOH (0.1M)	4g/L

19. ***Copper sulfate – sodium potassium tartarate solution***

$CuSO_4.5\ H_2O$	5g/L
Sodium-potassium tartarate	10g/L

20. ***Ehrlich reagent***

p-diaminobezaldehyde	0.1%
Acetic acid	3ml
Perchloric acid (70%)	2.4ml

21. ***EDTA*** 50.0 mM (pH 8.0)

22. ***Bromophenol blue*** 0.2% (w/v)

23. ***Folin lowry Reagents***

BSA stock solution 1mg/ml

Analytical reagents:

a) 50 ml of 2% sodium carbonate mixed with 50 ml of 0.1 N NaOH solution (0.4 gm in 100 ml distilled water.)

b) 10 ml of 1.56% copper sulphate solution mixed with 10 ml of 2.37% sodium potassium tartarate solution. Prepare analytical reagents by mixing 2 ml of (b) with 100 ml of (a)

c) Folin - Ciocalteau reagent solution (1N) Dilute commercial reagent (2N) with an equal volume of water on the day of use (2 ml of commercial reagent + 2 ml distilled water)

24. ***Bradford Protein Assay Reagents***

Dye stock - Coomassie Blue G (C.I.# 42655) (100 mg) is dissolved in 50 mL of methanol. The solution is added to 100 mL of 85% H_3PO_4, and diluted to 200 mL with water. The solution should be dark red, and have a pH of -0.01. The final reagent concentrations are 0.5 mg/mL Coomassie Blue G, 25% methanol, and 42.5% H_3PO_4. The solution is stable indefinitely in a dark bottle at 4°C.

Assay reagent - The assay reagent is prepared by diluting 1 volume of the dye stock with 4 volumes of distilled H_2O. The solution should appear brown, and have a pH of 1.1. It is stable for weeks in a dark bottle at 4°C.

Protein Standards - Protein standards should be prepared in the same buffer as the samples to be assayed. A convenient standard curve can be made using bovine serum albumin (BSA) with concentrations of 0, 250, 500, 1000, 1500, 2000 µg/mL for the standard assay, and 0, 10, 20, 30, 40, 50 µg/mL for the microassay

27***. Reagents used for total sugars***

(a) 95% Sulphuric acid: 95 ml of concentrated sulphuric acid was mixed with distilled water to make volume 100 ml.

(b) 5% phenol (w/v): it was prepared by dissolving 5 gm of phenol in 60 ml distilled water then volume was made to 100 ml with distilled water

28. **Reagents used for reducing sugars**

(a) Dinitrosalicylic acid (DNS) solution: Ten gram of DNS and 0.5 gm of sodium sulfate were added in 500 ml of 2% sodium hydroxide solution. The solution was allowed to cool, 2 gm of phenol was dissolved in it and final volume was made to 1000 ml, the solution was filtered and stored in dark bottle in refrigerator. (b) Potassium sodium tartarate solution (40%): 40 gm of potassium sodium tartarate was dissolved in distilled water to make its final volume 100 ml, the solution was filtered and stored at room temperature.

Fig. 1 Standard curve of polyphenols. Relationship between gallic acid (mg mL^{-1} equivalents) and absorbance using Folin–Ciocalteu method

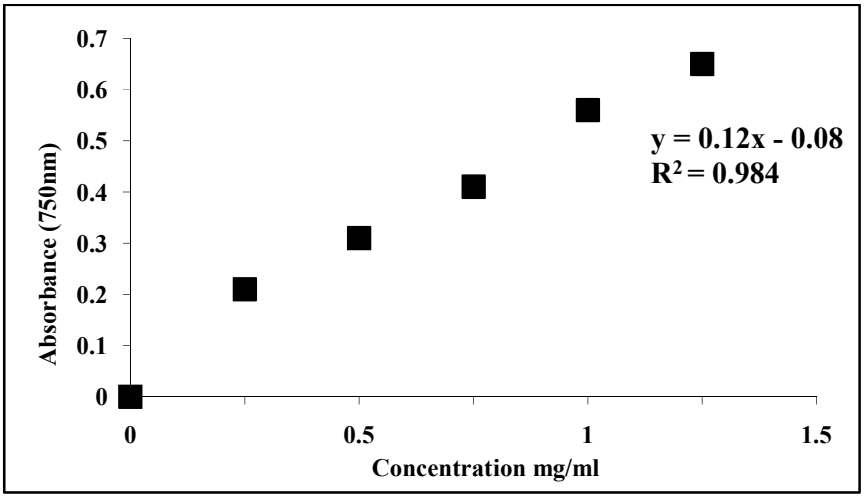

Fig. 2 Standard curve of flavomoids. Relationship between milligrams catechin equivalents (CE) per gram and absorbance using method explained by Dewanto et al. 2002

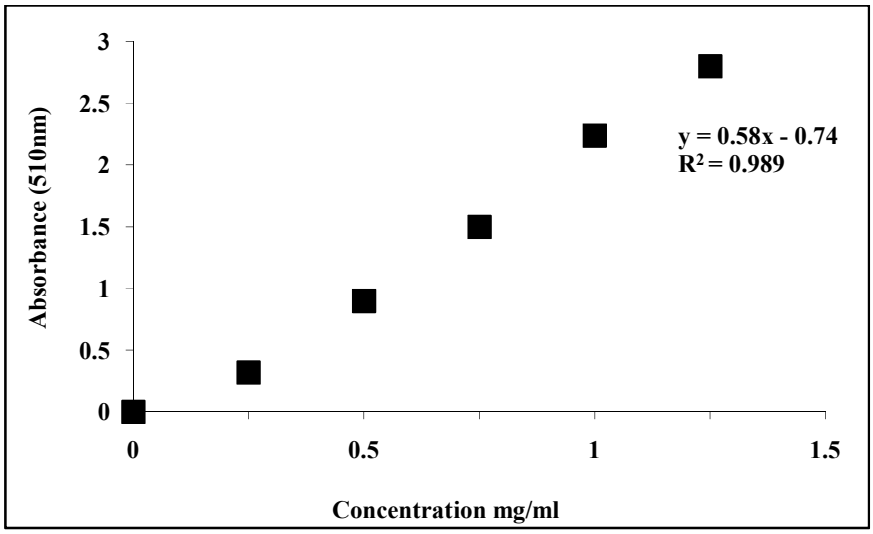

Fig.3 Standard curve of glutamate. Relationship between the concentration of glutamate (nmole) and absorbance at 450 nm was calculated as explained by the glutamate assay kit by Biovision

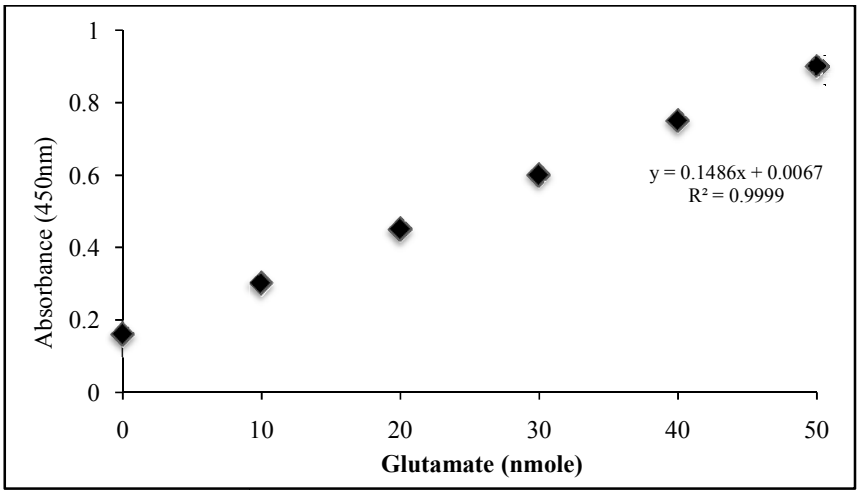

Fig. 4. Standard curve of protein assay. Relationship between protein (as mg bovine serum albumin) and absorbance using the Folin Lowry assay.

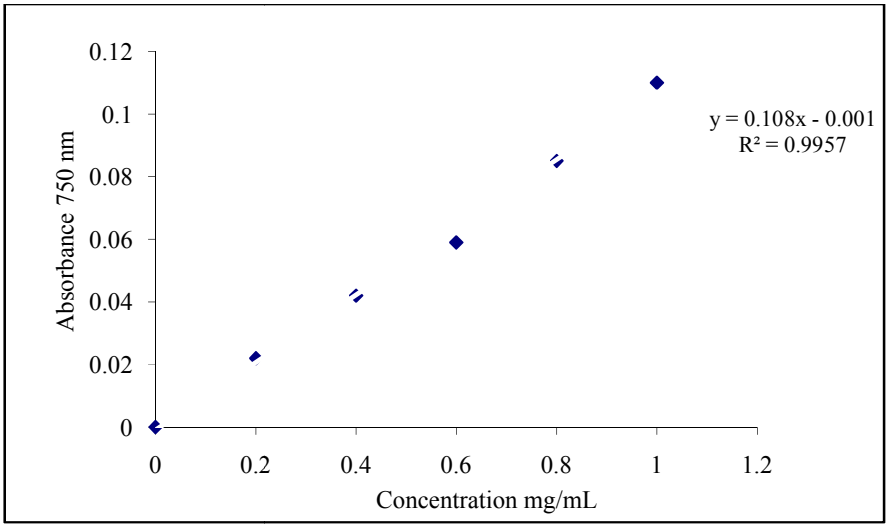

Fig. 5 PGEM-T easy vector map

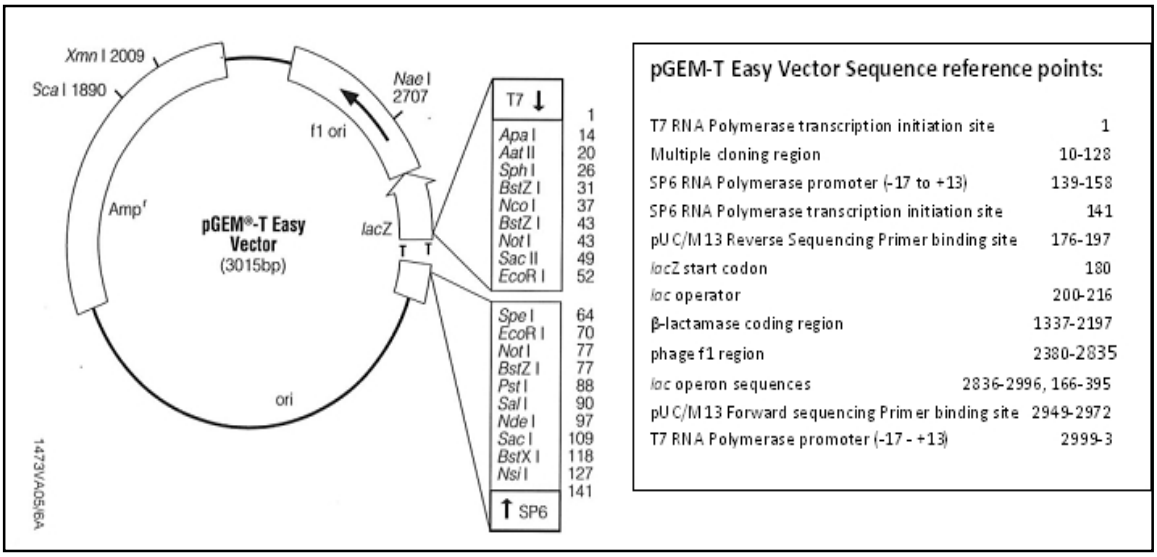

pGEM-T Easy Vector Sequence reference points:

T7 RNA Polymerase transcription initiation site	1
Multiple cloning region	10-128
SP6 RNA Polymerase promoter (-17 to +13)	139-158
SP6 RNA Polymerase transcription initiation site	141
pUC/M13 Reverse Sequencing Primer binding site	176-197
lacZ start codon	180
lac operator	200-216
β-lactamase coding region	1337-2197
phage f1 region	2380-2835
lac operon sequences	2836-2996, 166-395
pUC/M13 Forward sequencing Primer binding site	2949-2972
T7 RNA Polymerase promoter (-17 - +13)	2999-3

P86808 (LMDH_PSEPU) Reviewed, UniProtKB/Swiss-Prot

Last modified December 14, 2011. Version 4.

Names and origin

Protein names	*Recommended name:* **Limonin dehydrogenase** EC=1.2.1.-
Organism	**Pseudomonas putida (Arthrobacter siderocapsulatus)**
Taxonomic identifier	303 [NCBI]
Taxonomic lineage	Bacteria › Proteobacteria › Gammaproteobacteria › Pseudomonadales › Pseudomonadaceae › Pseudomonas

Protein attributes

Sequence length	308 AA.
Sequence status	Fragments.
Protein existence	Evidence at protein level

General annotation (Comments)

Function	Catalyzes the NAD^+-dependent conversion of limonin. Ref.1
Enzyme regulation	Completely inhibited by $HgCl_2$, $CoCl_2$ and $CaCl_2$. Ref.1
Subcellular location	Periplasm Ref.1.
Sequence similarities	Belongs to the aldehyde dehydrogenase family.
Biophysicochemical properties	Kinetic parameters: K_M=4.5 µM for limonin Ref.1 pH dependence: Optimum pH is 8.5. Ref.1 Temperature dependence: Optimum temperature is 35 degrees Celsius. Ref.1

Ontologies

Keywords

Cellular component	Periplasm
Ligand	NAD
Molecular function	Oxidoreductase

Gene Ontology (GO)

Cellular component	periplasmic space Inferred from electronic annotation. Source: UniProtKB-SubCell

Molecular function	nucleotide binding Inferred from electronic annotation. Source: InterPro oxidoreductase activity Inferred from electronic annotation. Source: UniProtKB-KW

Complete GO annotation...

Sequence annotation (Features)

Feature key	Position(s)	Length	Description	Graphical view	Feature identifier
Molecule processing					
Chain	‹1 – ›308	›308	Limonin dehydrogenase		PRO_0000406597
Experimental info					
Non-adjacent residues	14 – 15	2			
Non-adjacent residues	28 – 29	2			
Non-adjacent residues	46 – 47	2			
Non-adjacent residues	63 – 64	2			
Non-adjacent residues	69 – 70	2			
Non-adjacent residues	83 – 84	2			
Non-adjacent residues	94 – 95	2			
Non-adjacent residues	115 – 116	2			
Non-adjacent residues	135 – 136	2			
Non-adjacent residues	151 – 152	2			
Non-adjacent residues	167 – 168	2			
Non-adjacent residues	176 – 177	2			
Non-adjacent residues	189 – 190	2			
Non-adjacent residues	203 – 204	2			
Non-adjacent residues	209 – 210	2			
Non-adjacent residues	216 – 217	2			
Non-adjacent residues	222 – 223	2			
Non-adjacent residues	231 – 232	2			
Non-adjacent residues	243 – 244	2			
Non-adjacent residues	258 – 259	2			
Non-adjacent residues	276 – 277	2			
Non-adjacent residues	291 – 292	2			
Non-adjacent residues	302 – 303	2			
Non-terminal residue	1	1			
Non-terminal residue	308	1			

Sequences

Sequence		Length	Mass (Da)
P86808 [UniParc].	FASTA	308	31,977

Last modified April 5, 2011. Version 1.
Checksum: 1C7D5F7B6E275D66

```
        10         20         30         40         50         60
ALMKTKLFIN NTMASSGIGL ETDAIKAAQA VYCQGQICMS EEQEALCPFD RLEGEVAIVV

        70         80         90        100        110        120
GAGPSERRRL LLKVADVMES KTPKFIEVMA MEVGASALWA GFNVHASANV FREAASLATQ

       130        140        150        160        170        180
IQGTPLGFAV PTEAFEMATP DGTGALNYGV RRPKGVIGVI SPWNLPLLLM TWKVGPALAC

       190        200        210        220        230        240
GNTVVVKPSR INGLFKDAID KGAKVVCGGM AQGAVGVLNY LNRVNAVQPG GTVISLCGPA

       250        260        270        280        290        300
SAGFDIANDS VYGLSSGDDM IKQLTPLGFA AKPEDNVEPY LLGASRKQGK GITTTVISID


GGMALGAG
```

« Hide

References

[1] **"Enhancement of bioconversion of limonin by P.putida G7."**
Ghosh M., Malik M.
Submitted (SEP-2010) to UniProtKB
Cited for: IDENTIFICATION BY MASS SPECTROMETRY, FUNCTION, ENZYME REGULATION, BIOPHYSICOCHEMICAL PROPERTIES, SUBCELLULAR LOCATION.
Strain: ATCC 17485 / DSM 50208 / JCM 6158 / NCIMB 12092 / Stanier 111 / Biotype A.

Cross-references

3D structure databases

ModBase	Search...

Protocols and materials databases

StructuralBiologyKnowledgebase	Search...

Family and domain databases

InterPro	IPR016161. Ald_DH/histidinol_DH. IPR016162. Ald_DH_N.

	IPR015590. Aldehyde_DH_dom. IPR016040. NAD(P)-bd_dom. [Graphical view]
Gene3D	G3DSA:3.40.605.10. Aldehyde_dehydrogenase_N. 1 hit. G3DSA:3.40.50.720. NAD(P)-bd. 1 hit.
Pfam	PF00171. Aldedh. 1 hit. [Graphical view]
SUPFAM	SSF53720. Aldehyde_DH/Histidinol_DH. 1 hit.
PROSITE	PS00070. ALDEHYDE_DEHYDR_CYS. False negative. PS00687. ALDEHYDE_DEHYDR_GLU. False negative. [Graphical view]
ProtoNet	Search...

Entry information

Entry name	LMDH_PSEPU
Accession	Primary (citable) accession number: **P86808**
Entry history	Integrated into UniProtKB/Swiss-Prot: April 5, 2011 Last sequence update: April 5, 2011 Last modified: December 14, 2011 This is version 4 of the entry and version 1 of the sequence. [Complete history]
Entry status	Reviewed (UniProtKB/Swiss-Prot)
Annotation program	Prokaryotic Protein Annotation Program

Relevant documents

SIMILARITY comments
Index of protein domains and families

Nucleotide

Display Settings: GenBank (full)

Pseudomonas putida strain G7 glutamate transporter (gltS) gene, complete cds

GenBank: JQ990989.1

FASTA Graphics

Go to:

```
LOCUS       JQ990989               1206 bp    DNA     linear   BCT 10-SEP-2012
DEFINITION  Pseudomonas putida strain G7 glutamate transporter (gltS) gene,
            complete cds.
ACCESSION   JQ990989
VERSION     JQ990989.1  GI:403071656
KEYWORDS    .
SOURCE      Pseudomonas putida
  ORGANISM  Pseudomonas putida
            Bacteria; Proteobacteria; Gammaproteobacteria; Pseudomonadales;
            Pseudomonadaceae; Pseudomonas.
REFERENCE   1  (bases 1 to 1206)
  AUTHORS   Malik,M. and Ghosh,M.
  TITLE     Gene sequence coding for glutamate transporter (GltS) of
            Pseudomonas putida G7 implicated in limonin uptake
  JOURNAL   Unpublished
REFERENCE   2  (bases 1 to 1206)
  AUTHORS   Malik,M. and Ghosh,M.
  TITLE     Direct Submission
  JOURNAL   Submitted (27-APR-2012) Department of Biotechnology & Environmental
            Sciences, Thapar University, Badson Road, Patiala, Punjab 147004,
            India
FEATURES             Location/Qualifiers
     source          1..1206
                     /organism="Pseudomonas putida"
                     /mol_type="genomic DNA"
                     /strain="G7"
                     /db_xref="taxon:303"
                     /PCR_primers="fwd_seq: ttgaccccaacaccacctcta, rev_seq:
                     agatctcatgctggagttcttcgc"
                     /PCR_primers="fwd_seq: gaccttgcacagatagcgtggtcc, rev_seq:
                     gcagaagttatcatgaacgttacc"
     gene            <1..1206
                     /gene="gltS"
     CDS             1..1206
                     /gene="gltS"
                     /codon_start=1
                     /transl_table=11
                     /product="glutamate transporter"
                     /protein_id="AFR13889.1"
                     /db_xref="GI:403071657"
                     /translation="MFHLDTSATLVPATLTLLLGRKLVHSVSLGKKYTIPEPVAGGKL
                     VALALLVLFFCMGWEVKKDMSLRDPLMLANFATIGLNANIASLRAGGRVVGIFLIVVV
                     GLKVMLFAIGIGMASKLGLDPLGGLLAGSITLPGGHGTGAAWSKLFIERYGFTNATEV
                     AIPCATFFLVLPPLIFGPVARYLVKKSTTPNGIPDDQEVPTPFEKPDVGRMITSLVLI
                     ETIALIAICLTVGKIAAQPLAGTAGELPTFVCVLKVGVILSNGLSIMGKNRVPERAVK
                     MLPNVSLSLFLAMALMGLFLWELASLALPMLAGLVLQTINMALYAIFVTWRMMGFFYD
                     AAVLAAGHCGKGLGATPTAIANMQAITERKGPSHMAGGVVPMVGAFKIDIVNALVIKL
                     YLMLPRGAG"
ORIGIN
        1 atgtttcatc tcgatacttc agcaacgctt gttcccgcaa cgctgacgtt gctgctcggg
       61 cgtaagttgg tccattccgt ctccttgggg aagaaataca ccataccgga acctgttgcg
      121 ggtggaaagt tggtggcgct ggcgctacta gtactgtttt tttgcatggg ctgggaagtc
      181 aaaaaagata tgtccctgcg cgatccctta atgctggcaa acttcgccac cattggcctg
      241 aacgccaaca ttgccagttt gcgtgccggt gggcgtgtgg ttggcatctt cttgattgtg
      301 gttgttggtc tgaaggtgat gctttttgcc attggcattg gtatggctag caagttaggg
      361 cttgatccgc tgggggggct gttggccggt tctattactc tccccggcgg tcacggtacg
      421 ggcgctgcgt ggagtaaatt gttcattgaa cgttatggct tcaccaatgc gacggaagtg
      481 gcgatcccct gtgcaacgtt ttttctggtg ctccccccct tgatttttgg tccggtggcg
      541 cgctatctgg tgaaaaaatc caccacgccg aacggtattc cggatgacca ggaagtcccg
      601 accccgtttg aaaagcccga tgtgggacgc atgatcacct cgttggtgct gattgaaact
      661 atcgcgctga ttgctatctg cctgacggtg gggaaaattg ccgcgcaacc cctggctggc
      721 actgcggggg aactgccgac cttcgtctgt gtactgaaag ttggcgtgat tctgagcaac
      781 ggtctgtcaa taatgggcaa aaaccgcgtc cccgagcgtg cggtaaaaat gctccctaac
      841 gtaagcttgt cgttgttcct ggcgatggcg ttgatggggc tgtttctgtg ggagctggct
      901 tcgctggcgc tgccgatgct ggccggtctg gtcctacaga ccatcaacat ggcgttgtat
      961 gccatcttcg ttacctggcg catgatgggc tttttctacg atgcggcagt gctggctgcg
     1021 ggtcactgtg gaaaaggcct cggtgcaacg ccaacggcaa tcgccaacat gcaggcgatc
     1081 actgaacgca aaggcccgtc gcacatggcg gggggggtgg tgccgatggt cggtgcgttc
     1141 aaaatcgata tcgtcaatgc gctggtaatt aagttgtatt tgatgttgcc gaggggggcc
     1201 ggttaa
//
```

Council of Scientific & Industrial Research
Human Resource Development Group
(CSIR Complex, Opp. Institute of Hotel Management, Library Avenue, Pusa, New Delhi-110012)

ACK. No.: 113175/2K8/2 Dated:
FILE No. :

MEENAKSHI MALIK
DEPARTMENT OF BIOTECHNOLOGY,THAPAR
UNIVERSITY,PATIALA,PUNJAB,INDIA NA
PATIALA-147004

Award Letter

Sir/Madam,

With reference to your application and subsequent interview, I am happy to inform you that you have been selected for the award as per terms stated above. The award will be effective from the date mentioned above or from the date of joining research whichever is later. The duration of CSIR SRF and SRF (Extended) is as extended above.

The duration of the CSIR Research Associateship is one year and any further extension is at the discretion of CSIR, based on a three member Assessment Committee Report & Annual Progress Report. A copy of Terms & Conditions of CSIR Fellowship/ Associateship is available on HRDG website (http://www.csirhrdg.res.in). In case, the terms & conditions are acceptable to you, you may join the Fellowship/Associateship within the validity period and intimate to us.

The Director General, CSIR has also been pleased to sanction the Stipend and Contingency as stated above. In addition to Stipend & Contingency, House Rent Allowance & Medical Benefits will be payable as per rules of the host Institute limited to Central Govt. rates.

Please note that the validity of the award is for six months only from the effective date of award.

The award of CSIR Fellowship / Associateship does not imply any assurance or guarantee to subsequent employment by CSIR.

Yours faithfully,

SECTION OFFICER

Copy to :-

1 Registrar/Principal/Director, with the request to send the following documents to this office.
(A) Joining Report in the enclosed prescribed from.
(B) Undertaking in the enclosed prescribed form and consolidated bill claiming grants in respect of new awardees showing their names, fellowship letter number, date of joining and the amount admissible, in triplicate, as per enclosed bill form.
2. Sr. F&AO (EMR). The expenditure will be debitable to the Budget Head 'P-8I-101'.
3. Bill File.
4. Office Copy.

Appl Microbiol Biotechnol
DOI 10.1007/s00253-012-3880-z

Modeling of permeabilization process in *Pseudomonas putida* G7 for enhanced limonin bioconversion

Meenakshi Malik · Abhijit Ganguli · Moushumi Ghosh

Received: 2 September 2011 / Revised: 27 December 2011 / Accepted: 30 December 2011

Abstract A facile process of enhanced whole cell biotransformation to debitter the triterpenoid limonin in citrus juices was optimized in this work. To maximize bioconversion, permeabilization conditions were modeled using response surface methodology. A central composite rotatable design with four significant variables (concentration, temperature, pH, and treatment time) was employed. The second order polynomial equations with R^2 values above 0.9 showed good correspondence between experimental and predicted values. The concentration, temperature, pH, and treatment time as well as their interactions had significant effects ($p<0.001$) on limonin bioconversion. The optimum operating conditions for permeabilization were observed at a Na_2EDTA concentration of 1.5 μM, treatment time of 15 min, temperature of 28 °C, and pH 8. A maximum reduction of 76.71% in the limonin content was achieved within 150 min under selected conditions. The results are promising for refining permeabilization technique for whole cell biocatalysts thereby improving the debittering of citrus juices significantly.

Keywords Response surface methodology (RSM) · Limonin · Permeabilization · *Pseudomonas putida* G7 · Debittering

Introduction

The occurrence of limonoid aglycone limonin, responsible for bitterness in citrus juices, remains a major impediment for the citrus juice industry worldwide. Biotransformation of limonin for ameliorating bitterness has been unequivocally suggested to be the current method of choice (Puri et al. 2002; Canovas et al. 1998; Hasegawa and Maier 1983; Hasegawa et al. 1985). The applicability of purified enzyme(s) for limonin biotransformation, however, has been largely restricted due to inactivation of enzymes at low juice pH as well as their high cost. Whole cell biocatalysts provide several advantages in this regard and thus may be a feasible option for reducing limonin levels in citrus juices.

Microorganisms have gained renewed attention in recent years for developing a commercial viable debittering strategy in batch, continuous mode and by immobilization (Hasegawa et al. 1972; Hasegawa and Maier 1983; Hasegawa et al. 1985; Canovas et al. 1998), in several matrices. However, none of these processes based on whole cell catalysis were successful for practical purposes. The possible reason being diffusional restriction or the permeability barrier of cell envelope for substrates and or products that often results in low reaction rates when whole cells are used (Babu et al. 1991).

Reduction in the permeability barrier has been suggested to enhance the effectiveness of whole cell biocatalysts (Kondo et al. 2000). Perforation of cellular membrane (permeabilization) might ease and alleviate the permeability barrier to allow the free movement of substances across the cell envelope and produce high and stable enzymatic activities of the whole cell. The permeabilized microbial cells retain their inner organization, as well as cofactors necessary for functioning of several enzymes (Hewtter and Wang 1986; Felix 1982; Cheng et al. 2006; Siso et al. 1992).Various agents and methods like treatments with organic solvents, detergents, salt, enzymes, chemicals, and electropermeabilization have been described to permeabilize the bacterial whole cells (Chen 2007; Geckil et al. 2005; Cheng et al. 2006; Gough et al. 2001). However, the permeabilization

M. Malik · A. Ganguli · M. Ghosh (✉)
Department of Biotechnology and Environmental Sciences,
Thapar University,
Patiala 147004, Punjab, India
e-mail: mghosh@thapar.edu

parameters should be optimized to achieve high bioconversion efficiency. Response surface methodology (RSM) is an effective and widely used statistical modeling approach for studying the mutual interactions among the variables over a range of values in a statistically valid manner and optimization of multiple variables in order to predict the best performance conditions with a minimum number of experiments. These designs are used to find improved or optimal process settings (Gonzalez-Saiz and Pizarro 2001; Melo et al. 2005; Mundra et al. 2007; Potumarthi et al. 2008; Prakash et al. 2008; Senthilkumar et al. 2008; Liu et al. 2010; Mizumoto and Shoda 2007; Myers and Montgomery 2002).

Our earlier studies reported the ability of a *Pseudomonas putida* G7 to biotransform limonin (Ghosh et al. 2006) by virtue of a periplasmically located dehydrogenase which converts limonin to nonbitter derivatives (Verma et al. 2010). Recently, we reported that permeabilization could improve the limonin bioconversion potential of *P. putida* (Malik et al. 2011). This study aims to optimize the permeabilization process parameters of *P. putida* G7 by employing RSM, for maximizing the bioconversion of limonin.

Materials and methods

Chemicals and reagents

Standard limonin and protease (EC number 232-752-2, product number P5459, 7–15 units/mg protein) were purchased from Sigma (Sigma, MO, USA). Acetonitrile and other solvents were of HPLC and analytical grade, respectively, and were purchased from Merck (E. Merck, Darmstadt, Germany).

Microorganism and culture medium

Freeze-dried culture of *P. putida* G7 (MTCC 1658) was procured from microbial type culture collection and gene bank, Institute of Microbial Technology, Chandigarh, India. The nutrient medium for *P. putida* G7 was Luria–Bertani broth and mineral minimal medium (M63) supplemented with 0.5% limonin as carbon source. The strain was grown with shaking at 150 rpm at 30 °C. The revived culture was grown to log phase and was then used for limonin bioconversion.

Limonin bioconversion assay

Aliquots of the culture were aseptically withdrawn at a regular interval of every 1 h for up to 72 h. The aliquots were centrifuged at 10,000 rpm for 2 min at 4 °C; the pellets were resuspended in 1 ml of saline (0.85% NaCl), and the optical density was recorded at a wavelength of 600 nm. Residual limonin was estimated before and after biotransformation experiments by Vaks and Lifshitz (1981). Briefly, to 1 ml chloroform extract was added 1.5 ml Ehrlich reagent (0.1 g *p*-dimethylaminobenzaldehyde, 3 ml acetic acid, 2.4 ml 70% perchloric acid); the solutions were mixed vigorously and allowed to stand for 15–20 min. Absorbance of the red colored upper layer was taken at 503 nm. The absorbances were recorded spectrophotometrically (Hitachi U-2800, Japan). The limonin content in the juice serum was determined thereafter from a standard curve prepared by using standard limonin.

Permeabilization of whole cells of *P. putida* G7

For permeabilization, the method of Cheng et al. (2006) was followed with minor modifications. Log phase bacterial culture was centrifuged at 8,000 rpm for 10 min at 4 °C, washed with phosphate buffer (pH 7.0, 50 mM), and treated with lysozyme (100 μg/ml) at room temperature. The cells (~6 log CFU/ml) were centrifuged; pellet resuspended in 1.0 ml of phosphate buffer (pH 7.0, 50 mM) and subsequently treated with various permeabilizing agents viz 2% of the different organic solvents (toluene, chloroform, benzene, hexane), 1% of the detergents (CTAB, SDS, Triton X-100), besides protease (2 mM), and Na_2EDTA (ranging from 1–2 μM) were used separately in different experimental sets. The treatment time was varied between 10–30 min at variable temperatures of 20–37 °C. The treated cells were evaluated for limonin bioconversion activity in both model solutions viz the standard limonin solution and limonin present in citrus juice. The supernatant was also examined for limonin bioconversion activity. The storage stability of the permeabilized cells was determined by incubating them in sterile phosphate buffer (pH 7.0, 50 mM), at room temperature as well as at 4 °C, for a period of 30 days. Aliquots were removed at regular time intervals, washed with sterile saline, suspended in phosphate buffer, and assayed for limonin bioconversion activity. The viability of the cells was also examined by plating the diluted cells suspensions on Luria agar and minimal medium with limonin (0.5 gm/l) as the carbon source, before and after cell permeabilization, and was incubated at 30 °C for 48 h. The variation in the colony morphology was also monitored.

Optimization experiment design

RSM with central composite rotatable design (CCRD) was engaged to screen and determines the optimum levels of the significant parameters for permeabilization. The effect of the four independent variables, Na_2EDTA concentration, pH, temperature, and time duration, for the permeabilization of *P. putida* G7 cells was studied at five different levels (−2, −1, 0, +1, +2) (Table 1). The experimental trials were generated using statistical software Design-Expert Version 6.0.10 (Stat-

Table 1 Levels of variables tested in CCRD

	Variables	Coded levels				
		−2	−1	0	+1	+2
A	Na_2EDTA (μM)	0.5	1	1.5	2	2.5
B	Time duration (min)	5	10	15	20	25
C	Temperature (°C)	12	20	28	36	45
D	pH	2	5.0	8.0	9.0	12

Ease, Minneapolis, MN) using CCRD to augment experimental data with enough points to fit into a polynomial model. To examine the combined effect of the independent variables on limonin biotransformation, a factorial CCRD of $2^4=16+6$ six central points and eight star points leading to a total number of 30 experiments was employed (Table 2). The general form of the second degree polynomial equation is

$$Y_i = \beta_o + \sum \beta_i X_i + \sum \beta_{ii} X_i^2 + \sum \beta_{ij} X_i X_j$$

where Y_i is the response variable, X_iX_j are input variables which influence the response variable Y, β_o is the interception coefficient, β_i is the ith linear coefficient, β_{ii} is the ith quadratic coefficient, and β_{ij} is the ijth interaction coefficient. Regression analysis was performed on the data obtained from the design experiments in duplicate, followed by the calculation of second order polynomial coefficients to estimate the responses of the dependent variable (Y). F test was employed to evaluate the statistical significance of the quadratic

Table 2 Design matrix prepared using CCRD of RSM

Runs	Coded values				Limonin bioconversion (%)	
Runs	A	B	C	D	Actual value	Predicted value
1	1.00	−1.00	−1.00	−1.00	67.19	67.63
2	0.00	0.00	0.00	0.00	76.71	75.82
3	−1.00	−1.00	1.00	−1.00	65.72	66.41
4	−2.00	0.00	0.00	0.00	68.66	68.86
5	−1.00	−1.00	1.00	1.00	69.42	69.49
6	2.00	0.00	0.00	0.00	70.89	70.72
7	0.00	0.00	0.00	0.00	76.71	75.82
8	−1.00	1.00	−1.00	1.00	72.36	71.94
9	1.00	−1.00	1.00	1.00	70.02	69.99
10	0.00	−2.00	0.00	0.00	71.49	71.22
11	0.00	0.00	0.00	0.00	76.71	75.82
12	0.00	0.00	0.00	2.00	72.96	72.44
13	0.00	0.00	0.00	0.00	76.71	75.82
14	0.00	0.00	0.00	0.00	76.71	75.82
15	−1.00	1.00	1.00	1.00	75.19	74.30
16	1.00	−1.00	1.00	−1.00	76.66	75.52
17	−1.00	−1.00	−1.00	1.00	69.71	69.66
18	−1.00	1.00	−1.00	−1.00	71.18	72.11
19	1.00	1.00	−1.00	1.00	69.71	69.66
20	0.00	2.00	0.00	0.00	71.18	72.11
21	0.00	0.00	0.00	0.00	76.71	75.82
22	−1.00	1.00	1.00	−1.00	71.95	73.62
23	0.00	0.00	2.00	0.00	68.98	67.98
24	1.00	−1.00	−1.00	1.00	71.13	71.13
25	−1.00	−1.00	−1.00	−1.00	70.31	70.31
26	1.00	1.00	1.00	−1.00	71.13	71.13
27	1.00	1.00	−1.00	−1.00	70.31	70.31
28	0.00	0.00	−2.00	0.00	70.31	70.31
29	0.00	0.00	0.00	−2.00	70.11	70.11
30	1.00	1.00	1.00	1.00	71.13	71.13

A, B, C, D are the coded values for the significant variables—Na_2EDTA concentration, time duration, temperature, and pH, respectively. All the responses in the 30 runs were performed in triplicates. The calculated values were significant ($p<0.001$)

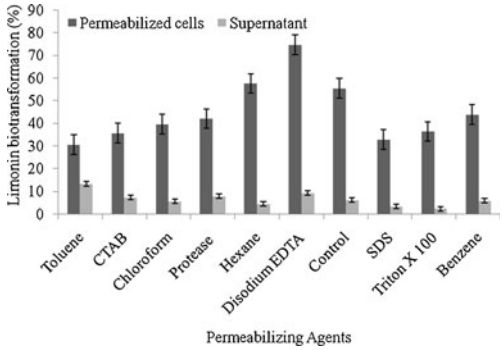

Fig. 1 Evaluation of the performance of different permeabilizing agents on the reduction in limonin by *P. putida* G7. Results are the mean of three independent replicates; (*dark gray square*) permeabilized cells, (*light gray square*) supernatant

polynomial. The performance of the regression equation was evaluated by determining the multiple coefficients of correlation R and the determination coefficient of correlation R^2. The response surface plots were used for determining the optimum level of the significant variables for maximal limonin bioconversion.

Entrapment of permeabilized cells

Dialysis tubing (Sigma, MO, USA) was washed in sterile triple-distilled water and clipped at one end to produce a sac. The permeabilized cells (1 g) were washed in phosphate buffer and were dialysis sac. The sac was tied at the upper end with string and submerged completely in a beaker containing 250 ml of model solutions where either the minimal media with limonin (50 ppm) as substrate or the citrus juice containing equivalent amounts of limonin was used.

HPLC analysis

Limonin determination was carried out using an HPLC system 10AVP (Shimadzu) equipped with a Nova-Pak C18 column (250×4.6 mm, 5-μm particle size, 100-Å unit pore size), a CLASS-VP software (Japan), and a UV visible detector. The mobile phase used for the assay was acetonitrile/deionized water (32:68) with a flow rate of 0.9 ml/min and an injection volume of 20 μl. The Nova-Pak C18 column was conditioned (rinsed) with 2 ml acetonitrile and 5 ml deionized water (17.5:65) with a flow rate of 0.5 ml/min and an injection volume of 5 μl. The samples collected from the experiments were filtered through a 0.45-μm Nylon filter (Waters, Milford, MA) and injected into the HPLC system. The cartridge was rinsed with 2.5 ml deionized water and 2.5 ml acetonitrile, and permeates were collected in small glass vials. The detection wavelength was 207 nm. The retention time of the working standards was used as an indicator to compare it with those of the unknown. The isocratic elution was performed as mobile phase composition remained constant throughout the procedure.

Statistical analysis

All experiments were carried out in triplicate. The data analyses were performed using Design-Expert Version 7.0 (Stat-Ease Inc., Minneapolis, MN). Treatment effect was analyzed using analysis of variance and Duncan multiple range test. Differences were considered to be significant at $p<0.05$ throughout the present study. Each point is the mean of replicate experiments.

Table 3 ANOVA of the experimental results of the central composite design (quadratic model)

Variables	Coefficient estimation	Sum of square	Standard error	*df*	*F* value	*p* value
Model	76.71	1245.25	0.078	17	11.58	0.001
A	0.61	23.36	0.014	1	1.098	0.032
B	0.62	24.51	0.014	1	1.083	0.025
C	1.55	41.28	0.014	1	3.078	0.013
D	1.78	42.64	0.014	1	4.002	0.125
AB	0.060	7.39	0.017	1	0.003	0.004
AC	0.078	8.91	0.017	1	0.004	0.012
AD	3.44	215.78	0.017	1	6.005	0.022
BC	0.098	9.36	0.017	1	0.007	0.009
BD	3.43	211.57	0.017	1	5.005	0.006
CD	3.39	201.38	0.017	1	5.006	0.007
A^2	0.14	17.56	0.010	1	1.030	0.153
B^2	0.14	17.56	0.010	1	1.030	0.318
C^2	0.058	21.56	0.010	1	1.007	0.125
D^2	0.32	19.89	0.010	1	0.810	0.431

A, B, C, D are the coded values for the significant variables—Na_2EDTA concentration, time duration, temperature, and pH, respectively

Results

For whole cell permeabilization, the concentrations of various permeabilizing agents that were optimized to achieve permeabilization were 2% for the organic solvents (toluene, chloroform, benzene, hexane), 1% for the detergents (CTAB, SDS, Triton X-100), 2 mM proteases, and 1–2 μM Na_2EDTA. A comparative study of their efficiency revealed that Na_2EDTA could permeabilize the *P. putida* G7 cells most efficiently amongst them (Fig. 1). It was speculated that the bioconversion efficiency may be impacted by the concentration of the permeabilizing agent, treatment time, pH, and temperature. Thus, optimization studies of permeabilization conditions were performed with Na_2EDTA. The permeabilized cells retained stability for up to 40 °C and pH 8.0 for 30 days (data not shown). The cells did not show any significant loss of the enzymatic activity when stored in sterile phosphate buffer (pH 7.0, 50 mM), distilled water, and tap water at room temperature as well as at 4 °C, for a period of 30 days.

Response surface modeling for maximum limonin bioconversion

RSM with CCRD was chosen to optimize the significant variables (Na_2EDTA concentration, pH, time duration, and temperature) for permeabilization of *P. putida* G7 cells. The coded levels for independent variables are presented in Table 1. The mean predicted and experimental bioconversion activity are presented as a response, as detected by central composite rotatable design experiments (Table 2). The analysis of variance (ANOVA) results demonstrate that the regression is highly significant (at 99% confidence level) and presents an excellent determination coefficient (R^2=0.904). This meant that 90.4% variability in the observed data could be explained by polynomial equation. The second order regression equation obtained after the ANOVA provided the levels of bioconversion activity as a function of values of the Na_2EDTA (1.5 μM) for time duration (15 min) at temperature (28 °C) and pH (8.0) (Table 3). The final estimative response model equation in terms of limonin bioconversion (Y) was

Limonin bioconversion

$$(Y) = +76.71 + 0.61 \times A + 0.62 \times B + 1.55 \times C + 1.78 \times D + 0.060 \times A \times B + 0.078 \times A \times C + 3.44 \times A \times D + 0.098 \times B \times C + 3.43 \times B \times D + 3.39 \times C \times D + 0.14 \times A^2 + 0.14 \times B^2 + 0.058 \times C^2 + 0.32 \times D^2$$

where A, B, C, and D are the coded values for Na_2EDTA (A), time duration (B), temperature (C), and pH (D).

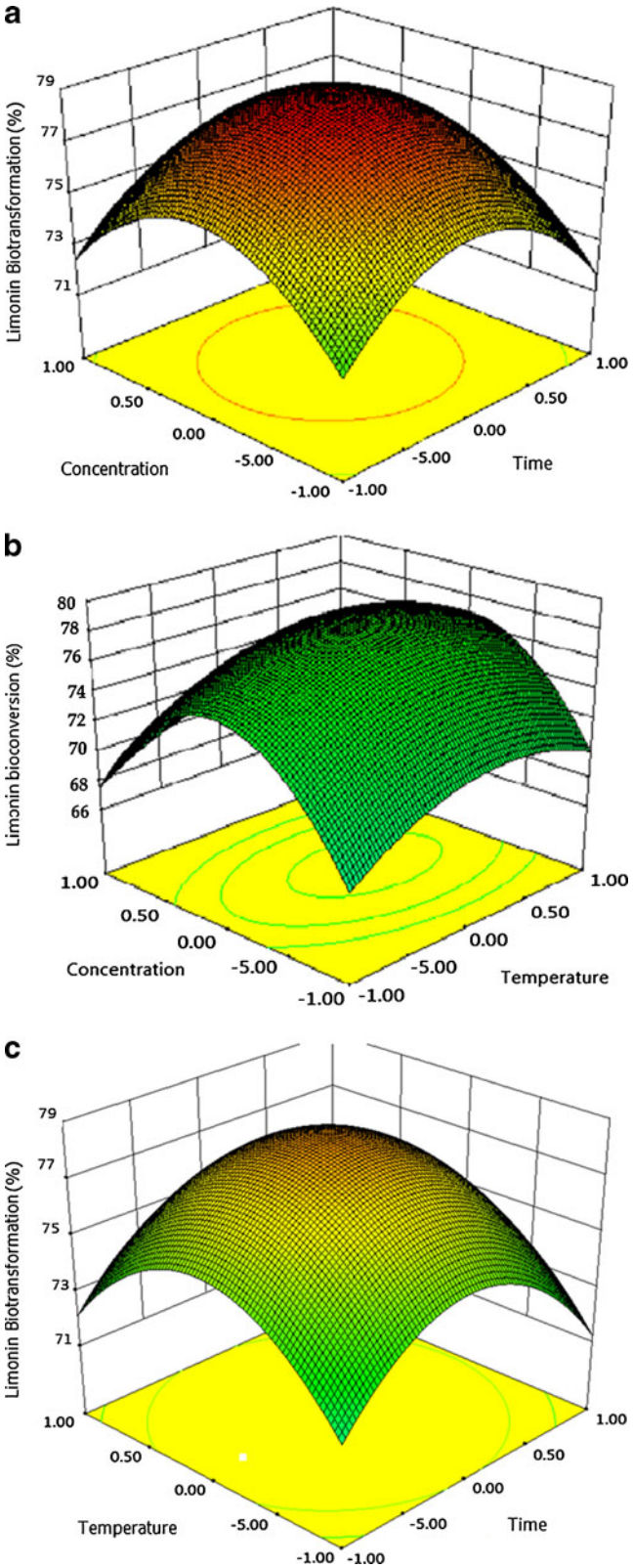

Fig. 2 **a**–**c** Response surface plots showing the combined effects of the significant variables in terms of limonin bioconversion. **a** Interaction effect between concentration and time, **b** interaction effect between concentration and temperature, and **c** interaction effect between time versus temperature

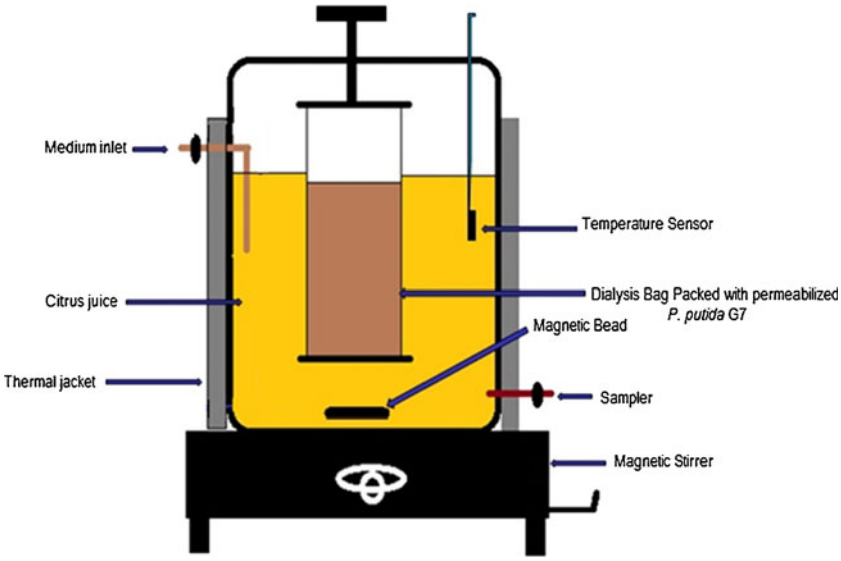

Fig. 3 A dialysis setup for entrapped permeabilized *P. putida* G7 cells

According to ANOVA, the model for activity of limonin biotransformation indicates that the *F* value of 11.58 and values of "Prob>*F*" less than 0.0500 infer that the model was significant. The R^2 value of 0.904, closer to 1, denotes a very high significance of the model. A higher reliability of the experiment is usually indicated by lower value of coefficient of variation (CV), i.e., 1.65 which indicates that the experiments performed were reliable. The "Adequate Precision" measures the signal to noise ratio, and a ratio greater than four is desirable. The ratio of 14.118 indicates an adequate signal and indicates that this model can be used to navigate the design space. The obtained responses from the CCRD were fitted to a second order polynomial equation to explain the dependence of catalysis of limonin on the optimization of the significant variables for permeabilization of *P. putida* G7 (Fig. 2a–c). As shown in Fig. 2a, the highest value of limonin bioconversion activity was obtained when the cells were exposed to a concentration of 1.5 μm Na_2EDTA for 15 min. The optimum operating conditions of temperature and pH (data not shown) for effective permeabilization was 28 °C and 8, respectively. The response surface plotted in Fig. 2b between Na_2EDTA concentration and temperature and the trend of the surface plot of temperature versus time in Fig. 2c depicted the similar activity of limonin bioconversion. In fact, the close interaction of temperature and pH with time was evident. Thus, the response shown was based on the interaction of the significant variables. The predicted response was aproximately 75.82% when the significant variables were taken at "0" level, whereas the experimental response (based on the best predicted combinations of significant variables showing maximum response in CCRD) was approximately 76.71%, which confirms the validity of the model.

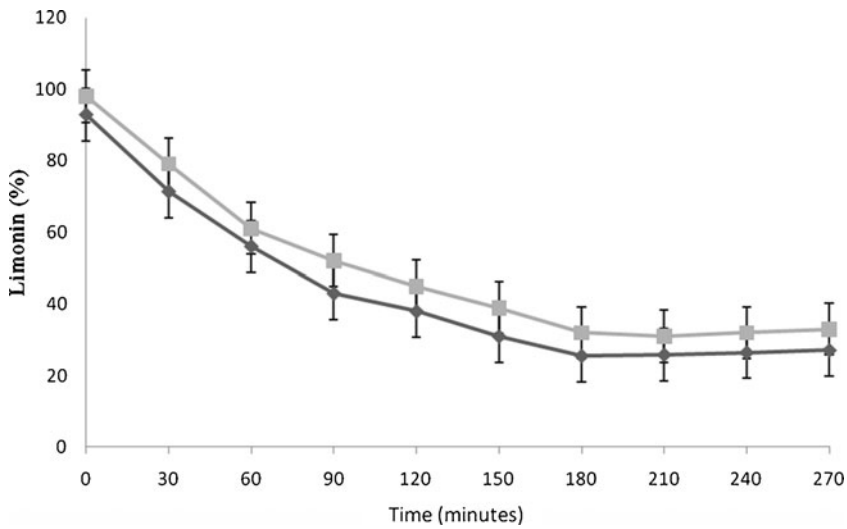

Fig. 4 Limonin bioconversion kinetics by permeabilized entrapped cells in juice (*dark gray line*) and in M63 minimal medium (*light gray line*) supplemented with equivalent amounts of limonin. Results are mean of three independent replicates

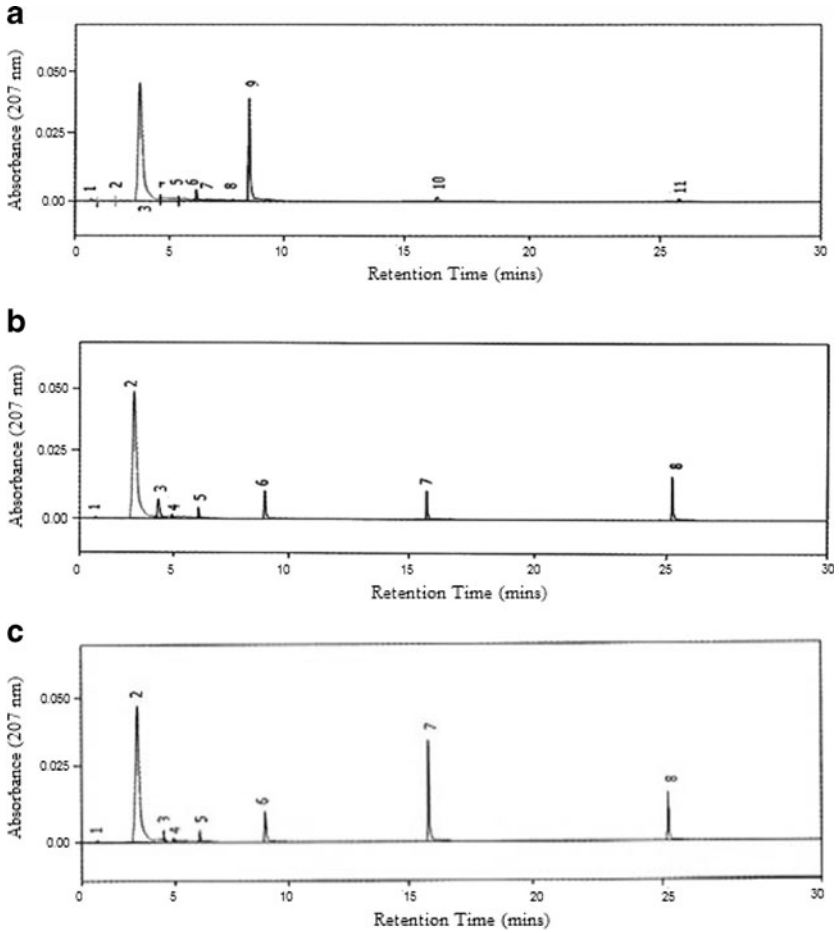

Fig. 5 **a** Representative HPLC chromatograms. **a** Standard limonin (control), **b** after bioconversion of limonin by permeabilized cells, and **c** by purified limonin biotransforming enzyme from *P. putida* G7. The results were recorded using acetonitrile/deionized water (32:68) with a flow rate of 0.9 ml/min and an injection volume of 20 μl

Performance of permeabilized cells

The performance of bioconversion of limonin was studied in an experimental setup (Fig. 3), in which the permeabilized cells of *P. putida* G7 were entrapped inside a dialysis membrane. The efficiency of the reduction of limonin was monitored in two model solutions, minimal medium (M63) with limonin as the substrate and in citrus juice with equivalent limonin content. Limonin bioconversion peaked typically at 3 h; thereafter, further reduction was not observed (Fig. 4). In citrus juices, 76.71% of limonin removal was achieved within 150 min. Further, the ability of entrapped permeabilized cells was compared with the efficiency of the purified enzyme by HPLC. A prominent peak, at a retention time of 9.3 min, was obtained with standard limonin (Fig. 5a). The peak area that represented limonin was reduced after biotransformation and appearance of two new peaks at retention times of 15.9 and 25.2 min were observed (Fig. 5b, c). As illustrated in Fig. 6, the peak area of 62% and 66% represented limonin in two respective model solutions of juice serum and standard limonin in the medium. A reduction in peak area to 9.07% and 7.09% was evidenced from the HPLC profile obtained after biotransformation by purified enzyme and the entrapped permeabilized cells, respectively. The same reduced the corresponding peak area to 18.08% and 17.08% in the juice medium with the equivalent limonin content. Thus, in both the model solutions, i.e., of juice serum and standard limonin in the minimal medium, the

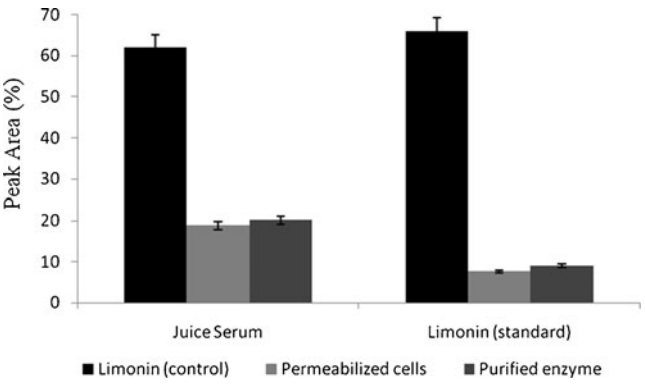

Fig. 6 Comparison of efficiency of limonin bioconversion in two model solutions (standard limonin and juice sample with same limonin content) using cells of *P. putida* G7 permeabilized with Na_2EDTA under specified conditions and the purified enzyme. The results are explained in terms of peak area (%) for residual limonin by HPLC

permeabilized cells proved to be equally efficient in biotransforming limonin as that of the purified enzyme.

Discussion

This is an innovative work conjugating the operational conditions inside the technological space, and the experimental domain used the potential microorganism *P. putida* G7 which was permeabilized effectively. Subsequently, a cell-based facile process was developed, where a substantial reduction of 76.71% of limonin in citrus juice was achieved within 150 mins. The efficient permeabilization is attributed to EDTA, a chelating agent which binds with the divalent cations of Ca^{2+} and Mg^{2+} where the latter stabilizes the outer membrane structure by bonding the lipopolysaccharides to each other. Once these cations are removed from the EDTA, the lipopolysaccharides are detached, resulting in perforations in areas of the outer walls (Siso et al. 1992). The increased permeability served as a whole cell process where the substrate limonin is transported to the cell without impedance and is transformed as dictated by the metabolic function of the cell. Thus improved whole cell biocatalysis was possible because permeability issues were resolved. Our earlier observation revealed that limonin biotransformation by *P. putida* G7 is mediated by a dehydrogenase located in the periplasm. It was postulated that periplasmic location of this enzyme with its catalytic site exposed to the external environment may present a unique arrangement for the cells for degradation of unusual compounds. The process of permeabilization rendered better contact between enzyme and substrate thereby enhancing limonin catalysis. The optimal permeabilization of the cells enabled retention of cofactors, especially NADH, for functioning of the dehydrogenase affording stability to the biocatalytic process. The availability of cofactors in whole cells is deemed crucial for operability of dehydrogenase-based biotransformations.

From the results of the RSM with CCRD, it was concluded that *P. putida* was able to biotransform limonin under all tested conditions. Concerning our findings, the RSM applied to the evolution of enhancement in limonin bioconversion showed that the R^2 value closer to 1, lower value of CV, and the Adequate Precisio denote a higher reliability of the experiments and a very high significance of the model (Venil and Lakshmanaperumalsamy 2009; Kaur and Satyanarayana 2010). Upon optimization of the significant variables for permeabilization of *P. putida* G7, the surface plots helped in the better understanding of the interactions of the significant variables and thus enabled the determination of the optimal level of each variable for maximizing limonin bioconversion. The slightly lower rates of limonin bioconversion by permeabilized cells observed while treating citrus juice may be attributed to the components of the juice (like essential oils) leading to a possible loss of enzyme activity (Verma et al. 2010).

The application of dialysis membrane for entrapment of *Acinetobacter* sp. for limonin reduction in orange juices has been reported earlier (Vaks and Lifshitz 1981). Entrapment of whole cells had resulted in slightly higher rate of limonin conversion as reported in some earlier studies; however, the operation time seemed to be too long which is an impeding factor for practical feasibility of the entrapped whole cells. In the present study, entrapment of permeabilized *P. putida* G7 cells afforded stability enabling a substantial increase in enzyme–substrate interaction thereby shortening the bioconversion time. The decrease in limonin content can be directly correlated with the reduction in bitterness (Soares and Hotchkiss 1998). The residual limonin in the treated citrus juice was far below the threshold limit of human detection. Therefore, it is speculated in comparison to the previous studies that the problem of delayed bitterness due to limonin could be better addressed through the present approach. A further technological development of this process is suggested before commercial use.

In conclusion, the enhanced stability and effective limonin bioconversion of permeabilized cells is relevant when process economics are considered. Thus, the process shows promise as an improvement made for citrus juice debittering application.

Acknowledgments This work was supported to M. Malik, as Senior Research Fellowship by Council of Scientific and Industrial Research, Human Research Development Group, New Delhi is duly acknowledged.

References

Babu S, Vaidya AN, Bal AS, Kapur E, Jueo A, Khanna P (1991) Kinetics of biosurfactant production by *Pseudomonas aeruginosa* strain BS2 from industrial wastes. Biotechnol Lett 18:263–268

Canovas M, Garcia-Cases L, Iborra J (1998) Limonin consumption at acidic pH values and absence of aeration by *Rhodococcus fascians* cells in batch and immobilized continuous systems. Enzym Microb Technol 22:111–116

Chen RR (2007) Permeability issues in whole-cell bioprocesses and cellular membrane engineering. Appl Microbiol Biotechnol 74:730–738

Cheng S, Dongzhi W, Song Q, Zhao X (2006) Immobilization of permeabilized whole cell penicillin G acylase from *Alcaligenes faecalis* using pore matrix cross linked with glutaraldehyde. Biotechnol Lett 28:1129–1133

Felix H (1982) Permeabilized cells. Anal Biochem 120:211–234

Geckil H, Ates B, Gencer S, Uckun M, Yilmaz I (2005) Membrane permeabilization of gram-negative bacteria with a potassium phosphate/hexane aqueous phase system for the release of l-asparaginase: an enzyme used in cancer therapy. Process Biochem 40:573–579

Ghosh M, Ganguli A, Mallik M (2006) Evidence of indigenous NAH plasmid of naphthalene degrading *Pseudomonas putida* PpG7 strain implicated in limonin degradation. J Microbiol 44:473–479

Gonzalez-Saiz JM, Pizarro C (2001) Polyacrylamide gels as support for enzyme immobilization by entrapment. Effect of polyelectrolyte carrier, pH and temperature on enzyme action and kinetics parameters. J Eur Polym 37:435–444

Gough S, Deshpande M, Scher M, Rosazza J (2001) Permeabilization of *Pichia pastoris* for glycolate oxidase activity. Biotechnol Lett 23:1535–1537

Hasegawa S, Bennett RD, Maier VP, King AD (1972) Limonoate dehydrogenase from *Arthrobacter globiformis*. J Agric Food Chem 20:1031–1034

Hasegawa S, Maier VP (1983) Solutions to the limonin bitterness problem of citrus juices. Food Technol 37:73–77

Hasegawa S, Vandercook CE, Choi GY, Herman Z, Ou P (1985) Limonoid debittering of citrus juice sera by immobilized cells of *Corynebacterium fascians*. J Food Sci 50:330–332

Hewtter DJ, Wang HY (1986) Protein released from chemically permeabilized *Escherichia coli*. In: Asenjo JA, Hong J (eds) Separation, recovery and purification in biotechnology. ACS symposium series 314. American Chemical Society, Washington, DC, pp 2–8

Kaur P, Satyanarayana T (2010) Improvement in cell-bound phytase activity of *Pichia anomala* by permeabilization and applicability of permeabilized cells in soymilk dephytinization. J Appl Microbiol 108:2041–2049

Kondo A, Liu Y, Furuta M, Fujita Y, Matsumoto T, Fukuda H (2000) Preparation of high activity whole cell biocatalyst by permeabilization of recombinant flocculent yeast with alcohol. Enzym Microb Technol 27:806–811

Liu L, Dong YS, Qi SS, Wang H, Xiu ZL (2010) Biotransformation of steriodal saponins in *Dioscorea zingiberensis* C. H. Wright to diosgenin by *Trichoderma harzianum*. Appl Microbiol Biotechnol 85:933–940

Malik M, Ganguli A, Ghosh M (2011) Enhancement of bioconversion efficiency of limonin by *Pseudomonas putida* G7. Int J Food Sci Nutr. doi:10.3109/09637486.2011.596823

Melo LLMM, Pastore GM, Macedo GA (2005) Optimized synthesis of citronellyl flavour esters using free and immobilized lipase from *Rhizopus* sp. Process Biochem 40:3181–3185

Mizumoto S, Shoda M (2007) Medium optimization of antifungal lipopeptide, iturin A, production by *Bacillus subtilis* in solid-state fermentation by response surface methodology. Appl Microbiol Biotechnol 76:101–108

Mundra P, Desai K, Lele SS (2007) Application of response surface methodology to cell immobilization for the production of palatinose. Bioresour Technol 98:2892–2896

Myers RH, Montgomery DC (2002) Response surface methodology: process and product optimization using designed experiments, 2nd edn. Wiley, New York

Potumarthi R, Subhaker C, Pavani A (2008) Evaluation of various parameters of calcium-alginate immobilization method for enhanced alkaline protease production by *Bacillus licheniformis* NCIM-2042 using statistical methods. Bioresour Technol 99:1776–1786

Prakash O, Talat M, Hasan SH (2008) Factorial design for the optimization of enzymatic detection of cadmium in aqueous solution using immobilized urease from vegetable waste. Bioresour Technol. doi:10.1016/j.biortech.2008.02.008

Puri M, Kaur L, Marwaha SS (2002) Partial purification and characterization of limonate dehydrogenase from *Rhodococcus fascians* for the degradation of limonin. J Microbiol Biotechnol 12:669–673

Senthilkumar SR, Dempsey M, Krishnan C (2008) Optimization of biobleaching of paper pulp in an expanded bed bioreactor with immobilized alkali stable xylanase by using response surface methodology. Bioresour Technol. doi:10.1016/j.biortech.2008.01.058

Siso MIG, Cerdan E, Picos MAF, Ramil E, Belmonte ER, Torres AR (1992) Permeabilization of *Kluyveromyces lactis* cells for milk whey saccharification: a comparison of different treatments. Biotechnol Tech 6:289–393

Soares NFF, Hotchkiss JH (1998) Naringinase immobilization in packaging films for reducing naringin concentration in grapefruit juice. J Food Sci 63:61–65

Vaks B, Lifshitz A (1981) Debittering of orange juice by bacteria which degrade limonin. J Agric Food Chem 29:1258–1261

Venil C, Lakshmanaperumalsamy P (2009) Application of statistical design to the optimization of culture medium for prodigiosin production by *Serratia marcescens* SWML08. Malays J Microbiol 1:55–61

Verma JP, Singh S, Shrivastava PK, Ghosh M (2010) Identification and characterization of cellular locus of limonin biotransforming enzyme in *Pseudomonas putida*. Int J Food Sci Technol 45:319–326

An amperometric biosensor developed for detection of limonin levels in kinnow mandarin juices

Raina Puri, Meenakshi Malik & Moushumi Ghosh

Annals of Microbiology

ISSN 1590-4261
Volume 62
Number 3

Ann Microbiol (2012) 62:1301-1309
DOI 10.1007/s13213-011-0376-5

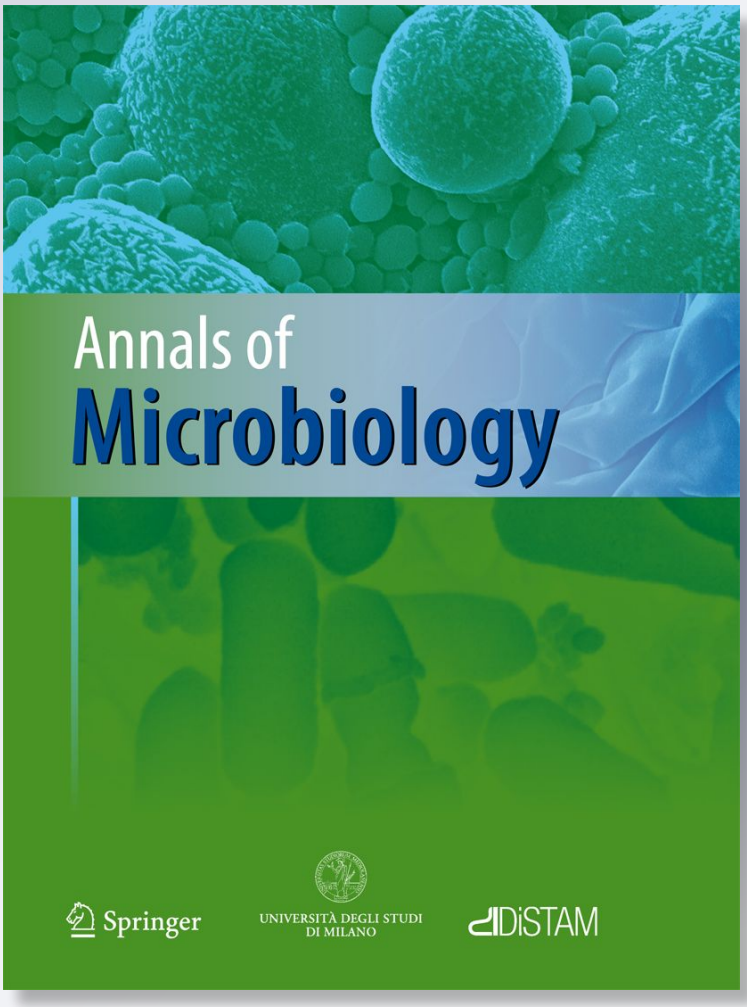

Springer

Ann Microbiol (2012) 62:1301–1309
DOI 10.1007/s13213-011-0376-5

ORIGINAL ARTICLE

An amperometric biosensor developed for detection of limonin levels in kinnow mandarin juices

Raina Puri · Meenakshi Malik · Moushumi Ghosh

Received: 6 June 2011 / Accepted: 12 October 2011 / Published online: 22 November 2011

Abstract The bitterness in kinnow mandarins (also in certain other citrus juices) has been ascribed to limonin that is gradually formed during processing of the juice, which lowers the consumer's acceptability. Thus, detection of limonin at various stages of processing is crucial for the employment of suitable debittering interventions. Owing to the lack of rapid, reliable and economical method for determining limonin levels during the juice production process, an attempt has been made to develop an amperometric microbial biosensor using a mutant (lim^+) of a strain *Pseudomonas putida* G7, that could selectively utilize limonin as a carbon source in the presence of other sugars in kinnow mandarin juice. Analytical determination was based on the respiratory activity of this stable, lim^+ auxotrophic mutant in the presence of the analyte, limonin. The temperature of 30°C, pH 6.5 and the mid-log phase cells at concentrations of 10^6 CFU/ml were the most optimal operating conditions. A consistent correlation between limonin concentrations of 20, 25, 30 ppm (i.e. an optimal substrate–to-cell mass concentration) and the dissolved oxygen (DO) was established. Response times of approximately 20 min for the steady-state method and 12 min for the initial slope method were recorded. The calibration curve for limonin was linear in the 15–50 ppm range of limonin. The performance of the biosensor was reproducible and remained unaffected following intermittent storage and reuse for at least 1 month. Overall, this study suggests the possible application of the developed biosensor for monitoring the limonin content in citrus juices during processing.

Keywords Limonin · Amperometric biosensor · *Pseudomonas putida* G7 · Debitterring

R. Puri · M. Malik · M. Ghosh (✉)
Department of Biotechnology and Environmental Sciences,
Thapar University,
Patiala 147004, Punjab, India
e-mail: mghosh@thapar.edu

Introduction

The phenomenon of delayed bitterness in certain citrus fruit juices continues to represent an important economic impediment for the citrus industry worldwide, especially with regard to achieving consumer acceptability of either processed or fresh products. Delayed bitterness has been attributed primarily to the formation of limonin (Hasegawa and Miyake 1996), which is a highly oxygenated triterpene derivative (composed of a furan ring and an epoxide group) and belongs to the class of limonoids. After juice extraction, acidic pH conditions facilitate the conversion of limonoate-A-ring lactone (LARL)—(non-bitter precursor) to limonin, present in citrus tissues. Different approaches have been used to avoid limonin formation or to eliminate this limonoid from citrus juices (Chern et al. 2001; Das et al. 1997; Krajewska et al. 2001). But all these methods have severe economic and technical limitations since they are non-specific in nature, alter the chemical composition of juice and affect the nutritional quality, texture, flavor, odor and stability of juices (Puri et al. 1996). In order to adopt suitable intervention strategies to reduce bitter limonoids from citrus juices, there is a strong need for a reliable economical, sensitive and direct method for determining limonin during processing of juices. The available techniques are either costly or are indirect methods not fit for on-line monitoring of limonin levels.

Use of a biosensor offers a clear and distinct advantage over standard analytical methods. Several configurations have been described in the past for many purposes (Chern et al. 2001; Das et al. 1997; Krajewska et al. 2001, 2004; Nikolelis et al. 1997). Recently, microbial biosensors have been advocated for their real-time analysis, simplicity of operation, portability, sensitivity, specificity and rapidity of use (Konig and Riedel 1998; Riedel et al. 1988, 1991; D'Souza 2001; Zhang et al. 2001; Liu and Mattiasson 2002). The use of microbial biosensors is based on the intimate contact between a biorecognition element that interacts with the analyte of interest by using the assimilation capacity of the appropriate microorganism as an index of the respiration activity or of the metabolic activity, and a transducer element converts the biorecognition event into a measurable signal. Common transducers include amperometric electrodes, optical wave guides or mass sensitive piezoelectric crystals (Karube et al. 1977; Karube and Suzuki 1981; An et al. 1998). Amperometric biosensors function by the production of a current when a potential is applied between two electrodes (Tan et al. 1994; Makarenko et al. 2002; Mulchandani et al. 2005). The simplest amperometric biosensor in common usage involves the Clark oxygen electrode (Yoo and Lee 2010).

In our previous studies, we demonstrated the ability of a *Pseudomonas putida* G7 strain to utilize limonin as a sole source of carbon (Ghosh et al. 2006) as the major part of aerobic metabolism which is accompanied by the oxygen consumption. Thus, in the present study, an auxotrophic mutant of this strain (lim^+) was generated that could selectively utilize limonin as the only carbon source in the presence of other sugars in kinnow mandarin juice, and was used for developing an amperometric biosensor for determining limonin content. Furthermore, the mutant can respond sensitively to very low concentration of limonin (i.e. 15 ppm). The robustness of the developed biosensor was further evaluated.

Materials and methods

Bacterial strain and culture conditions

A freeze-dried culture of *Pseudomonas putida* G7 (ATCC 17484, DSM 50222) was procured from microbial type culture collection and gene bank (MTCC), Institute of Microbial Technology, Chandigarh. The strain was stored frozen at −20°C in glycerol. The strain was grown with shaking at 150 rpm at a temperature of 30°C for 48 h prior to use. The complete media for growing *P. putida* and its mutant were Luria agar/broth and minimal medium M63 (KH_2PO_4, 13 g/l; $(NH4)_2SO_4$, 1 g/l; $FeSO_4$, 0.00005 g/l; adjusted pH to 7.0 by KOH, 1 N; $MgSO_4$, 1 mM; TTC, 0.1 %) with 0.5% limonin as sole source of carbon.

Extraction of juice from kinnow mandarins

Juice was extracted from 2 kg fresh kinnow mandarins using a commercial juice processor. The juice was pasteurized in an autoclaved screw-capped bottle. The juice was then stored at 4°C. Limonin content of the juice was estimated as described by Vaks and Lifshitz (1981). The limonin was extracted in chloroform and 1.5 ml Ehrlich reagent (0.1 g *p*-dimethylaminobenzaldehyde, 3 ml acetic acid, 2.4 ml 70% perchloric acid) was added to 1 ml chloroform extract. The solutions were mixed vigorously and allowed to stand for 15–20 min in airtight screw-capped tubes to minimize the solvent losses. Absorbance of the red-colored upper layer was recorded at 503 nm. The limonin content in the juice was determined thereafter from a standard curve prepared by using standard limonin.

Estimation of total sugars and reducing sugars

Total sugars in the kinnow mandarin juice were estimated by the phenol–sulphuric acid method of Dubois et al. (1956) using glucose as a standard. Briefly, 0.5 ml of prepared juice concentrate obtained from 10 ml of juice was made to 1 ml with distilled water. The color developed after the addition of 1 ml phenol and 5 ml sulphuric acid to the juice samples was measured at a wavelength of 490 nm by spectrophotometer (Hitachi U2900, Japan). The concentration of total sugar was calculated from the standard curve, prepared using glucose in the range of 10–100 μg/ml. The reducing sugars in the mandarin juice were estimated by the Dinitrosalicylic (DNS) acid method of Miller (1959). Briefly, to 1 ml of juice concentrate in 80% ethanol, 3 ml of DNS was added, boiled for 15 min and cooled. Then 1 ml of 2% sodium potassium tartarate was added and the intensity of the color which developed was recorded at 575 nm against a reagent blank. The corresponding sugar contents were estimated from a standard curve of glucose in the concentration range of 0–1,000 μg/ml.

Generation of auxotrophic mutant (lim^+) of *Pseudomonas putida* by transposon mutagenesis

A Tn5 mutagensis was carried out by biparental conjugation between *Escherichia coli S*171 (donor) and *P. putida* (recipient). The Tn5 element was harbored by the plasmid pGS9 of the donor strain (Reznikoff 2003). The selected exconjugants had the ability to utilize limonin as the only carbon source and could not use other sugars present in the kinnow mandarin juice. The variant was designated as lim^+ auxotrophic mutant.

Optimization of operational conditions

The age, size of cells, temperature and pH conditions of the medium containing limonin were optimized for the mutant as described by Ghosh et al. (2006). The temperature ranged from 15–37°C whereas the pH chosen ranged from 6 to 8. The pH at which microbial sensor was maximal (i.e. max. current) was taken as optimum pH. Similar studies were carried out to ascertain the optimum temperature.

Entrapment of *Pseudomonas putida* G7 in a polyvinyl alcohol (PVA) and adsorption on a dialysis membrane

Log phase cells of *P. putida* lim^+ auxotroph mutant was grown in minimal medium (M63) with limonin as the only carbon source. The culture aliquot (5 ml) was centrifuged and the cells were suspended in phosphate buffer. Suspensions in phosphate buffer of biomass concentrations 2, 4, 6, 8, 10 and 12 mg wet weight per ml were prepared. Four solutions of pre-P-medium (Na_2HPO_4: 13.5 g/l, KH_2PO_4: 0.7 g/l), PVA (4.8 g) and sodium alginic acid (0.36 g) were dissolved in 30 ml of the distilled water by stirring and heating on a hotplate (Hsieh et al. 2002). When the mixture was cooled to room temperature, 1 ml of PVA mixture was mixed with 1 ml of the concentrated cell suspension. This PVA solution containing cells was poured on a Petri dish, dried for 1 h, and solidified by soaking the membrane in a solidifying agent (50 % w/v $NaNO_3$ and 2 % w/v $CaCl_2$) for 1 h (Hsieh et al. 2002). The cell-entrapped membrane was then soaked twice in the distilled water. Cell suspension obtained as above was vacuum filtered with a Spectra/Pro®2 dialysis membrane (MWCO 12,000–14,000; Spectrum Laboratories, USA). A further three sets and proper controls were also prepared similarly for the experiment.

Biosensor assembly and configuration

A microbial sensor was developed with the mutant of *P. putida* (lim^+ auxotroph). A cell-free Spectra/Pro® 2 dialysis membrane was placed on the bottom, on which a cell-immobilized membrane was laid. Finally, a Teflon membrane (YSI standard membrane kit; YSI, USA) was placed on the top. This three-layered membrane was mounted on the tip of YSI 5719 DO probe (YSI) by clamping with a rubber O-ring (Konig et al. 1997; Dubey and Upadhyay 2001; Rastogi et al. 2003). The oxygen sensor consists of a platinum electrode and an Ag/AgCl electrode, as reference electrode, covered with an oxygen permeable membrane. Internal electrolyte is based on a 0.1 M KCl. Amperometric measurements were carried out using an electrochemical workstation BAS 100B/W (Bioanalytical System, West Lafayette, USA), at an applied potential of −650 mV, and data display and recording were supported by BAS electrochemical software version 3.2. The DO probe was placed in a phosphate buffer solution overnight to allow penetration of buffer into the microbe and permit the loss of entrapped air. The electrode was stored in the buffer in a refrigerator between uses.

Table 1 Analysis of sugar content in kinnow mandarin juice; figures in parentheses are SD

Total sugar (mg/ml)	Reducing sugar (mg/ml)
25.4 (±0.03)	15.6 (±0.02)

Biosensor calibration and evaluation

The microbial sensor was placed in a thermostatically controlled chamber where all the determinations were made

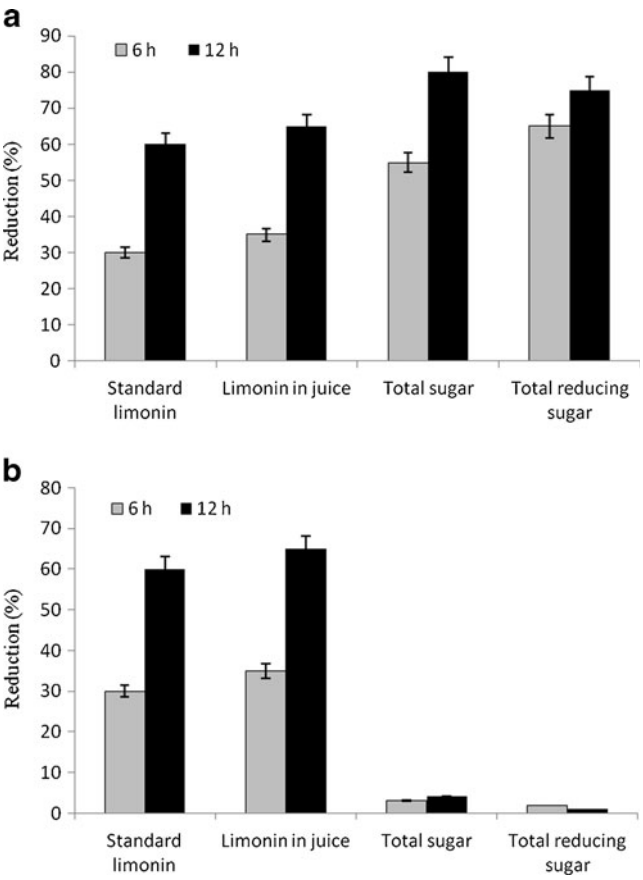

Fig. 1 **a** Utilization of limonin and sugars present in kinnow mandarin juice by *Pseudomonas putida* G7 (wild strain) after 6 12 h of growth. **b** Utilization of limonin and sugars present in kinnow mandarin juice by the mutant strain of *Pseudomonas putida* G7 after 6 12 h of growth

Table 2 Performance (in terms of limonin utilization) of an entrapped mutant of *Pseudomonas putida* G7 under optimal conditions of temperature (30°C), pH (6.5)

		10^4 (CFU/ml)								10^6 (CFU/ml)							10^8 (CFU/ml)						
			Time (min)							Time (min)							Time (min)						
Mid log phase	Standard limonon	Limonin (ppm)	0	5	10	15	20	25	30	0	5	10	15	20	25	30	0	5	10	15	20	25	30
		0	0	0	0	0	0	0	0	0	0	0	0	0	0	0	0	0	0	0	0	0	0
		5	5	4.92	4.86	4.83	4.74	4.75	4.76	5	4.98	4.90	4.84	4.77	4.72	4.65	5	4.96	4.89	4.81	4.75	4.69	4.62
		10	10	9.72	9.62	9.49	9.36	9.19	9.05	10	9.83	9.73	9.64	9.50	9.33	8.98	10	9.79	9.70	9.58	9.50	9.23	8.94
		15	15	14.58	13.79	13.56	13.36	12.93	12.27	15	14.7	13.94	13.11	12.58	12.04	11.33	15	14.63	13.91	12.98	12.46	11.87	11.28
		20	20	18.99	18.44	18.03	17.53	16.91	16.36	20	19.59	18.68	17.5	16.71	15.9	15.13	20	19.49	18.58	17.39	16.65	15.71	14.92
		25	25	23.81	23.23	22.91	22.42	21.21	20.42	25	24.21	23.29	21.91	21.05	19.9	18.92	25	24.16	23.19	21.74	20.86	19.79	18.77
		30	30	28.83	28.59	27.41	26.69	25.48	24.50	30	28.92	27.9	26.2	25.18	23.79	22.61	30	28.85	27.77	25.96	24.98	23.45	22.54
	Juice	Limonin (ppm)	0	5	10	15	20	25	30	0	5	10	15	20	25	30	0	5	10	15	20	25	30
		0	0	0	0	0	0	0	0	0	0	0	0	0	0	0	0	0	0	0	0	0	0
		5	5	4.93	4.85	4.82	4.75	4.76	4.77	5	4.98	4.89	4.83	4.78	4.72	4.67	5	4.95	4.89	4.83	4.75	4.70	4.63
		10	10	9.71	9.63	9.50	9.38	9.21	9.10	10	9.83	9.74	9.64	9.52	9.37	9.10	10	9.80	9.71	9.62	9.49	9.27	8.92
		15	15	14.59	13.79	13.59	13.38	12.99	12.29	15	14.74	14.19	13.17	12.58	11.99	11.27	15	14.66	13.96	13.12	12.51	11.90	11.25
		20	20	19.08	18.47	18.11	17.59	16.89	16.38	20	19.61	18.71	17.49	16.84	15.95	15.17	20	19.52	18.60	17.40	16.67	15.65	14.93
		25	25	23.86	22.94	22.92	21.26	21.24	20.51	25	24.18	23.26	22.15	21.20	19.89	18.88	25	24.22	23.16	21.84	20.94	19.88	18.81
		30	30	28.85	28.62	27.44	26.72	25.51	24.53	30	28.97	27.86	26.22	25.32	23.9	22.68	30	28.87	27.79	25.94	25.16	23.25	22.49
Late log pha se	Standard limonon	Limonin (ppm)	0	5	10	15	20	25	30	0	5	10	15	20	25	30	0	5	10	15	20	25	30
		0	0	0	0	0	0	0	0	0	0	0	0	0	0	0	0	0	0	0	0	0	0
		5	5	4.95	4.91	4.89	4.83	4.77	4.76	5	4.98	4.92	4.88	4.80	4.73	4.69	5	4.97	4.90	4.83	4.76	4.70	4.64
		10	10	9.79	9.71	9.57	9.46	9.31	9.21	10	9.83	9.73	9.64	9.51	9.33	9.15	10	9.80	9.73	9.61	9.49	9.31	8.96
		15	15	14.66	13.85	13.64	13.22	12.85	12.39	15	14.70	14.31	13.32	12.75	12.21	11.45	15	14.68	14.05	13.17	12.59	11.89	11.31
		20	20	19.08	18.64	18.35	17.64	17.25	16.44	20	19.69	18.84	17.59	16.78	15.98	15.26	20	19.54	18.70	17.50	16.75	15.90	14.98
		25	25	23.89	23.57	23.22	22.52	21.33	20.70	25	24.37	23.45	22.25	21.26	20.11	19.80	25	24.38	23.21	21.82	20.93	19.82	18.84
		30	30	29.14	28.76	28.42	26.81	25.64	24.73	30	29.13	28.17	26.33	25.29	24.51	22.72	30	28.88	27.81	26.14	25.22	23.92	22.58
	Juice	Limonin (ppm)	0	5	10	15	20	25	30	0	5	10	15	20	25	30	0	5	10	15	20	25	30
		0	0	0	0	0	0	0	0	0	0	0	0	0	0	0	0	0	0	0	0	0	0
		5	5	4.94	4.90	4.88	4.82	4.78	4.77	5	4.98	4.93	4.88	4.79	4.74	4.68	5	4.96	4.89	4.84	4.77	4.69	4.65
		10	10	9.80	9.71	9.58	9.47	9.32	9.22	10	9.82	9.74	9.65	9.53	9.33	9.12	10	9.80	9.72	9.60	9.49	9.28	8.99
		15	15	14.65	13.86	13.64	13.31	12.84	12.41	15	14.58	14.31	13.31	12.74	12.22	11.46	15	14.69	14.07	13.19	12.61	11.82	11.26
		20	20	19.05	18.67	18.38	17.67	17.22	16.41	20	19.71	18.89	17.87	16.92	16.15	15.28	20	19.54	18.7	17.51	16.77	15.92	12.54
		25	25	23.91	23.57	23.2	23.54	21.35	20.73	25	24.38	23.44	22.26	21.28	20.17	19.86	25	24.36	23.22	21.84	20.96	19.84	18.86
		30	30	29.08	28.76	28.47	26.83	25.63	24.75	30	29.78	28.23	26.36	25.31	24.53	22.78	30	28.89	27.83	26.20	25.26	23.95	22.59

The observations are with different cell sizes (10^4 –10^8 CFU/ml) from two different growth phases (mid-log and late log phase, representing age of cells), measured at intervals of 5 min for up to 30 min in medium (M63) containing standard limonin and in kinnow mandarin juice with specified equivalent amounts of limonin present. Values indicate the mean of three determinations

in a 10-ml measuring cell and all the solutions were previously saturated with oxygen. Before every determination, the biosensor was kept in an oxygen-saturated phosphate buffer solution. After the output signal of the microbial sensor became stable, aliquots of standard analyte (i.e. limonin) solution were added to the measuring chamber to generate a series of various concentration steps. The current decrease indicates that limonin passes through the membrane and is assimilated by the immobilized mutant of *P. putida* cells. Oxygen consumption due to respiratory activity of the microorganism caused a decrease in dissolved oxygen concentration and consequently brought about the decrease in output signal. Decrease of the oxygen concentration around the oxygen electrode is measured and correlated with limonin concentration. In principle, there are two possibilities of measuring biosensor response: (1) endpoint determination (steady-state method) and (2) kinetic measurements (initial slope method). Similarly for the real time study, the analytical determinations were made by immersing the sensor in the kinnow mandarin juice with known amounts of limonin. Subsequently, the amount of limonin now present in the juice was calculated and the DO was measured until the values stabilized. The response curve of the microbial biosensor was plotted between current and analyte concentrations.

Calculation of limit of detection and limit of determination

These were calculated by blank value procedure from the variation of blank probe and the empirical factors given by:

$$Y_L = B + 4.65\ S_B$$
$$Y_D = B + 14.1\ S_{B;}$$

Y_L = Limit of detection, Y_D = Limit of determination, S_B = Variation in the blank probe.

Stability

Long-term stability (1 month) of the microbial sensor response was examined by intermittent daily measurement of the current output of the biosensor.

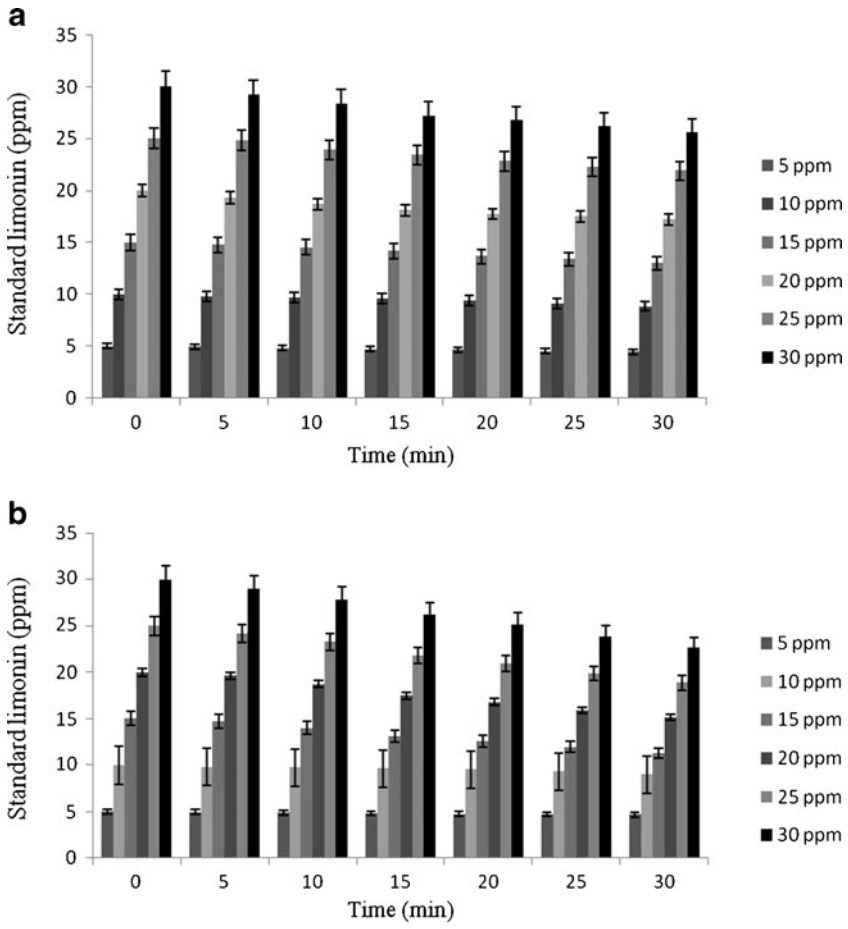

Fig. 2 **a** Kinetics of utilization of different concentrations of standard limonin (ranging from 5 to 30 ppm) by 10^6 CFU/ml mid log phase cells of entrapped lim^+ auxotroph mutant of *Pseudomonas putida* G7. **b** Kinetics of utilization of different concentrations of limonin (ranging from 5 to 30 ppm) present in the kinnow mandarin juice by 10^6 CFU/ml mid-log phase cells of entrapped lim^+ auxotroph mutant of *Pseudomonas putida* G7

Results and discussion

Development of lim$^+$ auxotrophic mutant of *Pseudomonas putida*

Although the unique ability of *P. putida* G7 to utilize limonin as a sole source of carbon has been reported earlier in our laboratory (Ghosh et al. 2006), this strain is also able to utilize a variety of sugars present in kinnow mandarin juice in addition to limonin. The inherent levels of total and reducing sugar in kinnow mandarin juice are presented in Table 1. The results are in agreement with that illustrated by Premi et al (1995). The utilization of total and reducing sugar of kinnow mandarin juice by the *P. putida* G7 cells, in the presence of limonin, were 8% and 82%, respectively, over a period 12 h (Fig. 1a) . This observation implied that the strain is non-selective for utilizing limonin in the presence of other sugars present in the juice. A lim$^+$ auxotrophic mutant of *P. putida* obtained by Tn5 mutagenesis was endowed with a selective property of utilizing limonin as the only carbon source even in presence of other sugars of kinnow mandarin juice (Fig. 1b). This attribute was important since it imparted selectivity for limonin detection to the biosensor; therefore, the possibility of using this mutant for development of limonin biosensor was envisaged.

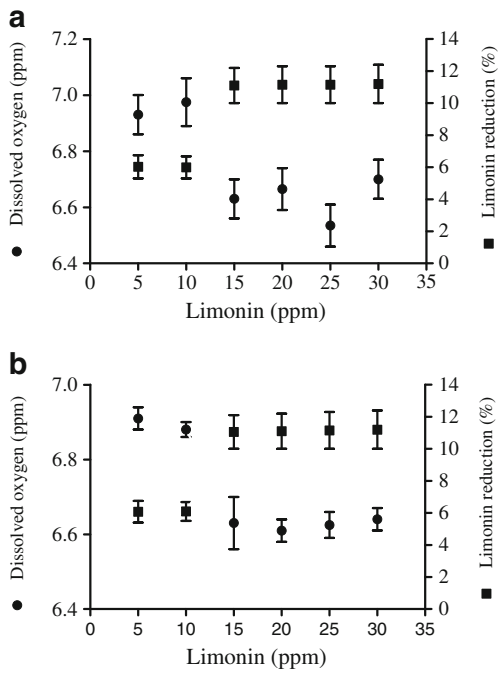

Fig. 3 **a** Biosensor response showing correlation between measured dissolved oxygen as indicator of percent limonin reduction (in standard limonin solution). **b** Biosensor response showing correlation between measured dissolved oxygen as indicator of percent limonin reduction (in juice)

Optimization of operating conditions

Optimal culture conditions such as age of culture, pH, and temperature as well as cell size are expected to enable an appropriateness of cellular physiology and thus afford maximal limonin utilization. The entrapped cells, previously grown to exponential, (mid and late log) phase were

Table 3 Correlation of dissolved oxygen with that of limonin utilization by entrapped lim$^+$ auxotroph in standard limonin under optimal conditions (steady state signal) of biosensor operation (i.e. mid-log phase cells of size 10^6 (CFU/ml), at medium temperature 30°C pH 6.5); values given as ±SD

Substrate concentration	Time (mins)	Dissolved oxygen	Residual limonin (ppm)
5 (ppm)	5	6.98±0.01	4.98±0.04
	10	6.77±0.04	4.82±0.03
	15	6.30±0.03	4.71±0.07
	20	5.89±0.02	4.67±0.04
	25	5.61±0.05	4.55±0.05
	30	5.43±0.06	4.48±0.03
10 (ppm)	5	6.97±0.03	9.82±0.08
	10	6.87±0.07	9.73±0.06
	15	6.23±0.04	9.64±0.02
	20	5.76±0.03	9.41±0.03
	25	4.93±0.08	9.12±0.05
	30	4.62±0.06	8.83±0.03
15 (ppm)	5	6.97±0.04	14.78±0.04
	10	6.55±0.03	14.53±0.03
	15	5.89±0.02	14.18±0.02
	20	5.62±0.01	13.68±0.03
	25	4.84±0.04	13.39±0.08
	30	4.38±0.02	13.02±0.05
20 (ppm)	5	6.97±0.03	19.3±0.02
	10	6.63±0.03	18.72±0.04
	15	5.81±0.02	18.11±0.03
	20	4.67±0.03	17.76±0.01
	25	4.53±0.03	17.53±0.02
	30	4.27±0.06	17.22±0.08
25 (ppm)	5	6.97±0.03	24.8±0.06
	10	5.98±0.08	23.9±0.03
	15	5.43±0.03	23.4±0.02
	20	4.72±0.04	22.8±0.01
	25	4.57±0.03	22.25±0.04
	30	4.18±0.07	21.92±0.01
30 (ppm)	5	6.91±0.03	29.2±0.02
	10	6.32±0.05	28.3±0.03
	15	5.57±0.03	27.2±0.06
	20	4.93±0.06	26.73±0.05
	25	4.52±0.03	26.13±0.03
	30	4.04±0.08	25.6±0.02

used at different cell size to determine residual limonin levels in both media spiked with different concentrations of limonin as well as in kinnow mandarin juice (Table 2). A cell size of 10^6 CFU/ml (corresponding to 0.8 g dry weight) mid-log phase cells of *P. putida* mutant could utilize 22% limonin (at a concentration of 10 ppm) at pH 6.5 and a temperature of 30°C. Limonin utilization kinetics using the same cell size, phase, pH and temperature conditions in kinnow mandarin juice samples did not differ notably over a period of 30 min (Fig. 2a, b). Furthermore, the utilization pattern in both standard limonin and juices could be correlated at higher concentrations of limonin (Fig. 3a, b). To ensure optimal operability of the biosensor, the cultural parameters for maximum limonin utilization by lim^+ *P. putida* were adopted.

Table 4 Correlation of dissolved oxygen with that of limonin utilization by entrapped lim^+ auxotroph in standard limonin under optimal conditions (base signal) of biosensor operation (i.e. mid-log phase cells of size 10^6 (CFU/ml), at medium temperature 30°C pH 6.5); values given as ±SD

Substrate concentration (juice serum)	Time (min)	Dissolved oxygen	Residual limonin
5 ppm	10	7.00±0.02	4.98±0.01
	20	6.99±0.01	4.90±0.04
	30	6.98±0.03	4.84±0.02
	40	6.97±0.05	4.77±0.06
	50	6.96±0.05	4.73±0.03
	60	6.93±0.06	4.68±0.05
10 ppm	10	6.98±0.07	9.82±0.03
	20	6.97±0.02	9.73±0.02
	30	6.96±0.01	9.64±0.03
	40	6.95±0.03	9.51±0.08
	50	6.93±0.04	9.32±0.08
	60	6.8±0.05	8.98±0.07
15 ppm	10	6.99±0.06	14.68±0.05
	20	6.93±0.03	14.0±0.04
	30	6.62±0.02	13.10±0.06
	40	6.1. ±0.01	12.59±0.03
	50	5.8±0.05	11.93±0.03
	60	5.6±0.06	11.30±0.05
20 ppm	10	6.97±0.07	19.6±0.03
	20	6.92±0.07	18.7±0.05
	30	6.63±0.08	17.47±0.08
	40	6.1±0.04	16.8±0.07
	50	5.81±0.03	15.91±0.06
	60	5.6±0.01	15.12±0.04
25 ppm	10	6.96±0.06	24.12±0.01
	20	6.92±0.02	23.25±0.02
	30	6.63±0.06	21.83±0.02
	40	6.15±0.07	20.97±0.05
	50	5.8±0.08	19.88±0.03
	60	5.66±0.02	18.85±0.01
30 ppm	10	6.96±0.03	28.97±0.04
	20	6.90±0.05	27.84±0.04
	30	6.63±0.02	26.2±0.02
	40	6.1±0.03	25.17±0.03
	50	5.8±0.02	23.85±0.01
	60	5.6±0.04	22.6±0.02

Biosensor response analysis

The membranes with immobilised lim + *P. putida* were tested using 5, 10, 15, 20, 25 and 30 ppm limonin. Dissolved oxygen levels were recorded at each concentration over a period of 30 min. The difference between steady state signal and base signal in oxygen-saturated buffer is represented in Tables 3 and 4. A consistent correlation of the observed DO levels with limonin utilization could be observed at all concentrations. These observations indicated that the cultural parameters as well as a cell mass of 10^6 CFU/ml performed optimally. Cell concentration is a critical parameter which can affect the biosensor response. For instance, it has been reported that low immobilized cell concentrations do not modify the base line of the biosensors whereas increasing the cell concentration on the surface of the membrane leads to a very low base signal. Additionally, the oxygen electrode loses the ability to detect dissolved oxygen around the biocatalytical membrane with a very high concentration of microbial cells. Utilization of limonin results in the consumption of oxygen leading to a change of DO level. The decrease in oxygen concentration to a new steady state reflects the endogenous respiration of the cells, which is represented by R_S of 18.76.

An intimate contact between the biocatalyst and the transducer element is the best possible by immobilization of the biocatalyst. In general for biosensors, immobilizations of microbial cells on the membrane allow easy handling besides a higher storage and working stability in compar-

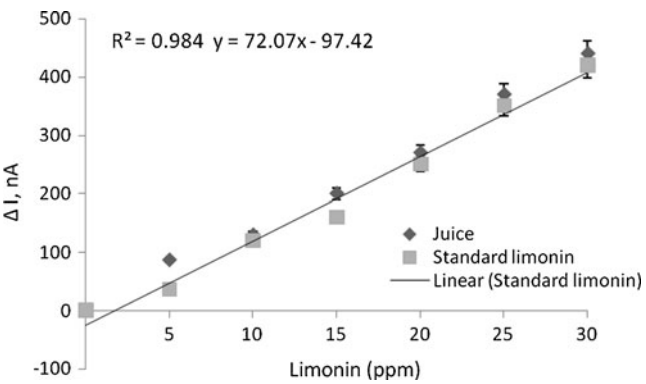

Fig. 4 Biosensor calibration curve (steady state pH 6.5 temperature 30°C) in standard limonin and kinnow mandarin juice

ison to microbial cells adsorbed on filters. The polymer used for immobilization possesses extremely high permeability and diffusivity for oxygen, thus the metabolic process of immobilized cells remains unimpeded, and this avoids discrepancy in the DO values. It has been suggested that suitable immobilization in addition to low microbial loading restricts diffusion limitation and improves sensitivity of biosensors (Hikuma et al. 1980).

The measurable output of the biosensor was tested with a range of limonin concentrations, both in standard limonin and juice as shown in Fig 4. A good correlation (R^2=0.984) between outputs with standard limonin, and that in juice samples were observed with all concentrations tested by the biosensor. The linearity and consistency in the output pattern (and thus DO level) observed within 20 min suggest uniformity in limonin utilization and may be attributed to an optimal substrate-to-cell mass concentration which is achieved during this period. This observation is further corroborated by the fact that DO levels steadily declined after this time period until 30 min.

Storage and stability

The biosensor stability was tested using 10 ppm limonin at a pH of 6.5 and temperature of 30°C, for 30 days with 2 determinations per day. In between, the sensor was kept in buffer solution at 4°C. No significant decrease in signal from the initial value obtained on the first day was observed after 30 days, suggesting the reusability and robustness of the developed biosensor.

Overall, the biosensor reported in this study using lim^+ *P. putida* was stable, reusable and sensitive. These results suggest the feasibility of the application of the developed biosensor in real-time processes. For commercial citrus juice debittering processes, an integration of this approach may prove to be effective in monitoring online reduction of limonin levels. Further experiments are, however, warranted for ascribing DO as an indicator for monitoring of the amount of limonin present in juice.

Acknowledgements This work was supported to M.G. by Department of Science and Technology, under the SERC Fast Track Scheme for young scientists.

References

An L, Niu H, Zeng H (1998) A new biosensor for rapid oxygen demand measurement. Water Environ Res 70:1070–1074

Chern LH, Heng LY, Musa A (2001) A potentiometric biosensor based on urease enzyme. Proc NSF Workshop, Kuala Lumpur

Das N, Prabhakar P, Kayastha AM, Srivastava RC (1997) Enzyme entrapped inside the reverse micelle in the fabrication of a new urea sensor. Biotechnol Bioeng 54:329–332

D'Souza SF (2001) Microbial biosensors (review). Biosens Bioelectron 16:337–353

Dubey RS, Upadhyay SN (2001) Microbial corrosion monitoring by an amperometric microbial biosensor developed using whole cell of *Pesudomosa.* sp. Biosens Bioelectron 16:995–1000

Dubois M, Gilles KA, Hamilton JK, Rebers PA, Smith F (1956) Colorimetric method for determination of sugars and related substances. Anal Chem 28:350–356

Ghosh M, Ganguli A, Mallik M (2006) Evidence of indigenous NAH plasmid of naphthalene degrading *Pseudomonas putida* G7 strain implicated in limonin degradation. J Microbiol 44:473–479

Hasegawa S, Miyake M (1996) Biochemistry and biological functions of citrus limonoids. Food Rev Int 12:413–415

Hikuma M, Obana H, Yasuda T (1980) Amperometric determination of total assimiable sugars in fermentation broths with use of immobilized whole cells. Enzyme Microbiol Technol 2:234–238

Hsieh YL, Tseng SK, Chang YJ (2002) Nitrification using polyvinyl alcohol-immobilized nitrifying biofilm on an O_2-enriching membrane. Biotechnol Lett 24:315–319

Karube I, Suzuki S (1981) Preliminary screening of mutagens with a microbial sensor. Anal Chem 53:1024–1026

Karube I, Matsunaga T, Mitsuda S, Suzuki S (1977) Microbial electrode BOD Sensor. Biotechnol Bioeng 19:1535–1547

Konig A, Riedel K (1998) A microbial sensor for detecting inhibitors of nitrification in wastewater. Biosens Bioelectron 13:869–874

Konig A, Secker J, Riedel K, Metzger JW (1997) A microbial sensor for measuring inhibitors and substrates for nitrification in wastewater. Am Lab 13:12–21

Krajewska B, Zaborska W, Leszko M (2001) Inhibition of chitosan-immobilized urease by slow-binding inhibitors: Ni^{2+}, F^- andacetohydroxamic acid. J Mol Catalysis B: Enzymes 101–109

Krajewska B, Zaborska W, Chudy M (2004) Multi-step analysis of Hg^{2+} ion inhibition of jack bean urease. J Inorg Biochem 98:1160–1168

Liu J, Mattiasson B (2002) Microbial BOD sensors for wastewater analysis. Water Res 36:3786–3802

Makarenko AA, Bezverbnaya IP, Kosheleva IA, Kuvichkina TN, II'yasov PV, Reshetilov AN (2002) Development of biosensors for phenol determination from bacteria found in petroleum fields of West Siberia. Appl Biochem Microbiol 38:23–27

Miller GL (1959) Use of dinitrosalicylic acid reagent determination reducing sugar. Anal Chem 31:426–428

Mulchandani P, Hangarter CM, Lei Y, Chen W, Mulchandani A (2005) Amperometric microbial sensor for *p*-nitrophenol using *Moraxella* sp. modifed carbon paste electrode. Biosensor Bioelectron 21:523–527

Nikolelis PD, Krull JU, Wang J, Mascini M (1997) Proceedings of the NATO Advanced research Workshop, Smolenice, Slovakia

Premi BR, Lal BB, Joshi VK (1995) Distribution pattern of bittering principles in kinnow fruit. J Food Sci 31:140–141

Puri JS, Kothari RM, Kennedy JF (1996) Biochemical basis of bitterness in citrus fruits and biotech approaches for dibittering. Crit Rev Biotech 16:145–155

Rastogi S, Kumar A, Mehra NK, Makhijani SD, Manoharan A, Gangal V, Kumar R (2003) Development and characterization of a novel immobilized microbial membrane for rapid determination

of biochemical oxygen demand load in industrial wastewater. Biosens Bioelectron 18:23–29

Reznikoff WS (2003) Tn5 as a model for understanding DNA transposition. Mol Microbiol 47:1199–1206

Riedel K, Renneberg R, Kuehn M, Scheller F (1988) A fast estimation of BOD with microbial sensors. Appl Microbiol Biotechnol 28:316–318

Riedel K, Naumov AV, Boronin LA, Golovleva LA, Stein J, Scheller F (1991) Microbial sensors for determination of aromatics and their chloroderivatives. Part II: Determination of 3-chlorobenzoate using a *Pseudomonas* containing biosensors. Appl Microbiol Biotechnol 35:557–562

Tan HM, Cheong SP, Tan TC (1994) An amperometric benzene sensor using whole cell *Pseudomonas putida* ML2. Biosens Bioelectro 9:1–8

Vaks B, Lifshitz A (1981) Debittering of Orange juice by bacteria which degrade limonin. J Agric Food Chem 29:1258–1261

Yoo EH, Lee SY (2010) Glucose biosensors: an overview of use in clinical practice. Sensor 10:4558–4576

Zhang S, Zhao H, John R (2001) Development of a quantitative relationship between inhibition percentage and both incubation time and inhibitor concentration for inhibition biosensors — theoretical and practical considerations. Biosens Bioelectron 16:1119–1126

International Journal of Food Sciences and Nutrition,
February 2012; 63(1): 59–65

informa
healthcare

Enhancement of bioconversion efficiency of limonin by *Pseudmonas putida* G7

MEENAKSHI MALIK, ABHIJIT GANGULI, & MOUSHUMI GHOSH

Department of Biotechnology and Environmental Sciences, Thapar University, Patiala-147004, Punjab, India

Abstract
The biocatalytic activity of periplasmic dehydrogenase of *Pseudomonas putida* G7 strain to catalyse limonin was enhanced when whole cells were permeabilized with EDTA (1 μM) lysozyme (100 μg/ml). The treated cells were entrapped in dialysis membranes to increase the stability. Permeabilized cells (1 g dry weight) entrapped in dialysis membrane could biotransform 73.67% of limonin in unpasteurized mandarin juices in a single-batch cycle of 3 h. Furthermore, permeabilized cells stored for 45 days in phosphate buffered saline (at 4 or 30°C) retained enzyme activity and were reusable for up to eight batch cycles of limonin reduction. The results of this study suggest a potential application of permeabilized *P. putida* G7 cells for reducing limonin levels in mandarin juices.

Keywords: P. putida *G7, dialysis membrane, permeabilization, limonin*

Introduction

Whole cell biocatalysts provide several advantages over purified enzymes in many processes. However, the permeability barrier of cell envelope for substrates and products often results in low reaction rates when whole cells are used. It is, therefore, important to develop an effective method to reduce the permeability barrier for preparing whole cell biocatalysts with enhanced activities (Kondo et al. 2000). Permeabilization is the process that eases the permeability barrier of the cell to allow the free movement of substances across the cell envelope. Thus, permeabilized microbial cells retain their inner organization, as well as cofactors necessary for functioning of several enzymes (Felix 1982; Hewtter and Wang 1986; Cheng et al. 2006). Limonoate dehydrogenase (LDase), an enzyme detected in different species of microorganisms (*Arthrobacter globiformis*, *Pseudomonas* sp. Strain 321-18 and *Rhodococcus fascians*), can prevent limonin production in certain varieties of freshly extracted mandarin juices, by catalysing the oxidation of limonoate A-ring lactone (LARL) to the corresponding 17-dehydrolimonoate form, a non-bitter derivative which cannot be converted into limonin (Puri et al. 2002).

Over decades, it has been a major goal of researchers to overcome the hindrance of delayed bitterness in citrus juices that the citrus industry faces worldwide due to consumers unacceptability (Hasegawa et al. 1973; Hasegawa and Maier 1983; Kimball 1991; Shaw et al. 2000; Sun et al. 2005; Roy and Saraf 2006). Following juice extraction, the acidic pH conditions facilitate the conversion of non-bitter limonoate A-ring lactone (LARL; Maier et al. 1969) during an enzymatic process. This slow conversion of LARL into limonin is known as 'delayed bitterness' (Hasegawa et al. 1972; Hasegawa and Maier 1983; Hasegawa and Maier 1990; Marawaha et al. 1994).

Among the various physicochemical approaches, the use of polyamides, adsorbents, such as cellulose acetate, nylon-based matrices, porous polymers, ion exchangers, activated magnesium silicate Florisil by Sigma Aldrich (St. Louis, Missouri, USA), and ultrafiltration selectively adsorbing significant quantities of limonin has been explored successfully (Chandler et al. 1968; Griffith 1969; Barmore

Correspondence: M. Ghosh, Department of Biotechnology and Environmental Sciences, Thapar University, Patiala 147004, Punjab, India. Tel: + 91-175-2393421. Fax: + 91-175-2364498 Ext. 2393020. E-mail: mghosh@thapar.edu

ISSN 0963-7486 print/ISSN 1465-3478 online © 2011 Informa UK, Ltd.
DOI: 10.3109/09637486.2011.596823

et al. 1986; Johnson and Chandler 1988; Hernandez et al. 1992). Treatments with ethylene, carbon dioxide at high pressures, cross-linked divinyl benzene (DVB) –styrene resin, polystyrene DVB resins, *P*-cyclodextrin were carried out for the adsorption of limonin from citrus juice (Hasegawa et al. 1973; Maier et al. 1973; Konno et al. 1982; Hasegawa et al. 1983; Shaw and Wilson 1983; Pun 1984; Shaw et al. 1984; Kimball 1987; Wagner et al. 1988; Martínez-Madrid et al. 1989; Kimball and Norman 1990; Manlan et al. 1990; Iborra et al. 1994; Puri et al. 2002; Ghosh et al. 2004; Patil et al. 2006). Thus far, *R. fascians* (CECT 3001) is the only organism that has been explored for a commercial viable debitterring strategy in batch, continuous mode and by immobilization (Canovas et al. 1996, 1998) in several matrices. Microorganism has the advantage of both survival in low-acidic juice pH and constitutively producing enzymes for the metabolism of limonoids. However, the dearth of genetic tools for genetic manipulation has hindered the full exploitation of *Rhodococcus* sp. The ability of *Pseudomonas putida* G7 in limonin biotransformation has been recently demonstrated (Ghosh et al. 2006; Verma et al. 2010). This strain produces a dehydrogenase which converts limonin to non-bitter derivatives (Verma et al. 2010), thus making it the enzyme of choice for debiterring of mandarin juices. However, limonin biotransformation by whole cells of *P. putida* G7 is low, impeding its feasibility for practical purposes (Gough et al. 2001). This investigation reports for the first time a process for significantly improving limonin biotransformation using permeabilized *P. putida* cells entrapped in dialysis membranes. The efficacy of the entrapped permeabilized cells to biotransform limonin in mandarin juices was also demonstrated.

Materials and methods

Microorganism and culture conditions

Freeze-dried culture of *P. putida* G7 (MTCC 1072) was procured from microbial type culture collection and gene bank (MTCC), Institute of Microbial Technology, Chandigarh, India. The complete medium for *P. putida* G7 was Luria–Bertani agar/broth and minimal medium (M63) supplemented with 0.5% limonin as sole source of carbon. The strain was grown by shaking at 150 rpm at 30°C for 48–72 h. Growth was monitored by measuring the increase in absorbance of the culture at 600 nm.

Biomass permeabilization

For permeabilization, the bacterial culture in its mid log-phase was centrifuged at 10,000 rpm for 10 min at 4°C, washed with phosphate buffer (pH 7.0, 50 mM) and subsequently treated with 100 μg/ml of lysozyme and 1 μM Na_2EDTA for 10 min at 30°C (Cheng et al. 2006). The lysozyme-treated cells were centrifuged and finally taken in 1.0 ml of phosphate buffer (pH 7.0, 50 mM) and lyophilized. To choose an effective permeabilization, other permeabilizing agents such as 5% organic solvents [toluene, hexane and chloroform with detergent Triton X-100 (1%)] cetyl trimethylammonium bromide (CTAB) (1%) and protease were added to the aqueous suspension. In each case, the cell permeabilization process was allowed to proceed for 1 h at 37°C, the flask being placed in a rotary shaker operated at 200 rpm. Normal cells were prepared in a similar manner but without any treatment with the enzyme, detergent or organic solvents.

Limonin biotransformation kinetics by free permeabilized cells

Limonin biotransformation by permeabialized cells in the unpasteurized mandarin juice and in M63 medium (200 ml) containing standard limonin was compared; the juice serum was diluted so as to achieve limonin concentrations in a range of 5–50 μg/ml. Similar concentrations of limonin were also prepared in M63 medium, inoculated with log-phase cultures to a final density of 5.5×10^8 CFU/ml and incubated at 30°C for 6 h. Aliquots (5 ml) were withdrawn after every hour, pelleted by centrifugation and the supernatant was used to estimate residual limonin (Vaks and Lifshitz 1981). The pellet was washed and resuspended in 0.85% saline before recording absorbance at 600 nm in a spectrophotometer (Hitachi, U-2800, Tokyo, Japan) so as to obtain the desired cell density.

Dialysis membrane entrapment

Dialysis tubing (Cellulose, MWCO 12000, Sigma-Aldrich, St. Louis, Missouri, USA) was thoroughly washed in sterile triple-distilled water and clipped at one end to produce a sac. The wet weight of permeabilized log-phase *P. putida* G7 cells (0.1 mg/ml), which corresponds to 5.5×10^8 CFU/ml, was packed in the dialysis sac and, after filling with bacterial culture, each sac was tied at the upper end with string and submerged completely in a beaker containing either M63 medium or juice. Solutions in each beaker were supplemented with different concentrations of limonin and the dialysis sacs containing the cultures were incubated with stirring at 30°C for 6 h. Aliquots (5 ml) of medium or effluent were withdrawn every hour and used to estimate residual limonin. In a parallel experiment, 1 ml aliquots of permeabilized cell mass were withdrawn every 2 h and processed for whole cell proteins for zymography and western blotting, as described below.

Zymography

A volume of 100 μl of permeabilized cell samples (80 μl of protein solutions with 20 μl of bromophenol

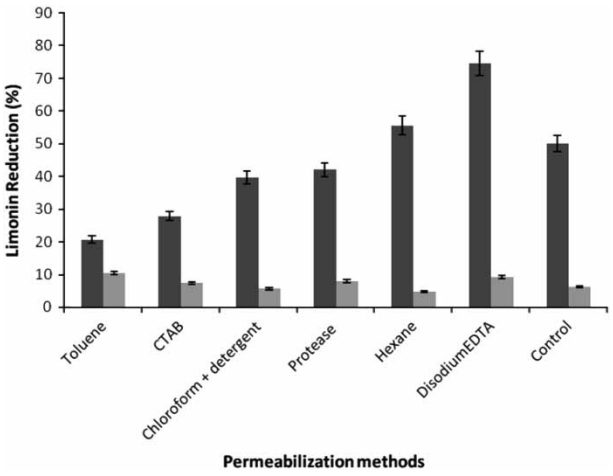

Figure 1. Comparison of different permeabilization methods to evaluate the reduction in limonin by *P. putida* G7. The reactions with the various methods were incubated for 1 h at 37°C, 200 rpm. Limonin estimation was carried out at 35°C. Results are mean of three independent replicates; (■) permeabilised cells and (■) supernatant.

blue) was applied to polyacrylamide gel (12% of acrylamide:*N*,*N*′-methylene bisacrylamide 37.5:1, 1 mm thickness, 8 × 6 cm, buffer:Tris/HCL, pH = 8.9). The migration was carried out in vertical mode in a Bio-Rad Protean II apparatus (Bio-Rad: Hercules, California, USA) at 150 V with Tris/glycine migration buffer (pH = 8.3) for 2 h until bromophenol blue (tracking dye) was 5 mm from the bottom of the gel. Following electrophoresis, the gels were incubated in 20 ml of modified assay mixture containing 375 mM Tris/HCl (pH 8.8), 0.5 mM NADH and 2 mM disodium limonoate. The gels were then placed on a UV light box and observed for a band of yellow fluorescence (due to NADH) after few minutes and later stained for protein detection with Coomassie blue. Known quantities of purified limonin dehydrogenase were used as standards. Unknown quantity bands were quantified using Quantity One Bio-Rad software (Version 4) in 'trace density' mode.

Western blot analysis

Permeabilized cell extracts were run in 12% sodium dodecyl sulphate gel and then transferred to 0.45 μm polyvinylidene difluoride membranes Roche (Penzberg, Germany) for 1 h at 100 mV and 4°C in a Mini Trans-Blot Electrophoretic Transfer Cell (Bio-Rad). The membranes were equilibrated with Tris-buffered saline solution with Tween 20 (TBST; 20 mM Tris/HCL, pH 7.5, 150 mM NaCl, 0.05% Tween 20), and then treated with anti-limonin dehydrogenase monospecific antibodies raised in rabbits (Ganguli and Tripathi 2002). The LDase antibodies were diluted 1:5,000 in TBST; unbound antibodies were removed by three 5-min washes with TBST. Immunodetection of bound antibodies was done by treatment with anti-mouse immunoglobulin G (heavy chain in addition with light chain) alkaline phosphatase conjugate Promega (Fitchburg, Wisconsin, USA) diluted 1:5,000, followed by a solution of nitroblue tetrazolium salt and 5-bromo-4-chloro-3-indolyl phosphate.

Batch cycle experiments and reusability of permeabilized cells

To determine the stability and reusability of dialysis sac entrapped permeabilized cells, the dialysis sac containing permeabilized cells after a batch was stored in phosphate buffered saline (PBS, pH 7.2) and distilled water in separate sets at 4 and 30°C for a period of 45 days. Aliquots were withdrawn periodically, washed with PBS buffer and assayed for limonin biotransformation as described above.

Satistical analysis

All experimental data were subjected to analysis of variance (ANOVA) and significant differences among means from triplicates analysis at ($p < 0.05$) were determined by Duncan's multiple range tests using the statistical analysis system (SPSS 12.0 for Windows, SPSS Inc., Chicago, USA).

HPLC analysis

HPLC system10AVP, Shimadzu, was used for limonin determination, a Novapak C18 column (250 × 4.6 mm, 5 μm particle size, 100 Å unit pore size) with class VP 6.12 software (Shimadzu Corp, Kyoto, Japan). The mobile phase used for the assay was acetonitrile/deionised water (32:68) with a flow rate 0.9 ml/min and an injection volume of 20 μl. The

Table I. Limonin biotransformation by permeabilized and non-permeabilized cells of *P. putida* G7.

	Mandarin juice		M 63 minimal medium*	
	Limonin biotransformation (%)			
Biomass (g/dry weight)	Unpermeabilized	Permeabilized	Unpermeabilized	Permeabilized
0.5	22.97 (± 0.06)	46.59 (± 0.02)	36.23 (± 0.05)	65.89 (± 0.03)
1.0	50.01 (± 0.07)	73.67 (± 0.01)	55.32 (± 0.04)	75.80 (± 0.05)
2.0	52.98 (± 0.02)	74.01 (± 0.04)	56.09 (± 0.04)	76.11 (± 0.06)

* Unpasteurized mandarin juice and M63 medium (200 ml volume with limonin concentrations in a range of 50 μg/ml) were treated with permeabilized and unpermeabilized cells, incubated at 30°C for 6 h, for limonin biotransformation.

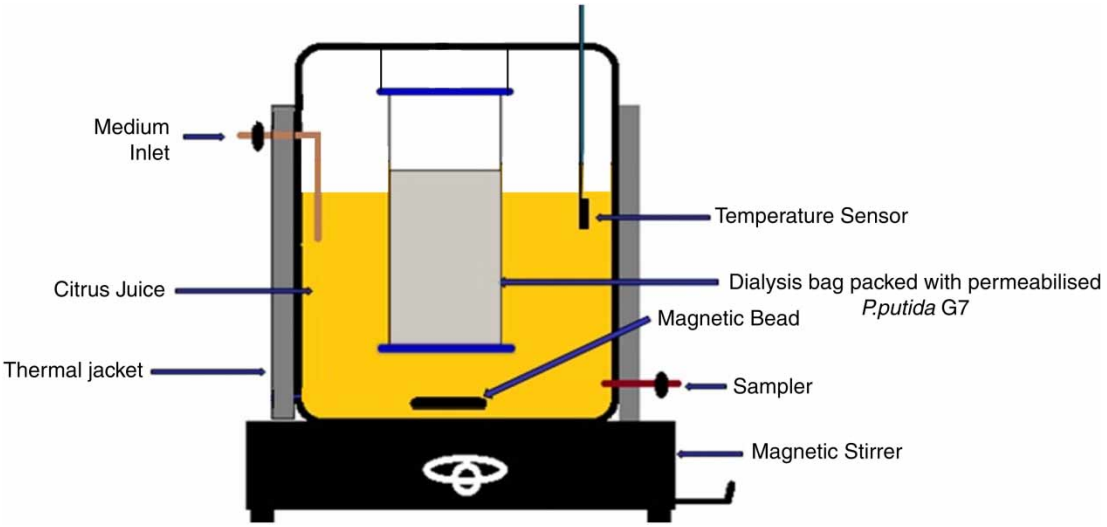

Figure 2. Experimental set-up for the study of limonin biotransformation by the dialysis membrane entrapped permeabilized *P. putida* G7. Volume of the mandarin juice in the vessel was 200 ml; temperature was monitored using temperature controller.

Novapak C18 column was conditioned (rinsed) with 2 ml acetonitrile and 5 ml deionized water. The samples were filtered through 0.45 μm Nylon filter (Waters, Milford, MA, USA) and injected into HPLC. The cartridge was rinsed with 2.5 ml deionized water and 2.5 ml acetonitrile, and permeates were collected in small glass vials. The detection wavelength was 207 nm (Abbasi et al. 2005). The retention time of the working standards was used as an indicator to compare it with those of the unknown.

Results

Permeabilization

The results on the effect of different methods of permeabilization of *P. putida* G7 cells on reduction of limonin are shown in Figure 1. The limonin biotransformation activity was found to be the maximum when Na_2EDTA was used as permeabilizing agent. The incubation of cells for a period of 10 min was considered as optimum because viability and enzyme activity were lost when the cells were incubated beyond the given time. Permeabilization with Na_2EDTA enhanced the enzyme activity up to 11.8 fold compared with the normal cells, within 3 h.

Limonin biotransformation kinetics by free permeabilized cells

Limonin biotransformation by the unpermeabilized cells of *P. putida* G7 was insignificant ($p < 0.05$) in comparison with that by the permeabilized cells of *P. putida* G7 (Table I). The limonin biotransformation by the permeabilzed cells in M63 medium as well as in mandarin juice (containing equivalent quantities of limonin) revealed a similar trend, though a difference in biotransformation rates was observed (74 and 55%, respectively). Permeabilized biomass of 1 g dry weight was considered optimum in terms of limonin biotransformation; increasing biomass concentration did not lead to higher biotransformation rate.

Performance of permeabilized, dialysis membrane entrapped P. putida *G7, its storage stability and reusability*

The performance of limonin biotransformation was studied in an experimental set-up as shown in Figure 2, in which the permeabilized cells of *P. putida* G7 were entrapped inside dialysis membrane. The efficiency of the reduction of limonin was monitored both in minimal medium and in mandarin juice, which consisted of equivalent amounts of limonin. The transformation of limonin by the permeabilized cells was found to be more in the minimal medium containing standard limonin than that observed in the mandarin juice. The maximum reduction was achieved within 180 min of incubation of permeabilized cells inside the dialysis sac. No reduction was observed thereafter (Figure 3). Whether the reduction

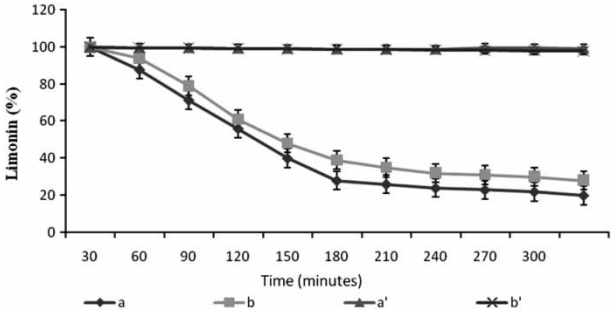

Figure 3. Limonin biotransformation kinetics by permeabilized entrapped cells in mandarin juice (a) (—); M63 minimal medium (b) (—) supplemented with equivalent amounts of limonin; (a′) adsorbed limonin in empty dialysis sac in M63 minimal medium and (b′) adsorbed limonin in empty dialysis sac in Mandarin juice. Results are mean of three independent replicates.

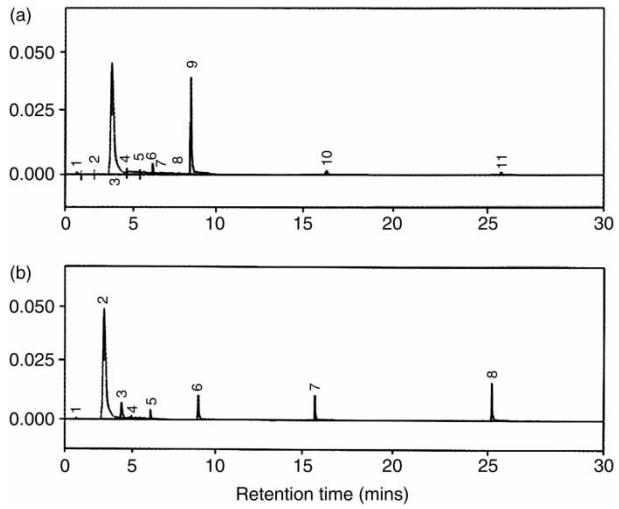

Figure 4. (a) Representative HPLC chromatograms of standard limonin (90 μg/ml) and (b) chromatograms of standard limonin (90 μg/ml) biotransformed by permeabilized cells of *P. putida* G7, using an acetonitrile/deionized water (32:68) with a flow rate 0.9 ml/min and an injection volume of 20 μl.

of limonin was solely due to biotransformation was evaluated by the estimation of limonin within the sac with or without cells. Limonin was not detected inside the dialysis sac during experiments also the empty dialysis sacs incubated in juice for a similar time span, indicated that removal of limonin was not due to adsorption (Figure 3).

HPLC was also used for demonstrating the biotransformation of limonin. A prominent peak at a retention time of 9.3 min was obtained with standard limonin (Figure 4). The area under the curve that represented limonin peak was reduced in the biotransformed sample. As illustrated in Figure 5, compared to the peak area of 62 and 66% of respective controls of juice serum and standard limonin in the medium, the biotransformation resulted in reduction in the peak area of 19.08 and 8.23%, respectively. Also, the biotransformation was evidenced from the appearance of two new peaks at retention times of 15.9 and 25.2 min (Figure 4). However, a complete disappearance of limonin peak was not observed due to the residual limonin in the medium, and these limonin levels (< 5 ppm) were far less than the sensorial property of the consumer. Furthermore, in Figure 5, the peak areas 39.64 and 27.03% corresponded to biotransformed limonin by the unpermeabilized free cells in juice serum and in medium containing standard limonin, respectively. The entrapped permeabilized *P. putida* G7 cells stored in PBS at 4 and 30°C for 45 days did not show any loss in its limonin removal efficiency for the subsequent eight batch cycles. A decline was observed thereafter (Figure 6(a)). This indicated the stability of the enzymes and hence reusability of permeabilized cells. The dialysis entrapment method thus proved to be quite effective for removing limonin.

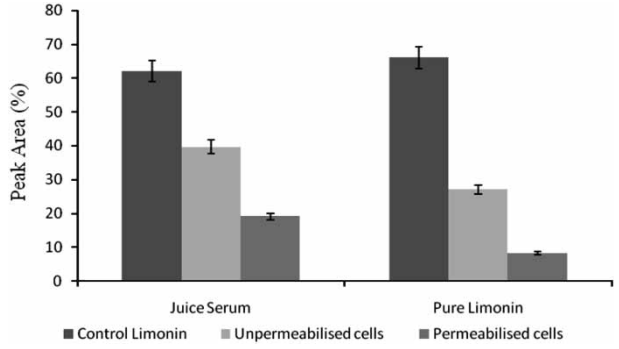

Figure 5. Comparison of limonin biotransformation using permeabilized and unpermeabilized cells of *P. putida* G7 in standard limonin and juice serum in terms of peak area (%) for residual limonin by HPLC.

Zymography

Zymography is a routine electrophoretic technique to identify proteolytic activities in polyacrylamide gels under non-denaturing conditions. This method was adopted to detect the functionality of the enzyme in permeabilized cells. Immersion of gels in a suspension containing 375 mM Tris/HCl (pH 8.8), 0.5 mM NADH and 2 mM disodium limonoate and exposure to UV light allowed visualization of a band of yellow fluorescence (due to NADH) after few minutes. Figure 6(b) shows the activity of the dehydrogenase over eight cycles. Intensity of spots decreased significantly following eighth batch cycle, indicating loss of enzyme activity.

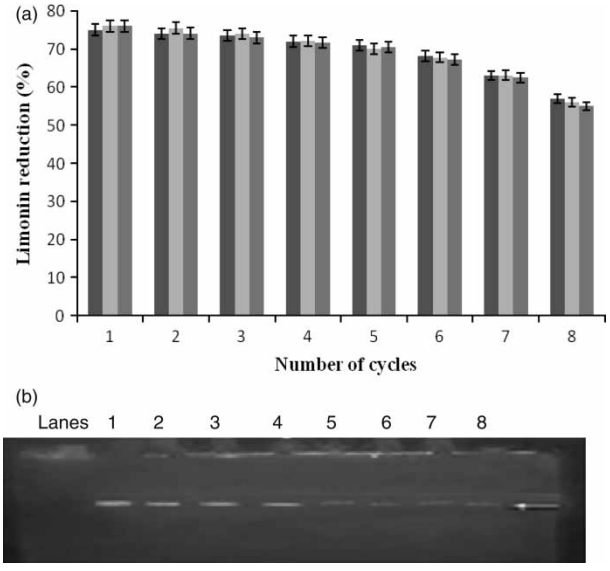

Figure 6. (a) Reusability and stability of permeabilized *P. putida* G7; limonin biotransformation of (■) freshly prepared permeabilized *P. putida* G7 cells, (■) stored at 4°C and (■) 30°C in phosphate buffer for 45 days. Results are mean of three independent replicates. (b) Zymogram showing the intensity of dehydrogenase activity in permeabilized cells (A) lanes 1–8: permeabilized cell extracts from batch cycles 1–8.

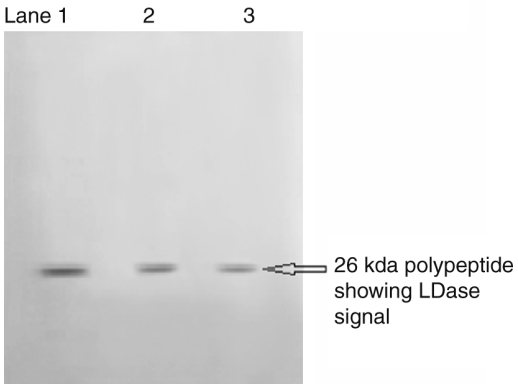

Figure 7. Western blots showing LDase signal of permeabilized cells fractions of *P. putida* G7 from batch cycles 1, 4 and 8 in lanes 1–3, respectively.

Western immunoblotting

The 26 kDa polypeptide of permeabilized cell lysates obtained during each batch cycle cross-reacted with monospecific anti-LDase antibodies raised against LDase from *R. fascians* (Figure 7).

Discussion

The application of microorganisms as a tool for converting bitter limonin to non-bitter derivative takes advantage over the other physicochemical methods employed. These existing methods have severe economic and technical limitations, because they also impair the stability and quality of the juice by affecting components other than limonin (Puri et al. 2002). *P. putida* is well characterized in terms of metabolic versatility and safety. Recent sequencing of the genome of *P. putida* KT 2440 has revealed important insights in terms of potential applications in biocatalysis and agriculture (Santos et al. 2004). The strain *P. putida* G7, in particular, has been studied thoroughly in terms of limonin utilization, the biotransformation of limonin being catalysed primarily by limonin dehydrogenase (Ghosh et al. 2006; Verma et al. 2010). A key parameter, from a process point of view, was to achieve good contact between the substrate, limonin and the enzyme. A feasible biotransformation strategy attempted with whole cells of *P. putida* was not possible on account of both of its slow growth and its low rate of limonin utilization. Permeabilization of *P. putida* cells resulted in a dramatic improvement of biotransformation rate. Highest limonin reduction was achieved with EDTA–lysozyme permeabilized cells; Na_2EDTA acted as a chelating agent by sequestering divalent cations that contribute to the stability of the outer membrane, thus creating a hydrophobic pathway for channelling of certain substances. Tris–EDTA has been reported to potentiate the activity of bacterial cell wall degrading agents (e.g. lysozyme and nisin; Kumar et al. 2008). An inherent disadvantage of permeabilized whole cell biocatalysts is the low specific activity of the desired enzyme for which immobilization or entrapment of the permeabilized cells has been proposed (Cheng et al. 2006). The rapid and simple HPLC method has potential for the regular analysis of limonin levels in citrus juice samples, which helps to determine whether the limonin levels meet the quality standard that requires an upper limit of 5 ppm of limonin.

The dialysis membrane entrapped permeabilized *P. putida* cells retained both viability and enzyme activity as demonstrated by zymograms during each batch cycles. Slightly lower rates of limonin biotransformation by permeabilized cells observed while treating mandarin juice may be attributed to the components of the juice (like essential oils), leading to a possible loss of enzyme activity (Verma et al. 2010). The stability of the biocatalyst is a result of the intracellular environment which protects the enzyme. The fact that entrapped, permeabilized cells stored in PBS retain enzyme activity assures its potential applicability for limonin reduction. The dialysis membrane may be important in compensating biocatalyst reuse by overcoming diffusion limitations typical of gel entrapment (Swaisgood 1991; Ganguli and Tripathi 2002; Kumar et al. 2008). Till date, an effective, economical biocatalyst for limonin reduction has not been reported (Canovas et al. 1998; Verma et al. 2010).

Conclusion

The enhanced limonin biotransformation by permeabilzed *P. putida* G7 cells, their operational and storage stability upon entrapment in dialysis membranes are important prerequisites for an industrial biocatalyst. The results obtained in this study suggest a feasibility of developing a continuous reactor system for limonin reduction in citrus juices using permeabilized, entrapped *P. putida* G7 as biocatalyst. To the best of our knowledge, this is the first report in which limonin biotransformation has been attempted using dialysis membrane entrapped permeabilized cells. Although further studies are required prior to commercially exploiting this method, the approach may be certainly useful for reducing bitter limonoids in citrus juices for practical purposes.

Acknowledgement

The funding for this research work provided to M. Malik, in form of Senior Research Fellowship, by Council of Scientific and Industrial Research, Human Resource Development Group, New Delhi, India, is duly acknowledged.

References

Abbasi S, Zandi P, Mirbagheri E. 2005. Quantitation of limonin in Iranian orange juice concentrates using high performance liquid chromatography and spectrophotometric methods. Euro Food Res Technol 221:202–207.

Barmore CR, Fisher JF, Feller PJ, Rouseff RL. 1986. Reduction of bitterness and tartness in grapefruit juice with florisil. J Food Sci 51:415–416.

Canovas M, Garcia-cases L, Iborra JL. 1996. pH influence on the consumption of limonin species by *Rhodococcus fascians* cells. Biotechnol Lett 18:423–428.

Canovas M, Garcia-Cases L, Iborra J. 1998. Limonin consumption at acidic pH values and absence of aeration by *Rhodococcus fascians* cells in batch and immobilized continuous systems. Enzyme Microbial Technol 22:111–116.

Chandler BV, Kefford JF, Ziemelis G. 1968. Removal of limonin from bitter orange juice. J Sci Food Agric 19:83–86.

Cheng S, Dongzhi W, Song Q, Zhao X. 2006. Immobilization of permeabilized whole cell penicillin G acylase from *Alcaligenes faecalis* using pore matrix cross linked with glutaraldehyde. Biotechnol Lett 28:1129–1133.

Felix H. 1982. Permeabilized cells. Annu Biochem 120:211–234.

Ganguli A, Tripathi AK. 2002. Bioremediation of toxic chromium from electroplating effluent by chromate-reducing *Pseudomonas aeruginosa* A2Chr in two bioreactors. Appl Microbiol Biotechnol 58:416–420.

Ghosh M, Prakash NT, Ganguli A. 2004. Quality issues of Kinnow-Mandarin juices sold by street vendors. J ASEAN Food 13: 143–148.

Ghosh M, Ganguli A, Mallik M. 2006. Evidence of Indigenous NAH plasmid of naphthalene degrading *Pseudomonas putida* PpG7 strain implicated in limonin degradation. J Microbiol 44:473–479.

Gough S, Deshpande M, Scher M, Rosazza JPN. 2001. Permeabilization of *Pichia pastoris* for glycolate oxidase activity. Biotechnol Lett 23:1535–1537.

Griffith FP. 1969. Process for reactivating polyamides resin used in debittering citrus juice, US Patent 3463763.

Hasegawa S, Maier VP. 1983. VP solutions to the limonin bitterness problem of citrus juices. Food Technol 37:73–77.

Hasegawa S, Maier VP. 1990. Biochemistry of limnoids in citrus juice bitter principles and biochemical debittering processes. In: Rouseff RL, editor. Bitterness in foods and beverages. New York, NY: Elsevier. p 293–308.

Hasegawa S, Bennett RD, Maier VP, King AD. 1972. Limonoate dehydrogenase from *Arthrobacter globiformis*. J Agric Food Chem 20:1031–1034.

Hasegawa S, Brewster LC, Maier VP. 1973. Use of limonoate dehydrogenase of *Arthrobacter globiformis* for the prevention or removal of limonin bitterness in citrus products. J Food Sci 38: 1153–1155.

Hernandez E, Couture R, Rouseff RL, Chen CS, Barros S. 1992. Evaluation of ultrafiltration and adsorption to debitter grapefruit juice and grapefruit pulp wash. J Food Sci 57:664–666.

Hewtter DJ, Wang HY. 1986. Protein released from chemically permeabilised *Escherichia coli*. In: Asenjo JA, Hong J, editors. Seperation, recovery and purification in biotechnology. ACS Symposium Series 314. Washington, DC: American Chemical Society. p 2–8.

Iborra JL, Manjon A, Canovas M, Lozano P, Martinez C. 1994. Continuous limonin degradation by immobilized *Rhodococcus fascians* cells in *k*-carragenaan. Appl Microbiol Biotechnol 41: 487–493.

Johnson RL, Chandler BV. 1988. Absorptive removal of bitter principles and titrable acid from citrus juices. Food Technol 45: 130–137.

Kimball DA. 1987. Debittering of citrus juices using supercritical carbon dioxide. J Food Sci 52:481–482.

Kimball DA. 1991. Bitterness in citrus juices Citrus processing: quality control technology. New York: Van Nostrand Reinhold. p 140–141.

Kimball DA, Norman SI. 1990. Processing effects during commercial debittering of California navel juice. J Agric Food Chem 38:1396–1400.

Kondo A, Liu Y, Furuta M, Fujita Y, Matsumoto T, Fukuda H. 2000. Preparation of high activity whole cell biocatalyst by permeabilization of recombinant flocculent yeast with alcohol. Enzyme Microbial Technol 27:806–811.

Konno A, Miyawaki M, Toda J, Wada T, Yasumatsu K. 1982. Bitterness reduction of naringin and limonin by β-cyclodextrin polymer. Agric Biol Chem 46:2203–2208.

Kumar SS, Kundu S, Pakshirajan K, Dasu VV. 2008. Cephalosporins determination with a novel microbial biosensor based on permeabilized *Pseudomonas aeruginosa*, whole cells. Appl Biochem Biotechnol 151:653–664.

Maier VP, Hasegawa S, Hera E. 1969. Limonin-d-ring lactone hydrolase. A new enzyme from citrus seeds. Phytochem 8:405–407.

Maier VP, Brewster LC, Hsu AC. 1973. Ethylene accelerated limonoids metabolism in citrus fruits: a process for reducing juice bitterness. J Agric Food Chem 21:490–495.

Manlan M, Mathews RF, Rouseff RL, Littell RC, Marshall MR, Moye HA, Texeira AA. 1990. Evaluation of the properties of polystyrene divinyl benzene adsorbents for debittering grapefruit juice. J Food Sci 55:440–445.

Marawaha SS, Puri M, Bhullar M, Kothari RM. 1994. Optimization of parameters for hydrolysis of limonin for debittering of kinnow mandarin juice by Rhodococcus fascians. Enzyme Microb Technol 16:723–725.

Martínez-Madrid C, Manjon A, Iborra JL. 1989. Degradation of limonin by entrapped *Rhodococcus fascians* cells. Biotechnol Lett 2:653–658.

Patil BS, Yu J, Dandekar DV, Toledo RT, Singh RK, Pike LM. 2006. Citrus bioactive limonoids and flavonoids extraction by supercritical fluids. In: Patil BS, Turner ND, Miller ED, Brodbelt JS, editors. Potential health benefits of citrus. vol. 1936. Washington, DC: American Chemical Society. p 18–33.

Pun A. 1984. Preparation and properties of citrus juices, concentrates and dried powders which are reduced in bitterness. US Patent 4439458.

Puri M, Kaur L, Marwaha SS. 2002. Partial purification and characterization of limonate dehydrogenase from *Rhodococcus facians* for the degradation of Limonin. J Microbiol Biotechnol 12:669–673.

Roy A, Saraf S. 2006. Limonoids: Overview of significant bioactive triterpenes distributed in plants kingdom. Biol Pharma Bull 29: 191–201.

Santos VAPMD, Heim S, Moore ERB, Strätz M, Timmis KN. 2004. Insights into the genomic basis of niche specificity of Pseudomonas putida KT2440. Environ Microbiol 6: 1264–1286.

Shaw PE, Wilson CW. 1983. Organic acids in orange, grapefruit and cherry juices quantified by high-performance liquid chromatography using neutral resin or propylamine columns. J Sci Food Agric 34:1285–1288.

Shaw PE, Tatum JH, Wilson CW, III. 1984. Improved flavour of navel orange and grapefruit juices by removal of bitter component with cyclodentrin polymer. J Agric Food Chem 32: 832–836.

Shaw PE, Moshonas MG, Hearn CJ, Goodner KL. 2000. Volatile constituents in fresh and processed juices from grapefruit and new grapefruit hybrids. J Agric Food Chem 48:2425–2429.

Sun C, Chen K, Chen Y, Chen Q. 2005. Contents and antioxidant capacity of limonin and nomilin in different tissues of citrus fruit of four cultivars during fruit growth and maturation. Food Chem 93:599–605.

Swaisgood HE. 1991. Immobilized enzymes: application to bioprocessing of food. Food Enzymol 2:309–341.

Vaks B, Lifshitz A. 1981. Debittering of orange juice by bacteria which degrade limonin. J Agric Food Chem 29:1258–1261.

Verma JP, Singh S, Shrivastava PK, Ghosh M. 2010. Identification and characterization of cellular locus of limonin biotransforming enzyme in *Pseudomonas putida*. Int J Food Sci Technol 45: 319–326.

Wagner JRCJ, Wilson CW, III, Shaw PE. 1988. Reduction of grapefruit bitter components in a fluidized P-cyclodextrin polymer bed. J Food Sci 53:516–518.

The Journal of Microbiology, October 2006, p. 473-479 Vol. 44, No. 5

Evidence of Indigenous NAH Plasmid of Naphthalene Degrading *Pseudomonas putida* PpG7 Strain Implicated in Limonin Degradation

Moushumi Ghosh*, Abhijit Ganguli, and Meenakshi Mallik

Department of Biotechnology and Environmental Sciences, Thapar Institute of Engineering and Technology, Patiala 147004, India

(Received February 3, 2006 / Accepted August 16, 2006)

A well characterized naphthalene-degrading strain, *Pseudomonas putida* PpG7 was observed to utilize limonin, a highly-oxygenated triterpenoid compound as a sole source of carbon and energy. Limonin concentrations evidenced a 64% reduction over 48 h of growth in batch cultures. Attempts were made to acquire a plasmid-less derivative via various methods (*viz*. Ethidium Bromide, SDS, elevated temperature & mitomycin C), among which the method involving mitomycin C (20 μg/ml) proved successful. Concomitant with the loss of plasmid in *P. putida* PpG7 strain, the cured derivative was identified as a lim$^-$ phenotype. The lim$^+$ phenotype could be conjugally transferred to the cured derivative. Based on the results of curing with mitomycin C, conjugation studies and presence of *ndo* gene encoding naphthalene 1,2 dioxygenase, it was demonstrated that genes for the limonin utilization were encoded on an 83 kb indigenous transmissible Inc. P9 NAH plasmid in *Pseudomonas putida Pp*G7 strain.

***Keywords*:** *Pseudomonas putida* PpG7, plasmid curing, NAH plasmid

The phenomenon of delayed bitterness in certain citrus fruit juices continues to represent an important economic impediment for the citrus industry worldwide, especially with regard to achieving consumer acceptability, of either processed or fresh products. Delayed bitterness has been attributed primarily to the formation of limonin, which is a highly oxygenated triterpene derivative (composed of a furan ring and an epoxide group) and belongs to a class of limonoids. The application of microorganisms as a tool for the conversion of bitter citrus juice to a non-bitter product relies on the existence of enzymes or whole bacterial cells capable of limonin metabolism. The successful use of microorganisms relies on the development of better insight into mechanisms adapted to limonin degradation. A few microorganisms assessed with regard to limonin degradation include *Arthrobacter globiformis*, (Hasegawa *et al.*, 1983), *Pseudomonas* 321-18 (Hasegawa *et al.*, 1974), *Acinetobacter* sp. (Vaks and Lifshitz, 1981), *Corynebacterium facians* (Hasegawa *et al.*, 1985) and *Rhodococcus fascians* (Martinez-Madrid *et al.*, 1989). Nevertheless no genetic characterization of the response of microorganisms to limonin has yet been conducted.

In view of the above we initiated studies of limonin metabolism via the exploration of limonin degradation ability in several strains of *Pseudomonas*, as the metabolic diversity of *Pseudomonas* has been thoroughly documented (Martinez-Madrid *et al.*, 1989). Here, we report for the first time, the ability of a well-characterized strain of *Pseudomonas putida* known as *Pp*G7 to utilize limonin as a sole carbon and energy source. Thus far this species has been shown repeatedly to carry out naphthalene oxidation via plasmid encoded naphthalene degradative pathway (Dunn and Gunsalus, 1973; Yen and Serdar, 1988) and also involved in degradation of other polycyclic aromatic hydrocarbons (PAHs) (Sanseverino, 1993). In this communication we describe our experiment designed to determine whether the indigenous NAH plasmid plays any role in limonin degradation.

Materials and Methods

Microorganism and culture conditions

Freeze dried culture of *Pseudomonas putida* PpG7 (DSM No. 4476) were obtained from Microbial Type Culture Collection and Gene Bank (MTCC1072), Institute of Microbial Technology (IMTECH), Chandigarh, India. The complete medium used for *Pseudomonas*

* To whom correspondence should be addressed.
(Tel) 91-175-239-3340/239-3481; (Fax) 91-175-239-3340
(E-mail) mghosh@tiet.ac.in

putida was Luria-Bertani Agar/Broth and limonin (Sigma, USA) or Naphthalene (Sigma, USA) used as carbon source in the minimal mineral medium 442 (Dunn and Gunsalus, 1973). All incubation was conducted at 30°C.

Growth of Pseudomonas putida PpG7 strain in limonin

Growth curve of *Pseudomonas putida* PpG7 was conducted with limonin (300 parts per million) as sole carbon source over time. *P. putida* was inoculated from log phase pregrown culture to minimal mineral medium containing limonin. Cultures were incubated at 30°C with agitation. Appropriate volumes of the culture were aseptically withdrawn from each set after every 4 h interval. The culture was then centrifuged for 2 min at 10,000 × g. The pellet was then re-suspended in 1 ml of saline and the optical density was recorded at a wavelength of 600 nm.

Residual limonin estimation

Limonin content was spectrophotometrically determined by a modified version of a previously described method (Vaks and Lifshitz, 1981). Aliquots (1 ml) of the culture were collected after regular growth intervals and centrifuged to create a cell-free extract. The 1 ml supernatant taken for estimation was extracted using 1 ml chloroform. The chloroform layer was separated out and kept overnight for drying. 500 µl chloroform was added to the beaker to dissolve limonin and 2.5 ml of Ehrlich reagent was prepared by mixing 0.1 g p-diamino benzaldehyde (Merck, Germany) to 3.0 ml acetic acid in 2.4 ml perchloric acid. The sample was then incubated for 30 min at room temperature and optical density was determined at 503 nm with appropriate controls.

Plasmid DNA extraction and molecular weight determination

The method described by Kado and Liu (1981) was modified for the extraction of indigenous plasmid of *P. putida*. Log-phase bacterial cells were washed in saline (0.85%) and centrifuged for 5 min at 10,000 × g. The cell pellet was resuspended in 100 µl E buffer (50 mM Tris acetate; pH 8.0). 200 µl of lysis buffer (3% SDS, 50 mM Tris; pH 12.0 using 0.1 M NaOH) mixed via gentle inversion. The mixture was incubated at 65°C for 30 min for complete lysis of cells. The crude lysate was then cooled at 4°C. 30 µl of phenol : chloroform : isoamyl alcohol was added to the lysates at a ratio of 24 : 24 : 1 and the tubes were inverted for mixing. Centrifugation was conducted for 25 min at 10,000 × g and 4°C. The supernatant was transferred into another fresh microfuge tube using a truncated tip. Sample (25 µl) was then mixed with 5 µl of loading dye, and subjected to 0.8% agarose gel electrophoresis for 3 h at 50 volts.

Aliquots of plasmid DNA were digested overnight at 37°C with ten units of various restriction enzymes (*Eco*RI, *Sma*I, Promega, USA). The fragments thus generated were then fractionated via electrophoreses on 0.7% agarose gel. The bands were then visualized under UV light, and digitized with the Mol Match program for calculations of molecular mass.

Plasmid curing

Plasmid curing was conducted in accordance with previously described method (Rheinwald *et al.*, 1973). Cells of *P. putida* (10^4 to 10^5 cfu/ml) from an overnight culture were inoculated in several tubes containing 5 ml of Luria broth and mitomycin C (Sigma, USA) in 5 µg increments at concentrations ranging from 5 to 25 µg/ml. Cultures were shaken at 30°C until growth became visible, as evidenced by turbidity. Aliquots from the highest concentration of mitomycin C that still allowed bacterial growth were then serially diluted and spread onto nutrient agar plates. Individual colonies were then tested on solid media for growth via replica plating on minimal media exposed to naphthalene vapors and on minimal media containing limonin (300 ppm). Colonies that proved unable to utilize naphthalene as sole carbon and energy source were tested for the presence of indigenous plasmid and those proved negative were further evaluated with regard to limonin degradation. The stability of the cured strains was monitored via the periodic cycling of cells under nonselective conditions and retesting for the ability to grow on naphthalene.

Calculation of curing frequencies

The frequency with which indigenous NAH7 plasmid of *Pseudomonas* was cured i.e. lost, as a result of mitomycin treatment, was calculated as described previously (Stephens and Dalton, 1987).

Amplification of gene encoding naphthalene 1, 2 dioxygenase located on the NAH7 plasmid

PCR was conducted to determine the presence of a catabolic gene *(ndo),* which is one of the genes responsible for Naphthalene degradation in *P. putida* G7. Primers *ndo* F; 5'-CACTCATGATAGCCTTGATTCCT GCCCCCGGCG-3' and *ndo* R; 5'-CCGTCCCACAA CACACCCATGCCGCTGCCG-3'were used, corresponding to positions 662 to 1663 on *P. putida*. Final concentrations of the reaction mix were 100 mM Tris–HCl (pH 8.0), 800 mM dNTP, 2.5 mM $MgCl_2$, and 2 U Taq polymerase (Amersham), reaction temperatures and times were arranged as follows: 96°C for 2min, 30 cycles at 94°C for 1 min, 55°C for 1 min. 72°C for 1 min and one cycle at 72°C for 7 min.

Generation of spontaneous mutants and conjugation by membrane filter mating

Prior to the conjugal mating between the wild type *P. putida* (donor) and the cured strain of *P. putida* (recipient), spontaneous mutants of wild type and cured *P. putida* were generated for resistance against antibiotic streptomycin (250 µg/ml) and rifampicin (100 µg/ml) respectively in order to generate selectable markers. Freshly prepared donor and recipient cultures were added to 5 ml Luria Bertani (LB) broth in tubes and incubated in a shaker (200 rpm) for 18 h at 30°C. Donor (3 ml) and recipient (2 ml) were mixed on a sterile petri dish and 3 ml were passed through sterile filter assembly with a 0.45 µm pore size membrane filter (Sartorius, Germany). The membrane was then placed onto the surface of Luria agar, and incubated for 24-48 h at 30°C. Mating was disrupted via vigorous shaking in 5 ml of sterile normal saline and serially diluted (10^{-2} to 10^{-8}). Each of the dilutions (0.1 ml) was spread into double antibiotic streptomycin-rifampicin containing Luria agar selective for transconjugants and recipients. The frequency of conjugation was then calculated as number of transconjugants divided by the number of recipient multiplied by the dilution factor. Simultaneously controls for donor and recipient were conducted in order to determine any spontaneous mutants.

Screening of transconjugants

The transconjugants on the Luria agar plates containing the antibiotics streptomycin and rifampicin were then replica plated on minimal media exposed to naphthalene vapors as well as on minimal media containing limonin. The plates were incubated at 30°C. Appropriate controls were utilized. The colonies evidenced growth both on limonin and naphthalene. Some colonies which proved unable to grow on limonin and naphthalene were evaluated for the presence of plasmids.

Results

Limonin utilization pattern by P. putida PpG7

A time course study was conducted to determine the rate of limonin utilization by *P. putida*. Thus, the growth of *P. putida* with limonin as sole carbon source and residual limonin levels in the media were monitored, as is shown in Fig. 1. A significant reduction of limonin content, 64% occurred in 48 h, and the residual limonin was shown to be only 36%. We also noted a proportionate reduction in the limonin content, occurring concomitantly with cell growth.

Interrelationship between optical density and viable cell numbers (biomass) of P. putida PpG7

In order to determine whether the structural gene encoding for enzymes implicated in limonin degradation is encoded for solely by the plasmid, it was essential to cure the wild-type strain of its indigenous NAH plasmid. *P. putida* samples were taken at different stages of growth and after the OD_{600} (LB-grown cultures) was recorded, a serial dilution was prepared and plated out, in duplicate, on LB agar. The number of viable cells was determined to be directly proportional to OD but only up to an OD of 1.0. Cultures with an OD values excess of 1.0 were therefore diluted with the same medium until they evidenced an OD below this threshold. An OD_{600} of 1.0 was determined to be equivalent 5.2×10^8 cells per ml.

Survival curve

An inoculum of *P. putida* (1.2×10^5 cells) was inoculated in LB-containing mitomycin C at different concentrations as well as LB without mitomycin C as a control. For each mitomycin C concentration, two tubes were prepared; one was inoculated with the

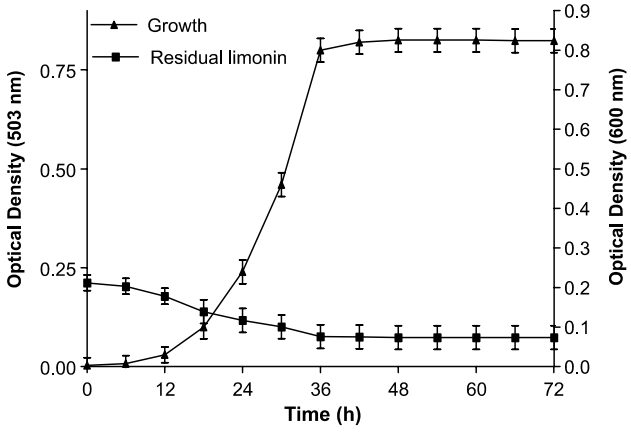

Fig. 1. Growth and limonin degradation profile of *Pseudomonas putida* PpG7.

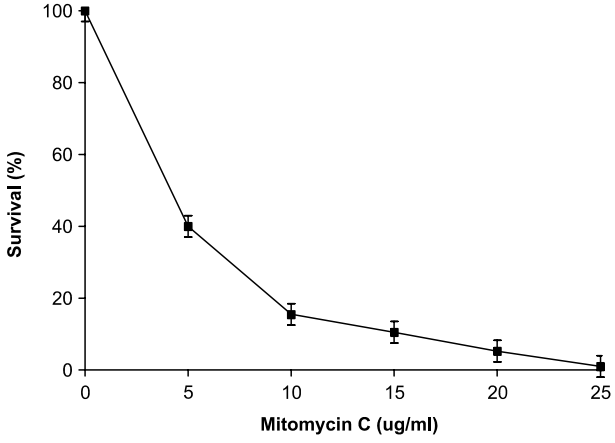

Fig. 2. Survival curve of *Pseudomonas putida* G7 as function of mitomycin C.

Table 1. Profile of four cured mutants

Putative cured derivatives	Growth on naphthalene (After 24 h)	Presence of *ndo* gene	Growth in limonin	Plasmid
PpC1	–	–	–	visible
PpC2	–	+	–	not visible
PpC3	–	–	–	not visible
PpC4	–	+	–	not visible

organism and the other was employed as a blank during the course of the experiment. After inoculation, the cultures were incubated with shaking at 30°C and OD_{600} values were intermittently determined. The number of viable cells was plotted as a function of mitomycin C (Fig. 2). A killing rate of 94.7% (±1.2, *n*=6) was observed in the presence of 20 ug/ml mitomycin C. Such a rate was considered sufficiently high for screening the remaining viable cells (5.3%) for plasmid loss. One ml of this culture was harvested, washed in 50 mM phosphate buffer pH 7.4, and resuspended in the same buffer to yield an OD_{600} of 1.0. A serial dilution was constructed in the same buffer and plated out on LB-agar plates then incubated overnight at 30°C. Among the resulting colonies, 1600 colonies were screened in terms of their ability to use naphthalene and limonin as sole carbon and energy sources. Among these, four colonies, viz. PpC1–PpC4, were selected. No growth was visible on naphthalene media after 24 h of incubation. However in two (PpC2, PpC4) colonies very faint growth was observed after 48 h. All the four suspected cured derivatives were further analyzed for plasmid loss. In only one of the four strains plasmid was visualized when resolved in agarose gel.

Molecular weight determination of plasmid

Aliquot of wild-type *P. putida* PpG7 indigenous plasmid were digested with two restriction enzymes *Eco*RI and *Sma*I in accordance with the recommended procedures. The resultant fragments were fractionated by agarose gel (0.7%) electrophoresis, as described in Materials and Methods. The fragments representing the genetic fingerprint of the plasmid were then fed into the Mol Match program for the determination of molecular weight, and the results indicated that the indigenous plasmid had a molecular mass in the region of approximately 83 kb (data not shown). This result is fully consistent with the size of NAH plasmid harbored by the previously reported PpG7 strain (Dunn and Gunsalus, 1973; Yen and Serdar, 1988).

Calculation of curing frequency

The data shown in table clearly demonstrate that out of four suspected cured derivatives (PpC1-PpC4); only one was a true cured strain (PpC3) as evidenced by utter loss of both plasmids, as well as its inability to grow on naphthalene as a sole carbon source. The other two cured strains viz. PpC2 and PpC4 appeared to have had the plasmid integrated into the genome, as evidenced by the absence of plasmid, but the very slow rate of growth on naphthalene. PpC1 was essentially a mutant, as the strain harbored the plasmid, but lost the ability to grow on naphthalene for one reason or another. According to these data and figures (Table. 1 and Fig. 2) a curing frequency with a mean of 4×10^{-4} i.e 1 per cell 1.6×10^{2}, (n=6), was calculated. Mitomycin C proved to be a very effective curing agent, as compared to other curing agents viz. EtBr, SDS, elevated temperature (data not shown).

Amplification of plasmid encoded ndo gene in P. putida PpG7

Total genomic DNA of all four suspected cured derivatives, as well as the DNA of the wild-type strain (control), were extracted and employed as templates for detection of of the *ndo* gene via PCR, using specific primers. Fig. 3 shows presence of bands approximately 640 bp in size in wild type and in other two of the four cured strains, viz. PpC2, PpC4. No bands were detected in PpC1 or PpC3. PpC3 was a true cured strain.

Verification of identity of the cured strain and confirmation of plasmid encoded limonin utilization

We then attempted to verify that cured strain was indeed a derivative of *P. putida* PpG7 and to confirm that the degradation of limonin is a plasmid-encoded function. The plasmid was transformed back to the cured strain via conjugation. The transconjugants obtained after screening (those growing on naphthalene) was once again monitored for the physical presence of plasmid as shown in Fig. 4. Also, it was determined to utilize limonin as a sole carbon and energy source.

Discussion

The diversity of complex carbon sources usable by *Pseudomonas* species led us to screen a number of known *Pseudomonas* species with regard to their ability

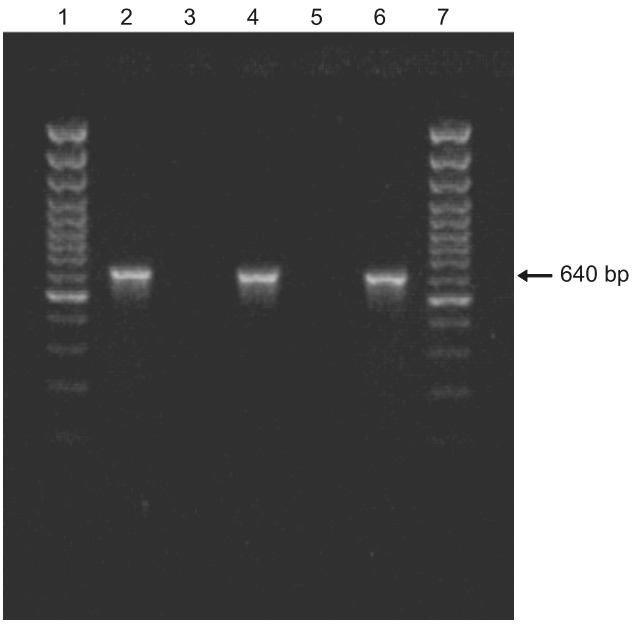

Fig. 3. Agarose (1.5%) gel of PCR products Lane 1, 100 bp ladder. Lane 2, presence of *ndo* gene encoding naphthalene 1, 2 dioxygenase (640 bp fragment) in wild-type PpG7. Lane 3, absence of *ndo* gene in PpC1 derivative. Lane 4, presence of *ndo* gene in PpC2 derivative. Lane 5, absence of *ndo* gene in PpC3 derivative. Lane 6, presence of *ndo* gene in PpC4 derivative. Lane 7, the 100 bp molecular weight marker.

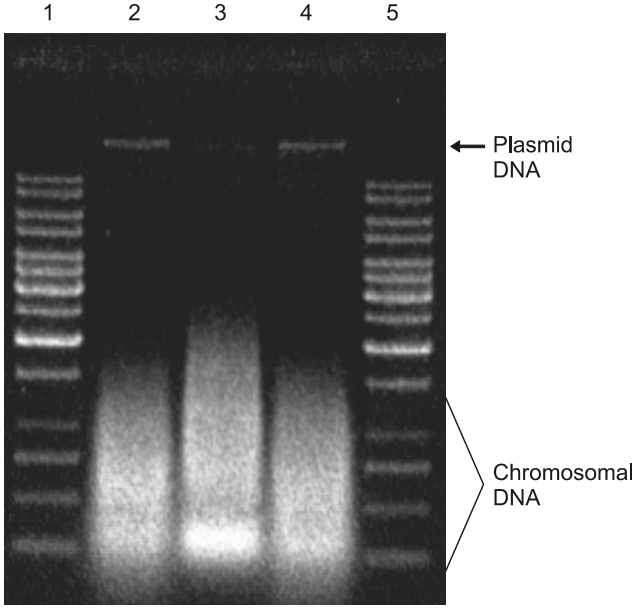

Fig. 4. Visualisation of plasmids in 0.7% agarose gel. Lane1, 1 kb molecular size marker. Lane 2, plasmid DNA of *Pseudomonas putida* G7 (wild-type) visualized by the method of Kado and Liu. Lane 3, DNA of cured strain absence of plasmid band. Lane 4, Plasmid DNA after conjugal transfer into cured derivative. Lane 5, 1 kb molecular size marker.

to utilize limonin as a sole carbon source. Among 14 strains of *Pseudomonas* thus far tested (data not shown) a well characterized strain of *Pseudomonas putida* PpG7 was determined to be the potential strain due to its ability to utilize limonin, a triterpenoid compound as sole source of carbon and energy. A significant reduction (64%) of limonin occurred at 48 h. Maximum reduction appears to occur during the exponential growth phase. However, as growth reaches saturation level and attains stationary phase we assume formation of other metabolites might render the cells unable to further utilize limonin (Furukawa and Chakrabarty, 1982; Chauhan and Jain, 2000; Thakur *et al.*, 2001). It was also previously reported (Williams and Murray, 1974; Chakrabarty, 1976) that plasmids harbored by the members of the genus *Pseudomonas* frequently harbor genetic information for the degradation of variety of organic compounds, thus contributing to the metabolic diversity of their hosts. Many of the exotic *Pseudomonas putida* phenotypes of predicated on plasmid encoded pathways which channelize substrates to metabolites that feed into central metabolic pathways (Timmis, 2001). Thus it became a focus of research to determine whether the indigenous NAH plasmid present in the strain PpG7 might be involved in limonin degradation. Loss of function at a rate higher than the expected rate of mutation and/or the ability to transfer a function to recipient cells are generally accepted properties that provide genetic evidence for the presence of a plasmid involved in conferring a particular function upon a cell. Also, curing of the indigenous plasmid from a bacterial strain is one effective by which the relationship between a genetic trait and the carriage of the specific trait within the plasmid can be substantiated (Trevors, 1986).

In a physical analysis and visualization of plasmid DNA conducted via a previously described method (Sanseverino *et al.*, 1993), a single large plasmid with a size 83 kb was determined to be present in this strain. Besides which, the test organism appeared to harbor no other small plasmid as several attempts with different isolation methods failed to reveal the presence of any other smaller plasmid. The size of the plasmid is also consistent with the earlier reports. It was clear that this plasmid belonged to the class of NAH plasmids and harbored genes that mediate naphthalene degradation pathway (Dunn and Gunsalus, 1973; Yen and Serdar, 1988). Phenotypes that have undergone a plasmid loss in *P. putida* PpG7 strain was easily screened principally on the basis of ability to grow on naphthalene (i.e. Nah^+/Nah^- phenotypes). As mentioned earlier the ability of this strain to utilize naphthalene as sole carbon and energy source is mediated by NAH plasmid. Attempts were made to acquire cured derivatives in order to determine the

role of the plasmid in degradation of limonin. The mutants which failed to grow in naphthalene medium (nah^-) were selected as this inability could be attributed to the loss of nah plasmid. Among variety of methods used for plasmid curing (viz. EtBr, SDS, and elevated temp.) success was only achieved when mitomycin C was used as curing agent (20 μg/ml). Mitomycin C owes its inhibitory activities to metabolic activation via reduction to a corresponding hydroquinone. The hydroquinone undergoes further changes, and generates a reactive intermediate, which can then react with the purine bases due to this type of nucleophilic attack; it inserts alkylating crosslinks between the two strands of double-stranded DNA. Any crosslink is sufficient to block transcription by RNA polymerase.

Concomitant with the loss of plasmid in the test organism *P. putida* PpG7 strain, all the cured derivatives were accessed for growth on limonin, cured derivatives no longer supported growth on limonin i.e. the true cured derivative turned out to be lim- phenotype. However loss of plasmid was encountered in three putative cured derivatives (PpC2, PpC3, PpC4) and nah^- trait was detected in only two of the four putative cured derivatives (PpC1, PpC3) (after 24 h of incubation time). Interestingly, out of these two, PpC1 evidenced the presence of plasmid whereas PpC3 did not. PpC1 appeared to have undergone mutation which may have resulted in the inactivation of the naphthalene catabolic gene. In case of PpC2, PpC4 plasmid remained undetected as they may have integrated into the genome of the test organism; consequently, the low copy number resulted in a reduced naphthalene (nah) catabolic activity. Another clear evidence for the identification of PpC3 as a true cured derivative resulted, when curing was verified in four putative cured derivatives via PCR analysis of total DNA. PCR products (640 bp) were detected in the wild-type as well as in three cured derivatives except for one, PpC3, in which the band corresponding *ndo* gene was absent.

Conjugation studies were conducted in an attempt to obtain Lim^+ phenotype. Transconjugants were obtained at a frequency of approximately 10×10^6 on the selection medium. The plasmid DNA isolated from these transconjugants was found to carry the same plasmid (approximately 83 kb), as was present in the wild type. Limonin degrading-ability was restored after plasmid was conjugally transferred into the cured strain. Therefore, on the basis of mutation, plasmid DNA isolation, conjugation studies and presence of *ndo* gene, it was clearly demonstrated that the genes for the limonin-degrading pathway are encoded on an indigenous NAH plasmid in the *Pseudomonas putida* PpG7 strain.

In conclusion, we report for the first time, the limonin utilization ability by the naphthalene-degrading *Pseudomonas putida* strain PpG7. However, whether direct linkage between plasmid-mediated catabolic genes implicated in naphthalene degradation with that of genes involved in limonin degradation has yet to be established. It appears that the highly oxygenated heterocyclic triterpenoid, limonin, due primarily to its structural resemblance with that of polycyclic aromatic hydrocarbons, may possess such metabolic potential. Moreover this report is of value in further resolving the as-yet-unknown plasmid mediated limonin degradation pathway.

Acknowledgments

This work was supported by Department of Science and Technology under SERC Fast Track Scheme for young scientists and by TIFAC under mission REACH, Govt. of India.

References

Chakrabarty, A.M. 1976. Plasmids in *Pseudomonas*. *Ann. Rev. Genet*. 10, 7-30.

Chauhan, A. and R.K. Jain. 2000. Degradation of o-Nitrobenzoate via Anthranilic Acid by *Arthrobacter protophormiae*. *Biochem. Biophys. Res. Commun.* 286, 109-113.

Dunn, N.W and I.C. Gunsalus. 1973. Transmissible plasmid coding early enzymes of naphthalene oxidation in *Pseudomonas putida*. *J. Bacteriol*. 114, 974-979.

Furukawa, K. and A.M. Chakrabarty. 1982. Involvement of plasmid in total degradation of chlorinated biphenyls. *Appl. Environ. Microbiol*. 44, 619-626.

Hasegawa, S., V.P. Maier, and A.D. King. 1974. Isolation of new limonoate dehydrogenase from *Pseudomonas*. *J. Agric. Food. Chem*. 22, 523-528.

Hasegawa, S., V.A. Pelton, and R.D. Bennet. 1983. Metabolism of limonoids by *Arthrobacter globiformis*. II. Basis for practical means of reducing the limonin content of orange juice by immoblized cells. *J. Agric. Food Chem.* 31, 102-107.

Hasegawa, S., C.E. Vander Cook, G.Y. Choi, and Z. Herman. 1985. Limonoid debittering of citrus juices by immobilized cells of *Corynebacterium fasciens*. *J. Food Sci*. 50, 330-338.

Kado, C.I. and S.T. Liu. 1981. Rapid procedure for detection and isolation of large and small plasmid. *J. Bacteriol.* 145, 1365-1373.

Martinez-Madrid, C., A. Manojon, and J.L. Iborra. 1989. Degradation of limonin by *Rhodococcus fascians* cells. *Biotech. Lett.* 2, 653-658.

Rheinwald, J.G., A.M. Chakrabarty, and I.C. Gunsalus. 1973. A transmissible plasmid containing camphor oxidation in *Pseudomonas putida*. *Proc. Natl. Acad. Sci. USA* 70, 1078-1089.

Sanseverino, J., B.M. Applegate, J.M. Henry King, and G.S. Sayler. 1993. Plasmid-Mediated Mineralization of Naphthalene, Phenanthrene and Anthracene. *Appl. Environ. Microbiol*.

59, 1931-1937.

Stephens, G.M. and H. Dalton. 1987. The effect of lipophilic acids on the segregational stability of TOL plasmids in *Pseudomonas putida. J. Gen. Microbiol.* 133, 1891-1899.

Thakur, I.S., P.K. Verma, and K.C. Upadhaya. 2001. Involvement of plasmid degradation of pentachlorophenol by *Pseudomonas* sp. From a chemostat. *Biochem. Biophys Res. Commun*. 286, 109-113.

Timmis, K. 2001. *Pseudomonas putida*: a cosmopolitan par excellence, *Env. Microbiol*. 4, 779-781.

Trevors, J.T. 1986. Plasmid curing in bacteria. *FEMS Microbiol. Rev.* 32, 149-157.

Vaks, B. and A. Lifshitz. 1981. Debittering of Orange juice by bacteria which degrade limonin. *J. Agric. Food Chem*. 29, 1258-1261.

Yen, K.M. and C.M. Serdar. 1988. Genetics of naphthalene catabolism in Pseudomonads. *Crit. Rev. Microbiol*. 15, 247-268.

Williams, P.A. and K. Murray. 1974. Metabolism of benzoate and the methyl benzoates by *Pseudomonas putida* mt-2: Evidence for existence of TOL plasmid. *J. Bacteriol.* 120, 416-423.

JOURNAL OF ADVANCED LABORATORY RESEARCH IN BIOLOGY

Title: Immobilization parameters statistically optimized for whole cells of *P. putida* G7 to enhance limonin biotransformation

Running title: Optimization of immobilization for *P. puitda*

Authors: Meenakshi Malik* and Moushumi Ghosh*

Affiliation: [a]Department of Biotechnology and Environmental Sciences, Thapar University, Patiala-147004, Punjab, India

Address for Correspondence:

Dr. Moushumi Ghosh*, Department of Biotechnology and Environmental Sciences,

Thapar University, Badson Road, Patiala-147004, Punjab, India

Email: mghosh@thapar.edu, Tel: +91-175-2393449, Fax: +91-175-2364498, 2393020

Abstract

This study was aimed for optimizing the immobilization parameters for Pseudomonas putida G7 in Ca-alginate beads, in order to establish a debittering strategy for citrus juices, by biotransforming the bitter principle - Limonin. Response Surface Methodology (RSM) with Central Composite Design (CCD) was employed to model the significant parameters for an enhanced response. An enhanced limonin bioconversion and immobilized bead stability was obtained with alginate concentration (2%), cell load (47.2 g/l), and a bead diameter (2.1 mm); which had significant effects ($p < 0.001$) on limonin biotransformation. The R^2 values of 0.9 showed good agreement between experimental and predicted response. Validation experiments under optimized parameters showed good association between experimental (limonin biotransformation and stability response of 65.8% and 0.97 OD respectively) and predicted responses (limonin biotransformation and stability of 65.1% and 0.094 respectively). Thus, the approach is promising to develop a strategy for debittering citrus juices by biotransforming limonin at a faster rate.

Introduction

Immobilized biocatalysts - whole microbial cells (viable or non viable) or their enzymes have some clear advantages over employing free cells in bioprocesses[1,2]. Cell immobilisation provides a physical incarceration or localization of microbial cells or enzymes to a certain defined space for the preservation of certain desired catalytic activity and subsequent continuous operation stability[3]. Industrial application of immobilized enzymes has been limited due to several factors like low stability, low recovery, low yield and expensive steps involved in isolation and purification of enzymes. Therefore, whole cell immobilization has been employed and offers many advantages over immobilized or free enzymes and free microbial cells. This method is cost effective, offers continuous operational stability and carry out multi-step cofactor requiring bioconversion[4,5] with minimum downstream processing, decreased product inhibition, simplified biocatalyst recovery, high reusability of cells, relative ease of product separation, high volumetric productivity and reduced susceptibility of cells to contamination[6]. Microbial cells and their enzymes (both in free form and immobilized forms) have been employed for the development of strategies for the eradication of bitterness from the citrus juices[7,8]. Among the various limonoids in citrus juices, limonin – a triterpenoid dilactone is a major cause which imparts bitterness to the citrus juices and is a hindrance for the citrus industries worldwide, in terms of bitterness and "delayed bitterness"[7,9,10]. The negative impact created by bitter taste in citrus juices made debittering a generally incorporated step in industrial juice processing technology. Previous studies explaining the usage of various immobilizing matrixes (for immobilizing various limonin degrading microbes for debittering citrus juices) like polyacryl amide gel, k-carrageenan and polyurethane foam has faced a number of constraints like

limitations for human consumption, low stability matrix at low pH of juice and delayed reduction of bitterness in citrus juices[11].

Various immobilization materials and techniques are being developed, making the immobilized biocatalysts more reachable for industrial applications. Entrapment technique has proved to be most significant of all immobilization techniques, for immobilizing whole cells into gel matrices[12]. Entrapment of living microbial cells in gel matrix of alginate has proved to be quite promising and has been widely used and the technique being simple, fast, cost effective, biocompatible, chemically inert, functional in the organic phase or biphasic system[13-15]. However, immobilized system faces a limitation of diffusional resistances to both substrate and product formed, which in turn determine the overall yield or biotransformation. Various physiological factors such as alginate concentration, cell loading and bead diameter are considerable parameters for immobilization[16]. Therefore, optimization of such parameters is an important prerequisite.

Response surface methodology (RSM) is a collection of statistical technique that has been applied successfully in biotechnology, for optimization and evaluation of significant parameters for desired responses in various processes[17,18]. The conventional approach is time consuming and involves variation of one variable at a time, and limits the evaluation of the combined effects of all the factors involved in the process. Based on the multivariate non-linear model (which reduces the number of experiments, improves statistical interpretation possibilities, reduction in number of experiments and time required for overall analysis), RSM is useful for the evaluation and better understanding of the interactions of the various significant parameters within a limited number of experiments[19,20].

The objective of this study was to employ response surface methodology for the best optimization of immobilization parameters (alginate concentration, cell load, and bead diameter) and to detect their interaction and combined effects to obtain maximum response (activity and stability).

MATERIALS AND METHODS

Microorganism and Culture Conditions

The lyophilized bacterial strain of *P. putida* G7 (MTCC 1658) was procured from microbial type culture collection and gene bank (MTCC), Institute of Microbial Technology (IMTECH), Chandigarh. The nutrient medium for *P. putida G7* was Luria-Bertani broth and mineral minimal medium (M63) supplemented with 0.5% limonin. The strain was grown with shaking at 150 rpm at 30^{o}C. The log phase cultures were used for agar and calcium alginate immobilization. All chemicals were purchased from Merck (Darmstad, Germany), except Na-alginate and agar, which were purchased from Sigma (St Louis, MO, USA).

Immobilization of whole cells

The limitation and low response of immobilization by adsorption and attachment[21,22] zzas compared to entrapment method, has helped to choose entrapment method for this study. The bacterial cells of *P. putida* G7 were immobilized by entrapment using different matrices like agar and sodium alginate as explained by Tapingkae et al. (2010). A sterile standard buffer containing a range of 0.5 % to 4 % (w/v) of sodium alginate and agar (Sigma, St Louis, MO, USA) were prepared by autoclaving it at 121°C (15 psi) for 15 min. Both the immobilizing solutions (Na-alginate and agar solution of variable concentrations) (2.5 ml) at 50°C were mixed with 2.5 ml of buffer containing 1 g of wet weight of cell at 60°C. Sterile syringes (2 ml) were then filled with the cell/alginate and cell/agar solutions and 0.5 ml was dropped through a 0.45 mm x 12 mm

needles into a 25 ml of stirring 0.2 M chilled $CaCl_2$ solution respectively. Another set of beads were prepared with Na- alginate and agar which does not harbored any bacterial cells and were taken as control. Each set of beads were transferred to sterile tubes and were kept in shaking condition in a 0.3 M $CaCl_2$ solution over night at 4°C.

Several different cell loads of 5, 10, 20, 30, 40, 50, 60 mg/ml were also used for immobilization with variable bead diameters of 1 -4 mm, during the maximum limonin biotransformation in citrus juice using immobilized cells.

Limonin biotranformation in citrus juices using immobilized cells of *P. putida* G7

The log phase revived culture of *P. putida* G7 with variable cell loads were used in immobilized forms (agar and Na-alginate), for limonin biotransformation in the citrus juice (100ml), taken in an Erlenmeyer flask and incubated at 30ºC. The regular aliquots of the juice sample from all the sets of free and immobilized (agar and Na-alginate) were aseptically withdrawn at a regular intervals of one hour, till 36 hours. The aliquots were centrifuged at 10,000 rpm for 2 minutes at 4ºC. The pellet was then resuspended in 1 ml of saline (0.85% NaCl) and the optical density was recorded at a wavelength of 600 nm.

Estimation of cell mass and viability

Cell growth was determined spectrophotometrically at 600 nm and converted to cell count using a conversion factor (one unit at 600 nm was equivalent to 10^5 CFU/ml, which corresponded to 28 mg protein that was calculated by plotting standard graphs). In case of all immobilized conditions (agar and Na-alginate), 5 beads were dissolved in 2ml of phosphate buffer (pH 7.0) and cells were collected by centrifugation at 5000 rpm at 37°C and were used for cell mass measurement, by serial dilution plate count method on luria agar plates and incubation at at 37°C for 24 h. At the end of each batch, the cell densities in the beads were enumerated using similar

method to study the total cell loss upon repeated use. Viable cell counts were performed in duplicates and expressed in CFU/ml of immobilized beads.

Estimation of limonin biotransformation

The extraction and quantification of biotransformed limonin in the supernatant of the aliquots was done by estimating the residual limonin as explained by Vaks et al. (1981). One milliliter of the solution containing limonin was extracted with 2ml chloroform. The chloroform was evaporated to dryness and the residue was dissolved in 0.2ml of chloroform. The limonin content was measured by developing it with 2.5ml reagent (0.1g of 4-(dimethylamino) benzaldehyde; 3ml of acetic acid, and 2.4ml of 70% perchloric acid). The red color that fully developed after 30 min had maximal absorbance at 503 nm. The limonin in the unknown samples was estimated from a standard curve of pure limonin prepared similarly.

Selection of immobilisation method

Whole cells immobilised by entrapment in agar and Na-alginate were analyzed for the limonin biotransformation activity, protein loading ratio, and immobilization yield, which were defined as explained by Tapingkae et al. (2010) as follows:

Biotransformation activity (units/g matrix) = Activity of immobilised whole cells (units) / Actual weight of cell immobilised (g)

Protein loading ratio (%) = Amount of protein bound (mg) / Amount of protein loaded (mg) x100%

Immobilisation yield (%) = Total activity of immobilised whole cells (units) / Total activity of free whole cells (units) x 100%

The immobilization method providing the maximal immobilization yield was chosen for further study.

Statistical optimization

After several preliminary tests based on one - factor experimental results, three critical parameters were selected which have a significant effect on whole cell immobilization. The Na-alginate concentration (X_1), Cell load (X_2) and bead diameter (X_3) were selected for further optimization. Response Surface Methodology (RSM) with Central Composite Design (CCD) was employed to detect the optimum levels and the interaction of significant variables. Table 1 represents the coded and non-coded values of the significant experimental variables at five coded ($-\alpha$, -1, 0, +1, $+\alpha$) levels. The zero levels of all the variables constitute to the central points while combination of experimental variables consisting of one at its lowest level (-1) and its highest (+1) levels. A total of 20 experimental runs with different combinations of the significant parameters were carried out in triplicate that were important to estimate the response (Mean of the triplicates). The relationship of the significant parameters and their response (limonin biotransformation and bead stability) was calculated by a second order polynomial equation.

$$Y= \beta_0 + \Sigma \beta_i \times X_i + \Sigma \beta_{ii} \times X_i^2 + \Sigma \beta_{ij} \times X_{ij}$$

where Y is the predicted response, X_i is the independent variable, β_0 is the intercept term, β_i the linear effect, β_{ii} the squared effect, and β_{ij} the interaction effect.

Design Expert software package (Version 2.05, Stat-Ease Inc., Minneapolis, USA) was used to estimate the response of dependent parameters and their optimum levels. Reusability of the immobilized microbial cells and free cells were evaluated under the optimized levels of significant variables.

Results and Discussion

Conventional studies

Among the various preliminary experiments performed for the selection of process parameters effecting limonin biotransformation in citrus juice, alginate concentration, cell load and bead diameter were screened as the most significant parameters for maximal limonin biotransformation by immobilized *P. putida* G7. Limonin in citrus juice was biotransformed upto 40% and 58% with *P. putida* G7 cells (cell load of 50 mg/ml) immobilized in agar and alginate respectively (Figure 1). Biotransformation response with cell immobilized in agar (concentration of 2.5% and bead diameter of 2.0 mm) was lower i.e. 30%, as compared to the cells immobilized in alginate (concentration of 3% and bead diameter of 2.5 mm) which showed a response of 57% in citrus juice (Figure 2). Based on the response of conventional studies, alginate was preferred as a matrix for immobilizing *P. putida* G7 cells to direct the further studies for limonin biotrasformation in citrus juices.

Statistical analysis

The combined effect or the inter-relationship of the parameters for limonin biotransformation response was observed with a face centred cube design of 2^3=8 + 6 centre points and 6 (2x3) star points which lead to a total of 20 experiments. Based on the optimization of process parameters and the experimental results (obtained from CCD and regression analysis) (Table 2), the relationship between the limonin biotransformation and the significant parameters (alginate concentration, cell load and bead diameter) was established in the form of a quadratic polynomial equation. The equation for the model in terms of coded factors is as follows:

Limonin biotransformation (R1)= +64.43 +0.70 * A +2.56 * B +1.40 * C -2.60 * A * B -1.07* A * C -0.37 * B * C -0.28 * A^2 -3.42 * B^2 -1.60 * C^2

Where Y is the response value for limonin biotransformation (%), A- Alginate concentration, B-Cell Load, C- Bead diameter, R1-Limonin Biotransformation (%), R2- Stability (O.D. 600 nm).

The analysis of variance (ANOVA) of the model for limonin biotransformation are presented in Table 3. The F value (14.97) of the model signifies the significane of the model and there was only 0.01 % chance that the model F value must have occurred due to noise. Regression analysis results has revealed R^2 (coefficient of determination, and the value more closer to 1 indicates the model fit of the experimental data) value of 0.9309, which signifies that the model was enable to explain only 7% of the total variations. The adjusted R^2 (adjusted determination coefficient) value of 0.8687 was quite high which indicates the high reliablity of the model and the quadratic polynomial equation. The values of "Prob>F" of the model far less than 0.05, indicates the significant and desirability of the model terms. The "Lack of Fit F-value" of 843.93 implies the Lack of Fit is significant. There is only a 0.01% chance that a "Lack of Fit F-value" this large could occur due to noise. "Adeq Precision" measures the signal to noise ratio (a ratio greater than 4 is desirable) and the ratio of 12.862 indicates an adequate signal. A low value of CV (coefficient of variation) of 2.76% signifies a high degree of precision and a good deal of realiablity of the experimental values. Accoring to this model, the significant parameters A-B has shown the highest interaction effect, followed by A-C and B-C with the least interaction, for the maximal response of limonin biotransformation.

The experimental relationship between stablity of the beads (response) and the three significant parameters in the coded values is presented as:

Stability (R2) = +0.11 +0.017*A + 8.660E - 003*B + 6.983E-003*C - 0.013*A*B - 7.625E-003*A*C -3.125E-003*B*C + 6.058E-003*A^2 +3.407E - 003* B^2 + 0.013*C^2

Where Y is the response value for limonin biotransformation (%), A- Alginate concentration, B- Cell Load, C- Bead diameter, R1-Limonin Biotransformation (%), R2- Stability (O.D. 600 nm). This response is of great importance in estimating the bead scabrousness for their potential to withstand mechanical stress[23]. The analysis of variance (ANOVA) for this model is presented in Table 4.

The F value (14.97) of the model signifies the significane of the model and there was only 0.01 % chance that the model F value must have occurred due to noise. Regression analysis results presenting the R^2 (coefficient of determination) and adjusted R^2 (adjusted determination coefficient) values of 0.9253 and 0.8581 respectively, was quite high which indicates the high reliablity of the model and the quadratic polynomial equation. The values of "Prob>F" of the model far less than 0.05, indicates the significant and desirability of the model terms. The "Lack of Fit F-value" of 5.31 implies the Lack of Fit is significant and the corresponding 0.01% chance that a "Lack of Fit F-value" this large could occur due to noise. "Adeq Precision" ratio value of 12.683 indicates an adequate signal which signifies a high degree of precision with a good deal of realiablity of the experimental values. According to this model, the significant varibales A-B has shown the highest interaction effect, followed by A-C and B-C with the least interaction, for the maximal response of high stability of the alginate beads.

RSM analysis

The response model developed was further represented in the form of contour plots for a better understanding of the interaction among the three significant parameters and for the detection of the optimum level of each parameter for a maximum response. The contours plot showed the interaction of two independent parameters when the third parameter is fixed at zero (Figure 3 a-

c), which represents the limonin biotransformation response. Limonin biotransformation increases moderately with increasing alginate concentration from 2% to 3% (w/v), with a high increase in cell load results in high biotransformation (Figure 3a). Fig. 3b demonstrates that response increases moderately with increase in bead diameter and alginate concentration. An increased response was observed with increase in cell load, and bead diameter (Figure 3c). The increase in limonin biotransformation when alginate concentration is increased (2-3%) can be a due to the facilitation of mass transfer rate of the substrate and product formed[24-27]. The increase in response with an increase in bead size and cell load can be attributed with effective utilization of the total cell load for limonin bioconversion, within an increased bead space which had protected the reaction from the unfavorable external pH of the juice.

The contours for stability with regard to the significant parameters of alginate concentration, cell load, and bead diameter are presented in Figure 4a-c. Figure 4a shows that higher stability could be obtained at a moderate alginate concentration and low cell load. Figure 4b dictates that stability increases with an increased bead diameter and at a moderate alginate concentration. Low cell load and a moderate bead diameter directs towards an increased response for stability (Figure 4c). Moderate concentration of alginate supports for stable beads as low concentrations causes cell leakage due to flimsy beads and high concentrations of alginate directs the beads to a brittle nature[24,28,29].

Validation of the model

The experimental model was validated by considering both activity and stability for a high limonin biotransformation and low OD600 nm responses, with the help of the regression equation. The experimental reactions (100 ml Erlenmeyer flask containing 50 ml citrus juice) with immobilized cells, for the maximum response included an alginate concentration of 2%, a

cell load of 47.2 g/l, and a bead diameter of 2.1 mm. The predicted values for the maximum response of limonin biotrasformation and stability giving these conditions were 65.1% and 0.094 respectively. The experiments were conducted in triplicates and maximum response with all the optimized conditions were 65.8% and 0.97 OD.

Reusability of immobilized cell

The reusability of the immobilized cells *P. putida* G7 was compared with free cells (20 beads, equivalent to 47 mg/ml cells and free cells - 47 mg/ml cells), for the evaluation of limonin biotransformation under the optimized parameters, at the original pH of citrus juice (4 pH) and at 35°C.

The immobilized bacterial cells and free cells were evaluated for their biotransformation potential in successive cycles. After each cycle the alginate beads were filtered and the free cells were collected by centrifugation, washed with saline and phosphate buffer and were then reused for limonin biotransformation in the next set of citrus juice. All the reactions conditions were kept constant for every batch cycle. The biotransformation reaction was carried out for 3 hr and the bioconversion during each cycle by immobilized and free cells is presented in Figure 5. The results depict a faster bioconversion and high reusability (till 8th cycle) of immobilized cells as compared to free cells (till 5^{th} cycle). This high performance of the immobilized cells indicates towards the higher rate of limonin biotransformation by *P. putida* G7, which indicate that the immobilization matrix has protected the cells from the external environment (low pH and other cell activity hampering essential oils or inhibitors in the juice), for a better performance. The optimization of immobilization parameters for immobilizing bacterial cells to get an enhanced response for limonin biotransformation of 65% in a time span of 3 hr has an advantage over the

other immobilizing matrices used so far (which shows a delayed limonin biotransformation in upto 50-60 hrs)[29].

Conclusion

The employment of immobilized *P. putida* G7 cells for an enhanced limonin biotransformation in a very short span of time, under optimized conditions, proves to be a promising technology for debittering citrus juices. This study indicates the significance and essentiality of statistical tools like RSM, for optimization of process parameters in order to improve the respective response.

Acknowledgement

This work was supported to M. Malik, as Senior Research Fellowship by Council of Scientific and Industrial Research, Human Research Development Group, New Delhi is duly acknowledged.

References

1) Krasaekoopt, W., Bhandari, B. and Deeth, H. (2003). Evaluation of encapsulation techniques for probiotics for yogurt. Int. Dairy J 13: 3-13.
2) Birgisson, H., Wheat, J.O., Hreggvidsson, G.O., Kristjansson, J.K. and Mattiasson, B. (2007). Immobilization of a recombinant *Escherichia coli* producing a thermostable a-L-rhamnosidase: creation of a bioreactor for hydrolyses of naringin. Enz Microbiol & Technol, 40: 1181–1187.
3) Karel, S.F., Libicki, S.B. and Robertson, C.R. (1985). The immobilization of whole cells: engineering principles. Chemical Eng & Sci 40: 1321–1354.
4) Haiau, L.T., Lee, W.C. and Wang. F.S. (1997). Immobilization of whole-cell penicillin G acylase by entrapping within polymethacrylamide beads. Appl Biochem Biotech 62: 303–315.

5) Babu, P.S.R. and Panda, T. (1991). Studies on improved techniques for immobilizing and stabilizing penicillin amidase associated with *E. Coli* cells. Enz Microbial Tech. 13: 676–682.

6) Bernal, V., Sevilla, Á., Cánovas, M., Iborra, J.L. (2007). Production of L-carnitine by secondary metabolism of bacteria. Microbial Cell Factories 6: 31–48.

7) Hasegawa, S. and Maier, V.P. (1983). Solutions to the limonin bitterness problem of citrus juices. Food Technol. 37: 73–77.

8) Canovas, M., Garcia-Cases, L. and Iborra, J. (1998). Limonin consumption at acidic pH values and absence of aeration by *Rhodococcus fascians* cells in batch and immobilized continuous systems. Enz Microbial Technol. 22: 111–116.

9) Sun, C., Chen, K., Chen, Y. and Chen, Q. (2005). Contents and antioxidant capacity of limonin and nomilin in different tissues of citrus fruit of four cultivars during fruit growth and maturation. Food Chem. 93: 599–605.

10) Roy, A. and Saraf, S. (2006). Limonoids: Overview of significant bioactive triterpenes distributed in plants kingdom. Biological Pharma Bullet. 29: 191–201.

11) Canovas, M., Garcia-cases, L. and Iborra, J.L. (1996). pH influence on the consumption of limonin species by *Rhodococcus fascians* cells. Biotechnol Lett. 18: 423-428.

12) Willaert, R.G., De Backer, L. and Baron, G.V. (1996). Mass transfer in immobilised cell systems. In: Willaert, R. G., Baron, G. V., De Backer L (eds) Immobilised living cell systems: modelling and experimental methods. John Wiley & Sons, Chichester, England, pp 21–45.

13) Gervais, T.R., Carta, G. and Gainer, J.L. (2003). Asymmetric synthesis with immobilized yeast in organic solvents: equilibrium conversion and effect of reactant partitioning on whole cell biocatalysis. Biotechnol Prog. 19: 389–395.

14) Li, Y.G., Xing, J.M., Xiong, X.C., Li, W.L., Gao, H.S. and Liu, H.Z. (2008). Improvement of biodesulfurization activity of alginate immobilized cells in biphasic systems. J Industrial Microbiol Biotechnol. 35: 145–150.

15) Garikipati, S.V.B.J., McIver, A.M., Peeples, T.L. (2009). Whole-cell biocatalysis for 1-naphthol production in liquid–liquid biphasic systems. Appl Environ Microbiol. 75: 6545–6552.

16) Dwevedi, A. and Kayastha, A.M. (2009). Optimal immobilization of beta-galactosidase from Pea (PsBGAL) onto Sephadex and chitosan beads using response surface methodology and its applications. Biores Technol. 100: 2667–2675.

17) Lee, J.H., Chae, M.S., Choi, G.H., Lee, N.K. and Paik, H.D. (2009). Optimization of medium composition for production of the antioxidant substances by *Bacillus polyfermenticus* SCD using response surface methodology. Food Sci Biotechnol. 18: 959–964.

18) Potumarthi, R., Subhakar, C., Pavani, A. and Jetty, A. (2008). Evaluation of various parameters of calcium-alginate immobilization method for enhanced alkaline protease production by *Bacillus licheniformis* NCIM-2042 using statistical methods. Bioresour Technol .99: 1776–1786.

19) Goksungur, S., Dagbagli, A. and Ucan, G.U. (2005). Optimization of pullulan production from synthetic medium by *Aureobasidium pullulans* in a stirred tank reactor by response surface methodology. J Chemical Technol Biotechnol. 80**:** 819–827.

20) Roig, M.G, Pedraz, M.A., Sanchez, J.M., Huska, J. and Toth, D. (1998). Sorption isotherms and kinetics in the primary biodegradation of anionic surfactants by immobilized bacteria: II *Comamonas terrigena* N3H. J Molecular Catalysis B: Enzymatic 4: 271–281.

21) Tapingkae, W., Parkin, K.L., Tanasupawat, S., Kruenate, J., Benjakul, S. and Visessanguan, W. (2010). Whole cell immobilisation of *Natrinema gari* BCC 24369 for histamine degradation. Food Chem. 120: 842-848.

22) Vaks and Lifshitz A. 1981. Debittering of orange juice by bacteria which degrade limonin. J Agric Food Chem. 29: 1258-1262.

23) Ertan, F., Yagar, H. and Balkan, B. (2007). Optimization of a-amylase immobilization in calcium alginate beads. Preparative Biochem Biotechnol. 37: 195–204.

24) Zhang, C.H., Ma, Y.J, Yang, F.X., Liu, W. and Zhang, Y.D. (2009). Optimization of medium composition for butyric acid production by Clostridium thermobutyricum using response surface methodology. Bioresour Technol. 100: 4284–4288.

25) Lei, L., Zhao, M. and Wang, Y. (2007). Immobilization of lactase by alginate-chitosan microcapsules and its use in dye decolorization. World J Microbiol Biotechnol. 23:159–166.

26) Urkut, Z., Dagbagli, S. and Goksungur, Y. (2007). Optimization of pullulan production using Ca-alginate-immobilized Aureobasidium pullulans by response surface methodology. J Chemical Technol Biotechnol. 82: 837–846.

27) Niladevi, K.N. and Prema, P. (2008). Immobilization of laccase from Streptomyces psammoticus and its application in phenol removal using packed bed reactor. World J Microbiol Biotechnol. 24: 1215–1222.

28) Elibol, M. and Moreira, A.R. (2003). Production of extracellular alkaline protease by immobilization of the marine bacterium *Teredinibacter turnirae*. Process Biochem. 38: 1445-50.

29) Iborra, J.L., Manjon, A. and Canovas, M. (1996). Immobilization in carrageenans. In: Bickerstaff E (ed) Methods in biotechnology, vol.I: immobilization of enzymes and cells. Humana, New Jersey, pp 53–60.

Tables:

Table 1 Coded and noncoded values of the experimental variables

Variables	**Coded Values**				
	-α	**-1**	**0**	**+1**	**+ α**
A- Alginate concentration (%, w/v)	0.32	1	2	3	3.68
B- Cell load (mg/ml)	36.5	40	45	50	53.41
C-Bead diameter (mm)	1.16	1.5	2	2.5	2.84

Table 2 Response surface central composite design (CCD) and experimental limonin biotransformation

Std. Order	Runs	A	B	C	Experimental (R1)	Predicted (R1)	Experimental (R2)	Predicted (R2)
1	10	1.00	40.00	1.50	49.7	50.42	0.07	0.072
2	8	3.00	40.00	1.50	61.8	59.17	0.16	0.15
3	11	1.00	50.00	1.50	62.7	61.49	0.13	0.12
4	13	3.00	50.00	1.50	60.1	59.83	0.138	0.15
5	4	1.00	40.00	2.50	56	56.12	0.12	0.11
6	15	3.00	40.00	2.50	59.5	60.57	0.15	0.15
7	18	1.00	50.00	2.50	63.2	65.69	0.138	0.14
8	9	3.00	50.00	2.50	60.6	59.74	0.145	0.14
9	2	0.32	45.00	2.00	63.8	62.47	0.089	0.094
10	17	3.68	45.00	2.00	63.3	64.83	0.15	0.15
11	1	2.00	36.59	2.00	50.1	50.45	0.092	0.10
12	14	2.00	53.41	2.00	59.2	59.05	0.132	0.13
13	3	2.00	45.00	1.16	55.6	57.54	0.126	0.13
14	19	2.00	45.00	2.84	64	62.25	0.15	0.15
15	16	2.00	45.00	2.00	64.5	64.43	0.11	0.11
16	7	2.00	45.00	2.00	64.4	64.43	0.11	0.11
17	20	2.00	45.00	2.00	64.5	64.43	0.11	0.11
18	12	2.00	45.00	2.00	64.4	64.43	0.1	0.11
19	6	2.00	45.00	2.00	64.3	64.43	0.11	0.11
20	5	2.00	45.00	2.00	64.5	64.43	0.11	0.11

[a]Alginate concentration, B- Cell Load, C- Bead diameter, R1-Limonin Biotransformation (%), R2- Stability (O.D. 600 nm)

Table 3 Analysis of variance (ANOVA) of the model for limonin biotransformation

Source	**Sum of Squares**	**df**	**Mean Square**	**F Value**	**p-value Prob > F**	
Model	379.49	9	42.17	14.97	0.0001	significant
A-Alginate conc.	*6.69*	*1*	*6.69*	*2.38*	*0.1543*	
B-Cell load	*89.21*	*1*	*89.21*	*31.67*	*0.0002*	
C-Bead diameter	*26.79*	*1*	*26.79*	*9.51*	*0.0116*	
AB	*54.08*	*1*	*54.08*	*19.20*	0.0014	
AC	*9.24*	*1*	*9.24*	*3.28*	0.1001	
BC	*1.12*	*1*	*1.12*	*0.40*	0.5416	
A^2	*1.09*	*1*	*1.09*	*0.39*	0.5476	
B^2	*168.74*	*1*	*168.74*	*59.91*	<0.0001	
C^2	*36.94*	*1*	*36.94*	*13.12*	0.0047	
Residual	28.16	10	2.82			
Lack of Fit	*28.13*	*5*	*5.63*	*843.93*	*< 0.0001*	significant
Pure Error	*0.033*	*5*	*6.667E-003*			
Cor Total	407.66	19				

Table 4 Analysis of variance (ANOVA) of the model for stability

Source	**Sum of Squares**	**df**	**Mean Square**	**F -value**	**p- Value Prob > F**	
Model	0.010	9	1.157E-003	13.76	0.0002	**significant**
A-Alginate conc.	*4.133E-003*	*1*	*4.133E-003*	*49.16*	*< 0.0001*	
B-Cell load	*1.024E-003*	*1*	*1.024E-003*	*12.18*	*0.0058*	
C-Bead diameter	*6.659E-004*	*1*	*6.659E-004*	*7.92*	*0.0183*	
AB	*1.378E-003*	*1*	*1.378E-003*	*16.39*	0.0023	
AC	*4.651E-004*	*1*	*4.651E-004*	*5.53*	0.0405	
BC	*7.812E-005*	*1*	*7.812E-005*	*0.93*	0.3578	
A^2	*5.289E-004*	*1*	*5.289E-004*	*6.29*	0.0310	
B^2	*1.672E-004*	*1*	*1.672E-004*	*1.99*	0.1888	
C^2	*2.288E-003*	*1*	*2.288E-003*	*27.21*	0.0004	
Residual	8.407E-004	10	8.407E-005			
Lack of Fit	*7.074E-004*	*5*	*1.415E-004*	*5.31*	*0.045*	**significant**
Pure Error	*1.333E-004*	*5*	*2.667E-005*			
Cor Total	0.011	19				

Figure Captions

Figure 1 Effect of cell load concentration (mg/ml) in alginate beads on limonin biotransformation

Figure 2 Effect of alginate and agar concentration (%) with their respective bead size (mm) on limonin biotransformation with immobilized *P. puitda* G7 cells

Figure 3 Contour plots of limonin biotransformation which depicts the interaction among **a.** alginate concentration (%) and bead diameter (mm), **b.** alginate concentration (%) and cell load(mg/ml) **c.** bead diameter and cell load (mg/ml)

Figure 4 Contour plots of stability which depicts the interaction among **a.** alginate concentration (%) and cell load (mg/ml), **b.** bead diameter (mm) and cell load (mg/ml), **c.** alginate concentration (%) and bead diameter (mm),

Figure 5 Reusability of free and alginate immobilized *P. putida* G7 cells for limonin biotransformation

Figures

Figure 1

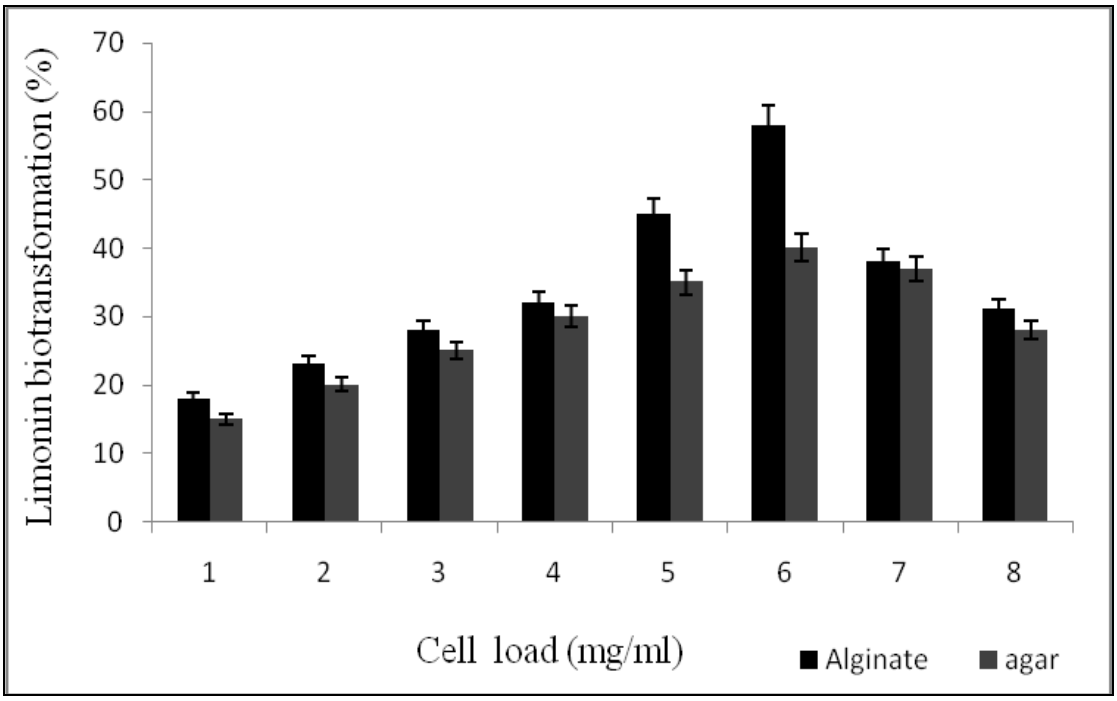

Figure 2

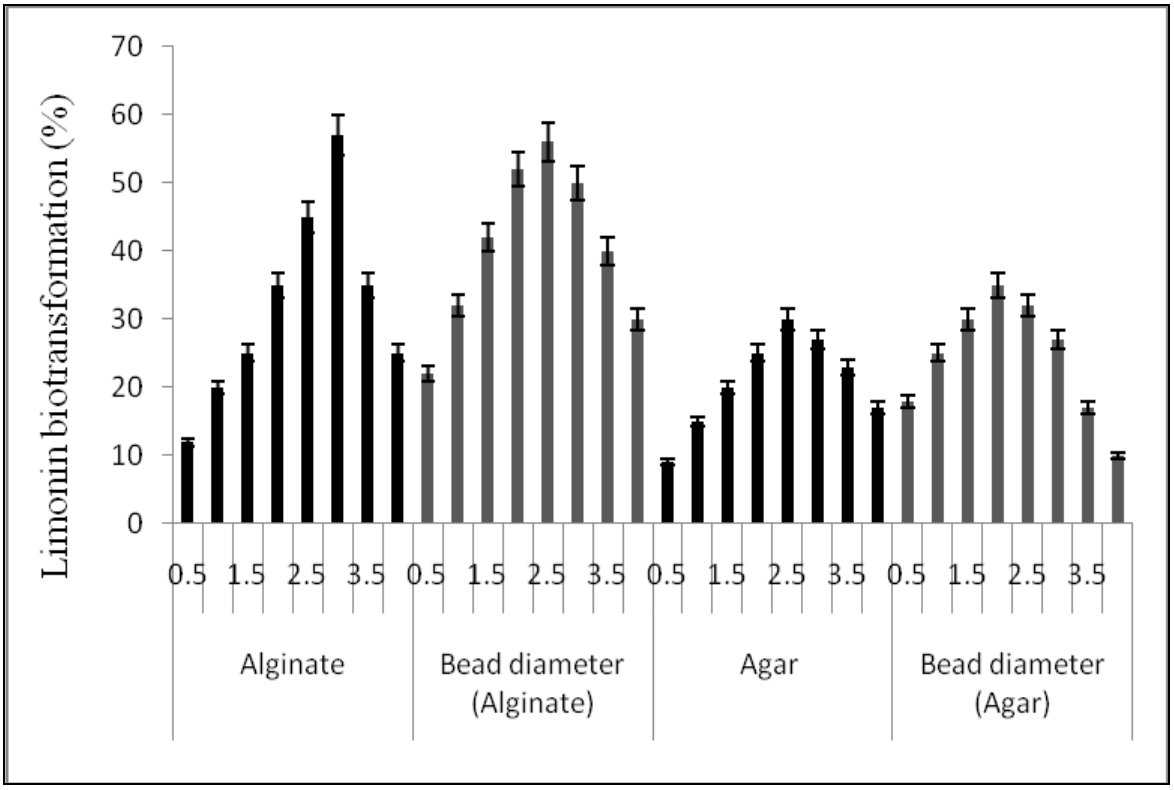
Limonin biotransformation (%)
70
60
50
40
30
20
10
0
0.5 1.5 2.5 3.5 0.5 1.5 2.5 3.5 0.5 1.5 2.5 3.5 0.5 1.5 2.5 3.5
Alginate
Bead diameter (Alginate)
Agar
Bead diameter (Agar)

Figure 3

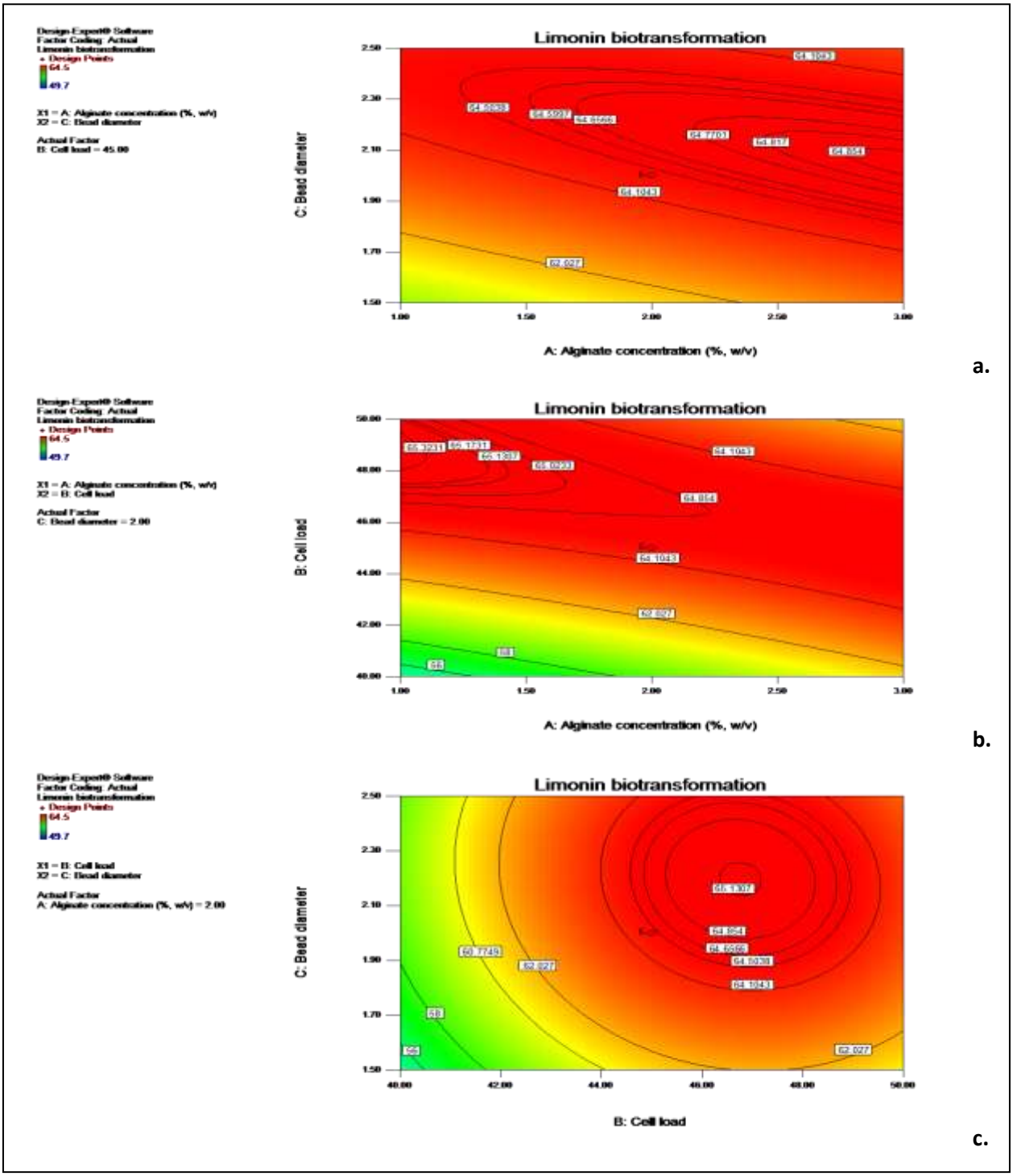
Design-Expert® Software
Factor Coding: Actual
Limonin biotransformation
Design Points
64.5
49.7
X1 = A: Alginate concentration (%, w/v)
X2 = C: Bead diameter
Actual Factor
B: Cell load = 45.00
Limonin biotransformation
C: Bead diameter
A: Alginate concentration (%, w/v)
a.
Design-Expert® Software
Factor Coding: Actual
Limonin biotransformation
Design Points
64.5
49.7
X1 = A: Alginate concentration (%, w/v)
X2 = B: Cell load
Actual Factor
C: Bead diameter = 2.00
Limonin biotransformation
B: Cell load
A: Alginate concentration (%, w/v)
b.
Design-Expert® Software
Factor Coding: Actual
Limonin biotransformation
Design Points
64.5
49.7
X1 = B: Cell load
X2 = C: Bead diameter
Actual Factor
A: Alginate concentration (%, w/v) = 2.00
Limonin biotransformation
C: Bead diameter
B: Cell load
c.

Figure 4

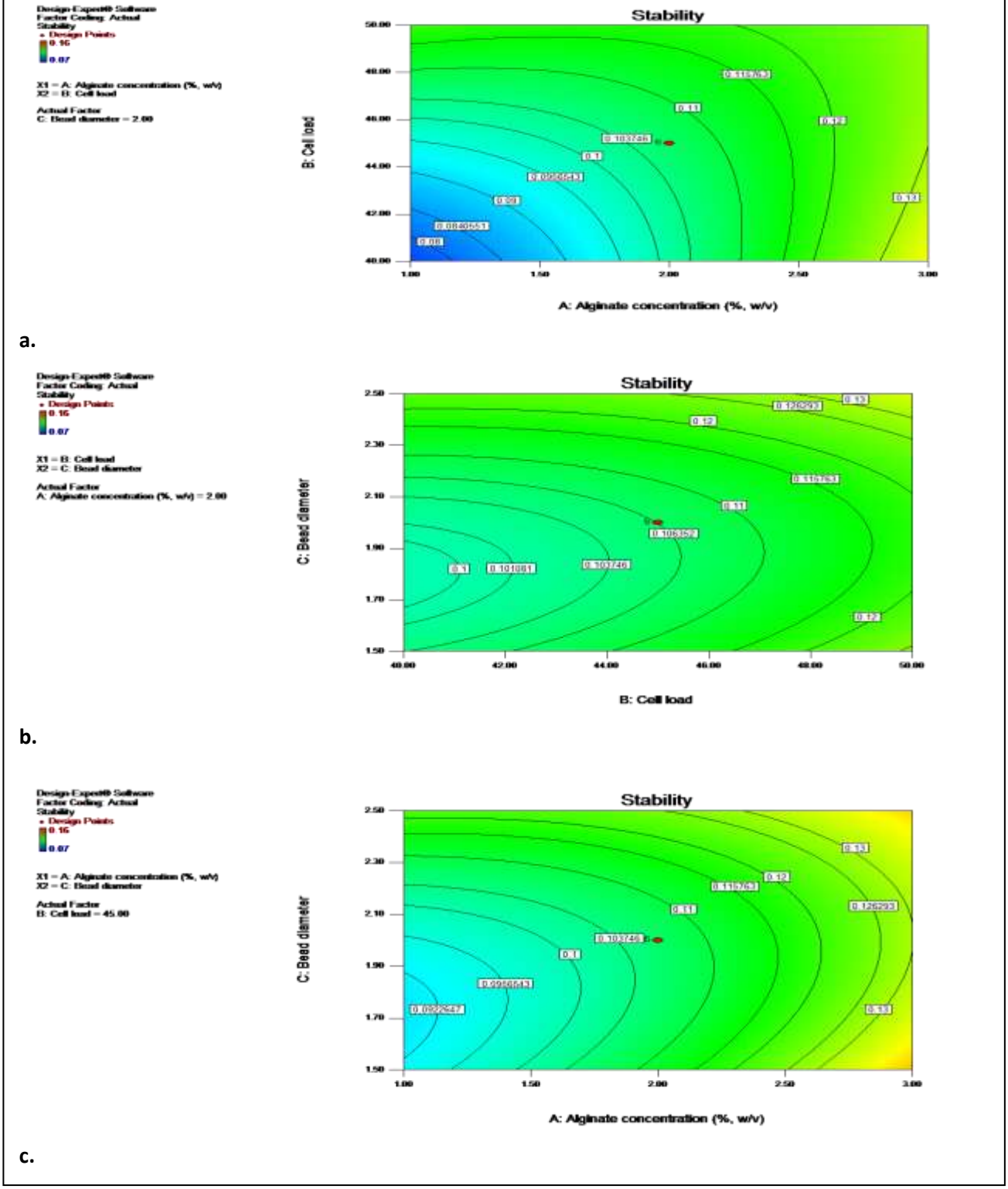
Design-Expert® Software
Factor Coding: Actual
Stability
Design Points
0.16
0.07
X1 = A: Alginate concentration (%, w/v)
X2 = B: Cell load
Actual Factor
C: Bead diameter = 2.00
Stability
B: Cell load
A: Alginate concentration (%, w/v)
a.
Design-Expert® Software
Factor Coding: Actual
Stability
Design Points
0.16
0.07
X1 = B: Cell load
X2 = C: Bead diameter
Actual Factor
A: Alginate concentration (%, w/v) = 2.00
Stability
C: Bead diameter
B: Cell load
b.
Design-Expert® Software
Factor Coding: Actual
Stability
Design Points
0.16
0.07
X1 = A: Alginate concentration (%, w/v)
X2 = C: Bead diameter
Actual Factor
B: Cell load = 45.00
Stability
C: Bead diameter
A: Alginate concentration (%, w/v)
c.

Figure 5

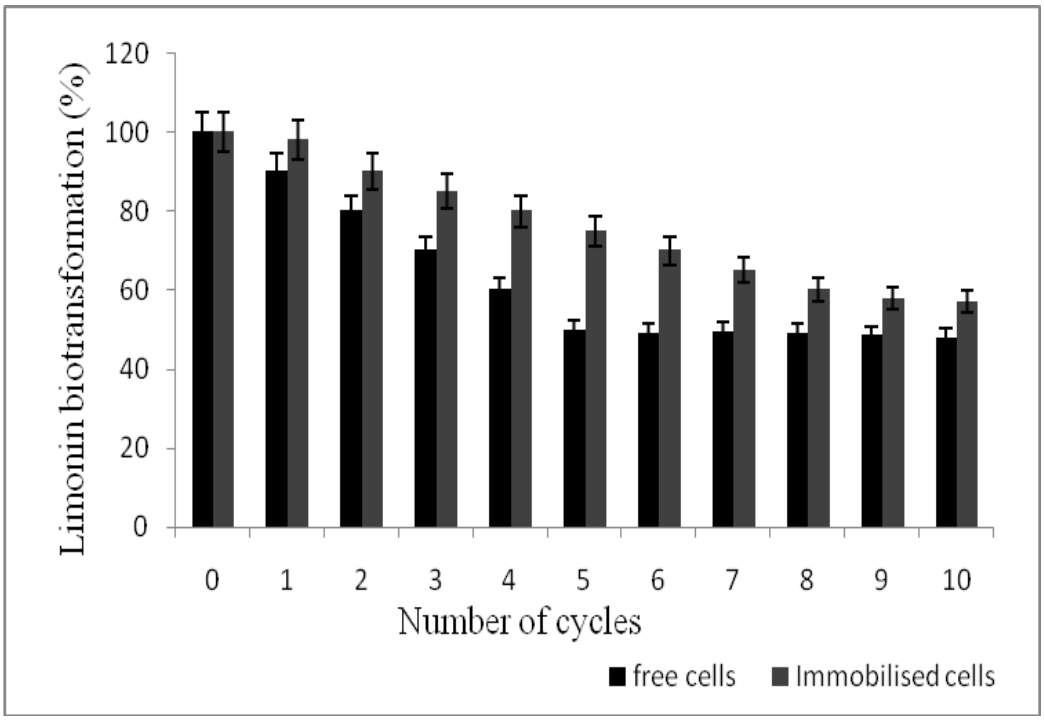
Limonin biotransformation (%)
120
100
80
60
40
20
0
0
1
2
3
4
5
6
7
8
9
10
Number of cycles
free cells
Immobilised cells